Impact of Growth Stage, Supplemental Red LED, and Salinity Stress on the Quality and Aroma Attributes of Hydroponic Fennel (*Foeniculum vulgare* Mill.)

Jingsi Liu

Dissertation submitted to the faculty of the Virginia Polytechnic Institute and State University in partial fulfillment of the requirements for the degree of

Doctor of Philosophy
In
Food Science and Technology

Yun Yin, Chair
David C. Haak
Sean F. O'Keefe
E. Kenneth Hurley
Laban K. Rutto
Renee Eriksen

November 14, 2024
Blacksburg, VA

Keywords: fennel, aroma, GC-MS-O, RNA sequencing, secondary metabolism

Impact of Growth Stage, Supplemental Red LED, and Salinity Stress on the Quality and Aroma Attributes of Hydroponic Fennel (*Foeniculum vulgare* Mill.)

Jingsi Liu

ABSTRACT

Fennel (*Foeniculum vulgare* Mill.) is a widely used culinary herb valued for its distinct flavor, rich essential oil content, and health-promoting secondary metabolites. Due to its diverse culinary, medicinal, and industrial applications, optimizing fennel aroma, the key quality characteristic of fennel and its products, is of significant interest. The production of aroma compounds, which arise from secondary metabolism, is influenced by factors such as growth stage and environmental conditions. Understanding how secondary metabolite biosynthesis are affected by these factors is crucial for optimizing the quality and flavor of fennel. In particular, supplemental red light and salinity are known to modulate the production of aroma compounds in herbs, but the molecular mechanisms underlying these effects remain largely unexplored. Controlled environment agriculture (CEA) provides an ideal platform for studying plant responses to environmental stimuli. Accordingly, this dissertation aims to investigate the influences of growth stage, supplemental red LED light, and salinity stress on the quality and aroma compounds of fennel cultivated by CEA.

Fennel was cultivated with nutrient film technique (NFT) hydroponic systems under controlled conditions. Solid phase microextraction (SPME) - gas chromatography - mass spectrometry olfactometry (GC-MS-O) was utilized for aroma characterization. RNA sequencing was used to generate transcriptome profiles of fennel under different

environmental treatments. A total of 32 aroma-active compounds were identified in fennel microgreens, compared to 28 in mature fennel. Compared to mature plants, fennel microgreens contained a significantly higher level of monoterpenes, showing an 81.4-98.1% increase when compared to mature fennel. Supplemental red LED significantly increased both fennel yield and aroma compounds accumulation, particularly phenylpropanoids such as *(E)*-anethole ("sweet", "anise"), estragole ("anise", "herbal"), and *p*-anisaldehyde ("floral", "sweet"). Transcriptome analysis showed upregulation of key genes involved in phenylpropanoid biosynthesis, including eugenol synthase and isoeugenol synthase, which likely contributed to the increased phenylpropanoid concentrations under red LED light. Salinity stress, while significantly reducing plant growth, did not notably affect the overall content of aroma-active compounds. However, salinity triggered defense mechanisms in fennel, particularly through the activation of plant hormone signal transduction and mitogen-activated protein kinase (MAPK) signaling pathways. The findings of this study enhanced understanding of aroma formation of fennel in response to environmental factors at molecular and transcriptomic levels. These results also offer opportunities for growers to optimize fennel flavor through precise control of environmental conditions.

Impact of Growth Stage, Supplemental Red LED, and Salinity Stress on the Quality and Aroma Attributes of Hydroponic Fennel (*Foeniculum vulgare* Mill.)

Jingsi Liu

GENERAL AUDIENCE ABSTRACT

Fennel (*Foeniculum vulgare* Mill.) is a popular herb known for its unique anise-like aroma. It's widely used in different cuisines, traditional medicine, and in industrial products due to its rich essential oils and health-promoting compounds. The aroma of fennel comes from natural chemicals produced by the plant, which can be influenced by factors such as growth stage and environmental conditions. This study explores how different factors, specifically growth stage, additional red LED light, and salt stress, affect the flavor chemistry of fennel grown in controlled environments.

Fennel was grown using hydroponic systems, which allowed precise control of water and nutrients, at Virginia Tech greenhouse. To identify important chemicals responsible for the aroma profile of fennel, instrumental analysis was used to pick out and measure the levels of these compounds. In addition, the gene expression of fennel under different treatments was quantified by RNA sequencing. The results showed that fennel microgreens had a higher level of aroma compounds compared to mature plants. Adding red LED light boosted both the yield and aroma content of fennel, especially those aroma compounds that are responsible for sweet, anise-like and herbal notes. In addition, red light activated certain genes in fennel that are responsible for producing these aroma compounds. On the other hand, exposing fennel to salt stress reduced its growth, but did not significantly affect its overall aroma content. Salinity triggered the defense mechanisms

in fennel, which helped the plant adjust its responses to stress conditions. Overall, this study provides new insights into how different environmental conditions affect the flavor chemistry of fennel. The knowledge can help farmers and growers improve the quality of fennel and other herbs by fine-tuning their growing environments to produce more flavorful plants.

Acknowledgements

There are countless people who have been a part of my journey at Virginia Tech, and I owe each of them my deepest gratitude. To my advisor, Dr. Yun Yin, thank you for giving me the opportunity to pursue what I love, for showing me great mentorship, and for helping me become the scientist I am today. To my past and current committee, Drs. David Haak, Sean O'Keefe, Ken Hurley, Renee Eriksen, Laban Rutto and Song Li, who generously offered their time, wisdom, and support, thank you for being my endless source of information and encouragement. To Dr. Bastiaan Bargmann, for welcoming me to his lab, and guiding me through the complexities of working with plant RNA. To Dr. Jacob Lahne, for showing me writing codes in R can be really fun (sometimes). I would also like to thank Ann Sandbrook, our food chemistry lab manager, Dr. Hengjian Wang, laboratory specialist, and Jeff Burr, greenhouse manager, for always making sure I have what I need to continue my experiment.

I've had the privilege of working alongside many brilliant graduate students, Xueqian Su, Hope Xu, Rebekah Miller, Isabel Gutierrez, Alisa Holst, Wangyi Wei, Billy Tu, Adam Sumner, Alex Harris, Joseph Taylor, Kelsey Reed, Dajun Yu, Virell To, Megan Mershon, Felicia Fianu, Jiakun Yi, Zane Xu, Mico Li, Journey Yang, Fujunzhu Zhao, and Saehah Yi. You have all made this experience richer with your camaraderie, help, and shared laughter. To undergraduate students Ray Huang, Tiffany Nguyen, Ishaan Agarwal, and Sofia Palacios, thank you for your hard work and positivity.

To my best friend, Ruoling Xu. There were times when I thought I would lose my way, but even from afar, you keep me grounded. Thank you for always being by my side.

To my parents, Hongjun Yang and Wenlian Liu, you have loved me unconditionally, stood by my decisions even when we disagreed, and believed in me at every step. This work is didecated to you.

Table of Contents

List of Figures

List of Tables

List of Abbreviations

Abbreviation	Full Name
4CL	4-coumaroyl-CoA ligase
AEDA	aroma extraction dilution analysis
AIMT1	*trans*-anol O-methyltransferase
ALDH2C4	aldehyde dehydrogenase family 2 member C4
AMC	apparent moisture content
ANOVA	analysis of variance
ARF	auxin response factors
B	blue
BP	biological process
CAD	cinnamyl alcohol dehydrogenase
CCR	cinnamoyl CoA reductase
CEA	controlled environment agriculture
CFAT	coniferyl alcohol acyltransferase
CHS	chalcone synthase
COMT	caffeic acid 3-O-methyltransferase
CPK28	calcium-dependent protein kinase 28
CYP73A	*trans*-cinnamate 4-monooxygenase
DASD	directorate of arecanut and spices development
DEG	differentially expressed gene
DFT	deep flow technique
DLI	daily light integral
DMAPP	dimethylallyl diphosphate
DNA	deoxyribonucleic acid
DVB/CAR/PDMS	divinylbenzene/carboxen/polydimethylsiloxane
DWC	deepwater culture
EC	electrical conductivity
EOMT1	eugenol O-methyltransferase
EGS1	eugenol synthase
FAO	Food and Agriculture Organization
FID	flame ionization detector
FR	far-red
GC	gas chromatography
GC-O	gas chromatography-olfactometry
GI	growth index
GO	Gene Ontology
IGS1	isoeugenol synthase
IPP	isopentenyl pyrophosphate
KEGG	Kyoto Encyclopedia of Genes and Genomes
LED	light-emitting diode
LOD	limit of detection
LOQ	limit of quantitation
MAPK	mitogen-activated protein kinase
MEP	methylerythritol phosphate

mRNA	messenger RNA
MS	mass spectrometry
MSD	mass selective detector
MVA	mevalonic acid
NFT	nutrient film technique
OAV	odor activity value
OD	optical density
PAL	phenylalanine ammonialyase
PAR	photosynthetically active radiation
PCA	principal component analysis
PGK	phosphoglycerate kinase
PP2C	protein phosphatases 2C
PPFD	photosynthetic photon flux density
PSI	photosystem I
PSY2	phytoene synthase 2
R	red
RI	retention index
RIN	RNA Integrity
RNA	ribonucleic acid
RNA-seq	RNA sequencing
ROS	reactive oxygen species
rRNA	ribosomal RNA
SAFE	solvent assisted flavor evaporation
SAM	standard addition methods
SD	standard deviation
SDE	simultaneous distillation-extraction
SFE	supercritical fluid extraction
SIDA	stable isotope dilution analysis
SPME	and solid phase microextraction
TAL	tyrosine ammonia lyase
TF	transcription factor
Tukey’s HSD	Tukey’s honest significant difference
UVR8	ultraviolet resistance locus 8 photoreceptor
VOC	volatile organic compound

Chapter 1 Introduction and Justification

Fennel (*Foeniculum vulgare* Mill.) is a biennial or perennial herb from the Apiaceae family, widely cultivated for culinary, medicinal, and industrial uses (Kooti, Moradi, Ali-Akbari, Sharafi-Ahvazi, Asadi-Samani, & Ashtary-Larky, 2015). Its unique, anise-like aroma is attributed to various secondary metabolites, particularly phenylpropanoids and terpenoids. These compounds not only contribute to the characteristic aroma of fennel, but also offer health benefits, including antioxidant, anti-inflammatory, antimicrobial, and gastroprotective properties (Mehra, Tamta, & Nand, 2021; Noreen, Tufail, Badar-Ul-Ain, & Awuchi, 2023; Rafieian, Amani, Rezaei, Karaça, & Jafari, 2024). As a result, fennel is a specialty crop with significant economic impact, with applications in both fresh and processed markets (Malhotra, 2012). Its global production has expanded into a multimillion-dollar industry, with most productions in India, Turkey, and Mexico (FAO, 2022).

Aroma is a critical quality parameter for fennel and other culinary herbs. The yield and aroma quality of these herbs are influenced by many factors, including growth stage (El-Zaeddi, Calín-Sánchez, Noguera-Artiaga, Martínez-Tomé, & Carbonell-Barrachina, 2020) and environmental conditions, such as light (Litvin, Currey, & Wilson, 2020) and salinity (Aktsoglou et al., 2021). Understanding how these factors affect the concentration and composition of aroma compounds is crucial for enhancing the quality and commercial value of fennel.

Aroma compounds in plants vary across different developmental stages, with certain compounds peaking at different times of growth. Previous studies have primarily focused on plant biomass and essential oil content at different stages, such as pre- and post-

flowering or seed formation (Huopalahti & Linko, 1983; Rohloff, Dragland, Mordal, & Iversen, 2005; Souza, Ming, Santos, Simon, Juliani, & Saad, 2021). However, limited studies have examined the effect of harvest times on the aroma composition of fennel leaves and stem during vegetative growth stage (El-Zaeddi et al., 2020). This is an important aspect for leafy fennel, as it is harvested and consumed prior to flowering. Additionally, microgreens have been shown to contain a higher level of bioactive phytochemicals compared to their mature counterpart, making them valuable sources of functional compounds (Choe, Yu, & Wang, 2018). However, the differences in aroma profile between herb microgreens and the mature plants are species-dependent (Choe et al., 2018), and no studies have specifically investigated this aspect for fennel. Determining the optimal harvest stage based on aroma composition and other key traits could enable growers to enhance the quality, marketability, and value of fennel.

Light is one of the most important environmental factors affecting plant growth and the biosynthesis of secondary metabolites. Light spectrum, intensity, and photoperiod are key aspects that influence photosynthesis and secondary metabolite production (Alrifai, Hao, Marcone, & Tsao, 2019). In the visible spectrum, red light is particularly important due to its strong absorption by chlorophylls and phytochromes, making it more efficiently utilized than other wavelengths by plants (Brazaityte et al., 2019). Recent studies have demonstrated that red light-emitting diode (LED) light significantly increased the growth and secondary metabolite content in Apiaceae herbs, such as dill (*Anethum graveolens* L.), chervil (*Anthriscus cerefolium* L. Hoffm.), and parsley (*Petroselinum crispum*) (El Haddaji et al., 2023; Litvin et al., 2020). Despite these findings, there is still very limited research on the influence of red LED light on fennel growth and aroma development.

The increasing global salinization, driven by climate change, saltwater intrusion, and other anthropological activities, is a growing concern for agriculture productivity and food security (Cunillera-Montcusí et al., 2022; Tarolli et al., 2023). Salinity negatively affects plant growth and secondary metabolism by disrupting ion balance, osmotic pressure, and cellular homeostasis (Yang & Guo, 2018). It is also known to induce oxidative stress, leading to changes in the production of aroma compounds and other secondary metabolites in various plant species (Corrado, Vitaglione, Chiaiese, & Rouphael, 2021; Isayenkov & Maathuis, 2019; Sarmoum, Haid, Biche, Djazouli, Zebib, & Merah, 2019). Fennel is moderately tolerant to salinity (Shafeiee & Ehsanzadeh, 2019), and well-suited for cultivation in arid and semi-arid environments (Ashraf & Akhtar, 2004). However, previous study has shown that salinity significantly impacted fennel essential oil content and composition (Rebey, Rahali, Tounsi, Marzouk, & Ksouri, 2016), leading to changes in fennel quality. Furthermore, the molecular mechanisms underlying salinity-induced changes in fennel aroma biosynthesis are still largely unknown.

Driven by consumer demand for fresh, flavorful, and healthy ingredients, the cultivation of culinary herbs in controlled environment agriculture (CEA), including hydroponic systems, has expanded rapidly over the past three decades (USDA, 2019). Although fennel can be grown outdoors or within controlled environments, year-round production in regions with extreme climates is only feasible with CEA (Walters & Currey, 2015). CEA offers precise control over environmental factors such as light, temperature, and humidity, as well as recycled water usage (Benke & Tomkins, 2017). This makes CEA an ideal platform for studying the effects of environmental factors on plant growth and quality. This is particularly relevant for aromatic herbs like fennel, whose secondary

metabolites, particularly aroma compounds, are highly sensitive to cultivation conditions. Light and salinity were selected in this study because both factors have been reported to modulate the production of aroma compounds in several culinary herbs (Alrifai et al., 2019; Corrado et al., 2021; Massa, Kim, Wheeler, & Mitchell, 2008; Tsamaidi, Daferera, Karapanos, & Passam, 2017). Additionally, both factors can be effectively manipulated in CEA systems, offering opportunities for herb growers to optimize and refine the flavor and aroma profiles of their crops.

The characterization of fennel aroma compounds and gene expression levels in response to environmental stresses requires advanced analytical techniques. Gas chromatography - mass spectrometry, coupled with olfactometry, is widely used for the identification and quantitation of aroma-active compounds (Song & Liu, 2018). RNA sequencing is a powerful tool for studying the transcriptome in response to environmental stimuli (Wolf, 2013). The integration of transcriptome analysis with metabolic profiling of aroma compounds offers a novel approach to understand how gene expression patterns are linked to aroma formation in fennel, and other crops of interest, under different environmental conditions.

Thus, the overarching goal of this study is to understand how key aroma compounds in fennel are influenced by growth stage, supplemental red LED light, and varying levels of salinity stress. Specifically, this research aims to: investigate and compare the aroma characteristics of fennel microgreens and mature plants (chapter 3); determine the impact of supplemental red LED light on the growth, aroma, and gene expression of hydroponic grown fennel, and identify key genes that contribute to aroma formation and accumulation under red LED light (chapter 4); examine the effects of different salinity levels on the

growth, aroma composition, and gene expression of fennel, and identify key metabolic pathways and candidate genes that could serve as makers for breeding of salt-tolerant crops (chapter 5). Overall, this study seeks to provide new insights into the aroma formation in fennel and contribute to the development of strategies for enhancing the flavor and quality of culinary herbs through precise environmental control in CEA.

References

Aktsoglou, D.-C., Kasampalis, D. S., Sarrou, E., Tsouvaltzis, P., Chatzopoulou, P., Martens, S., & Siomos, A. S. (2021). Improvement of the quality in hydroponically grown fresh aromatic herbs by inducing mild salinity stress is species-specific. *Folia Horticulturae*, *33*(2), 265-274. https://doi.org/10.2478/fhort-2021-0020.

Alrifai, O., Hao, X., Marcone, M. F., & Tsao, R. (2019). Current review of the modulatory effects of led lights on photosynthesis of secondary metabolites and future perspectives of microgreen vegetables. *Journal of Agriculture and Food Chemistry*, *67*(22), 6075-6090. https://doi.org/10.1021/acs.jafc.9b00819.

Ashraf, M., & Akhtar, N. (2004). Influence of salt stress on growth, ion accumulation and seed oil content in sweet fennel. *Biologia Plantarum*, *48*(3), 461-464. https://doi.org/10.1023/B:BIOP.0000041105.89674.d1.

Benke, K., & Tomkins, B. (2017). Future food-production systems: vertical farming and controlled-environment agriculture. *Sustainability: Science, Practice and Policy*, *13*(1), 13-26. https://doi.org/10.1080/15487733.2017.1394054.

Brazaityte, A., Virsile, A., Samuoliene, G., Vastakaite-Kairiene, V., Jankauskiene, J., Miliauskiene, J., Novičkovas, A., Duchovskis, P. (2019). Response of mustard microgreens to different wavelengths and durations of UV-A LEDs. *Frontiers in Plant Science, 10*. https://doi.org/10.3389/fpls.2019.01153.

Choe, U., Yu, L. L., & Wang, T. T. Y. (2018). The science behind microgreens as an exciting new food for the 21st century. *Journal of Agricultural and Food Chemistry, 66*(44), 11519-11530. https://doi.org/10.1021/acs.jafc.8b03096.

Corrado, G., Vitaglione, P., Chiaiese, P., & Rouphael, Y. (2021). Unraveling the modulation of controlled salinity stress on morphometric traits, mineral profile, and bioactive metabolome equilibrium in hydroponic basil. *Horticulturae*, 7(9), 273. https://doi.org/10.3390/horticulturae7090273.

Cunillera-Montcusí, D., Beklioğlu, M., Cañedo-Argüelles, M., Jeppesen, E., Ptacnik, R., Amorim, C. A., Arnott, S. E., Berger, S. A., Brucet, S., Dugan, H. A., Gerhard, M., Horváth, Z., Langenheder, S., Nejstgaard, J. C., Reinikainen, M., Striebel, M., Urrutia-Cordero, P., Vad, C. F., Zadereev, E., & Matias, M. (2022). Freshwater salinisation: a research agenda for a saltier world. *Trends in Ecology & Evolution, 37*(5), 440-453. https://doi.org/10.1016/j.tree.2021.12.005.

El Haddaji, H., Akodad, M., Skalli, A., Moumen, A., Bellahcen, S., Elhani, S., Urrestarazu, M., Kolar, M., Imperl, J., Petrova, P., & Baghour, M. (2023). Effects of light-emitting diodes (LEDs) on growth, nitrates and osmoprotectant content in microgreens of aromatic and medicinal plants. *Horticulturae*, 9(4). 494. https://doi.org/10.3390/horticulturae9040494.

El-Zaeddi, H., Calín-Sánchez, Á., Noguera-Artiaga, L., Martínez-Tomé, J., & Carbonell-Barrachina, Á. A. (2020). Optimization of harvest date according to the volatile composition of Mediterranean aromatic herbs at different vegetative stages. *Scientia Horticulturae*, 267, 109336. https://doi.org/10.1016/j.scienta.2020.109336.

FAO (2022). Fennel, In *Food and Agriculture Organization of the United Nations: Value of Agricultural Production*. Retrieved October 15, 2024, from https://www.fao.org/faostat/en/#data/QCL.

Huopalahti, R., & Linko, R. R. (1983). Composition and content of aroma compounds in dill, *Anethum graveolens* L., at three different growth stages. *Journal of Agricultural and Food Chemistry*, *31*(2), 331-333. https://doi.org/10.1021/jf00116a036.

Isayenkov, S. V., & Maathuis, F. J. M. (2019). Plant salinity stress: Many unanswered questions remain. *Frontiers in Plant Science*, *10*, https://doi.org/10.3389/fpls.2019.00080.

Kooti, W., Moradi, M., Ali-Akbari, S., Sharafi-Ahvazi, N., Asadi-Samani, M., & Ashtary-Larky, D. (2015). Therapeutic and pharmacological potential of *Foeniculum vulgare* Mill: a review. *Journal of HerbMed Pharmacology*, 4(1), 1-9.

Litvin, A. G., Currey, C. J., & Wilson, L. A. (2020). Effects of supplemental light source on basil, dill, and parsley growth, morphology, aroma, and flavor. *Journal of the American Society for Horticultural Science, 145*(1), 18-29. https://doi.org/10.21273/JASHS04746-19.

Malhotra, S. K. (2012). Fennel and fennel seed. In K. V. Peter (Eds.), *Handbook of herbs and spices* (pp. 275-302). Elsevier.

Massa, G. D., Kim, H.-H., Wheeler, R. M., & Mitchell, C. A. (2008). Plant productivity in response to LED lighting. *HortScience, 43*(7), 1951-1956. https://doi.org/10.21273/HORTSCI.43.7.1951.

Mehra, N., Tamta, G., & Nand, V. (2021). A review on nutritional value, phytochemical and pharmacological attributes of *Foeniculum vulgare* Mill. *Journal of*

Pharmacognosy and Phytochemistry, 10(2), 1255-1263. https://doi.org/10.22271/phyto.2021.v10.i2q.13983.

Noreen, S., Tufail, T., Badar Ul Ain, H., & Awuchi, C. G. (2023). Pharmacological, nutraceutical, functional and therapeutic properties of fennel (*Foeniculum vulgare*). *International Journal of Food Properties, 26*(1), 915-927. https://doi.org/10.1080/10942912.2023.2192436.

Rafieian, F., Amani, R., Rezaei, A., Karaça, A. C., & Jafari, S. M. (2024). Exploring fennel (*Foeniculum vulgare*): Composition, functional properties, potential health benefits, and safety. *Critical Reviews in Food Science and Nutrition, 64*(20), 6924-6941. https://doi.org/10.1080/10408398.2023.2176817.

Rebey, I. B., Rahali, F. Z., Tounsi, M. S., Marzouk, B., & Ksouri, R. (2016). Variation in fatty acid and essential oil composition of sweet fennel (*Foeniculum vulgare* Mill) seeds as affected by salinity. *Journal of New Sciences*, *62*.

Rohloff, J., Dragland, S., Mordal, R., & Iversen, T.-H. (2005). Effect of harvest time and drying method on biomass production, essential oil yield, and quality of peppermint (*Mentha × piperita* L.). *Journal of Agricultural and Food Chemistry, 53*(10), 4143-4148. https://doi.org/10.1021/jf047998s.

Sarmoum, R., Haid, S., Biche, M., Djazouli, Z., Zebib, B., & Merah, O. (2019). Effect of salinity and water stress on the essential oil components of rosemary (*Rosmarinus officinalis* L.). *Agronomy,* 9(5), 214. https://doi.org/10.3390/agronomy9050214.

Shafeiee, M., & Ehsanzadeh, P. (2019). Physiological and biochemical mechanisms of salinity tolerance in several fennel genotypes: Existence of clearly-expressed

genotypic variations. *Industrial Crops and Products*, *132*, 311-318. https://doi.org/10.1016/j.indcrop.2019.02.042.

Song, H. L., & Liu, J. B. (2018). GC-O-MS technique and its applications in food flavor analysis. *Food Research International, 114*, 187-198. https://doi.org/10.1016/j.foodres.2018.07.037.

Souza, J. V. R. S., Ming, L. C., Santos, M. A. L., Simon, J. E., Juliani, H. R., & Saad, J. C. C. (2021). Effect of water regime and harvest stage on essential oil accumulation in basil plant growing in sandy soil. *Irrigation Science, 39*(4), 493-503. https://doi.org/10.1007/s00271-021-00719-1.

Tarolli, P., Luo, J., Straffelini, E., Liou, Y.-A., Nguyen, K.-A., Laurenti, R., et al. (2023). Saltwater intrusion and climate change impact on coastal agriculture. *PLOS Water, 2*(4), e0000121. https://doi.org/10.1371/journal.pwat.0000121.

Tsamaidi, D., Daferera, D., Karapanos, I. C., & Passam, H. C. (2017). The effect of water deficiency and salinity on the growth and quality of fresh dill (*Anethum graveolens* L.) during autumn and spring cultivation. *International Journal of Plant Production*, *11*(1), 33-46. http://doi.org/10.22069/ijpp.2017.3308.

USDA (2019). Census of horticultural specialties. Census of Agriculture. Retrieved October 15, 2024, from https://www.nass.usda.gov/Publications/AgCensus/2017/Online_Resources/Census_of_Horticulture_Specialties/index.php.

Walters, K. J., & Currey, C. J. (2015). Hydroponic greenhouse basil production: comparing systems and cultivars. *Horttechnology, 25*(5), 645-650. https://doi.org/10.21273/Horttech.25.5.645.

Wolf, J. B. W. (2013). Principles of transcriptome analysis and gene expression quantification: an RNA‐seq tutorial. *Molecular Ecology Resources*, *13*(4), 559-572. https://doi.org/10.1111/1755-0998.12109.

Yang, Y., & Guo, Y. (2018). Elucidating the molecular mechanisms mediating plant salt-stress responses. *New Phytologist, 217*(2), 523-539. https://doi.org/10.1111/nph.14920.

Chapter 2 Literature Review

2.1 Fennel

Fennel (*Foeniculum vulgare* Mill.), commonly known as anise or sweet fennel, is a biennial or perennial herb widely used for culinary and medicinal purposes. *Foeniculum vulgare,* its name meaning of or related to hay, due to the aroma of fennel resembling the smell of hay (Saddiqi & Iqbal, 2011). The earliest botanical description of fennel dates to the 4th century BC in Theophrastus's *Historia Plantarum* (Inquiry into Plants) (Jarmusch, 2015). Fennel belongs to the Apiaceae (Umbelliferae) family, one of the largest families of flowering plants with over 3000 species (Sayed-Ahmad, Talou, Saad, Hijazi, & Merah, 2017). Characterized by its feathery leaves, umbels-containing inflorescences, and anise-like aroma, fennel has many wild and cultivated varieties that differ in shape, size, color, and flavor (Verma & Saxena, 2024).

Fennel is thought to originate from the Mediterranean region and thrives under temperate climates (Ziółkowska, Strzedulla, Śnit, Szczyra, & Kuźniewicz, 2024). Today, it is widely distributed across Europe, Asia, and North America (Badgujar, Patel, & Bandivdekar, 2014). Historically, ancient Egyptians utilized fennel both as food and medicine. In ancient China, it was valued as a remedy for snake bite, rheumatism, back pain, and hernias (Chevallier, 2016). Fennel seeds have also been used by the Romans since the first century AD (Saddiqi et al., 2011).

Depending on the variety, fennel has different uses. Bitter fennel is commonly grown for its seeds and essential oil, while sweet fennel is cultivated for its fresh leaves, stems, and bulbs, which are used as a vegetable (Verma et al., 2024). All parts of the fennel plants are edible. Fresh fennel leaves, stems, bulbs, and inflorescences are frequently used

in different cuisines, enhancing the flavor and texture of dishes such as salads, stews, and grilled foods (Barros, Carvalho, & Ferreira, 2010). Fennel seeds are usually used as a spice in foods such as liquors, bread, and cheese (Saxena, Agarwal, John, Dubey, & Lal, 2018). Due to its rich essential oil content and secondary metabolites, fennel is also an important ingredient in the cosmetic and pharmaceutical industries (Kooti, Moradi, Ali-Akbari, Sharafi-Ahvazi, Asadi-Samani, & Ashtary-Larky, 2015). These secondary metabolites are largely responsible for the health benefits of fennel, which include antioxidant, anti-inflammatory, antimicrobial, and gastroprotective properties (Mehra, Tamta, & Nand, 2021; Noreen, Tufail, Badar Ul Ain, & Awuchi, 2023; Rafieian, Amani, Rezaei, Karaça, & Jafari, 2024).

Proximate analysis of fennel from previous studies is shown in table 2.1 (Barros et al., 2010; Mittal et al., 2016). Fennel is a rich source of vitamins A, B (such as pantothenic acid and niacin), C, as well as calcium and potassium (Verma et al., 2024). Fresh fennel parts, such as shoots, leaves, stems, and inflorescences, have a high moisture content, while carbohydrates are the predominant macronutrient in fennel seeds. Carbohydrates plays an essential role in plant metabolism and cell structure, while lipids are vital for the plant membrane. Compared to fennel seeds, fresh fennel has a relatively low concentration of lipids. In fennel, fatty acids are synthesized from acetyl-CoA through plastids, then transported to endoplasmic reticulum, where they are assembled into various lipids (Ohlrogge, 1994). Fennel seeds contain 10% ~ 14% fatty acids, including palmitic acid (C16:0), petroselinic acid (C18:1 *cis*-6), oleic acid (C18:1 *cis*-9), and linoleic acid (C18:2) as the principal fatty acids (Coşge, Kiralan, & Gürbüz, 2008). In fresh fennel, the most

abundant fatty acid is linoleic acid (C18:2), followed by α-linolenic (C18:3) and palmitic (C16:0) acids (Barros et al., 2010).

Table 2-1. Chemical composition of different parts of fennel on a fresh weight basis (g/100g)

	Seeds[1]	Shoots[2]	Leaves[2]	Stems[2]	Inflorescences[2]
Moisture	6.3	73.9	76.4	77.5	71.3
Protein	9.5	1.3	1.2	1.1	1.4
Carbohydrate	60.8	21.9	18.4	19.4	22.8
Lipid	10.0	0.5	0.6	0.5	1.3
Ash	13.4	2.4	3.4	1.6	3.2

[1]Data from Rather, Dar, Sofi, Bhat, & Qurishi, 2016. [2] Data from Barros et al., 2010.

According to the latest data from Food and Agriculture Organization of the United Nation (FAO), global production of fennel, combined with other herbs and spices like anise, coriander, and cumin, was approximately 2.8 million tons in 2022, spanning a total harvest area of 2.3 million hectares (FAO, 2022). The production was mainly from India, Turkey, Mexico, Russia, Iran, China, Syria, and Egypt. As a relatively minor crop, country-specific production values of fennel are often not available. In the United States, domestic fennel production is mainly from California and Arizona (IPM Data, 2000), and most of the fennel seeds sold commercially are imported from Egypt (Herb Society of America, n.d.). India is the world's largest producer and exporter of fennel, estimated to produce around 300,000 tons in 2023 to 2024, with a 92% increase from the previous year (DASD, 2024), highlighting the great economic potential of this specialty crop.

Traditionally, fennel is grown by sowing seeds in open fields. It is hardy as a perennial or biennial in USDA hardiness zones up to Zone 7, but may grow as an annual in colder regions, as far north as Zone 4 (Herb Society of America, n.d.). In recent years,

there is a growing interest in cultivating fennel and other culinary herbs in controlled environment agriculture (CEA), such as hydroponic systems and protected structures, to enable local, year-round production and improve sustainability (USDA, 2019).

2.2 Controlled environment agriculture

Controlled environment agriculture refers to a form of agriculture where environmental conditions, such as light, temperature, humidity, and other variables can be precisely monitored and controlled for optimal plant growth and production (Folta, 2019; Shamshiri et al., 2018). CEA can be implemented in a modern greenhouse, where the entire system can be managed in an integrated manner (Shamshiri et al., 2018). With nearly 70% of the global population projected to reside in cities by 2050 (UN DESA, 2024), CEA has emerged as a crucial strategy for securing a steady supply of fresh fruit and vegetables for urban population. Although most culinary herbs can be grown outdoors or in a controlled environment, year-round production in regions with harsh climates is only feasible with CEA (Walters & Currey, 2015). Additionally, CEA offers a wide range of advantages, including recycled water usage, solar-powered lighting and heating, and 24-hour control of lighting, temperature, and humidity (Benke & Tomkins, 2017). Recent agricultural innovations, such as hydroponics or aeroponics, have also been introduced to CEA (Shamshiri et al., 2018), which simplify nutrient control and reduces the need for herbicides or pesticides.

Among all the hydroponic systems used in greenhouse production, the most common techniques for leafy greens and culinary herbs include deep flow technique (DFT), nutrient film technique (NFT), and deepwater culture (DWC) systems (Niu & Masabni, 2022). Previous studies have shown that the type of hydroponic system does not

significantly affect the fresh mass of basil or lemon balm, especially in a commercial production setting (Son, Park, Kim, Yoo, & Nho, 2021; Walters et al., 2015). Primarily, the choice of hydroponic systems should be tailored to the operational needs of growers, as each system offer unique advantages and challenges. NFT systems, which are normally placed at a height convenient for greenhouse workers, may be better suitable for herbs harvested multiple times, such as cut fresh varieties, while DFT and DWC systems are often more appropriate for single-harvest crops (Walters et al., 2015).

In the United States, the domestic production of fresh herbs can occur both outdoors and under protected environments, such as in greenhouses. According to the USDA Census of Horticultural Specialties, the value of food crops grown under protection (include herbs and hydroponic food crops) exceeded $703 million in 2019, accounting for more than 51% of the total horticultural crop production (USDA, 2019). Greenhouse herb production has increased tremendously over the past decade. Between 2009 and 2019, the number of greenhouse operations for cut fresh herbs rose by 216.7%, from 323 to 700. In 2019, the total value of cut fresh herbs grown under production was over $65 million, with 22.6% of production from hydroponic systems (USDA, 2019). The growth is largely because herbs share similar cultivation requirements with bedding plants (which are generally cultivated for planting in flower beds), which makes it easy for greenhouse growers to incorporate herbs into their production schedule (Gibson, Whipker, & Cloyd, 2001). Additionally, growers also favor culinary herbs due to their short turnaround time, low-cost seeds, and high profitability compared to bedding plants (Gibson, 2001). Furthermore, greenhouses and other CEA facilities support a year-round supply of locally grown herbs, that meet consumer demand for fresh, high-quality ingredients.

2.3 Aroma compounds in fennel

Aroma compounds are products of plant secondary metabolism, which involves pathways and compounds that are not essential for the immediate survival of plants but play critical roles in defense and signaling (L. Yang, Wen, Ruan, Zhao, Wei, & Wang, 2018). These secondary metabolites can be classified based on their distinct structures and biosynthetic pathways. Due to their biological activities, secondary metabolites are valuable for pharmaceutical, nutritional, and cosmetic applications, largely enhancing the commercial value and industrial interest of fennel.

Fennel is particularly known for its sweet, anise-like aroma, which is also a key feature of its essential oils. Fennel essential oils are rich in phenylpropanoids, terpenoids, aldehydes, ketones, and alcohols (Xiao, Chen, Niu, & Chen, 2017; Zayed, Sobeh, & Farag, 2022). Varietiy, geographical location, and harvesting time can greatly affect the composition and concentrations of aroma compounds in fennel. To date, more than 110 volatile aroma compounds have been identified in fennel and its products from different origins, with phenylpropanoids and terpenoids being the main constituents.

Phenylpropanoids are a class of compounds composed of a benzene ring linked to a three-carbon side chain (Zhu, Chen, & Zhang, 2024). These compounds are derived from the shikimic acid pathway via the aromatic amino acids phenylalanine and tyrosine (Vogt, 2010), with biosynthesis primarily occurring in the cytosol (Barman, Tenhaken, & Dötterl, 2023). In fennel, phenylpropanoids such as *(E)*-anethole, estragole, and methyl eugenol are the most prominent. Previous studies have consistently identified phenylpropanoids as the most dominant aroma group in many fennel varieties, with *(E)*-anethole being the most abundant compound (Bilia, Flamini, Taglioli, Morelli, & Vincieri, 2002; Díaz-Maroto,

Díaz-Maroto Hidalgo, Sánchez-Palomo, & Pérez-Coello, 2005; Zeller & Rychlik, 2006). *(E)*-Anethole imparts a characteristic sweet, anise-like aroma. Other phenylpropanoids such as eugenol and *(Z)*-anethole are usually present in lower amounts, but also contribute to the nuanced aroma profile of fennel.

Terpenoids, derived from five-carbon precursors, isopentenyl pyrophosphate (IPP) or its interconvertible isomer dimethylallyl diphosphate (DMAPP), are formed through methylerythritol phosphate (MEP) pathway in plastids or mevalonic acid (MVA) pathway in the cytoplasm, endoplasmic reticulum, and peroxisomes (Vranová, Coman, & Gruissem, 2013; Zhou & Pichersky, 2020). Terpenoids represent a highly diverse group of plant secondary metabolites, which can be divided into subgroups such as monoterpenes, sesquiterpenes, triterpenes, each varying in chemical structure and function (Zhou et al., 2020). In fennel, common terpenoids include α-pinene, camphene, β-pinene, myrcene, cymene, and γ-terpinene (Verma et al., 2024). Interestingly, certain terpenoids are unique to specific fennel cultivars. For example, sabinene is found exclusively in *F. vulgare* subsp. *piperitum* (Afifi, El-Mahis, Heiss, & Farag, 2021). Terpenoids typically exhibit woody, herbal, and spice odor attributes (Xiao et al., 2017), representing an important aspect of fennel aroma.

In addition to phenylpropanoids and terpenoids, fennel also contains ketones, aldehydes, alcohols, and esters, although these are generally present in smaller quantities and can vary widely across cultivars and growing conditions. For example, ketones account for 17.6% of the total volatile compounds in the variety “Fino” from Austria, but only account for 0.5% in variety “Dulce” from Italy; similarly, esters have been found to be more abundant in fennel grown in Egypt and Sudan (Afifi et al., 2021). These variations

suggested that origins, cultivars, and cultivation conditions significantly influence the aroma compounds accumulation in fennel. Additionally, dynamic interactions between different secondary metabolites happen as the plant progresses through different development stages.

2.4 Changes of aroma compounds during development stages

Secondary metabolites production in plants is highly influenced by developmental stages and environmental factors (Li, Kong, Fu, Sussman, & Wu, 2020). As plants progress through various developmental stages, the concentration and composition of secondary metabolites also change across different plant parts, such as roots, leaves, stems, inflorescences, and seeds (Birenboim et al., 2022). Germination and seedling growth stages are crucial for any plant species because plants are most vulnerable to environmental stress during this period (De-la-Cruz Chacón, Riley-Saldaña, & González-Esquinca, 2013). In some species, secondary metabolite levels are highest during early development and decline as plants mature. For example, in *Camptotheca acuminata,* the content of camptothecin was highest in the early development stage but dropped drastically upon reaching maturity (Valletta, Santamaria, & Pasqua, 2007).

Dynamic changes of secondary metabolite composition also occur during development. Aroma profiles of culinary herbs can also shift with plant maturity. Dimita et al. (2022) found that microgreens of perilla mint (Chinese basil) had a higher aroma content compared to mature plants. In cinnamon leaves, the highest content of the main volatile compound eugenol was found in 1-year-old branches during vegetative growth stage (Li et al., 2016). However, these changes often vary with species. In dill, the major aroma compound α-phellandrene peaked before bud formation but decreased significantly

during the flowering stage (Huopalahti & Linko, 1983). In contrast, essential oil content in basil was highest at the end of the flowering stage, while the essential oil of dill peaked right before bud formation (Souza, Ming, Santos, Simon, Juliani, & Saad, 2021).

Understanding how secondary metabolite levels fluctuate throughout plant growth and development is essential for optimizing herb quality and determining the ideal harvest time. While studies have examined the essential oil content and composition of fennel seeds at different developmental stages (Anwar, Hussain, Sherazi, & Bhanger, 2009; Saharkhiz & Tarakeme, 2011; Telci, Demirtas, & Sahin, 2009), research on the aroma compounds and composition of fresh fennel parts during different growth stages remain limited. Further investigation could offer valuable insights for improving fresh fennel production and eventually benefit fennel growers.

2.5 Lighting and aroma compounds

Various environmental factors, such as light (Litvin, Currey, & Wilson, 2020) and salinity (Zrig, Tounekti, Elgawad, Hegab, Ali, & Khemira, 2016), can influence the formation of aroma compounds and ultimately the quality of culinary herbs. These factors affect the biosynthesis pathways of secondary metabolites, which further alters the composition and of aroma profiles of herbs.

Light is a particularly important environmental factor that significantly influences both plant growth and the biosynthesis of secondary metabolites. Key aspects of light that modulate aroma compounds include light spectrum, intensity, and photoperiod (Alrifai, Hao, Marcone, & Tsao, 2019). Plants contain specialized photoreceptors that can detect various wavelengths of light and trigger responses that support photosynthesis and secondary metabolite production (Alrifai et al., 2019). The main photoreceptors in plants

are phytochromes, cryptochromes, phototropins, zeitlupes, and ultraviolet resistance locus 8 (UVR8) photoreceptor (Zhang et al., 2021). They are sensitive to different light spectra. Namely, phytochromes respond to red and far-red light, cryptochromes respond to blue light and ultraviolet A radiation, phototropins respond to blue light, zeitlupes to blue and green light, and UVR8s respond to ultraviolet B radiation (Zhang et al., 2021). The activation of these receptors leads to the regulation of specific genes and enzymes involved in secondary metabolism, as shown in Figure 2-1.

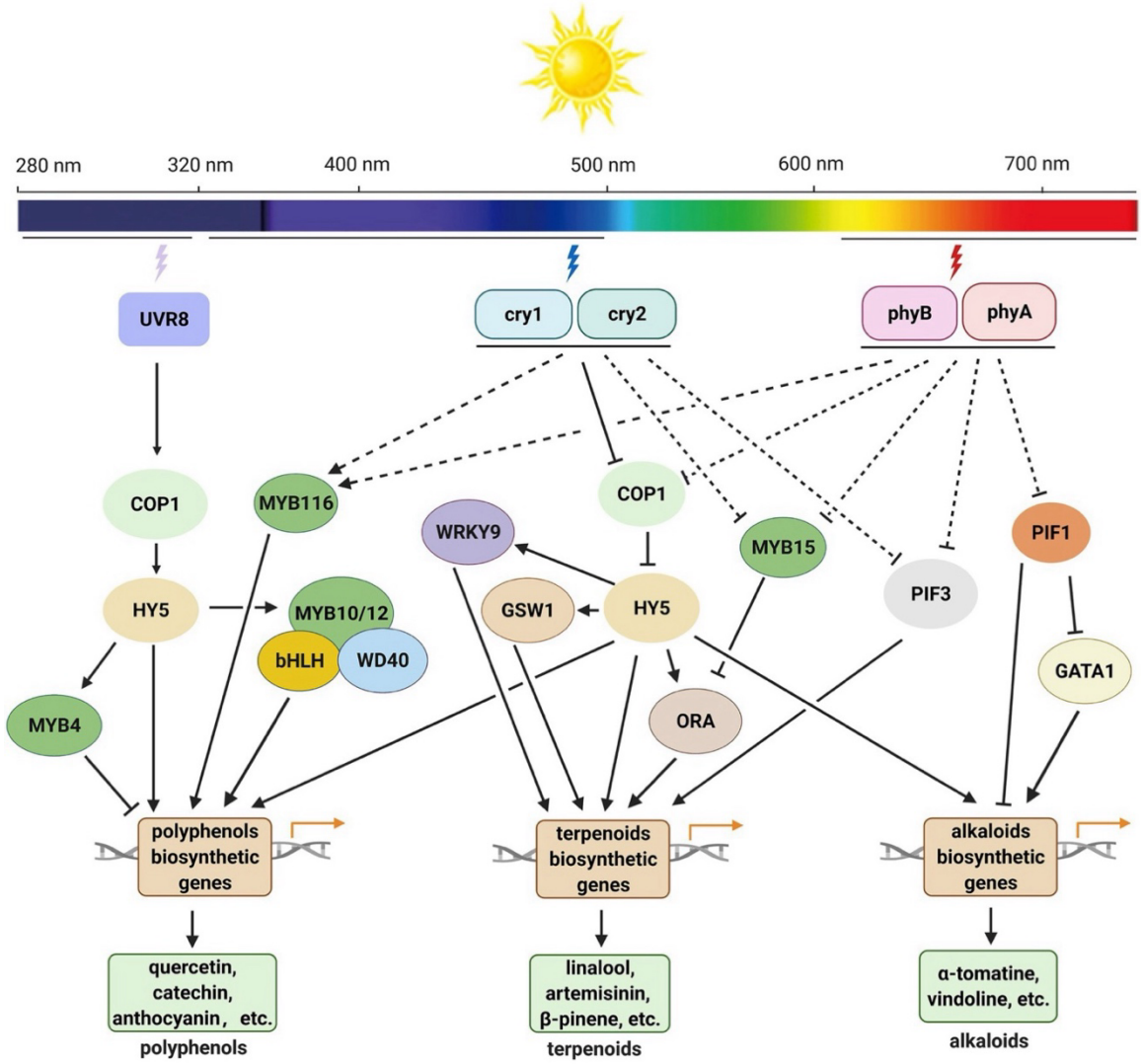

Figure 2-1. Light-mediated biosynthesis of polyphenols, terpenoids, and alkaloids in plants (Zhang et al., 2021).

For aroma compounds, light spectrum plays a critical role in modulating their biosynthesis. For example, research has demonstrated that supplemental red and blue LED increased the level of myristicin, a phenylpropanoid, in basil and dill (Litvin et al., 2020). The underlying mechanism of this regulation has not been fully understood, but likely involves the regulation of key enzymes in phenylpropanoid pathways, such as phenylalanine ammonialyase (PAL), 4-coumaroyl-CoA ligase (4CL), and chalcone

synthase (CHS), as shown in *Cyclocarya paliurus* (Liu, Fang, Yang, Shang, & Fu, 2018). Similarly, studies have suggested that both red and blue light promoted terpenoid accumulation in many plant species by affecting the expressions of genes involved in terpenoid biosynthesis (Takshak & Agrawal, 2019; D. Zhang, Sun, Shi, Wu, Zhang, & Xiang, 2018).

Light intensity is another factor influencing the synthesis of secondary metabolites. The total amount of photosynthetically active photons received by a specific area over an entire day, known as the daily light integral (DLI), has a significant impact on plant growth (Faust & Logan, 2018). High light intensity can increase stress, which impacts photosynthetic activity and may alter the biosynthesis of aroma compounds. For example, in tomatoes, increased light intensity has been shown to enhance the biosynthesis of phenolics and carotenoids (Ahmadi, Hao, & Tsao, 2018). In the context of aroma compounds, similar light-induced stress responses may influence enzymes that regulate the production of volatile organic compounds (VOCs) (Lefsrud, Kopsell, & Sams, 2008). However, the relationship between light intensity and aroma compound accumulation can vary largely depending on the plant species. For example, exposure to higher photosynthetic photon flux density (PPFD) has been found to increase carotenoid content in certain microgreens, but in *Orthosiphon stimaneus*, it resulted in reduced flavonoids and phenolic contents (Brazaitytė et al., 2015; Ibrahim & Jaafar, 2012).

Photoperiod, or the duration of light exposure, also affects secondary metabolite production, though the effects can be species-specific. For example, in wild cabbage, prolonged photoperiod increased the content of sinigrin (Charron & Sams, 2004). Photoperiod regulates circadian rhythm, help plants to adapt to seasonal variations, and

triggers key life cycle transitions, for example, dormancy or flowering (Creux & Harmer, 2019). While studies suggest that longer photoperiods are often associated with enhanced secondary metabolite production in some medicinal plants, there is no universal correlation between light duration and aroma compound biosynthesis (Alrifai et al., 2019).

2.6 Salinity and aroma compounds

Climate change presents many serious challenges to the agricultural and food system. In the United States, the production of fresh market crops has been declining annually since 2017, due to the negative influences of extreme heat and the shortages of irrigation water, particularly in California (Davis, Weber, Lucier, & Gallagher, 2022). In addition to impacting crop yield, climate change also affects various aspects of plant growth through environmental stressors, with salinity being a prominent factor.

Salinity can restrict water uptake by plants from the growth media, and it can also trigger oxidative stress by increasing the production of reactive oxygen species (ROS) (Ahmad, John, Sarwat, & Umar, 2008; Farooq et al., 2021). ROS includes free radicals and non-radicals that can harm cell membranes and damage cellular macromolecules (Anjum et al., 2017). The generation of ROS is commonly linked to the increased escape of electrons to oxygen in mitochondria or chloroplasts (Ahmad et al., 2008). Plant responses to salinity stress vary depending on the severity of the stress, and the plant response is usually species-specific (Aktsoglou et al., 2021).

The effect of salinity on the biosynthesis of aroma compounds, especially essential oils, has been widely studied in various culinary herbs and spices. For example, Aziz et al. (2008) evaluated the effect of salinity stress on three mint varieties and found that all three mint varieties showed decreased essential oils after being exposed to salt stress, although

the severity was different. In rosemary, salinity stress decreased the total essential oil yield, but increased the concentration of esters, hydrocarbon sesquiterpenes, and oxygenated sesquiterpenes (Sarmoum, Haid, Biche, Djazouli, Zebib, & Merah, 2019). Similar results were observed in fennel, an herb with partial salinity tolerance (Shafeiee & Ehsanzadeh, 2019). The major aroma compound *(E)*-anethole decreased, while several minor aroma compounds, include estragole, limonene, and fenchone showed increased level under salinity stress (Rebey, Rahali, Tounsi, Marzouk, & Ksouri, 2016). These finding suggested that salinity not only affect plant growth, but also the biosynthesis of secondary metabolites that contribute to herb flavor.

Salinity stress impacts the biosynthesis of secondary metabolites through several mechanisms. It is known to disrupt the balance of ions within plant cells, leading to metabolic shifts that can alter the biosynthesis of VOCs (Isayenkov & Maathuis, 2019). However, the response is complex, and in some species, salinity stress can enhance the concentration of certain secondary metabolites as part of a defense mechanism against stress (Corrado, Vitaglione, Chiaiese, & Rouphael, 2021). These secondary metabolites, such as terpenes and phenolic compounds, can act as antioxidants to reduce ROS damage caused by salinity stress (Yang & Guo, 2018). In addition, salinity stress influences biosynthetic pathways of secondary metabolites in plants. For example, genes related to carotenoids and flavonoids biosynthesis, such as phytoene synthase 2 (PSY2), phenylalanine ammonialyase (PAL), and chalcone synthase (CHS) were induced by NaCl, with increased production of *β*-carotene, lutein, and quercetin 3-*β*-d-glucoside in *Solanum nigrum* L. (Abdallah et al., 2016). These results suggests that moderate salinity levels could

be strategically applied to enhance the aroma profile of herbs, although the results might be highly species and condition dependent.

Among the environmental factors affecting the production of secondary metabolites, especially aroma compounds in fennel, light and salinity have been selected for further investigation in this dissertation. This is because that both factors have been reported to modulate the production of aroma compounds in several culinary herbs, such as basil, mint, and dill (Alrifai et al., 2019; Corrado et al., 2021; Massa, Kim, Wheeler, & Mitchell, 2008; Tsamaidi, Daferera, Karapanos, & Passam, 2017). Additionally, both light and salinity can be effectively implemented and regulated in controlled environment agriculture (CEA) systems, providing herb growers with valuable tools to optimize and refine the flavor and aroma profiles of their crops.

2.7 Analytical methods for aroma characterization

Aroma compounds play an important role in defining the quality of culinary herbs. These compounds are typically volatile or semi-volatile with low molecular weights (Bordiga & Nollet, 2019). Table 2-2 summarized previous studies on fennel aroma compounds and their analytical approaches. Generally speaking, analytical methods used to study the aroma compounds must meet a few requirements: first, they should capture compounds contributing to the overall flavor without neglecting any compounds; second, the experimental conditions should not change the key aroma compounds in the food matrix; third, non-volatile compounds that may interfere with separation or identification should be completely removed (Engel, Bahr, & Schieberle, 1999). The process of aroma analysis generally involves four steps: extraction, separation, identification, and quantification.

The extraction of aroma compounds, or VOCs, from a complex food matrix is the critical first step in aroma analysis. Main extraction methods that have been applied to fennel include steam distillation, hydrodistillation, solvent extraction, simultaneous distillation-extraction (SDE), supercritical fluid extraction (SFE), solvent assisted flavor evaporation (SAFE), and solid phase microextraction (SPME). The selection of extraction method typically depends on the specific objectives and feasibility of the study. Since many VOCs are present in low or trace concentration, the choice of extraction method and solvent also significantly affects the extraction results (Bordiga et al., 2019).

Table 2-2. Summary of previous studies on fennel aroma characterization

Sample	Method	References
Fennel seeds	Hydrodistillation, GC-MS	Miraldi, 1999
Sweet fennel seeds and tea	Solvent extraction, GC-FID, GC-MS	Bilia et al., 2002
Fennel seeds	SDE/SFE, GC-MS/O	Díaz-Maroto et al., 2005
Bitter fennel seeds and tea	SAFE, GC-MS/O, AEDA, SIDA	Zeller et al., 2006
Seeds of bitter and sweet fennel	Hydrodistillation, GC-MS	Coşge et al., 2008
Fennel seeds	Hydrodistillation, GC-MS	Saharkhiz et al., 2011
Florence fennel leaves	Hydrodistillation, GC-MS	Senatore et al., 2013
Fennel seeds	Steam distillation, GC-MS/O, AEDA	Xiao et al., 2017
Fennel seeds	SPME, GC-MS	Afifi et al., 2021

Traditional extraction methods such as hydrodistillation and solvent extraction are commonly used in early research on fennel aroma. However, hydrodistillation may alter the aroma profile due to the heat-induced artifacts, and solvent extraction often involves the use of harmful solvents (Augusto, Lopes, & Zini, 2003; Engel et al., 1999). Additionally, solvent extraction may cause interferences between volatile and non-volatile compounds. To minimize the formation of artifacts from high temperature in steam distillation, SAFE was developed. This method extracts VOCs under a mild temperature

by evaporating them at a mild temperature (such as 45°C) in an ultra-vacuum environment and then condensing them using liquid nitrogen (-196°C), thus removing any non-volatiles. While SAFE is the gold standard for avoiding artifact formation in flavor research, it requires expensive equipment and technical expertise (Schlumpberger, Stübner, & Steinhaus, 2022).

SPME is widely used due to its rapid analytical speed, high sensitivity, and ease of use. A coated fiber is placed directly in the headspace of a sample, where VOCs are absorbed into the fiber's coating. After reaching absorption equilibrium, the fiber is then inserted into gas chromatography and the VOCs are desorbed for further analysis (Bordiga et al., 2019). However, SPME has limitations, such as potential artifact formation due to the high temperature of injection port (Schlumpberger et al., 2022). Nevertheless, the goal of extraction is to obtain representative volatile data that can represent the true aroma profile.

Separation of aroma compounds is usually performed through gas chromatography (GC), according to the partitioning of volatile compounds between two phases, the mobile phase (such as helium gas) and the stationary phase (such as the coating inside GC column) (Bordiga et al., 2019). The compounds are separated in the GC column between the sample inlet and the detector, with an appropriate temperature program applied for better peak separation. While one-dimensional GC is the most common technique, more powerful alternatives such as two-dimensional GC×GC have also been employed in aroma analysis of culinary herbs to overcome the issue of co-elution (Petronilho, Maraschin, Delgadillo, Coimbra, & Rocha, 2011).

GC is often coupled with detectors for compound identification. Some of the commonly used detectors include the flame ionization detector (FID), which is cost-effective and mostly used for targeted analysis; and mass spectrometry (MS), which is ideal for comprehensive aroma profiling. By comparing the mass spectrum fragmentation pattern with the MS database, as well as comparing retention index (RI), the VOCs can be identified. Fennel contains a broad range of VOCs with different moieties, and their contributions to the overall aroma profile of fennel are not equally important. Thus, simply identifying VOC is not sufficient for fully understanding fennel's aroma profile.

Gas chromatography-olfactometry (GC-O) combines instrumental analysis with human sensory perception, allowing panelists to assess different VOCs at the sniffing port of GC-O as they elute from the GC column. This technique helps assign odor descriptors and intensity ratings to VOCs, providing a precise and descriptive analysis of aroma compounds (Song & Liu, 2018). To determine the contribution of individual VOCs, aroma extraction dilution analysis (AEDA) is often used. In this method, the sample is consecutively diluted until the odor of each compound is no longer detectable. The contribution of different compounds can be represented by their dilution factor, the highest dilution value when the compound is still detectable (Zellner, Dugo, Dugo, & Mondello, 2008).

For quantification, the peak area of each aroma compounds obtained from chromatography are compared to the peak area of standards. By establishing standard calibration curves using standard addition method and internal standards, the concentration of target compounds can be calculated based on the peak area ratio between the sample and internal standard (Bordiga et al., 2019). Internal standards are selected based on the polarity

of VOCs and the analytical technique. Stable isotope dilution analysis (SIDA) is often preferred in many flavor labs due to its high precision and accuracy (Bordiga et al., 2019). In SIDA, the internal standard is isotope-labeled, which allows for more accurate quantification as the internal standard and target analyte have similar chemical and physical behavior during ionization, therefore, the matrix effect can be reduced. Similarly, standard addition method (SAM) with nearly odorless samples can effectively minimize matrix effect. In addition, using *n*-alkanes and RI further enhances identification accuracy. The RI of a certain compound can be calculated through the equation described by van Den Dool and Kratz, where N represents the carbon number of lower alkane, n represents the difference in carbon number of the two alkanes next to the target analyte, t_{Ra}, t_{RN}, and $t_{R(N+n)}$ represent the retention time of unknown analyte, the lower alkane, and the upper alkane (van Den Dool & Dec. Kratz, 1963).

$$RI = 100N + 100n\frac{t_{Ra} - t_{R_N}}{t_{R_{(N+n)}} - t_{R_N}}$$

2.8 RNA sequencing and transcriptome analysis

With the rapid development of next-generation sequencing technologies and assembly algorithms over the past two decades, whole genome and whole transcriptome analysis have become standard practices in molecular biology studies (Wolf, 2013). Transcriptome refers to the full set of RNA transcripts produced in a specific cell or tissue type (Martin & Wang, 2011). RNA sequencing (RNA-seq) is an essential tool for characterizing species' transcriptome, generating large, complex datasets of gene expressions that offer valuable biological insights (Wolf, 2013). Figure 2-2 demonstrates the typical pipeline for RNA-seq analysis. This process begins with experimental design

and include key steps such as RNA extraction, quality control, read alignment, quantification of gene or transcript levels. These are followed by a multitude of bioinformatics analyses, such as differential expression analysis, co-expression network, and pathway enrichment analysis (Conesa et al., 2016; Han, Gao, Muegge, Zhang, & Zhou, 2015).

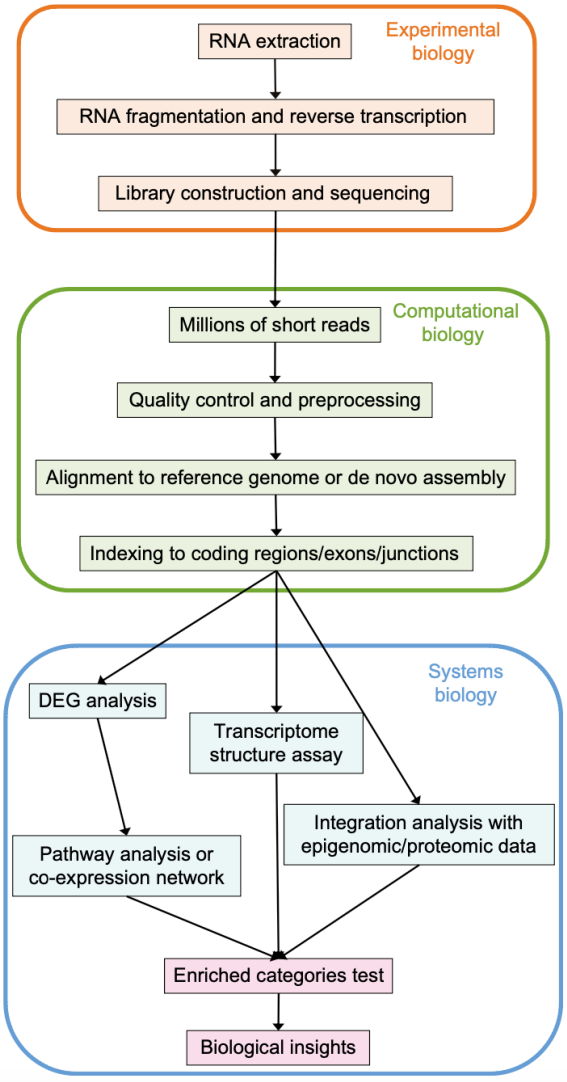

Figure 2-2. Overview of the typical RNA sequencing pipeline (Han et al., 2015).

In the experimental design phase, it is crucial to decide the appropriate library type, sequencing depth, and number of replicates to ensure the generated data can effectively

address the biological questions of interest (Conesa et al., 2016). RNA-seq library construction typically begins with the depletion of ribosomal RNA (rRNA) or the enrichment of messenger RNA (mRNA), as rRNA is highly abundant and needs to be removed (Shi, Zhou, Jia, Pan, Bai, & Ge, 2021). Poly(A) enrichment is commonly used to prepare RNA-seq libraries for plants (Zhu, Sanz-Jimenez, Ning, Tahir ul Qamar, & Chen, 2024). Paired-end sequencing is generally preferred over single-read sequencing for *de novo* transcript discovery, as it provides better transcript identification, especially when using longer reads (Garber, Grabherr, Guttman, & Trapnell, 2011). For hypothesis generation, 3 biological replicates may be sufficient for statistical analysis, but a more extensive experiment can require 6-12 replicates per treatment (Van den Berge et al., 2019). Composite sampling is frequently applied in plant studies, but attention should be given to tissue consistency and batch effects, as well as diurnal and circadian influences, since RNA-seq data is highly sensitive to biological variability and technical artifacts (Upton et al., 2023).

Obtaining high-quality RNA is critical for good sequencing results. However, isolating high-quality RNA can be challenging due to the presence of widespread RNA degrading enzymes (RNases) (Gayral, Weinert, Chiari, Tsagkogeorga, Ballenghien, & Galtier, 2011). Two commonly used methods for RNA extraction are TRIzol (phenol-chloroform extraction) and Qiagen kits (silica-gel-based column procedures) (Shi et al., 2021). These methods were primarily designed to extract long mRNAs. Following RNA extraction, RNA quality should be assessed using methods such as electrophoresis, a Bioanalyzer, or optical density (OD) measurement. RNA purity can be confirmed by

assessing the 260/280 ratio, with an OD260/280 >1.8 and a high OD260/230 ratio generally indicating acceptable RNA quality (Die & Román, 2012).

The next step of RNA-seq is preprocessing and quality control of raw sequencing reads. Although sequencing centers often perform this step, in-house data quality checks are also recommended (Upton et al., 2023). Read alignment can be performed using either a reference genome or *de novo* assembly methods. For fennel, while transcriptome data has been previously published (Palumbo, Vannozzi, Vitulo, Lucchin, & Barcaccia, 2018), a complete reference genome is not yet available. In this case, *de novo* transcriptome assembly using tools like Trinity (Grabherr et al., 2011) is an appropriate approach. This method involves reconstructing transcripts from raw reads (Wolf, 2013). Once alignment is finished, transcript expression levels across different samples can be quantified and summarized into an expression matrix for downstream analyses (Van den Berge et al., 2019).

To gain deeper insights into transcriptional profiles, a wide array of analytical approaches can be applied to expression matrix, including differential expression analysis, co-expression network analysis, and pathway enrichment analysis (Conesa et al., 2016). Differential expression helps understand plant plasticity under different environmental conditions, as well as the molecular mechanisms underlying plant responses to biotic and abiotic stress (Upton et al., 2023). Tools such as edgeR (Robinson, McCarthy, & Smyth, 2010) and DESeq2 (Love, Huber, & Anders, 2014) are commonly used to conduct robust differential analysis and identify differentially expressed genes (DEGs). By investigating the up- and down-regulated genes under stress, it helps to understand how genes involved in secondary metabolite biosynthesis pathways are affected and how plants cope with

stress. For example, genes associated with chitin response, response to abscisic acid, and regulation of jasmonic acid mediated signaling pathway were significantly upregulated in *Aeluropus littoralis* under high salinity stress (400 mM NaCl) (Younesi-Melerdi, Nematzadeh, Pakdin-Parizi, Bakhtiarizadeh, & Motahari, 2020).

Co-expression network analysis identifies clusters of genes with similar expression patterns across samples, providing insights into gene regulatory networks from large transcriptomic datasets (Zhang & Horvath, 2005). This approach can clarify the complex molecular mechanisms of secondary metabolism. For example, a linalool synthase, CsLIN, was identified through co-expression analysis, shedding light on the formation of characteristic aroma compounds in oolong tea (Zheng et al., 2022). Additionally, co-expression network analysis is suitable for time-series expression data and can provide insights into the dynamic co-regulation of genes (Wang, Waterman, & Huang, 2014).

Pathway enrichment analysis, which focuses on gene lists or gene sets (for example, DEGs or co-expressed genes), combines functional annotation through ontologies like Gene Ontology (GO) (Ashburner et al., 2000) and Kyoto Encyclopedia of Genes and Genomes (KEGG) (Kanehisa, Furumichi, Tanabe, Sato, & Morishima, 2017). For example, Yue et al. reported pathway enrichment analysis for investigating the molecular mechanism of floral scent formation and regulation in *Hedychium coronarium* and identified enzymes and their coding genes involved in flavor-related esters biosynthesis (Yue, Yu, & Fan, 2015).

In recent years, there has been a growing trend toward integrating metabolic and transcriptomic data to study complex biological processes (Cavill, Jennen, Kleinjans, & Briedé, 2016). This approach, while adding complexity to the analysis, provides a powerful

framework for studying aroma biosynthesis in fennel under different environmental conditions.

References

Afifi, S. M., El-Mahis, A., Heiss, A. G., & Farag, M. A. (2021). Gas chromatography–mass spectrometry-based classification of 12 fennel (*Foeniculum vulgare* Miller) varieties based on their aroma profiles and estragole levels as analyzed using chemometric tools. *ACS Omega*, *6*(8), 5775-5785. https://doi.org/10.1021/acsomega.0c06188.

Ahmad, P., John, R., Sarwat, M., & Umar, S. (2008). Responses of proline, lipid peroxidation and antioxidative enzymes in two varieties of *Pisum sativum* L. under salt stress. *International Journal of Plant Production*, *2*(4), 353-365. https://doi.org/10.22069/ijpp.2012.626.

Ahmadi, L., Hao, X. M., & Tsao, R. (2018). The effect of greenhouse covering materials on phytochemical composition and antioxidant capacity of tomato cultivars. *Journal of the Science of Food and Agriculture, 98*(12), 4427-4435. https://doi.org/10.1002/jsfa.8965.

Alrifai, O., Hao, X., Marcone, M. F., & Tsao, R. (2019). Current review of the modulatory effects of LED lights on photosynthesis of secondary metabolites and future perspectives of microgreen vegetables. *Journal of Agriculture and Food Chemistry, 67*(22), 6075-6090. https://doi.org/10.1021/acs.jafc.9b00819.

Anwar, F., Hussain, A. I., Sherazi, S. T. H., & Bhanger, M. I. (2009). Changes in composition and antioxidant and antimicrobial activities of essential oil of fennel (*Foeniculum vulgare* Mill.) fruit at different stages of maturity. *Journal of Herbs, Spices & Medicinal Plants, 15*(2), 187-202. https://doi.org/10.1080/10496470903139488.

Ashburner, M., Ball, C. A., Blake, J. A., Botstein, D., Butler, H., Cherry, J. M., Davis, A. P., Dolinski, K., Dwight, S. S., Eppig, J. T., Harris, M. A., Hill, D. P., Issel-Tarver, L., Kasarskis, A., Lewis, S., Matese, J. C., Richardson, J. E., Ringwald, M., & Rubin, G. M., & Sherlock, G. (2000). Gene Ontology: tool for the unification of biology. *Nature Genetics, 25*(1), 25-29. https://doi.org/10.1038/75556.

Augusto, F., Lopes, A. L., & Zini, C. A. (2003). Sampling and sample preparation for analysis of aromas and fragrances. *TrAC Trends in Analytical Chemistry, 22*(3), 160-169. https://doi.org/10.1016/S0165-9936(03)00304-2.

Badgujar, S. B., Patel, V. V., & Bandivdekar, A. H. (2014). *Foeniculum vulgare* Mill: a review of its botany, phytochemistry, pharmacology, contemporary application, and toxicology. *BioMed Research International*, 1, 842674. https://doi.org/10.1155/2014/842674.

Barman, M., Tenhaken, R., & Dötterl, S. (2023). A review on floral scents and pigments in cucurbits: their biosynthesis and role in flower visitor interactions. *Scientia Horticulturae*, *322*, 112402. https://doi.org/10.1016/j.scienta.2023.112402.

Barros, L., Carvalho, A. M., & Ferreira, I. C. F. R. (2010). The nutritional composition of fennel (*Foeniculum vulgare*): Shoots, leaves, stems and inflorescences. *LWT - Food Science and Technology, 43*(5), 814-818. https://doi.org/10.1016/j.lwt.2010.01.010.

Abdallah, S. B., Aung, B., Amyot, L., Lalin, I., Lachâal, M., Karray-Bouraoui, N., & Hannoufa, A. (2016). Salt stress (NaCl) affects plant growth and branch pathways

of carotenoid and flavonoid biosyntheses in Solanum nigrum. *Acta Physiologiae Plantarum, 38*(3), 72. https://doi.org/10.1007/s11738-016-2096-8.

Benke, K., & Tomkins, B. (2017). Future food-production systems: vertical farming and controlled-environment agriculture. *Sustainability: Science, Practice and Policy*, *13*(1), 13-26. https://doi.org/10.1080/15487733.2017.1394054.

Bilia, A. R., Flamini, G., Taglioli, V., Morelli, I., & Vincieri, F. F. (2002). GC-MS analysis of essential oil of some commercial Fennel teas. *Food Chemistry, 76*(3), 307-310. https://doi.org/10.1016/S0308-8146(01)00277-1.

Birenboim, M., Chalupowicz, D., Maurer, D., Barel, S., Chen, Y. R., Falik, E., Kengisbuch, D., & Shimshoni, J. A. (2022). Optimization of sweet basil harvest time and cultivar characterization using near-infrared spectroscopy, liquid and gas chromatography, and chemometric statistical methods. *Journal of the Science of Food and Agriculture, 102*(8), 3325-3335. https://doi.org/10.1002/jsfa.11679.

Bordiga, M., & Nollet, L. M. L. (2019). *Food aroma evolution: During food processing, cooking, and aging*. CRC Press. https://doi.org/10.1201/9780429441837.

Brazaitytė, A., Sakalauskienė, S., Samuolienė, G., Jankauskienė, J., Viršilė, A., Novičkovas, A., Sirtautas, R., Miliauskienė, J., Vaštakaitė, V., & Dabašinskas, L. & Duchovskis, P. (2015). The effects of LED illumination spectra and intensity on carotenoid content in Brassicaceae microgreens. *Food Chemistry*, *173*, 600-606. https://doi.org/10.1016/j.foodchem.2014.10.077.

Cavill, R., Jennen, D., Kleinjans, J., & Briedé, J. J. (2016). Transcriptomic and metabolomic data integration. *Briefings in bioinformatics, 17*(5), 891-901. https://doi.org/10.1093/bib/bbv090.

Charron, C. S., & Sams, C. E. (2004). Glucosinolate content and myrosinase activity in rapid-cycling Brassica oleracea grown in a controlled environment. *Journal of the American Society for Horticultural Science*, *129*(3), 321-330. https://doi.org/10.21273/Jashs.129.3.0321.

Chevallier, A. (2016). *Encyclopedia of herbal medicine: 550 herbs and remedies for common ailments*. Penguin.

Conesa, A., Madrigal, P., Tarazona, S., Gomez-Cabrero, D., Cervera, A., McPherson, A., Szcześniak, M. W., Gaffney, D. J., Elo, L. L., Zhang, X., & Mortazavi, A. (2016). A survey of best practices for RNA-seq data analysis. *Genome biology, 17*, 1-19. https://doi.org/10.1186/s13059-016-0881-8.

Corrado, G., Vitaglione, P., Chiaiese, P., & Rouphael, Y. (2021). Unraveling the modulation of controlled salinity stress on morphometric traits, mineral profile, and bioactive metabolome equilibrium in hydroponic basil. *Horticulturae, 7*(9), 273. https://doi.org/10.3390/horticulturae7090273.

Coşge, B., Kiralan, M., & Gürbüz, B. (2008). Characteristics of fatty acids and essential oil from sweet fennel (*Foeniculum vulgare* Mill. var. dulce) and bitter fennel fruits (*F. vulgare* Mill. var. vulgare) growing in Turkey. *Natural Product Research*, *22*(12), 1011-1016. https://doi.org/10.1080/14786410801980675.

Creux, N., & Harmer, S. (2019). Circadian rhythms in plants. *Cold Spring Harbor Perspectives in Biology, 11*(9), a034611. https://doi.org/10.1101/cshperspect.a034611.

DASD, Calicut & Spice Board India (2024). Major spice state wise area production 2023-24. Retrived October 15, 2024.

Davis, W. V., Weber, C., Lucier, G., & Gallagher, N. (2022). Vegetables and pulses outlook: April 2022. USDA Economic Research Service, No. (VGS-368). 71.

De-la-Cruz Chacón, I., Riley-Saldaña, C. A., & González-Esquinca, A. R. (2013). Secondary metabolites during early development in plants. *Phytochemistry Reviews, 12*(1), 47-64. https://doi.org/10.1007/s11101-012-9250-8.

Díaz-Maroto, M. C., Díaz-Maroto Hidalgo, I. J., Sánchez-Palomo, E., & Pérez-Coello, M. S. (2005). Volatile components and key odorants of fennel (*Foeniculum vulgare* Mill.) and thyme (*Thymus vulgaris* L.) oil extracts obtained by simultaneous distillation−extraction and supercritical fluid extraction. *Journal of Agricultural and Food Chemistry*, *53*(13), 5385-5389. https://doi.org/10.1021/jf050340.

Die, J. V., & Román, B. (2012). RNA quality assessment: a view from plant qPCR studies. *Journal of Experimental Botany*, *63*(17), 6069-6077. https://doi.org/10.1093/jxb/ers276.

Dimita, R., Min Allah, S., Luvisi, A., Greco, D., De Bellis, L., Accogli, R., Mininni, C., Negro, C. (2022). Volatile compounds and total phenolic content of perilla

frutescens at microgreens and mature stages. *Horticulturae, 8*(1), 71. https://doi.org/10.3390/horticulturae8010071.

Engel, W., Bahr, W., & Schieberle, P. (1999). Solvent assisted flavour evaporation – a new and versatile technique for the careful and direct isolation of aroma compounds from complex food matrices. *European Food Research and Technology, 209*(3), 237-241. https://doi.org/10.1007/s002170050486.

FAO (2022). Food and Agriculture Organization of the United Nations: Value of Agricultural Production. Retrived October 15, 2024, from https://www.fao.org/faostat/en/#data/QCL.

Farooq, M., Ahmad, R., Shahzad, M., Sajjad, Y., Hassan, A., Shah, M. M., Naz, S., Khan, S. A. (2021). Differential variations in total flavonoid content and antioxidant enzymes activities in pea under different salt and drought stresses. *Scientia Horticulturae, 287*, 110258. https://doi.org/10.1016/j.scienta.2021.110258.

Faust, J. E., & Logan, J. (2018). Daily light integral: A research review and high-resolution maps of the United States. *HortScience*, *53*(9), 1250-1257. https://doi.org/10.21273/HORTSCI13144-18.

Folta, K. M. (2019). Breeding new varieties for controlled environments. *Plant Biology*, *21*(S1), 6-12. https://doi.org/10.1111/plb.12914.

Garber, M., Grabherr, M. G., Guttman, M., & Trapnell, C. (2011). Computational methods for transcriptome annotation and quantification using RNA-seq. *Nature methods*, 8(6), 469-477. https://doi.org/10.1038/nmeth.1613.

Gayral, P., Weinert, L., Chiari, Y., Tsagkogeorga, G., Ballenghien, M., & Galtier, N. (2011). Next-generation sequencing of transcriptomes: a guide to RNA isolation in nonmodel animals. *Molecular ecology resources, 11*(4), 650-661. https://doi.org/10.1111/j.1755-0998.2011.03010.x.

Gibson, J., B. Whipker, and R. Cloyd. (2000). Success with container production of twelve herb species. North Carolina State University Cooperative Extension. Horticulture Information Leaflet 509.

Grabherr, M. G., Haas, B. J., Yassour, M., Levin, J. Z., Thompson, D. A., Amit, I., Adiconis, X., Fan, L., Raychowdhury, R., Zeng, Q., Chen, Z., Mauceli, E., Hacohen, N., Gnirke, A., Rhind, N., di Palma, F., Birren, B. W., Nusbaum, C., Lindblad-Toh, K., Friedman, N., & Regev, A. (2011). Full-length transcriptome assembly from RNA-Seq data without a reference genome. *Nature Biotechnology*, *29*(7), 644-652. https://doi.org/10.1038/nbt.1883.

Han, Y., Gao, S., Muegge, K., Zhang, W., & Zhou, B. (2015). Advanced applications of RNA sequencing and challenges. *Bioinformatics and Biology Insights, 9*(1), 29-46. https://doi.org/10.4137/BBI.S28991.

Herb Society of America (n.d.). Quick Fact Sheets: Fennel. Retrieved October 15, 2024, from https://www.herbsociety.org/hsa-learn/herb-information/hsa-quick-fact-sheets.html.

Huopalahti, R., & Linko, R. R. (1983). Composition and content of aroma compounds in dill, *Anethum graveolens* L., at three different growth stages. *Journal of*

Agricultural and Food Chemistry, 31(2), 331-333. https://doi.org/10.1021/jf00116a036.

Ibrahim, M. H., & Jaafar, H. Z. E. (2012). Primary, secondary metabolites, H_2O_2, malondialdehyde and photosynthetic responses of *Orthosiphon stimaneus* Benth. to different irradiance levels. *Molecules, 17*(2), 1159-1176. https://doi.org/10.3390/molecules17021159.

IPM Data (2000). Crop Profile for Fennel in California. National IPM Database. Retrived October 15, 2024, from https://ipmdata.ipmcenters.org/documents/cropprofiles/CAfennel.pdf.

Isayenkov, S. V., & Maathuis, F. J. M. (2019). Plant salinity stress: Many unanswered questions remain. *Frontiers in Plant Science*, *10*. https://doi.org/10.3389/fpls.2019.00080.

Jarmusch, S. A. (2015). *Ancient Pharmacology: Theophrastus' Historia Plantarum and Pliny the Elder's Historia Naturalis*. [Master's thesis, University of Liverpool].

Kanehisa, M., Furumichi, M., Tanabe, M., Sato, Y., & Morishima, K. (2017). KEGG: new perspectives on genomes, pathways, diseases and drugs. *Nucleic Acids Research, 45*(D1), D353-D361. https://doi.org/10.1093/nar/gkw1092.

Kooti, W., Moradi, M., Ali-Akbari, S., Sharafi-Ahvazi, N., Asadi-Samani, M., & Ashtary-Larky, D. (2015). Therapeutic and pharmacological potential of *Foeniculum vulgare* Mill: a review. *Journal of HerbMed Pharmacology*, 4(1), 1-9.

Lefsrud, M. G., Kopsell, D. A., & Sams, C. E. (2008). Irradiance from distinct wavelength light-emitting diodes affect secondary metabolites in kale. *HortScience, 43*(7), 2243-2244. https://doi.org/10.21273/Hortsci.43.7.2243.

Li, Y., Kong, D., Fu, Y., Sussman, M. R., & Wu, H. (2020). The effect of developmental and environmental factors on secondary metabolites in medicinal plants. *Plant Physiology and Biochemistry, 148*, 80-89. https://doi.org/10.1016/j.plaphy.2020.01.006.

Li, Y., Kong, D., Lin, X., Xie, Z., Bai, M., Huang, S., Nian, H., & Wu, H. (2016). Quality evaluation for essential oil of *Cinnamomum verum* leaves at different growth stages based on GC–MS, FTIR and microscopy. *Food Analytical Methods, 9*(1), 202-212. https://doi.org/10.1007/s12161-015-0187-6.

Litvin, A. G., Currey, C. J., & Wilson, L. A. (2020). Effects of supplemental light source on basil, dill, and parsley growth, morphology, aroma, and flavor. *Journal of the American Society for Horticultural Science, 145*(1), 18-29. https://doi.org/10.21273/JASHS04746-19.

Liu, Y., Fang, S., Yang, W., Shang, X., & Fu, X. (2018). Light quality affects flavonoid production and related gene expression in *Cyclocarya paliurus*. *Journal of Photochemistry and Photobiology B: Biology, 179*, 66-73. https://doi.org/10.1016/j.jphotobiol.2018.01.002.

Love, M. I., Huber, W., & Anders, S. (2014). Moderated estimation of fold change and dispersion for RNA-seq data with DESeq2. *Genome biology, 15*, 550. https://doi.org/10.1186/s13059-014-0550-8.

Martin, J. A., & Wang, Z. (2011). Next-generation transcriptome assembly. *Nature Reviews Genetics*, *12*(10), 671-682. https://doi.org/10.1038/nrg3068.

Massa, G. D., Kim, H.-H., Wheeler, R. M., & Mitchell, C. A. (2008). Plant productivity in response to LED lighting. *HortScience, 43*(7), 1951-1956. https://doi.org/10.21273/HORTSCI.43.7.1951.

Mehra, N., Tamta, G., & Nand, V. (2021). A review on nutritional value, phytochemical and pharmacological attributes of *Foeniculum vulgare* Mill. *Journal of Pharmacognosy and Phytochemistry, 10*(2), 1255-1263. https://doi.org/10.22271/phyto.2021.v10.i2q.13983.

Miraldi, E. (1999). Comparison of the essential oils from ten *Foeniculum vulgare* Miller samples of fruits of different origin. *Flavour and Fragrance Journal, 14*(6), 379-382. https://doi.org/10.1002/(SICI)1099-1026(199911/12)14:6<379::AID-FFJ833>3.0.CO;2-8.

Mittal, G. K., Shivran, A. C., Singh, D., Saxena, S. N., Rathore, S. S., Sharma, L. K., Singh, B. & Singh, B. (2016). Variation in essential oil constituents of fennel (*Foeniculum vulgare* Mill) varieties. *The International Journal of Seed Spices*, *6*(1), 74-77.

Niu, G., & Masabni, J. (2022). Chapter 9 - Hydroponics. In T. Kozai, G. Niu & J. Masabni (Eds.), *Plant Factory Basics, Applications and Advances* (pp. 153-166). Academic Press.

Noreen, S., Tufail, T., Badar Ul Ain, H., & Awuchi, C. G. (2023). Pharmacological, nutraceutical, functional and therapeutic properties of fennel (*Foeniculum*

vulgare). *International Journal of Food Properties, 26*(1), 915-927. https://doi.org/10.1080/10942912.2023.2192436.

Ohlrogge, J. B. (1994). Design of new plant products: Engineering of fatty acid metabolism. *Plant physiology, 104*(3), 821-826. https://doi.org/10.1104/pp.104.3.821.

Palumbo, F., Vannozzi, A., Vitulo, N., Lucchin, M., & Barcaccia, G. (2018). The leaf transcriptome of fennel (*Foeniculum vulgare* Mill.) enables characterization of the t-anethole pathway and the discovery of microsatellites and single-nucleotide variants. *Scientific Reports, 8*(1), 10459. https://doi.org/10.1038/s41598-018-28775-2.

Petronilho, S., Maraschin, M., Delgadillo, I., Coimbra, M. A., & Rocha, S. M. (2011). Sesquiterpenic composition of the inflorescences of Brazilian chamomile (*Matricaria recutita* L.): Impact of the agricultural practices. *Industrial Crops and Products, 34*(3), 1482-1490. https://doi.org/10.1016/j.indcrop.2011.05.005.

Rafieian, F., Amani, R., Rezaei, A., Karaça, A. C., & Jafari, S. M. (2024). Exploring fennel (*Foeniculum vulgare*): Composition, functional properties, potential health benefits, and safety. *Critical Reviews in Food Science and Nutrition*, *64*(20), 6924-6941. https://doi.org/10.1080/10408398.2023.2176817.

Rather, M. A., Dar, B. A., Sofi, S. N., Bhat, B. A., & Qurishi, M. A. (2016). *Foeniculum vulgare*: A comprehensive review of its traditional use, phytochemistry, pharmacology, and safety. *Arabian Journal of Chemistry*, *9*, S1574-S1583. https://doi.org/10.1016/j.arabjc.2012.04.011.

Rebey, I. B., Rahali, F. Z., Tounsi, M. S., Marzouk, B., & Ksouri, R. (2016). Variation in fatty acid and essential oil composition of sweet fennel (*Foeniculum vulgare* Mill) seeds as affected by salinity. *Journal of New Sciences*, 15.

Robinson, M. D., McCarthy, D. J., & Smyth, G. K. (2010). edgeR: a Bioconductor package for differential expression analysis of digital gene expression data. *Bioinformatics, 26*(1), 139-140. https://doi.org/10.1093/bioinformatics/btp616.

Saddiqi, H. A., & Iqbal, Z. (2011). Chapter 55 - Usage and Significance of Fennel (Foeniculum vulgare Mill.) Seeds in Eastern Medicine. In V. R. Preedy, R. R. Watson & V. B. Patel (Eds.), *Nuts and Seeds in Health and Disease Prevention* (pp. 461-467). Academic Press.

Saharkhiz, M. J., & Tarakeme, A. (2011). Essential oil content and composition of fennel (*Foeniculum vulgare* L.) fruits at different stages of development. *Journal of Essential Oil Bearing Plants, 14*(5), 605-609. https://doi.org/10.1080/0972060X.2011.10643978.

Sarmoum, R., Haid, S., Biche, M., Djazouli, Z., Zebib, B., & Merah, O. (2019). Effect of salinity and water stress on the essential oil components of rosemary (*Rosmarinus officinalis* L.). *Agronomy, 9*(5), 214. https://doi.org/10.3390/agronomy9050214.

Saxena, S., Agarwal, D., John, S., Dubey, P. N., & Lal, G. (2018). Analysis of fennel (*Foeniculum vulgare*) essential oil extracted from green leaves, seeds and dry straw. *International Journal Seed Spices, 8*(1), 60-64.

Sayed-Ahmad, B., Talou, T., Saad, Z., Hijazi, A., & Merah, O. (2017). The Apiaceae: Ethnomedicinal family as source for industrial uses. *Industrial Crops and Products, 109*, 661-671. https://doi.org/10.1016/j.indcrop.2017.09.027.

Schlumpberger, P., Stübner, C. A., & Steinhaus, M. (2022). Development and evaluation of an automated solvent-assisted flavour evaporation (aSAFE). *European Food Research and Technology, 248*(10), 2591-2602. https://doi.org/10.1007/s00217-022-04072-1.

Senatore, F., Oliviero, F., Scandolera, E., Taglialatela-Scafati, O., Roscigno, G., Zaccardelli, M., & De Falco, E. (2013). Chemical composition, antimicrobial and antioxidant activities of anethole-rich oil from leaves of selected varieties of fennel [*Foeniculum vulgare* Mill. ssp. vulgare var. azoricum (Mill.) Thell]. *Fitoterapia, 90*, 214-219. https://doi.org/10.1016/j.fitote.2013.07.021.

Shafeiee, M., & Ehsanzadeh, P. (2019). Physiological and biochemical mechanisms of salinity tolerance in several fennel genotypes: Existence of clearly-expressed genotypic variations. *Industrial Crops and Products, 132*, 311-318. https://doi.org/10.1016/j.indcrop.2019.02.042.

Shamshiri, R. R., Kalantari, F., Ting, K. C., Thorp, K. R., Hameed, I. A., Weltzien, C., Ahmad, D., & Shad, Z. M. (2018). Advances in greenhouse automation and controlled environment agriculture: A transition to plant factories and urban agriculture. *International Journal of Agricultural and Biological Engineering, 11*(1), 1-22. https://doi.org/10.25165/j.ijabe.20181101.3210.

Shi, H., Zhou, Y., Jia, E., Pan, M., Bai, Y., & Ge, Q. (2021). Bias in RNA-seq library preparation: current challenges and solutions. *BioMed Research International*, 6647597. https://doi.org/10.1155/2021/6647597.

Son, Y.-J., Park, J.-E., Kim, J., Yoo, G., & Nho, C. W. (2021). The changes in growth parameters, qualities, and chemical constituents of lemon balm (*Melissa officinalis* L.) cultivated in three different hydroponic systems. *Industrial Crops and Products, 163*, 113313. https://doi.org/10.1016/j.indcrop.2021.113313.

Song, H. L., & Liu, J. B. (2018). GC-O-MS technique and its applications in food flavor analysis. *Food Research International, 114*, 187-198. https://doi.org/10.1016/j.foodres.2018.07.037.

Souza, J. V. R. S., Ming, L. C., Santos, M. A. L., Simon, J. E., Juliani, H. R., & Saad, J. C. C. (2021). Effect of water regime and harvest stage on essential oil accumulation in basil plant growing in sandy soil. *Irrigation Science, 39*(4), 493-503. https://doi.org/10.1007/s00271-021-00719-1.

Takshak, S., & Agrawal, S. B. (2019). Defense potential of secondary metabolites in medicinal plants under UV-B stress. *Journal of Photochemistry and Photobiology B: Biology, 193*, 51-88. https://doi.org/10.1016/j.jphotobiol.2019.02.002.

Telci, I., Demirtas, I., & Sahin, A. (2009). Variation in plant properties and essential oil composition of sweet fennel (*Foeniculum vulgare* Mill.) fruits during stages of maturity. *Industrial Crops and Products, 30*(1), 126-130. https://doi.org/10.1016/j.indcrop.2009.02.010.

Tsamaidi, D., Daferera, D., Karapanos, I. C., & Passam, H. C. (2017). The effect of water deficiency and salinity on the growth and quality of fresh dill (*Anethum graveolens* L.) during autumn and spring cultivation. *International Journal of Plant Production, 11*(1), 33-46.

UN DESA (2024). The Sustainable Development Goals Report 2024. Retrieved October 17, 2024, from https://unstats.un.org/sdgs/files/report/2024/SG-SDG-Progress-Report-2024-advanced-unedited-version.pdf.

Upton, R. N., Correr, F. H., Lile, J., Reynolds, G. L., Falaschi, K., Cook, J. P., & Lachowiec, J. (2023). Design, execution, and interpretation of plant RNA-seq analyses. *Frontiers in Plant Science*, *14*, 1135455. https://doi.org/10.3389/fpls.2023.1135455.

USDA (2019). Census of horticultural specialties. Census of Agriculture. Retrieved October 15, 2024, from https://www.nass.usda.gov/Publications/AgCensus/2017/Online_Resources/Census_of_Horticulture_Specialties/index.php.

Valletta, A., Santamaria, A. R., & Pasqua, G. (2007). CPT accumulation in the fruit and during early phases of plant development in *Camptotheca acuminata* Decaisne (Nyssaceae). *Natural Product Research, 21*(14), 1248-1255. https://doi.org/10.1080/14786410701755482

Van den Berge, K., Hembach, K. M., Soneson, C., Tiberi, S., Clement, L., Love, M. I., Patro, R., & Robinson, M. D. (2019). RNA sequencing data: Hitchhiker's guide to

expression analysis. *Annual Review of Biomedical Data Science, 2*(1), 139-173. https://doi.org/10.1146/annurev-biodatasci-072018-021255.

van Den Dool, H., & Dec. Kratz, P. (1963). A generalization of the retention index system including linear temperature programmed gas—liquid partition chromatography. *Journal of Chromatography A, 11*, 463-471. https://doi.org/10.1016/S0021-9673(01)80947-X.

Verma, A. K., & Saxena, S. N. (2024). Fennel. In P. N. Ravindran, K. Sivaraman, S. Devasahayam & K. N. Babu (Eds.), *Handbook of Spices in India: 75 Years of Research and Development* (pp. 2349-2383). Springer Nature Singapore.

Vogt, T. (2010). Phenylpropanoid biosynthesis. *Molecular Plant, 3*(1), 2-20. https://doi.org/10.1093/mp/ssp106.

Vranová, E., Coman, D., & Gruissem, W. (2013). Network analysis of the MVA and MEP pathways for isoprenoid synthesis. *Annual Review of Plant Biology, 64*(1), 665-700. https://doi.org/10.1146/annurev-arplant-050312-120116.

Walters, K. J., & Currey, C. J. (2015). Hydroponic greenhouse basil production: comparing systems and cultivars. *HortTechnology, 25*(5), 645-650. https://doi.org/10.21273/Horttech.25.5.645.

Wang, Y. X. R., Waterman, M. S., & Huang, H. (2014). Gene coexpression measures in large heterogeneous samples using count statistics. *Proceedings of the National Academy of Sciences, 111*(46), 16371-16376. https://doi.org/10.1073/pnas.1417128111.

Wolf, J. B. W. (2013). Principles of transcriptome analysis and gene expression quantification: an RNA‐seq tutorial. *Molecular Ecology Resources*, *13*(4), 559-572. https://doi.org/10.1111/1755-0998.12109.

Xiao, Z., Chen, J., Niu, Y., & Chen, F. (2017). Characterization of the key odorants of fennel essential oils of different regions using GC–MS and GC–O combined with partial least squares regression. *Journal of Chromatography B, 1063*, 226-234. https://doi.org/10.1016/j.jchromb.2017.07.053.

Yang, L., Wen, K. S., Ruan, X., Zhao, Y. X., Wei, F., & Wang, Q. (2018). Response of plant secondary metabolites to environmental factors. *Molecules, 23*(4). https://doi.org/10.3390/molecules23040762.

Yang, Y., & Guo, Y. (2018). Elucidating the molecular mechanisms mediating plant salt-stress responses. *New Phytologist, 217*(2), 523-539. https://doi.org/10.1111/nph.14920.

Younesi-Melerdi, E., Nematzadeh, G.-A., Pakdin-Parizi, A., Bakhtiarizadeh, M. R., & Motahari, S. A. (2020). *De novo* RNA sequencing analysis of *Aeluropus littoralis* halophyte plant under salinity stress. *Scientific Reports, 10*(1), 9148. https://doi.org/10.1038/s41598-020-65947-5.

Yue, Y., Yu, R., & Fan, Y. (2015). Transcriptome profiling provides new insights into the formation of floral scent in *Hedychium coronarium*. *BMC Genomics, 16*, 470. https://doi.org/10.1186/s12864-015-1653-7.

Zayed, A., Sobeh, M., & Farag, M. A. (2022). Dissecting dietary and semisynthetic volatile phenylpropenes: A compile of their distribution, food properties, health

effects, metabolism and toxicities. *Critical Reviews in Food Science and Nutrition*, *63*(32), 11105-11124. https://doi.org/10.1080/10408398.2022.2087175.

Zeller, A., & Rychlik, M. (2006). Character impact odorants of fennel fruits and fennel tea. *Journal of Agricultural and Food Chemistry*, *54*(10), 3686-3692. https://doi.org/10.1021/jf052944j.

Zellner, B. A., Dugo, P., Dugo, G., & Mondello, L. (2008). Gas chromatography-olfactometry in food flavour analysis. *Journal of Chromatography A, 1186*(1-2), 123-143. https://doi.org/10.1016/j.chroma.2007.09.006.

Zhang, B., & Horvath, S. (2005). A general framework for weighted gene co-expression network analysis. *Statistical Applications In Genetics And Molecular Biology, 4*(17). https://doi.org/10.2202/1544-6115.1128.

Zhang, D., Sun, W., Shi, Y., Wu, L., Zhang, T., & Xiang, L. (2018). Red and blue light promote the accumulation of artemisinin in *Artemisia annua* L. *Molecules, 23*(6), 1329. https://doi.org/10.3390/molecules23061329.

Zhang, S., Zhang, L., Zou, H., Qiu, L., Zheng, Y., Yang, D., & Wang, Y. (2021). Effects of light on secondary metabolite biosynthesis in medicinal plants. *Frontiers in Plant Science, 12*, 781236. https://doi.org/10.3389/fpls.2021.781236.

Zheng, Y., Hu, Q., Wu, Z., Bi, W., Chen, B., Hao, Z., Wu, L., Ye, N., & Sun, Y. (2022). Volatile metabolomics and coexpression network analyses provide insight into the formation of the characteristic cultivar aroma of oolong tea (*Camellia sinensis*). *LWT, 164*, 113666. https://doi.org/10.1016/j.lwt.2022.113666.

Zhou, F., & Pichersky, E. (2020). More is better: the diversity of terpene metabolism in plants. *Current Opinion in Plant Biology, 55*, 1-10. https://doi.org/10.1016/j.pbi.2020.01.005.

Zhu, X.-T., Sanz-Jimenez, P., Ning, X.-T., Tahir ul Qamar, M., & Chen, L.-L. (2024). Direct RNA sequencing in plants: Practical applications and future perspectives. *Plant Communications*, 101064. https://doi.org/10.1016/j.xplc.2024.101064.

Zhu, Z., Chen, R., & Zhang, L. (2024). Simple phenylpropanoids: Recent advances in biological activities, biosynthetic pathways, and microbial production. *Natural Product Reports, 41*(1), 6-24. https://doi.org/10.1039/D3NP00012E.

Ziółkowska, P., Strzedulla, M., Śnit, M., Szczyra, D., & Kuźniewicz, R. (2024). The (un) known herb–fennel. *Herba Polonica*, 70(1), 57-65. https://doi.org/10.5604/01.3001.0054.4607.

Zrig, A., Tounekti, T., Elgawad, H., Hegab, M. M., Ali, S. O., & Khemira, H. (2016). Essential oils, amino acids and polyphenols changes in salt-stressed *Thymus vulgaris* exposed to open–field and shade enclosure. *Industrial Crops and Products, 91*, 223-230. https://doi.org/10.1016/j.indcrop.2016.07.012.

Chapter 3 Characterization of Key Aroma Compounds in Microgreens and Mature Plants of Hydroponic Fennel (*Foeniculum vulgare* Mill.)

This chapter has been published in *Food Research International* and reproduced here with minor modifications.

Author Details: Jingsi Liu[1], Song Li[2], Sean O'Keefe[1], Ken Hurley[1], Laban Rutto[3], Renee Eriksen[4], Yun Yin[1]

[1] Department of Food Science and Technology, Virginia Tech, Blacksburg, VA

[2] School of Plant and Environmental Sciences, Virginia Tech, Blacksburg, VA

[3] College of Agriculture, Virginia State University, Petersburg, VA

[4] Crop Improvement and Protection Research, USDA Agricultural Research Service, Salinas, CA

Abstract

Fennel is a popular culinary herb known for its unique flavor. In this study, we identified key aroma-active compounds in fresh fennel (*Foeniculum vulgare* Mill.) and its microgreens. Fennel was cultivated hydroponically with soilless substrates. Upon harvesting, samples were ground with liquid nitrogen, and headspace solid phase microextraction (SPME) gas chromatography-mass-spectrometry-olfactometry (GC-MS-O) was used for volatile analysis. Thirty-two and 28 key aroma-active compounds were identified in fennel microgreens and mature leaves, respectively. Phenylpropenes, especially *(E)*-anethole, were the predominant aroma-active compound in all samples (36.3-83.4%). Quantitation results showed that fennel microgreens contained a significantly higher amount of monoterpenes, showing an 81.4-98.1% increase when compared to mature fennel. Principal component analysis (PCA) of identified volatiles indicated a distinctive difference in the overall aroma profile between microgreens and mature leaf. The changes in aroma contents over different growth stages revealed the underlying volatile biosynthesis discrepancy. This study provided baseline information for understanding the aroma evolution from microgreen to mature fennel herbs.

Keywords

Leaf fennel, aroma characterization, gas chromatography-mass-spectrometry-olfactometry (GC-MS-O), secondary metabolites, phenylpropenes, monoterpenes

3.1 Introduction

The COVID-19 pandemic has shifted food preferences towards healthier and more sustainable choices (Skalkos & Kalyva, 2023; Timpanaro & Cascone, 2022). Driven by this change, there is a growing interest and consumer demand for high-quality fresh produce with potential health benefits (Celik & Dane, 2020; Filimonau et al., 2022; Maire et al., 2022). Diets rich in plant-derived foods have been shown to promote health by reducing the risk of chronic diseases (Wallace et al., 2020). Against this backdrop, new food sources such as microgreens are emerging as novel culinary ingredients with health-promoting functions (Choe, Yu, & Wang, 2018; Zhang et al, 2021).

Microgreens are young, tender greens produced from the seeds of herbs, vegetables, or grains (Xiao et al., 2012). Microgreens consist of the stem, seed leaves (cotyledons), and young true leaves. With a short production cycle, microgreens can be harvested 7 to 21 days after seed germination, depending on the species (Kyriacou et al., 2016). Microgreens production can be easily adopted into controlled environment agriculture (CEA) due to their short production cycle, and they are usually grown hydroponically (Zhang et al., 2021). CEA refers to a controlled plant production space where environmental factors such as light, nutrients, and temperature are precisely regulated (Folta, 2019; Kozai & Niu, 2016). CEA enables year-round production of fresh produce and supports the supply of local food. Hydroponic production has the advantages of reduced water usage and recycling of organic waste (Folta, 2019). Recent advances have shown that many culinary herbs, such as chives, dill (González-García et al., 2009), basil (Walters & Currey, 2015), and lemon balm (Son et al., 2021) adapt well to CEA and hydroponic production.

Studies have shown that microgreens have higher levels of bioactive phytochemicals than their mature counterparts, making them reliable sources of functional compounds (Choe et al., 2018). In other words, a small amount of microgreens may provide equal nutritional effects similar to a large quantity of mature plants. For example, compared to mature cilantro, cilantro microgreens contain a 10 times higher concentration of lutein and zeaxanthin, which are two major carotenoids that function as antioxidants and can prevent age-related eye disease (Xiao et al., 2012). Recently, microgreens of plants belonging to Brassicaceae, Apiaceae, and Lamiaceae families, have also been identified as excellent sources of dietary antioxidants, such as vitamin C and polyphenols (Ghoora, Haldipur, & Srividya, 2020).

Compared to numerous studies focusing on the nutritional value of microgreens, their aroma remains largely unexplored, despite the importance of aroma in sensory quality and food consumption. So far, the comparison of aroma compounds of microgreens and their mature counterpart has only been studied in a few species, such as cilantro (Oruña-Concha et al., 2018) and perilla mint (Dimita et al., 2022). Moreover, the differences in aroma compounds between herb microgreens and their mature plants are species-specific, and to date, no information is found for fennel.

Fennel (*Foeniculum vulgare* Mill.) is a widely used culinary herb native to the Mediterranean region. The plant contains many volatile compounds with industrial interest (Guillén & Manzanos, 1996; Valduga et al., 2019), and the aroma characteristics of mature fennel have been previously studied. Bilia *et al*. (2002) identified anethole and anisaldehyde as the main constituents of fennel tea essential oil using gas chromatography-mass spectrometry (GC-MS). Díaz-Maroto et al. (2005) characterized odor-active

compounds in dried fennel seeds with gas chromatography-mass spectrometry-olfactometry (GC-MS-O), finding *(E)*-anethole, estragole, fenchone, and 1-octen-3-ol as the most intense aroma compounds. Zeller and Rychlik (2006) conducted aroma extract dilution analysis (AEDA) on fennel seeds and tea, identifying *(E)*-Anethole, estragole, and fenchone as the compounds with the highest odor activity value (OAV). Saharkhiz and Tarakeme (2011) found that the essential oil content of fennel seeds varies largely with ripening stage. Xiao et al. (2017) identified seven sensory terms correlated to aroma constitutes in fennel essential oil through GC-MS-O. Most recently, Afifi *et al.* (2021) analyzed the volatile composition of fennel seeds from 12 varieties using solid phase microextraction (SPME), though GC-O or detailed volatile quantitation was not conducted.

Notably, most previous studies have focused primarily on fennel seeds rather than fresh leaves. Barros *et al.* (2010) analyzed the nutritional composition of different fennel parts (shoots, leaves, stems, and inflorescences), but did not evaluate volatile compounds. Fennel seeds were found to exhibit low to moderate antioxidant capacity due to phenolic compounds (Lu et al., 2011). In contrast, fennel microgreens have been shown to possess high antioxidant capacities (Ghoora et al., 2020) and nutritional potential (Uher et al., 2023), yet their aroma profile remains uncharacterized.

Our research aims to fill this gap by identifying and comparing the key aroma compounds in hydroponically grown fennel microgreens and mature plants using SPME-GC-MS-O, multiple internal standards, and the standard addition method. These techniques minimize matrix effects and ensure accurate quantitation (Penton, 1999). This approach has demonstrated good precision and accuracy for the quantitation of volatile aroma compounds in different food samples (Zhang et al., 2015; Fortini et al., 2017; Su &

Yin, 2021). Understanding the differences in these important secondary metabolites during plant growth can enhance the quality of hydroponic fennel, helping herb growers determine the optimal harvest time.

3.2 Materials and method

3.2.1 Plant materials and growth conditions

Fennel (*Foeniculum vulgare* Mill., cv. Grosfruchtiger) seeds were purchased from Johnny's Selected Seeds (Winslow, ME). Seeds were sown into rockwool propagation cubes saturated with water in a germination tray. The trays were placed in a glass-glazed greenhouse in Blacksburg, VA (lat. 37.2°N) and the plant growth experiment lasted from October to December 2022. Seedlings were irrigated daily with water and allowed to grow for 3 weeks before being transplanted to an NFT hydroponic system (NFT0406, CropKing, Lodi, OH). Fennel microgreens were harvested 3 weeks after seed germination. The rest of the seedlings from the same batch were transplanted into NFT hydroponic systems, which included nutrient solution supplemented with 2-1-6 and 5-0-1 (nitrogen-phosphate potash) liquid fertilizers (FloralGro and FloraMicro, General Hydroponics, Sebastopol, CA).

To investigate the changes in key aroma compounds of fennel plants during the vegetative growth stage, twelve mature fennel plants were destructively harvested at 8, 9, and 10 weeks after seed germination. During the plant material collection, data on plant height, growth index (GI), fresh biomass, number of branches, and apparent moisture content were also collected. Plant height was measured perpendicularly from the surface of the growing substrate to the tallest point of the canopy. Growth index was calculated using the formula $GI = \frac{W1+W2}{H}$, , where W1 and W2 represent two perpendicular canopy widths, and H represents plant height. Fresh biomass was recorded as the fresh weight of

aerial parts of the plant upon harvesting. Number of branches was recorded as the total count of branches originating from fully expanded nodes. Apparent moisture content (AMC) was determined by placing a specific amount of fresh tissue in a forced-air oven at 105°C for 2 hours (Ahn et al., 2014), recording the dry weight, and calculating using the formula $AMC = \frac{Fresh\ weight - Dry\ weight}{Fresh\ weight} \times 100\%$. Growth parameters were measured for all twelve plants, and six plants (three from hydroponic system 1 and three from hydroponic system 2) were used for aroma characterization by GC-MS. For microgreens, three replicates from germination tray 1 and three replicates from germination tray 2 were analyzed by GC-MS. Immediately after harvesting, the fennel samples were stored at -80°C until further analysis.

During the growth experiment, the day and night temperature of greenhouse were set to 24°C and 21°C, respectively. The greenhouse temperature was maintained with an environmental controller (Step Control, Wadsworth Control Systems, Arvada, CO). The temperature and humidity were recorded at 5 min intervals by a data logger (Watchdog 1650 Micro Station, Spectrum Technologies, Aurora, IL). Light was measured with a quantum PAR light sensor (3668I, Spectrum Technologies, Aurora, IL) in a radiation shield (3663A, Spectrum Technologies, Aurora, IL). The greenhouse environmental conditions, such as average daylight hours, daily light integral (DLI), maximum and minimum greenhouse temperature, and humidity were shown in Supplemental Table 3-1.

The pH and electrical conductivity (EC) of each NFT unit were monitored daily, and pH of the nutrient solution was maintained at the range of 5.8-6.2 while EC was maintained at the range of 1.4-1.6 $dS \cdot m^{-1}$ with a portable pH/EC meter (HI98131, HANNA Instruments, Smithfield, RI). The pH was adjusted with phosphoric and citric acid (pH

Down, General Hydroponics, Sebastopol, CA) and potassium hydroxide and potassium carbonate (pH Up, General Hydroponics, Sebastopol, CA). EC was adjusted with deionized water and 2-1-6 and 5-0-1 liquid fertilizers.

3.2.2 Chemicals and standards

The chemicals and authentic standards are purchased from the following companies: α-Pinene (98%), α-phellandrene (≥75%), 1-octen-3-ol (≥98%), anisketone (≥97%), β-ionone (96%), 3-octanol acetate (≥98%), *(Z)*-3-hexen-1-ol (≥98%), carvacrol (≥99%), γ-terpinene (≥95%), (±)-camphor (≥95.5), estragole (≥96%), fenchyl acetate (≥96%, mix of α- and β- isomers), *p*-cymenene (≥98%), *p*-anisaldehyde (≥97.5%), phenyl acetaldehyde (≥95%), *p*-propyl-anisole (≥99%), methyl eugenol (≥98%), linalool (≥97%), myristicin (≥97%), *(E)*-anethole (≥99%), decane (≥99.8%), 2-octanol (≥97%), 1-phenylethanol (98%), and *n*-alkanes (C_7-C_{30}) were purchased from Sigma-Aldrich (St. Louis, MO). *(Z)*-3-Hexenal (50% in triacetin) and *(E)*-2-hexenal (98%) were provided by Bedoukian Research Inc. (Danbury, CT). Tridecane (>99%) and 4-methoxycinnamaldehyde (>97%) were purchased from Tokyo Chemical Industry Co., Ltd. America (Portland, OR). (-)-Bornyl acetate (95%) was purchased from Alfa Aesar (Haverhill, MA). *(Z)*-Anethole was purchased from Toronto Research Chemicals (Toronto, Canada) and methanol (HPLC grade, 99.9%) was purchased from Fisher Scientific (Fair Lawn, NJ).

3.2.3 Aroma compound extraction by solid phase micro extraction (SPME)

Frozen fennel leaves were ground with a mortar and a pestle in liquid nitrogen to fine powders. Fennel powder (50 ± 0.5 mg) was weighed in a 20 mL clear and odorless

vial (Supelco, Bellefonte, PA), spiked with 1 μL internal standard (IS) and then sealed with a PTFE lined screw cap (Supelco, Bellefonte, PA). Specifically, the internal standard solution consisted of 36.4 ng/μL decane, 4.8 ng/μL 2-octanol, and 99.0 ng/μL 1-phenylethanol dissolved in methanol. The IS were selected based on the following principles (McNair, Miller, & Snow, 2019; Xia et al., 2023): (1) the IS are not present in fennel samples; (2) they are stable and do not interfere with any sample components; (3) the peak of IS does not overlay with peak of any compounds of interest. The vial containing sample was then kept in the autosampler agitator for 10 min at 50°C with a stirring speed of 250 rpm so that the headspace was equilibrated. After equilibration, a 1 cm 50/30 divinylbenzene/carboxen/polydimethylsiloxane (DVB/CAR/PDMS) fiber (Supelco, Bellefonte, PA) was exposed to the headspace of the vial for 30 min at 50°C with a stirring speed of 250 rpm to extract the volatile compounds. The SPME-GC-MS measurement was performed in six replicates for each harvest time, with each replicate containing leaf tissue from different fennel plants.

3.2.4 Gas chromatography-mass spectrometry-olfactometry (GC-MS-O)

The system consisted of an Agilent 6890N GC (Santa Clara, CA) equipped with a DB-WAX capillary column (30 m × 0.25 mm i.d., film thickness = 0.25 μm) (Supelco, Bellefonte, PA), a 5975B mass selective detector (MSD) (Agilent Technologies Inc., Santa Clara, CA) and a PHASER sniff port (GL Sciences, Eindhoven, the Netherlands). The injection port was held at 230°C in splitless mode and the column temperature was programmed as follows: 5min at 40°C, followed by a temperature increase at 8°C/min to 80°C, 5°C/min to 152°C, 8°C/min to 225°C, and hold 15min at 225°C. The carrier gas was helium at the flow rate of 2 mL/min (67.9 cm/s). The interface temperature of MSD is

230°C; the ionization energy was 70 eV; the mass range was 33-500 amu; the EM voltage was Atune + 200V; and the scan rate was 5.15 scans/s. Column effluent was split 1:1 between sniff port and MSD using the 0.25 mm i.d. deactivated capillary column. The sniff port temperature was 230°C and the eluting volatile compounds were combined with humidified air at the flow rate of 5 mL/min.

GC-O of fennel samples was performed by three trained panelists (two females, one male, aged between 20 and 27 years old). Each panelist participated in three training sessions where they sniffed pure standards of common aroma compounds found in fennel through the sniff port. The purpose of training was for panelists to recognize and describe different aroma attributes of odorants (Jonas & Schieberle, 2021). For each sample, panelists recorded retention time, aroma descriptors, and aroma intensity of each perceived odorant. Panelists rated the intensity of odorant on a five-point scale: very weak (1), weak (2), medium (3), strong (4), and very strong (5). A volatile compound is considered aroma-active if only (1) two or more panelists smelled the compounds; (2) only one panelist smelled the aroma compound, the odor intensity was weak or above. The results of three panelists were averaged. The fennel samples used for GC-O were not spiked with IS.

3.2.5 Identification of aroma-active compounds

Aroma-active compounds were first selected based on the results of GC-O. These compounds were then identified by: (1) matching electron-impact (EI) mass spectra with NIST Mass Spectral Library (NIST 17), (2) matching retention indices on the polar GC column with previous references, (3) matching odor characteristics with authentic standards. Retention indices were calculated based on the equation described by a previous

publication (van Den Dool & Kratz, 1963) with the retention time of a C_7-C_{30} alkane solution.

3.2.6 Quantitation of aroma-active compounds with standard addition method

The quantitation of identified aroma-active compounds was performed by GC-MS with standard addition method. Fennel powder (50 ± 0.5 mg) was spiked with IS (1 μL, containing 36.4 ng/μL decane, 4.8 ng/μL 2-octanol, and 99.0 ng/μL 1-phenylethanol) and the aroma compounds were extracted by SPME as described in section 2.3. To build a calibration curve of each aroma-active compound, a known concentration of authentic standards of aroma-active compounds were first mixed and dissolved in methanol, and then the stock solution was stepwise diluted to levels of known concentrations. Levels of standards mixture solution (1 μL) were added to an "odorless" or "blank" fennel powder, which was achieved by incubating the sample under 50°C for about 15 hours with regular nitrogen purge of the headspace (Su & Yin, 2021). The "blank" state of fennel powder was confirmed when GC-MS peaks were negligible. The "odorless" fennel powder was also spiked with the same amount of IS (1 μL, containing 36.4 ng/μL decane, 4.8 ng/μL 2-octanol, and 99.0 ng/μL 1-phenylethanol). The regression equation was constructed based on the peak area ratio and mass ratio of a target aroma-active compound and its internal standard (McNair et al., 2019). At each dilution point, GC-MS was performed in duplicate.

The aroma-active compounds were divided into three major groups against particular IS applied. For each group, the IS has similar molecular structure and/or chemical formula to the target analytes. For the compounds using decane as the IS, the stock solution contained 7.16 μg/μL *α*-pinene, 24.23 μg/μL *α*-phellandrene, 9.88 μg/μL *γ*-terpinene, 0.38 μg/μL tridecane, and 1.67 μg/μL *p*-cymenene. The stock solution was then

diluted with methanol at 1:2, 1:4, 1:20, 1:200, and 1:400 ratios. For the compounds using 2-octanol as the IS, the stock solution contained 3.33 µg/µL *(E)*-2-hexenal, 0.42 µg/µL *(Z)*-3-hexen-1-ol, 0.08 µg/µL 1-octen-3-ol, 0.17 µg/µL linalool, 0.20 µg/µL phenyl acetaldehyde, 2.18 µg/µL *p*-anisaldehyde, and 0.10 µg/µL 4-methoxycinnamaldehyde. The stock solution was, likewise, diluted with methanol at 1:2, 1:4, 1:20, 1:200, and 1:400 ratios. For the compounds using 1-phenylethanol as the IS, the stock solution contained 2.39 µg/µL camphor, 3.76 µg/µL bornyl acetate, 1.46 µg/µL carvacrol, 0.08 µg/µL 3-octanol acetate, 0.36 µg/µL *p*-propyl-anisole, 14.27 µg/µL methyl eugenol, and 1.56 µg/µL anisketone. It was diluted with methanol at 1:2, 1:4, 1:20, 1:200, 1:400, and 1:4000 ratios.

The following standards were run individually with IS because their authentic standards contained isomers: the concentration of stock solution of 3-hexenal, fenchyl acetate, and *β*-ionone are 0.08 µg/µL, 28.22 µg/µL, and 3.19 µg/µL, respectively. *(E)*-Anethole and estragole were also run individually with IS due to their high concentrations in fennel samples. The stock solution concentration of *(E)*-anethole and estragole was 294.03 µg/µL and 76.05 µg/µL, respectively. *(Z)*-Anethole and myristicin were run individually with IS because their authentic standards came in small quantity (50 mg and 10 mg, respectively) and the total volume of their stock solution was lower than other standards mixtures. For *(Z)*-anethole, the concentration of stock solution is 10.67 µg/µL and for myristicin, the concentration of stock solution is 0.78 µg/µL. The above-mentioned stock solutions were diluted with methanol at 1:2, 1:4, 1:20, 1:200, and 1:400 ratios. For compounds without authentic standards, compounds with similar chemical structures were used to build the calibration curve (Su & Yin, 2021; Wei et al., 2018). Specifically, allo-

ocimine, γ-muurolene, germacrene D, and α-cadinene were quantified against *p*-cymenene; methyl isoeugenol and apiol were quantified against methyl eugenol.

The quantitation capability of each calibration curve was validated with limit of detection (LOD) and limit of quantitation (LOQ) based on the lowest concentration point of each calibration curve. The equations for the calculation of LOD and LOQ are as follows (MacDougall et al., 1980; Su & Yin, 2021), where SD is the standard deviation of the response and b is the slope of calibration curve:

$$LOD = \frac{3SD}{b}$$

$$LOQ = \frac{10SD}{b}$$

3.2.7 Calculation of odor activity value (OAV)

The odor activity value was calculated by dividing the concentration of aroma-active compounds in fennel samples and their previous published odor detection threshold in water (Erten & Cadwallader, 2017).

3.2.8 Statistical analysis

Concentration of aroma-active compounds in fennel microgreens and mature plants were compared by one-way analysis of variance (ANOVA) based on Tukey's honest significant difference (HSD) test for post hoc comparisons using JMP (JMP® Pro 16.0.0). The significance level was set at $p<0.05$. For multivariate analysis, principal component analysis (PCA) was conducted to reduce the dimensionality of data and to identify patterns in the overall variances in key aroma compounds across different harvest stages. In addition, a heatmap with hierarchical clustering was generated using the pheatmap package

(Kolde & Kolde, 2015) in R (version 4.3.1) to visualize the relative concentration of the key aroma compounds in samples harvested at different growth stages. The dendrogram in the heatmap was constructed based on Ward's method and Euclidean distances as the similarity measure.

3.3 Results and discussion

3.3.1 Growth and morphological evaluation

The plant growth and morphological data is shown in Table 3-1. The apparent moisture content was similar between microgreens and earlier harvested mature fennel, but decreased in week 10 samples, in addition to significant increases in plant height, number of branches, and fresh biomass. Plant fresh biomass and the number of branches on each plant gradually increased with growth period. Notably, the average fresh biomass of week 10 sample (43.60 g/plant) is nearly three times as the week 9 sample (15.21 g/plant), suggesting drastic vegetative growth during this period. The fresh biomass of hydroponic fennel is comparable to that of field-grown fennel. According to Moosavi et. al (2015), the fresh biomass of field-grown fennel ranged from 4.27g/plant to 48.31g/plant, depending on plant density in the field and sowing date. Plant height was relatively consistent for mature fennel ranging from week 8 to week 9, with a small increase at week 10. However, the growth index of fennel exhibited a clear increase trend during late harvest, which indicated that greater growth changes on branches length and width, instead of plant heigh, were happening for later harvested samples. At week 10, we also observed a larger standard deviation in all growth parameters, suggesting there were larger variances due to differences in growth conditions. Nevertheless, positive plant growth data suggested the

fennel cultivar (Grosfruchtiger) used in this study was well suited to hydroponic cultivation and produced good yield.

Table 3-1. Morphological and growth data of fennel at different growth stages

	Microgreen	Mature Herbs		
Weeks after germination	3	8	9	10
Apparent moisture content (%)	88.66±0.78[a]	90.24±1.00[a]	88.95±0.35[a]	83.03±2.69[b]
Fresh biomass (g)	0.06±0.02[d]	7.76±2.45[c]	15.21±4.46[b]	43.60±19.79[a]
Number of branches	2.96±0.27[c]	6.58±0.51[b]	9.00±1.76[b]	12.83±6.01[a]
Height (cm)	5.56±1.11[c]	20.35±3.19[b]	19.02±3.57[b]	22.75±6.55[a]
Growth index	1.35±0.43[b]	1.24±0.19[b]	1.73±0.30[a]	2.14±0.72[a]

[abcd] represent the mean separation between harvest time by Tukey's HSD at $p < 0.05$. The results are expressed as mean ± SD.

3.3.2 Aroma-active compounds in fennel microgreens and mature plants

The aroma-active compounds found in fennel microgreens and mature plants, the identification methods, their odor descriptors, and the intensity are shown in Table 3-2. A total of 35 aroma-active compounds were identified in fennel microgreens and mature plants, including 5 monoterpenes, 3 sesquiterpenes, 1 alkane, 3 alcohols, 5 aldehydes, 4 monoterpenoids, 1 ester, 2 ketones, 8 phenylpropenes, and 3 unknown compounds that cannot be identified by GC-MS due to invisible peaks. The peaks not identified by GC-MS were below the detection limit of mass spectrometer but above the human sensory threshold. The number of identified aroma-active compounds is similar to previous studies focusing on fennel. Twenty-seven and 30 aroma compounds were identified by GC-MS-O from fennel seeds (Díaz-Maroto et al., 2005) and commercial fennel essential oils (Xiao et al., 2017), respectively. However, in both studies, volatile compounds were extracted using either simultaneous distillation extraction (SDE) or supercritical fluid extraction (SFE)

instead of SPME. In our study, fourteen compounds, namely *p*-cymenene, *γ*-muurolene, germacrene D, *α*-cadinene, tridecane, *(E)*-2-hexenal, phenyl acetaldehyde, 4-methoxycinnamaldehyde, bornyl acetate, carvacrol, 3-octanol acetate, *p*-propyl-anisole, methyl eugenol, and apiol, were first identified as aroma-active compounds by GC-MS-O in fennel.

Fennel microgreens contained more aroma-active compounds compared to mature leaves. Thirty-two aroma compounds were identified in fennel microgreens, while 23, 23, and 28 aroma-active compounds were identified in mature fennel harvested at week 8, 9, 10, respectively. *(E)*-Anethole was the most potent and characteristics aroma-active compound among all samples, with a strong and distinct sweet, anise aroma. *(E)*-Anethole was also reported by previous work as the main aroma constituent of fennel tea and fennel seeds (Díaz-Maroto et al., 2005; Zeller et al., 2006). Due to its sweet, anise-like aroma, *(E)*-anethole is commonly used in the cosmetics and food industries (Wang et al., 2020). In addition, *(E)*-anethole has been reported to have several bioactive functions, such as antioxidant and antibacterial activities (Senatore et al., 2013). In a recent study, *(E)*-anethole was added to the emitting sachets inside the packages of ready-to-eat lettuce, and the results showed that the added *(E)*-anethole reduced discoloration and improved overall freshness and odor of lettuce (Wieczyńska & Cavoski, 2018). *p*-Cymenene and myristicin were only identified in fennel microgreens. *p*-Cymenene exhibited a medium woody, terpenic aroma, and myristicin exhibited a weak woody, spicy aroma. Allo-ocimene and anisketone were only identified in early harvest of mature fennel. Allo-ocimene exhibited a medium to strong herbal, terpenic aroma and anisketone exhibited a weak licorice, sweet aroma. 3-Octanol acetate was only detected in week 10 fennel with a medium woody,

herbal aroma. Six aroma compounds had a stronger intensity in mature fennel, namely *α*-pinene (pine, woody), γ-muurolene (spice, woody), germacrene D (spice, clove), 1-octen-3-ol (earthy, mushroom), *(E)*-2-hexenal (leafy, green), and *β*-ionone (floral, sweet). On the other hand, carvacrol (herbal, oregano) showed a stronger odor intensity in fennel microgreens compared with mature fennel. While the differences in aroma profiles observed across different stages of fresh fennel are evident, it remains uncertain whether these differences are perceptible to consumers. A future sensory study may be necessary to validate the differences, although this is beyond the scope of the current investigation.

Table 3-2. Aroma-active compounds identified in fennel microgreens and mature plants

no.	Compound	IS	RI	RI Ref. [a]	Identification Method [b]	Odor Description	Odor Intensity [c]			
							Week 3	Week 8	Week 9	Week10
	Monoterpenes									
1	*α*-pinene	decane	1011	1011	MS, RI, OD, AS	Pine, woody	W	M	W	M
2	*α*-phellandrene	decane	1153	1157	MS, RI, OD, AS	Herbal, woody	M	M	W	M
3	*γ*-terpinene	decane	1239	1233	MS, RI, OD, AS	Oily, herbal	M	W	W	M
4	allo-ocimene	decane	1371	1366	MS, RI, OD	Herbal, terpenic		S	M	
5	*p*-cymenene	decane	1435	1435	MS, RI, OD	Woody, terpenic	M			
	Sesquiterpenes									
6	*γ*-muurolene	decane	1697	1690	MS, RI, OD	Spice, woody	W	W	M	S
7	germacrene D	decane	1719	1717	MS, RI, OD	Spice, clove	W	M	M	S
8	*α*-cadinene	decane	1816	1815	MS, RI, OD	Woody, fresh	M	M	M	M
	Alkane									
9	tridecane	decane	1303	1300	MS, RI, OD, AS	Mushroom, gasoline-like	M	W	W	M
	Alcohols									
10	*(Z)*-3-hexen-1-ol	2-octanol	1384	1377	MS, RI, OD, AS	Leafy, green	M			M
11	1-octen-3-ol	2-octanol	1451	1451	MS, RI, OD, AS	Earthy, mushroom	M	M	M	S
12	linalool	2-octanol	1552	1552	MS, RI, OD, AS	Floral	M	M		
	Aldehydes									
13	*(Z)*-3-hexenal	2-octanol	1130	1134	MS, RI, OD, AS	Leafy, grassy	M	S	W	M
14	*(E)*-2-hexenal	2-octanol	1218	1218	MS, RI, OD, AS	Leafy, green	W	M		M
15	phenyl acetaldehyde	2-octanol	1634	1632	MS, RI, OD, AS	Floral, sweet	M			M
16	*p*-anisaldehyde	2-octanol	2019	2016	MS, RI, OD, AS	Floral, sweet	M	M	M	M
17	4-methoxycinnamaldehyde	2-octanol	2554	2544	MS, RI, OD	Cinnamon, sweet	M			M
	Monoterpenoids									
18	fenchyl acetate	1-phenylethanol	1495	1481	MS, RI, OD, AS	Herbal, pine	W			W
19	camphor	1-phenylethanol	1518	1519	MS, RI, OD	Camphor	W			W

no.	Compound	IS	RI	RI Ref. [a]	Identification Method [b]	Odor Description	Odor Intensity [c]			
							Week 3	Week 8	Week 9	Week10
20	bornyl acetate	1-phenylethanol	1583	1580	MS, RI, OD, AS	Woody, pine	M	M	W	M
21	carvacrol	1-phenylethanol	2231	2233	MS, RI, OD	Herbal, oregano	M	W	W	W
	Ester									
22	3-octanol acetate	1-phenylethanol	1335	1344	MS, RI, OD	Woody, herbal				M
	Ketones									
23	*β*-ionone	1-phenylethanol	1940	1940	MS, RI, OD, AS	Floral, sweet	M	S	S	S
24	anisketone	1-phenylethanol	2150	2170	MS, RI, OD, AS	Licorice, sweet			W	
	Phenylpropenes									
25	*p*-propyl-anisole	1-phenylethanol	1612	1606	MS, RI, OD, AS	Anise, green	M	W		
26	estragole	1-phenylethanol	1669	1661	MS, RI, OD, AS	Anise, herbal	M	W	M	S
27	*(Z)*-anethole	1-phenylethanol	1754	1732	MS, RI, OD	Sweet, anise	M	M	M	W
28	*(E)*-anethole	1-phenylethanol	1846	1838	MS, RI, OD, AS	Sweet, anise	S	VS	S	VS
29	methyl eugenol	1-phenylethanol	2000	2003	MS, RI, OD, AS	Clove, sweet	M	M	M	M
30	methyl isoeugenol	1-phenylethanol	2174	2176	MS, RI, OD	Clove, woody	M		W	M
31	myristicin	1-phenylethanol	2262	2257	MS, RI, OD	Woody, spicy	W			
32	apiol	1-phenylethanol	2361	2431	MS, RI, OD	Parsley, green	W	W		M
	Unknown									
33	Unknown 1	NA	1538	NA	OD	Woody, floral	M		W	W
34	Unknown 2	NA	2058	NA	OD	Fruity, metal	M	M	M	M
35	Unknown 3	NA	2300	NA	OD	Floral, fruity	W		W	
		Total number of aroma-active compounds identified					32	23	23	28

[a] Reference retention indices are from a NIST publication (Babushok, Linstrom, & Zenkevich, 2011). [b] Identification method: mass spectra (MS), retention index (RI), odor descriptors (OD) against authentic aroma standards (AS). [c] Odor intensity: very weak (VW), weak (W), medium (M), strong (S), and very strong (VS).

Two out of three panelists smelled the compound.

One out of three panelists smelled the compound.

3.3.3 Quantification of aroma-active compounds and odor activity values

The 32 known aroma-active compounds were quantitated with standard addition methods (SAM). The representative SPME-GC-MS total ion chromatograms of aroma compounds from microgreen and mature fennel were shown in Supplemental Figure 3-1. The regression equations of aroma-active compounds built from SAM and their details were shown in Table 3-3. The quantification results and odor activity values (OAV) of aroma-active compounds in fennel microgreens and mature fennel leaves were shown in Table 3-4. Six replicates were measured at each growth stage, with each replicate analyzed twice by GC-MS. The large variation in the concentration of some compounds was due to individual differences between plants (as shown in Supplemental Table 3-2, 3-3, 3-4, and 3-5), not the analytical method. Quantitatively, *(E)*-anethole was present in all fresh fennel samples with the highest concentration above 492 μg/g. Two aroma compounds with concentrations above 100 μg/g were *α*-phellandrene and apiol. Other aroma compounds ranging from 1 to 100 μg/g were *α*-pinene, *γ*-terpinene, *(Z)*-3-hexenal, *(E)*-2-hexenal, *p*-anisaldehyde, 4-methoxycinnamaldehyde, *β*-ionone, anisketone, *(Z)*-anethole, methyl eugenol, and methyl isoeugenol. It is worth noting that microgreens contained a significant higher level of *α*-phellandrene (herbal, woody), *γ*-terpinene (oily, herbal), *p*-cymenene (woody, terpenic), germacrene D (spice, clove), tridecane (mushroom, oily), linalool (floral), and apiol (parsley, green), while mature fennel contained a higher level of *(Z)*-3-hexen-1-ol (leafy, green). The concentration of *(Z)*-3-hexenal and *(E)*-2-hexenal also seemed to gradually decrease when plants were allowed to grow older. Both *(Z)*-3-hexenal and *(E)*-2-hexenal reached the highest concentration in the samples taken at week 8, an

early mature stage. The differences suggested the discrepancy of secondary metabolites biosynthesis at different growth stages.

The contribution of aroma compounds depends on the concentration as well as their odor detection threshold. OAV of aroma compounds was calculated based on previous published odor detection thresholds in water (moisture content of fresh fennel >83%) (Jonas et al., 2021). *(E)*-Anethole also possessed a high OAV, with week 8 sample being the highest value. It is greatly contributing to the "anise", "sweet" odor of both fennel microgreens and mature plants. *(Z)*-3-Hexenal was the compound with the highest OAV because of its low odor detection threshold, despite its concentration being relatively low. It was contributing a "leafy", "grassy" odor of fennel. Other aroma compounds with a high OAV and contribution to fennel aroma profiles were *α*-pinene (OAV 4044-7134), estragole (OAV 3027-5550), *β*-ionone (OAV 2097-3415), *(E)*-2-hexenal (OAV 591-1604), *α*-phellandrene (OAV 441-985), *p*-anisaldehyde (OAV 139-248), which was also in agreement with GC-O results. These compounds contributed to the "woody", "herbal", "leafy", and "floral" notes of fennel aroma. What's more, the results were in accordance with previous reports published by other researchers. For example, Xiao et al. (2017) also found that *(E)*-anethole, estragole, *p*-anisaldehyde, *α*-phellandrene, and *α*-pinene were compounds with high OAV in fennel essential oils produced in different regions of China. Similarly, Zeller and Pychlik (2006) reported *(E)*-anethole and estragole as the main aroma contributing compounds of tea made from bitter fennel from Hungary. However, there were some aroma compounds that have been reported but were not found in our study, such as fenchone and limonene (Miraldi, 1999; Zeller & Rychlik, 2006), which suggested that the aroma constitutes of fennel may be related to variety and geographical origins.

The comparison of different aroma constitutes of fennel over harvest time was shown in Figure 3-1. In general, the total concentration of all aroma-active compounds in fennel was not significantly different between samples (Figure 3-1A), but numerically fennel microgreens contained the highest average value of total concentration of aroma-compounds. Phenylpropenes, including *(E)*-anethole, *(Z)*-anethole, estragole, methyl eugenol, methyl isoeugenol, *p*-propyl-anisole, myristicin, and apiol, were the most abundant group of aroma-active compounds in fennel. They largely determined the total concentration of aroma-active compounds and showed similar trend over different harvest times (Figure 3-1B). Although not significantly different, fennel microgreens also contained the highest average value of phenylpropenes (735.09 μg/g), higher than the phenylpropene content of all mature fennel. Among the aroma compounds, myristicin exhibited the highest OAV in microgreens at week 3, while *(E)*-anethole had the highest OAV in early mature samples at week 8, and estragole showed the highest OAV in late mature samples at week 10. In contrast, the OAVs of methyl eugenol and methyl isoeugenol did not show clear trends across harvest times.

Table 3-3. Regression equations for selected aroma-active compounds in fennel by standard addition method

No.	Compound	IS	Regression Equation[a]	R^2	Linear range (ug/g)	LOD	LOQ
1	*α*-pinene	decane	y = 0.3418x + 0.0527	0.9975	0.36~143.28	0.39	1.29
2	*α*-phellandrene	decane	y = 0.7269x + 3.6977	0.9947	1.21~484.50	0.11	0.38
3	*γ*-terpinene	decane	y = 1.1434x + 1.8957	0.9948	0.49~197.60	0.33	1.10
4	allo-ocimene	decane	y = 3.3571x - 1.0863	0.9941	0.08~33.32	0.01	0.04
5	*p*-cymenene	decane	y = 3.3571x - 1.0863	0.9941	0.08~33.32	0.01	0.04
6	*γ*-muurolene	decane	y = 3.3571x - 1.0863	0.9941	0.08~33.32	0.01	0.04
7	germacrene D	decane	y = 3.3571x - 1.0863	0.9941	0.08~33.32	0.01	0.04
8	*α*-cadinene	decane	y = 3.3571x - 1.0863	0.9941	0.08~33.32	0.01	0.04
9	tridecane	decane	y = 2.3394x - 0.4302	0.9941	0.02~7.52	0.00	0.01
10	*(Z)*-3-hexen-1-ol	2-octanol	y = 0.2213x + 0.6373	0.9970	0.02~8.33	0.04	0.14
11	1-octen-3-ol	2-octanol	y = 0.4363x + 1.3773	0.9955	0.01~1.65	0.16	0.54
12	linalool	2-octanol	y = 0.5871x - 0.1086	0.9965	0.01~3.34	0.01	0.05
13	*(Z)*-3-hexenal	2-octanol	y = 0.0035x + 0.0266	0.9942	0.01~16.00	0.07	0.25
14	*(E)*-2-hexenal	2-octanol	y = 0.1129x + 3.1690	0.9886	0.17~66.64	1.17	3.90
15	phenyl acetaldehyde	2-octanol	y = 0.0836x + 1.4775	0.9957	0.01~3.91	0.20	0.67
16	*p*-anisaldehyde	2-octanol	y = 0.0581x - 0.7592	0.9822	0.11~43.68	0.65	2.15
17	4-methoxycinnamaldehyde	2-octanol	y = 0.0105x - 0.0005	0.9766	0.01~1.94	0.03	0.10
18	fenchyl acetate	1-phenylethanol	y = 1.2779x + 18.9400	0.9729	1.41~564.48	0.69	2.29
19	camphor	1-phenylethanol	y = 1.3442x + 1.7364	0.9861	0.12~47.75	0.08	0.26
20	bornyl acetate	1-phenylethanol	y = 2.0570x + 0.8921	0.9966	0.19~75.24	0.07	0.22
21	carvacrol	1-phenylethanol	y = 0.8875x - 0.0478	0.9989	0.07~29.11	0.02	0.05
22	3-octanol acetate	1-phenylethanol	y = 3.6567x + 0.1126	0.9847	0.01~1.69	0.00	0.02

No.	Compound	IS	Regression Equation[a]	R^2	Linear range (ug/g)	LOD	LOQ
23	*β*-ionone	1-phenylethanol	y = 0.5634x + 0.3565	0.9971	0.16~63.84	0.02	0.07
24	anisketone	1-phenylethanol	y = 0.4849x - 0.0254	0.9973	0.08~31.14	0.03	0.11
25	*p*-propyl-anisole	1-phenylethanol	y = 5.3344x - 0.1859	0.9982	0.02~7.13	0.00	0.00
26	estragole	1-phenylethanol	y = 3.7210x - 3.4301	0.9999	3.80~1520.96	0.38	1.01
27	*(Z)*-anethole	1-phenylethanol	y = 3.4311x - 14.1430	0.9799	0.53~213.41	0.04	0.11
28	*(E)*-anethole	1-phenylethanol	y = 2.9579x + 62.2620	0.9935	14.70~5880.60	1.96	6.52
29	methyl eugenol	1-phenylethanol	y = 0.7534x - 0.4722	0.9996	0.07~285.38	0.18	0.61
30	methyl isoeugenol	1-phenylethanol	y = 0.7534x - 0.4722	0.9996	0.07~285.38	0.18	0.61
31	myristicin	1-phenylethanol	y = 0.2460x + 0.0209	0.9970	0.04~15.52	0.01	0.03
32	apiol	1-phenylethanol	y = 0.7534x - 0.4722	0.9996	0.07~285.38	0.18	0.61

[a] Regression equation: $y = \frac{Peak\ area\ of\ analyte}{Peak\ area\ of\ IS}$, $x = \frac{Mass\ of\ analyte}{Mass\ of\ IS}$

Pure standards not available, calibration curve was built based against compounds with similar chemical structure. Specifically, allo-ocimine, *γ*-muurolene, germacrene D, and *α*-cadinene were quantified against *p*-cymenene; methyl isoeugenol and apiol were quantified against methyl eugenol.

Table 3-4. Concentration (μg/g based on fresh weight) of aroma-active compounds found in leafy fennel

No.	Compound	Odor threshold in water (μg/g)	Concentration (μg/g fennel, fresh weight)				OAV			
			Microgreen		Mature fennel		Microgreen		Mature fennel	
			Week 3	*Week 8*	*Week 9*	*Week 10*	*Week 3*	*Week 8*	*Week 9*	*Week 10*
1	*α*-pinene	0.006[A]	24.26 ± 11.85[a]	42.80 ± 15.30[a]	29.04 ± 18.96[a]	33.97 ± 26.38[a]	4044	7134	4840	5661
2	*α*-phellandrene	0.2[B]	196.92 ± 56.56[a]	90.71 ± 26.16[b]	99.48 ± 35.21[b]	88.17 ± 26.82[b]	985	454	497	441
3	*γ*-terpinene	1[D]	28.49 ± 5.83[a]	3.90 ± 2.41[b]	6.02 ± 4.13[b]	3.65 ± 3.20[b]	28	4	6	4
4	allo-ocimene	0.727[F]	0.27 ± 0.01[a]	0.25 ± 0.01[a]	0.26 ± 0.05[a]	0.25 ± 0.01[a]	0.4	0.3	0.4	0.3
5	*p*-cymenene	11.4[G]	0.30 ± 0.03[a]	0.26 ± 0.01[b]	0.26 ± 0.01[b]	0.26 ± 0.01[b]	0.03	0.02	0.02	0.02
6	*γ*-muurolene	ND	0.53 ± 0.08[a]	0.54 ± 0.19[a]	0.38 ± 0.06[a]	0.43 ± 0.14[a]	ND	ND	ND	ND
7	germacrene D	ND	0.85 ± 0.16[a]	0.36 ± 0.03[b]	0.36 ± 0.08[b]	0.61 ± 0.25[ab]	ND	ND	ND	ND
8	*α*-cadinene	ND	0.25 ± 0.01[a]	0.28 ± 0.02[a]	0.26 ± 0.02[a]	0.26 ± 0.02[a]	ND	ND	ND	ND
9	tridecane	ND	0.51 ± 0.18[a]	0.15 ± 0.01[b]	0.14 ± 0.00[b]	0.14 ± 0.01[b]	ND	ND	ND	ND
10	*(Z)*-3-hexen-1-ol	0.07[A]	0.12 ± 0.07[c]	1.29 ± 0.69[ab]	2.40 ± 1.22[a]	0.36 ± 0.31[bc]	2	19	34	5
11	1-octen-3-ol	0.001[A]	ND	ND	ND	0.04	ND	ND	ND	35
12	linalool	0.006[A]	0.09 ± 0.05[a]	0.03 ± 0.01[b]	0.03 ± 0.01[b]	0.04 ± 0.03[b]	15	5	4	7
13	*(Z)*-3-hexenal	0.00025[A]	4.56 ± 2.96[ab]	6.75 ± 1.41[a]	4.12 ± 2.22[ab]	1.97 ± 1.41[b]	18233	27011	16485	7865
14	*(E)*-2-hexenal	0.017[A]	22.92 ± 6.16[ab]	27.27 ± 9.37[a]	14.97 ± 5.26[bc]	10.05 ± 7.37[c]	1348	1604	881	591
15	phenyl acetaldehyde	0.004[A]	ND	ND	ND	ND	ND	ND	ND	ND
16	*p*-anisaldehyde	0.047[E]	9.15 ± 2.74[a]	11.66 ± 9.17[a]	6.54 ± 4.33[a]	6.91 ± 3.01[a]	195	248	139	147
17	4-methoxycinnamaldehyde	ND	1.70 ± 0.55[a]	1.59 ± 0.79[a]	1.26 ± 1.02[a]	1.22 ± 0.52[a]	ND	ND	ND	ND
18	fenchyl acetate	ND	3.17 ± 4.30	ND	ND	ND	ND	ND	ND	ND
19	camphor	1.47[E]	0.77	0.78	ND	0.52	0.5	0.5	ND	0.4
20	bornyl acetate	0.075[A]	0.74 ± 0.35[a]	0.04[a]	ND	0.43[a]	10	0.5	ND	6
21	carvacrol	1.7[F]	0.22 ± 0.07[a]	0.20 ± 0.05[a]	0.16 ± 0.03[a]	0.19 ± 0.06[a]	0.1	0.1	0.1	0.1
22	3-octanol acetate	ND	ND	ND	ND	0.02 ± 0.02	ND	ND	ND	ND
23	*β*-ionone	0.0005[B]	1.11 ± 0.39[a]	1.71 ± 0.89[a]	1.05 ± 0.80[a]	1.56 ± 0.93[a]	2212	3415	2097	3127
24	anisketone	1.8[E]	2.30 ± 0.49[a]	2.92 ± 1.71[a]	1.71 ± 1.26[a]	2.02 ± 1.19[a]	1	2	1	1

No.	Compound	Odor threshold in water (μg/g)	Concentration (μg/g fennel, fresh weight)				OAV			
			Microgreen		Mature fennel		Microgreen		Mature fennel	
			Week 3	*Week 8*	*Week 9*	*Week 10*	*Week 3*	*Week 8*	*Week 9*	*Week 10*
25	*p*-propyl-anisole	ND	0.08 ± 0.00[a]	0.12 ± 0.08[a]	0.08 ± 0.01[a]	0.09 ± 0.01[a]	ND	ND	ND	ND
26	estragole	0.0075[B]	22.70 ± 4.58[a]	31.42 ± 17.13[a]	22.81 ± 20.09[a]	41.62 ± 43.91[a]	3027	4190	3041	5550
27	*(Z)*-anethole	ND	9.54 ± 0.19[b]	12.35 ± 1.75[a]	10.65 ± 2.40[ab]	10.06 ± 1.36[ab]	ND	ND	ND	ND
28	*(E)*-anethole	0.073[E]	543.11 ± 140.97[a]	765.66 ± 506.40[a]	492.08 ± 548.75[a]	514.75 ± 450.89[a]	7440	10488	6741	7051
29	methyl eugenol	0.82[A]	1.52 ± 0.12[ab]	1.47 ± 0.06[ab]	1.40 ± 0.08[b]	1.69 ± 0.23[a]	2	2	2	2
30	methyl isoeugenol	1.6[E]	2.67 ± 0.37[a]	3.00 ± 1.18[a]	1.93 ± 0.78[a]	2.03 ± 1.00[a]	2	2	1	1
31	myristicin	0.025[C]	3.85 ± 2.76[a]	0.08 ± 0.07[a]	0.21[a]	3.05 ± 6.04[a]	154	3	9	122
32	apiol	ND	151.60 ± 32.91[a]	4.59 ± 4.05[b]	2.31 ± 0.48[b]	2.98 ± 1.44[b]	ND	ND	ND	ND

[abc] represent the mean separation between harvest time by Tukey's HSD at $p < 0.05$. Results are expressed as mean ± SD (unless the compound is detected in only one of the six replicates). ND = not determined

[A] Odor threshold obtained from Leffingwell & Associates (http://www.leffingwell.com/odorthre.htm).

[B] Odor threshold obtained from literature (Rychlik, Schieberle, & Grosch, 1998).

[C] Odor threshold obtained from literature (Buttery et al., 1968).

[D] Odor threshold obtained from literature (van Gemert, 2003).

[E] Odor threshold obtained from literature (Zeller et al., 2006).

[F] Odor threshold obtained from literature (Zhang et al., 2023).

[G] Odor threshold obtained from literature (Liang et al., 2022).

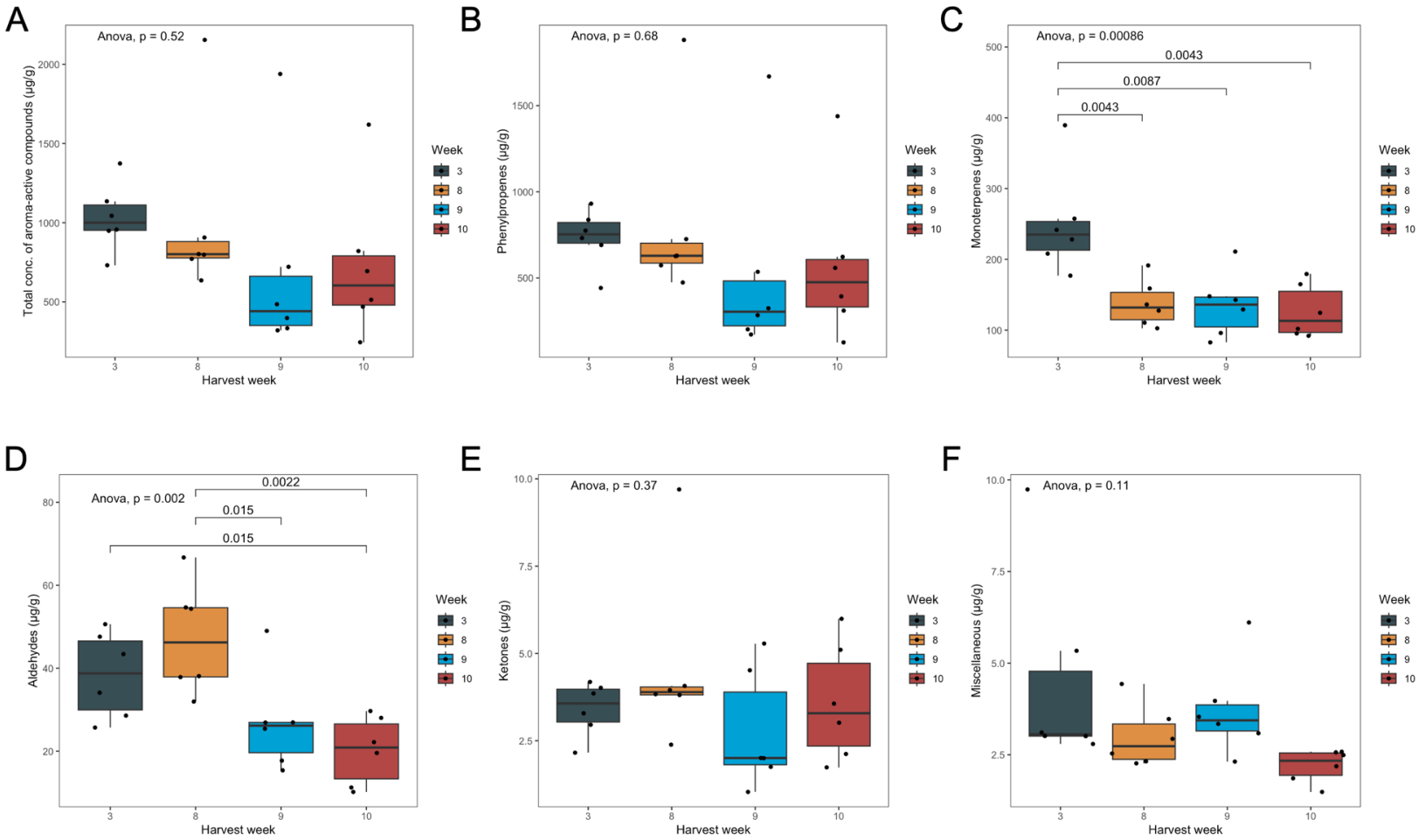

Figure 3-1. Concentration of (A) total aroma-active compounds, (B) phenylpropenes, (C) monoterpenes, (D) aldehydes, (E) ketones, and (F) miscellaneous compounds found in fennel sample harvested at different weeks.

Monoterpenes were the second largest group of aroma-active compounds in fennel, and the average value ranging from 126.30 to 250.23 μg/g among all samples. One-way ANOVA results showed that microgreens contained a significantly higher level of monoterpenes than mature fennel (Figure 3-1C). *α*-Phellandrene was the monoterpene with highest concentration, but *α*-pinene had the highest OAV due to its low odor detection threshold, making it an important contributor to the overall fennel aroma profile. The other monoterpenes, such as *γ*-terpinene, allo-ocimene, and *p*-cymenene, had relatively lower concentrations and OAV values, therefore, were considered not as important as *α*-phellandrene and *α*-pinene. *α*-Pinene exhibited the highest OAV in early mature samples at week 8, while *α*-phellandrene and *γ*-terpinene exhibited the highest OAVs in microgreens at week 3.

Aldehydes were also found to have relatively high concentrations in fennel. Fennel sample from week 8 harvest showed the highest content in aldehydes, significantly higher than other mature samples, and numerically higher than the aldehyde content of fennel microgreens (Figure 3-1D). *(Z)*-3-hexenal and *(E)*-2-hexenal were aldehydes with highest OAV and they contributed a green, leafy aroma. Both *(Z)*-3-hexenal and *(E)*-2-hexenal showed the highest OAV in early mature samples at week 8, and the OAV continued to decrease as growth time increased. Phenyl acetaldehyde and *p*-anisaldehyde were aldehydes contributing to the floral and sweet note of fennel aroma profile. Similar to other aldehydes, *p*-anisaldehyde also exhibited the highest OAV in the samples collected at week 8. *β*-Ionone and anisketone were the two ketones identified as aroma-active compounds in this study, and no significant differences were found in the level of ketones over microgreens and mature fennel samples (Figure 3-1E). However, both ketones showed the

highest OAVs at early mature fennel plants harvest at week 8. Other miscellaneous compounds, including sesquiterpenes, monoterpenoids, alcohols, ester, and alkane, only took up less than 1% of total aroma-active compounds, and showed no significant differences between fennel samples collected at different times (Figure 3-1F).

Phenylpropanoids are a part of the chemical defense mechanism and contribute to plant resistance against pests and herbivores (Chang & Ahn, 2002; Sousa et al., 2013). Additionally, phenylpropanoids and terpenoids found in plant essential oils exhibit activity against a wide range of fungi and pathogens (Basaid et al., 2021). These defense compounds, derived from specialized metabolism, are typically found in higher concentrations in young plants to protect them from abiotic and biotic stresses (Gershenzon & Ullah, 2022). This may explain why fennel microgreens contain higher levels of phenylpropanoids and monoterpenes.

3.3.3 Multivariate statistical analysis of aroma-active compounds in fennel microgreens and mature plants

To further evaluate the overall variance in aroma profiles of fennel microgreens and mature plants, principal component analysis (PCA) was applied to the concentrations of different aroma-active compounds and the results were shown in Figure 3-2A and 3-2B. Five compounds, namely 1-octen-3-ol, phenyl acetaldehyde, fenchyl acetate, camphor, and 3-octanol acetate, were excluded due to the presence of many zero values, which could bias the model due to zero-inflation. The samples were well differentiated by the first two principal components (PC1 and PC2), which accounted for 30.1% and 24.0% of the total variance, respectively. As shown in Supplemental Table 2-5, individual differences among plant samples could contribute to the overall variance. Considering the total variances

explained by the first two principal components were less than 60%, we also visualized the variances explained by other principal components (Supplemental Figure 3-2). Subsequent principal components, such as PC3 and PC4, also captured significant portions of the variance (9.2% and 6.7%, respectively), reflecting the complex interaction among variables. In total, the first ten principal components covered more than 90% of the total variances. In Figure 3-2, there was some overlapping between mature fennel samples, but no overlapping was observed between microgreens and mature fennel, suggesting a clear distinction of aroma-active compounds between microgreens and mature plants. All samples representing fennel microgreens were in the positive side of PC1, which were also positively correlated to a higher concentration of certain aroma-active compounds, such as α-phellandrene, γ-terpinene, germacrene D, tridecane, linalool, and apiol. Supplemental Figure 3-3A and Supplemental Figure 3-3B showed the sample distribution on the first and third principal components. All points representing microgreens were located on the positive side of PC1, while the majority of points for mature fennel were located on the negative side of PC1. Additionally, all points representing Week 10 samples were located on the positive side of PC3, while samples from week 3, week 8, and week 9 were predominantly on the negative side. These results indicated that the aroma-active compounds associated with PC1 more effectively distinguish between microgreens and mature fennel, while the aroma-active compounds associated PC3 better differentiate week 10 samples from earlier time points (week 3, 8, and 9). Supplemental Figure 3-3C and Supplemental Figure 3-3D showed the distribution of samples on the second and third principal components. All the data points representing microgreens were located on the positive side of PC2, while most points representing mature fennels were positioned on the

negative side of PC2. The results suggest that fennel microgreens are positively associated with higher concentrations of aroma-active compounds such as bornyl acetate and α-phellandrene, whereas mature fennel contains lower amount of these compounds.

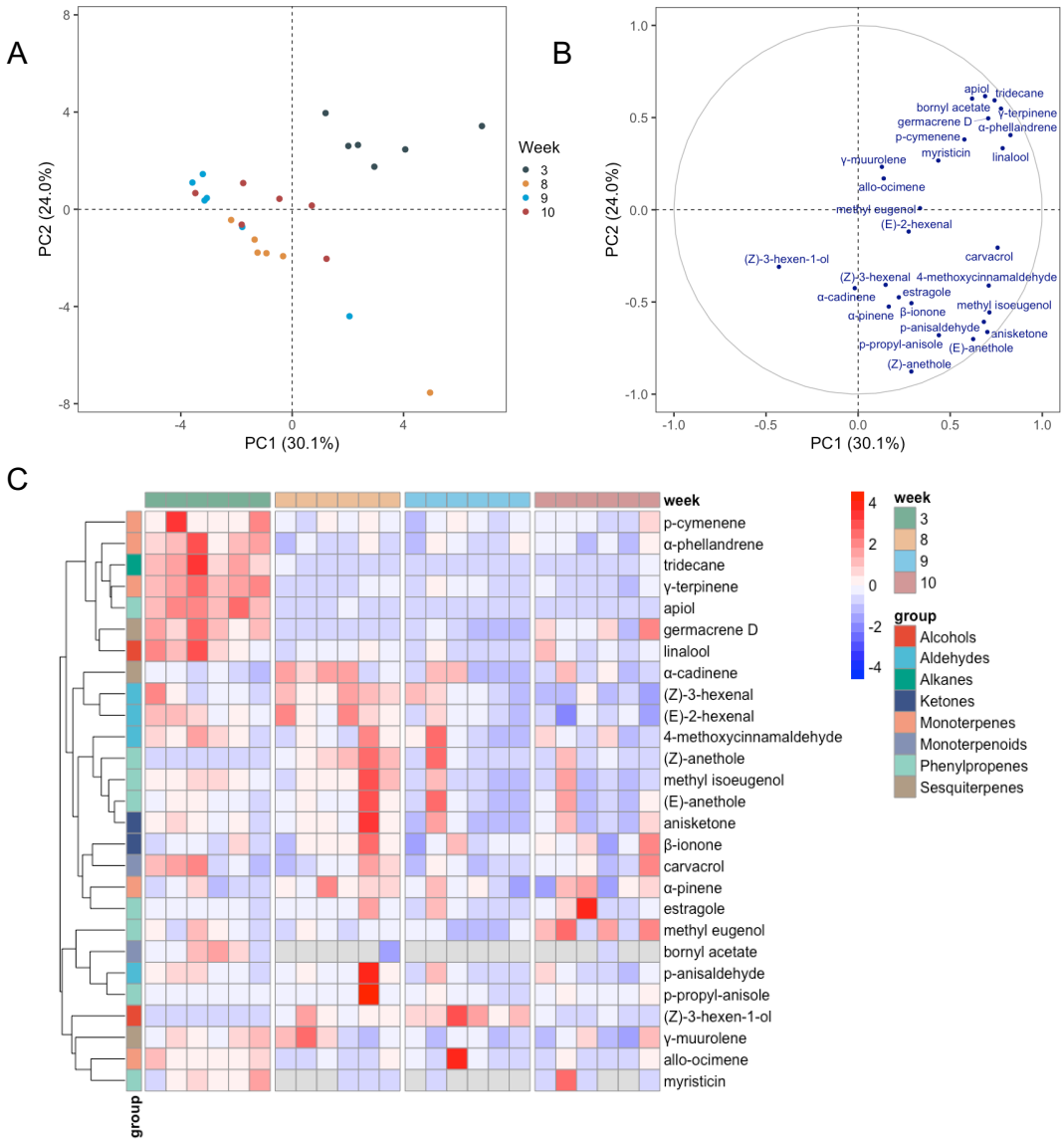

Figure 3-2. Multivariate statistical analysis of aroma-active compounds found via SPME-GC-MS in fennel samples. (A) Principal component analysis (PCA), (B) the loading plot of PCA, and (C) heatmap of aroma-active compounds in fennel from different harvest week.

To visually illustrate the pattern of change in aroma-active compounds present in fennel samples from different harvest time, a heatmap with hierarchical clustering analysis was applied. The results are shown in Figure 3-2C, where aroma-active compounds were labeled by chemical groups, indicated by different colors on the left side of the heatmap. It can be observed that seven compounds, specifically *p*-cymenene, *α*-phellandrene, tridecane, *γ*-terpinene, apiol, germacrene D, and linalool, in the same cluster showed a clear decreasing pattern from week 3 to week 10. It is also worth mentioning that more than half of these compounds are terpenes. This pattern is similar to findings in dill, another Apiaceae family herb, where terpenes such as *α*-phellandrene and apiol also decreased with harvest time (Huopalahti & Linko, 1983).

In addition, a decreasing trend was observed for 4-methoxycinnamaldehyde, methyl isoeugenol, *(E)*-anethole, and anisketone. Young plants tend to accumulate high levels of certain volatile compounds, such as phenylpropanoids, as part of their defense mechanism; however, the specific levels and types of the secondary metabolites can vary largely depending on factors including plant cultivar, phenotype, physiological traits, the type of secondary metabolites, and the specific stress conditions (Brunetti et al., 2020; Francini, Giro, & Ferrante, 2019; Petruľová, Dučaiová, & Repčák, 2014; Wang et al, 2023). Methyl isoeugenol and *(E)*-anethole are phenylpropanoids synthesized from the aromatic amino acid phenylalanine through enzymatic reactions. In contrast to the observation for fennel, methyl isoeugenol was found only in mature leaves of orange carrot, another Apiaceae plant, and not in young leaves (Yahyaa et al., 2019). This suggests that volatile composition is influenced not only by growth stage but also by the specific plant species.

A similar decreasing trend was observed for *(Z)*-3-hexenal and *(E)*-2-hexenal in another cluster. Both compounds are C-6 aldehydes that have a leafy, grassy odor produced by linoleic acid peroxidation via lipoxygenase (Thomas, 2017). Interestingly, *(Z)*-3-hexen-1-ol, a C6 alcohol and another green leaf volatile, showed an increasing trend from week 3 to week 9, followed by a decrease thereafter. These findings indicate a metabolic shift during plant growth, with volatile compounds serving different biological functions at various stages.

Additionally, in Figure 3-2C, some mature samples, such as sample 5 from week 8 (the fifth column of week 8) and sample 2 from week 9 (the second column of week 9), showed higher concentrations of compounds than other replicates, suggesting variability in growth conditions among individual plants.

3.4 Conclusion

In this study, the aroma profile and volatile constitute of hydroponic fennel at different growth stages were investigated. In general, more aroma-active compounds were detected in microgreens, and the overall content of aroma-active compounds was also higher in fennel microgreens. In terms of the volatile profiles, phenylpropenes were the major aroma constitutes of hydroponic fennel, regardless of growth stage. Compared with mature fennel, microgreens showed a significantly higher level of monoterpenes, and early harvested mature fennel contained a higher level of aldehydes. The results from multivariate statistical analysis revealed clear differences in the overall aroma profile of fennel microgreens and mature plants, and many aroma-active compounds, especially terpenes, exhibited a decrease trend with growth period. Although distinct differences in aroma profiles across growth stages of fresh fennel leaves were identified, it is unclear

whether these differences are perceivable to consumers. A future sensory study could be necessary to confirm consumer perception of these differences. Our study determined for the first time the differences in aroma quality between fennel microgreens and mature fennel and provided information on aroma compounds to herb growers for the cultivation of hydroponic fennel. Other than aroma quality, farmers and herb growers are encouraged to take production cycle and cost into consideration when deciding the best harvest time. Future studies could investigate the impact of different cultivation techniques and environmental factors on the aroma and quality of hydroponic herbs, and the identification and regulation of genes and enzymes responsible for the biosynthesis of key aroma volatiles.

References

Afifi, S. M., El-Mahis, A., Heiss, A. G., & Farag, M. A. (2021). Gas chromatography–mass spectrometry-based classification of 12 fennel (*Foeniculum vulgare* Miller) varieties based on their aroma profiles and estragole levels as analyzed using chemometric tools. *ACS Omega*, *6*(8), 5775-5785. https://doi.org/10.1021/acsomega.0c06188.

Ahn, J. Y., Kil, D. Y., Kong, C., & Kim, B. G. (2014). Comparison of oven-drying methods for determination of moisture content in feed ingredients. *Asian-Australasian Journal of Animal Sciences*, *27*(11), 1615. https://doi.org/10.5713/ajas.2014.14305.

Babushok, V. I., Linstrom, P. J., & Zenkevich, I. G. (2011). Retention indices for frequently reported compounds of plant essential oils. *Journal of Physical and Chemical Reference Data, 40*(4), 043101. https://doi.org/10.1063/1.3653552.

Barros, L., Carvalho, A. M., & Ferreira, I. C. F. R. (2010). The nutritional composition of fennel (*Foeniculum vulgare*): Shoots, leaves, stems and inflorescences. *LWT - Food Science and Technology, 43*(5), 814-818. https://doi.org/10.1016/j.lwt.2010.01.010.

Basaid, K., Chebli, B., Mayad, E. H., Furze, J. N., Bouharroud, R., Krier, F., Barakate M., & Paulitz, T. (2021). Biological activities of essential oils and lipopeptides applied to control plant pests and diseases: a review. *International Journal of Pest Management, 67*(2), 155-177. https://doi.org/10.1080/09670874.2019.1707327.

Bilia, A. R., Flamini, G., Taglioli, V., Morelli, I., & Vincieri, F. F. (2002). GC-MS analysis of essential oil of some commercial Fennel teas. *Food Chemistry, 76*(3), 307-310. https://doi.org/10.1016/S0308-8146(01)00277-1.

Brunetti, C., Gori, A., Moura, B. B., Loreto, F., Sebastiani, F., Giordani, E., & Ferrini, F. (2020). Phenotypic plasticity of two *M. oleifera* ecotypes from different climatic zones under water stress and re-watering. *Conservation Physiology*, *8*(1), coaa028.

Buttery, R. G., Seifert, R. M., Guadagni, D. G., Black, D. R., & Ling, L. (1968). Characterization of some volatile constituents of carrots. *Journal of Agricultural and Food Chemistry, 16*(6), 1009-1015. https://doi.org/10.1021/jf60160a012.

Celik, B., & Dane, S. (2020). The effects of COVID-19 pandemic outbreak on food consumption preferences and their causes. *Journal of Research in Medical and Dental Science, 8*(3), 169-173.

Chang, K.-S., & Ahn, Y.-J. (2002). Fumigant activity of *(E)*-anethole identified in *Illicium verum* fruit against *Blattella germanica. Pest Management Science, 58*(2), 161-166. https://doi.org/10.1002/ps.435.

Choe, U., Yu, L. L., & Wang, T. T. Y. (2018). The science behind microgreens as an exciting new food for the 21st century. *Journal of Agricultural and Food Chemistry, 66*(44), 11519-11530. https://doi.org/10.1021/acs.jafc.8b03096.

Díaz-Maroto, M. C., Díaz-Maroto Hidalgo, I. J., Sánchez-Palomo, E., & Pérez-Coello, M. S. (2005). Volatile components and key odorants of fennel (*Foeniculum vulgare* Mill.) and thyme (*Thymus vulgaris* L.) oil extracts obtained by

simultaneous distillation−extraction and supercritical fluid extraction. *Journal of Agricultural and Food Chemistry, 53*(13), 5385-5389. https://doi.org/10.1021/jf050340+.

Dimita, R., Min Allah, S., Luvisi, A., Greco, D., De Bellis, L., Accogli, R., Mininni, C., & Negro, C. (2022). Volatile compounds and total phenolic content of perilla frutescens at microgreens and mature stages. *Horticulturae, 8*(1), 71. https://doi.org/10.3390/horticulturae8010071.

Erten, E. S., & Cadwallader, K. R. (2017). Identification of predominant aroma components of raw, dry roasted and oil roasted almonds. *Food Chemistry, 217*, 244-253. https://doi.org/10.1016/j.foodchem.2016.08.091.

Filimonau, V., Vi, L. H., Beer, S., & Ermolaev, V. A. (2022). The Covid-19 pandemic and food consumption at home and away: An exploratory study of English households. *Socio-Economic Planning Sciences, 82*, 101125. https://doi.org/10.1016/j.seps.2021.101125.

Folta, K. M. (2019). Breeding new varieties for controlled environments. *Plant Biology, 21*(S1), 6-12. https://doi.org/https://doi.org/10.1111/plb.12914.

Fortini, M., Migliorini, M., Cherubini, C., Cecchi, L., & Calamai, L. (2017). Multiple internal standard normalization for improving HS-SPME-GC-MS quantitation in virgin olive oil volatile organic compounds (VOO-VOCs) profile. *Talanta*, 165, 641-652. https://doi.org/10.1016/j.talanta.2016.12.082.

Francini, A., Giro, A., & Ferrante, A. (2019). Biochemical and molecular regulation of phenylpropanoids pathway under abiotic stresses. In *Plant Signaling Molecules* (pp. 183-192). Woodhead Publishing.

Gershenzon, J., & Ullah, C. (2022). Plants protect themselves from herbivores by optimizing the distribution of chemical defenses. *Proceedings of the National Academy of Sciences, 119*(4), e2120277119.

Ghoora, M. D., Haldipur, A. C., & Srividya, N. (2020). Comparative evaluation of phytochemical content, antioxidant capacities and overall antioxidant potential of select culinary microgreens. *Journal of Agriculture and Food Research, 2*, 100046. https://doi.org/10.1016/j.jafr.2020.100046.

González-García, J. L., Rodríguez-Mendoza, M. N., Sánchez-García, P., Osorio-Rosales, B., Trejo-Téllez, L. I., Alcántar-González, G., & Sandoval-Villa, M. (2009). Ammounium/nitrate ratios in hydroponic production of aromatic herbs. *Acta Horticulturae*, *843*, 123-128. https://doi.org/10.17660/ActaHortic.2009.843.14.

Guillén, M. D., & Manzanos, M. J. (1996). A study of several parts of the plant *Foeniculum vulgare* as a source of compounds with industrial interest. *Food Research International*, *29*(1), 85-88. https://doi.org/10.1016/0963-9969(95)00047-X.

Huopalahti, R., & Linko, R. R. (1983). Composition and content of aroma compounds in dill, *Anethum graveolens* L., at three different growth stages. *Journal of Agricultural and Food Chemistry, 31*(2), 331-333. https://doi.org/10.1021/jf00116a036.

Jonas, M., & Schieberle, P. (2021). Characterization of the key aroma compounds in fresh leaves of garden sage (*Salvia officinalis* L.) by means of the sensomics approach: influence of drying and storage and comparison with commercial dried sage. *Journal of Agricultural and Food Chemistry, 69*(17), 5113-5124. https://doi.org/10.1021/acs.jafc.1c01275.

Kolde, R., & Kolde, M. R. (2015). Package 'pheatmap'. *R package*, *1*(7), 790.

Kozai, T., & Niu, G. (2016). Chapter 2 - Role of the plant factory with artificial lighting (PFAL) in urban areas. In Kozai, T., Niu, G., & Takagaki, M. (Eds.), *Plant Factory* (pp. 7-33). San Diego: Academic Press.

Kyriacou, M. C., Rouphael, Y., Di Gioia, F., Kyratzis, A., Serio, F., Renna, M., De Pascale, S., & Santamaria, P. (2016). Micro-scale vegetable production and the rise of microgreens. *Trends in Food Science & Technology, 57*, 103-115. https://doi.org/10.1016/j.tifs.2016.09.005.

Leffingwell & Associates. (1999). *Odor & Flavor Detection Thresholds in Water (In Parts per Billion)*. Retrieved from http://www.leffingwell.com/odorthre.htm. Accessed April 9, 2024.

Liang, M., Yang, Y., Zheng, F.-P., Sun, B.-G., Wang, X.-P., & Yu, A.-N. (2022). Comparison of free and bound volatile profiles of immature *Litsea mollis* fruits grown in five distinct regions of China. *Food Science and Technology, 42*, Article e28821. https://doi.org/10.1590/fst.28821.

Lu, M., Yuan, B., Zeng, M., & Chen, J. (2011). Antioxidant capacity and major phenolic compounds of spices commonly consumed in China. *Food Research International, 44*(2), 530-536. https://doi.org/10.1016/j.foodres.2010.10.055.

MacDougall, D., Crummett, W. B., & et al. (1980). Guidelines for data acquisition and data quality evaluation in environmental chemistry. *Analytical Chemistry, 52*(14), 2242-2249. https://doi.org/10.1021/ac50064a004.

Maire, J., Sattar, A., Henry, R., Warren, F., Merkle, M., Rounsevell, M., & Alexander, P. (2022). How different COVID-19 recovery paths affect human health, environmental sustainability, and food affordability: a modelling study. *The Lancet Planetary Health, 6*(7), e565-e576. https://doi.org/10.1016/S2542-5196(22)00144-9.

McNair, H. M., Miller, J. M., & Snow, N. H. (2019). Qualitative and Quantitative Analysis. In *Basic Gas Chromatography* (pp. 139-155). John Wiley & Sons, Incorporated.

Miraldi, E. (1999). Comparison of the essential oils from ten *Foeniculum vulgare* Miller samples of fruits of different origin. *Flavour and Fragrance Journal*, *14*(6), 379-382.

Moosavi, S. G., Seghatoleslami M. J., & Ansarinia E. (2015). Effect of sowing date and plant density on yield and yield components of fennel (*Foeniculum vulgare*). *International Journal of Biosciences, 6*(1), 334-342.

Oruña-Concha, M. J., Lignou, S., Feeney, E. L., Beegan, K., Kenny, O., & Harbourne, N. (2017, September). *Investigating the phytochemical , flavour and sensory*

attributes of mature and microgreen coriander (Coriandrum sativum). In Flavour Science: proceedings of the 15th Weurman Symposium, Graz, Austria. https://doi.org/10.3217/978-3-85125-593-5.

Penton, Z. (1999). Method development with solid phase microextraction. In *Solid Phase Microextraction: A Practical Guide* (pp. 27-57). Boca Raton: CRC, Taylor & Francis.

Petruľová, V., Dučaiová, Z., & Repčák, M. (2014). Short‐term UV‐B Dose stimulates production of protective metabolites *in Matricaria chamomilla* leaves. *Photochemistry and Photobiology*, 90(5), 1061-1068.

Rychlik, M., Schieberle, P., & Grosch, W. (1998). *Compilation of odor thresholds, odor qualities and retention indices of key food odorants*. Garching: Deutsche Forschungsanstat für Lebensmittelchemie and Instit für Lebensmittelchemie der Technischen Universität München Garching.

Saharkhiz, M. J., & Tarakeme, A. (2011). Essential oil content and composition of fennel (*Foeniculum vulgare* L.) fruits at different stages of development. *Journal of Essential Oil Bearing Plants, 14*(5), 605-609. https://doi.org/10.1080/0972060X.2011.10643978.

Senatore, F., Oliviero, F., Scandolera, E., Taglialatela-Scafati, O., Roscigno, G., Zaccardelli, M., & De Falco, E. (2013). Chemical composition, antimicrobial and antioxidant activities of anethole-rich oil from leaves of selected varieties of fennel [*Foeniculum vulgare* Mill. ssp. *vulgare* var. *azoricum* (Mill.) Thell]. *Fitoterapia, 90*, 214-219. https://doi.org/10.1016/j.fitote.2013.07.021.

Skalkos, D., & Kalyva, Z. C. (2023). Exploring the impact of COVID-19 pandemic on food choice motives: a systematic review. *Sustainability, 15*(2), 1606. https://doi.org/10.3390/su15021606.

Son, Y.-J., Park, J.-E., Kim, J., Yoo, G., & Nho, C. W. (2021). The changes in growth parameters, qualities, and chemical constituents of lemon balm (*Melissa officinalis* L.) cultivated in three different hydroponic systems. *Industrial Crops and Products, 163*, 113313. https://doi.org/10.1016/j.indcrop.2021.113313.

Sousa, R. M. O. F., Rosa, J. S., Oliveira, L., Cunha, A., & Fernandes-Ferreira, M. (2013). Activities of Apiaceae Essential Oils against Armyworm, *Pseudaletia unipuncta* (Lepidoptera: Noctuidae). *Journal of Agricultural and Food Chemistry, 61*(32), 7661-7672. https://doi.org/10.1021/jf403096d.

Su, X., & Yin, Y. (2021). Aroma characterization of regional Cascade and Chinook hops (*Humulus lupulus* L.). *Food Chemistry, 364*, 130410. https://doi.org/10.1016/j.foodchem.2021.130410.

Thomas, B. (2017). Genetic engineering for postharvest quality. In B. Thomas, B. G. Murray & D. J. Murphy (Eds.), *Encyclopedia of Applied Plant Sciences (Second Edition)* (pp. 300-307). Oxford: Academic Press.

Timpanaro, G., & Cascone, G. (2022). Food consumption and the Covid-19 pandemic: The role of sustainability in purchasing choices. *Journal of Agriculture and Food Research, 10*, 100385. https://doi.org/10.1016/j.jafr.2022.100385.

Uher, S. F., Radman, S., Opačić, N., Dujmović, M., Benko, B., Lagundžija, D., Mijić, V., Prša, L., Babac, S., & Šic Žlabur, J. (2023). Alfalfa, cabbage, beet and fennel

microgreens in floating hydroponics-perspective nutritious food? *Plants, 12*(11), 2098. https://doi.org/10.3390/plants12112098.

Valduga, A. T., Gonçalves, I. L., Magri, E., & Finzer, J. R. D. (2019). Chemistry, pharmacology and new trends in traditional functional and medicinal beverages. *Food Research International*, 120, 478-503. https://doi.org/10.1016/j.foodres.2018.10.091.

van Den Dool, H., & Kratz, P. D. (1963). A generalization of the retention index system including linear temperature programmed gas—liquid partition chromatography. *Journal of Chromatography A, 11*, 463-471. https://doi.org/10.1016/S0021-9673(01)80947-X.

van Gemert, A. F. (2003). *Compilations of Odour Threshold Values in Air, Water and Other Media*. Boelens Aroma Chemical Information Service.

Wallace, T. C., Bailey, R. L., Blumberg, J. B., Burton-Freeman, B., Chen, C. y. O., Crowe-White, K. M., Drewnowski, A., Hooshmand, S., Johnson, E., Lewis, R., Murray, R., Shapses, S. A., & Wang, D. D. (2020). Fruits, vegetables, and health: A comprehensive narrative, umbrella review of the science and recommendations for enhanced public policy to improve intake. *Critical Reviews in Food Science and Nutrition, 60*(13), 2174-2211. https://doi.org/10.1080/10408398.2019.1632258.

Walters, K. J., & Currey, C. J. (2015). Hydroponic greenhouse basil production: Comparing systems and cultivars. *Horttechnology, 25*(5), 645-650. https://doi.org/10.21273/Horttech.25.5.645.

Wang, B., Lin, L., Yuan, X., Zhu, Y., Wang, Y., Li, D., He, J., & Xiao, Y. (2023). Low-level cadmium exposure induced hormesis in peppermint young plant by constantly activating antioxidant activity based on physiological and transcriptomic analyses. *Frontiers in Plant Science*, *14*, 1088285.

Wang, C., Sun, J., Tao, Y., Fang, L., Zhou, J., Dai, M., Liu, M., & Fang, Q. (2020). Biomass materials derived from anethole: conversion and application. *Polymer Chemistry, 11*(5), 954-963. https://doi.org/10.1039/C9PY01513B.

Wei, X., Song, M., Chen, C., Tong, H., Liang, G., & Gmitter, F. G. (2018). Juice volatile composition differences between Valencia orange and its mutant Rohde Red Valencia are associated with carotenoid profile differences. *Food Chemistry, 245*, 223-232. https://doi.org/10.1016/j.foodchem.2017.10.066.

Wieczyńska, J., & Cavoski, I. (2018). Antimicrobial, antioxidant and sensory features of eugenol, carvacrol and *trans*-anethole in active packaging for organic ready-to-eat iceberg lettuce. *Food Chemistry, 259*, 251-260. https://doi.org/10.1016/j.foodchem.2018.03.137.

Xia, T., Su, S., Guo, K., Wang, L., Tang, Z., Huo, J., & Song, H. (2023). Characterization of key aroma-active compounds in blue honeysuckle (*Lonicera caerulea* L.) berries by sensory-directed analysis. *Food Chemistry, 429*, 136821. https://doi.org/10.1016/j.foodchem.2023.136821.

Xiao, Z., Chen, J., Niu, Y., & Chen, F. (2017). Characterization of the key odorants of fennel essential oils of different regions using GC–MS and GC–O combined with

partial least squares regression. *Journal of Chromatography B, 1063*, 226-234. https://doi.org/10.1016/j.jchromb.2017.07.053.

Xiao, Z., Lester, G. E., Luo, Y., & Wang, Q. (2012). Assessment of vitamin and carotenoid concentrations of emerging food products: Edible microgreens. *Journal of Agricultural and Food Chemistry, 60*(31), 7644-7651. https://doi.org/10.1021/jf300459b.

Yahyaa, M., Berim, A., Nawade, B., Ibdah, M., Dudareva, N., & Ibdah, M. (2019). Biosynthesis of methyleugenol and methylisoeugenol in *Daucus carota* leaves: Characterization of eugenol/isoeugenol synthase and *O*-Methyltransferase. *Phytochemistry, 159*, 179-189. https://doi.org/10.1016/j.phytochem.2018.12.020.

Zeller, A., & Rychlik, M. (2006). Character impact odorants of fennel fruits and fennel tea. *Journal of Agricultural and Food Chemistry, 54*(10), 3686-3692. https://doi.org/10.1021/jf052944j.

Zhang, Y., Hartung, N. M., Fraatz, M. A., & Zorn, H. (2015). Quantification of key odor-active compounds of a novel nonalcoholic beverage produced by fermentation of wort by shiitake (*Lentinula edodes*) and aroma genesis studies. *Food Research International*, 70, 23-30. https://doi.org/10.1016/j.foodres.2015.01.019.

Zhang, Y., Xiao, Z., Ager, E., Kong, L., & Tan, L. (2021). Nutritional quality and health benefits of microgreens, a crop of modern agriculture. *Journal of Future Foods, 1*(1), 58-66. https://doi.org/10.1016/j.jfutfo.2021.07.001.

Zhang, Z., Guan, W., Liang, M., Wang, R., Wu, Y., & Liu, Y. (2023). Characterization of the key odorants in fresh *Amomum tsao-ko* Crevost et Lemaire fruit by gas

chromatography-olfactometry, quantitative analysis and aroma reconstitution. *LWT, 185*, 115154. https://doi.org/10.1016/j.lwt.2023.115154.

Chapter 4 Narrow-wavelength Red LED Lighting on Quality and Aroma Expression of Hydroponic Fennel (*Foeniculum vulgare* Mill.)

This chapter is in preparation for submission to *Food Chemistry.*

Author Details: Jingsi Liu[1], Adam Sumner[2], Alex Harris[2], Song Li[2], Bastiaan Bargmann[2], David Haak[2], Yun Yin[1]

[1] Department of Food Science and Technology, Virginia Tech, Blacksburg, VA

[2] School of Plant and Environmental Sciences, Virginia Tech, Blacksburg, VA

Abstract

Fennel (*Foeniculum vulgare* Mill.) is an aromatic herb cultivated worldwide. Narrow-wavelength red LED light is sensed by plant phytochromes and can regulate the accumulation of secondary metabolites such as aroma compounds, but the effects of supplemental red light on fennel aroma remain unclear. The study aimed to investigate the effects of narrow-wavelength red LED light on fennel aroma. Fennel was grown using nutrient film technology hydroponic systems with two treatments: natural greenhouse light (control) and supplemental red LED lighting (PPFD 100 $\mu mol \cdot m^{-2} \cdot s^{-1}$, $14h \cdot d^{-1}$). GC-MS-O was used for aroma characterization. RNA-seq was performed to study the gene expression changes. The results showed that supplemental red LED light positively affected fennel growth, increasing plant height and fresh biomass. Additionally, it significantly increased the total concentration of aroma-active compounds in fennel leaves, particularly phenylpropanoids such as *(E)*-anethole (sweet, anise) and estragole (anise, herbal). Differential expression analysis identified 1958 upregulated genes and 278 downregulated genes (> 1.5-fold change and adjusted $p < 0.05$). Supplemental red light regulated several genes involved in phenylpropanoid biosynthesis, such as eugenol synthase and isoeugenol synthase. Transcripts encoding the regulatory elements of phenylpropanoid biosynthesis pathway were also identified as differentially expressed. Our results provide insights into the molecular mechanism of aroma biosynthesis in fennel and demonstrate the potential of controlled environment and LED lighting to accelerate aroma improvement of culinary herbs.

Keywords

Fennel, red LED, hydroponic system, aroma, gene expression

4.1 Introduction

With rising awareness of health and wellbeing, consumers are seeking high-quality fresh produce rich in flavor and beneficial phytochemicals, or plant secondary metabolites. Controlled environment agriculture (CEA) is a promising strategy to provide year-round supply of fresh produce while enhancing product quality through the regulation of environmental factors (Benke & Tomkins, 2017; Rouphael, Kyriacou, Petropoulos, De Pascale, & Colla, 2018; Zhang et al., 2024). Light, the primary energy source for plant growth and development, is of particular interest to CEA growers and researchers. Supplemental lighting is often used in CEA to extend the photoperiod or enhance light quantity for crop production. In recent years, the use of light-emitting diodes (LED) in CEA and indoor agriculture has increased due to their energy efficiency and precise spectral control (Ibaraki, 2017). Studies have shown that light spectral quality, intensity, and photoperiod can impact the accumulation of secondary metabolites in plants grown under controlled conditions and largely affect their flavor, appearance, and nutritional value (Alrifai, Hao, Marcone, & Tsao, 2019; Meng & Runkle, 2018; Zhang et al., 2021).

It is crucial to understand how lighting regulates the biosynthesis of important secondary metabolites for cultivating high-quality fresh produce in controlled environments. However, this area has not been fully understood, with mixed results observed across different plant species and different lighting systems applied (Appolloni et al., 2022; Livadariu, Maximilian, Rahmanifar, & Cornea, 2023). Plants respond to light through photoreceptors, which are proteins that sense light signals and trigger downstream morphological and physiological responses (Paik & Huq, 2019). The main photoreceptors in plants include phytochromes, cryptochromes, phototropins, zeitlupes, and UVR8, each

sensitive to different part of the light spectrum (Appolloni et al., 2022). Since LEDs can emit light at specific wavelengths within and near the photosynthetically active radiation (PAR) range, they can be used to regulate the production of plant secondary metabolites by targeting different photoreceptors. Within the PAR range (400-700 nm), red (R) light wavelengths (~650 nm) fall within the absorption spectra of chlorophylls and phytochromes, making them more efficiently absorbed than other wavelengths in the visible spectrum (Brazaityte et al., 2019; Alrifai et al., 2019). Phytochromes also sense far-red (FR) light due to their two interconvertible forms, Pr and Pfr, which have absorption peaks at approximately 660 nm and 730 nm, respectively. The R/FR ratio is an important regulatory factor for phytochrome-mediated photomorphogenic responses (Quail, Boylan, Parks, Short, Xu, & Wagner, 1995), significantly impacting many phytochrome-dependent processes and ultimately affecting plant biomass. A combination of R and blue (B) LED light (~450 nm) is also commonly used because their absorption peaks correspond to those of chlorophyll *a* and *b* (Amoozgar, Mohammadi, & Sabzalian, 2017), which makes RB LED light suitable for enhancing photosynthesis and aiding plant growth. LEDs emitting R and B wavelengths are considered to have higher photon efficiency, making them widely used in CEA (Contreras-Avilés, Heuvelink, Marcelis, & Kappers, 2024). Notably, many studies have shown that supplemental red LED light can increase the content of certain secondary metabolites in various vegetables and herbs (Bantis, Smirnakou, Ouzounis, Koukounaras, Ntagkas, & Radoglou, 2018; Chen, Xue, Guo, Wang, & Qiao, 2016; Zhang et al., 2021) by regulating genes that encode enzymes involved in the secondary metabolite biosynthetic pathways.

Fennel (*Foeniculum vulgare* Mill.), a biennial or perennial herb in the Apiaceae family, has been used by humans since ancient times for both culinary and medicinal purposes. Fennel has become an economically important crop and is cultivated worldwide. Its annual production, along with several other herbs and spices, exceeded 2,803,164 tons in 2022 (FAO, 2022). Fennel is highly aromatic with a sweet, anise-like flavor. As the key quality characteristic, its unique aroma has been studied using different extraction methods combined with gas chromatography-mass spectrometry (GC-MS) (Afifi, El-Mahis, Heiss, & Farag, 2021; Díaz-Maroto, Díaz-Maroto Hidalgo, Sánchez-Palomo, & Pérez-Coello, 2005; Xiao, Chen, Niu, & Chen, 2017; Zeller & Rychlik, 2006). Over 110 volatile organic compounds have been identified in fennel plants and their products, such as fennel seeds, tea, or essential oils. These compounds are mainly phenylpropanoids, terpenoids, aldehydes, and ketones produced through secondary metabolism. Among these, *(E)*-anethole is considered as the main aroma compound of fennel flavor due to its sweet, licorice odor and, in most cases, being the most abundant compound. Other volatile compounds in relatively high amounts include *α*-phellandrene, *α*-pinene, estragole, and *p*-anisaldehyde, with some variations relating to genotype and growing region. These volatile compounds not only contribute to fennel aroma and taste, but also have potential health benefits including antioxidant, antimicrobial, and anti-inflammatory activities (Badgujar, Patel, & Bandivdekar, 2014). Interestingly, recent studies have found that red LED light significantly increased the growth and secondary metabolites content in herbs belonging to the Apiaceae family, such as dill (*Anethum graveolens* L.), chervil (*Anthriscus cerefolium* L. Hoffm.), and parsley (*Petroselinum crispum*) (El Haddaji et al., 2023; Litvin, Currey, & Wilson, 2020). However, there is still very limited research on the influence of red LED

light on fennel growth and aroma development, despite the great economic value associated with this herb. In addition, few genetic studies have been conducted on fennel and many challenges remain, including incomplete transcriptome assembly and partial sequence annotation (Palumbo, Vannozzi, Vitulo, Lucchin, & Barcaccia, 2018).

To fill this research gap, the present study aims to determine the influence of supplemental red LED light on the growth, aroma, and gene expression of hydroponic grown fennel and identify key genes that contribute to aroma formation and accumulation triggered by red LED light in fennel. The key aroma-active compounds in fennel were identified by GC-MS coupled with olfactometry and quantified using multiple quantitation internal standards and standard addition method. Moreover, RNA sequencing (RNA-seq) was applied to generate gene expression profiles of fennel grown under supplemental red LED light and control conditions. Since a complete fennel genome is not yet available, we used *de novo* transcriptome assembly, which also enables discovery of novel genes involved in light-induced aroma formation. Our study focused on differentially expressed genes (DEGs) involved in secondary metabolite biosynthesis pathways and the transcription factors (TFs) that may modulate light regulation of fennel aroma. Overall, we provide new insights into the light regulation of aroma development in fennel and enhanced flavor profiles of culinary herbs using LED technology in controlled environmental conditions.

4.2 Materials and methods

4.2.1 Plant materials and growth conditions

Fennel (*Foeniculum vulgare* Mill., cv. Grosfruchtiger) was grown in a glass-glazed greenhouse located in Blacksburg, VA (lat. 37.2 °N) from March to May 2023. Fennel

seeds were obtained from a commercial source (Johnny's Selected Seeds, Winslow, ME) and were sown in rockwool propagation cubes saturated with water. Seedlings were irrigated daily and were allowed to grow for three weeks under natural sunlight before being transplanted into nutrient film technology (NFT) hydroponic units (NFT0406, CropKing, Lodi, OH). After transplanting, all plants continued to receive natural sunlight, while half of them received supplemental red LED light. Reflective color of fennel leaves was measured in CIE *L a b* color scale with a Minolta CR-300 Chroma Meter (Minolta Co., Osaka, Japan). Fennel leaves and stems from each plant were collected after six weeks, flash frozen in liquid nitrogen, and stored at -80 °C until further analysis.

Greenhouse temperature was maintained using an environmental controller (Step Control, Wadsworth Control Systems, Arvada, CO). The temperature was set to 24 °C during the day and 21 °C during the night. Temperature and humidity were recorded at 5-minute intervals with a data logger (Watchdog 1650 Micro Station, Spectrum Technologies, Aurora, IL). The pH and electrical conductivity (EC) of each NFT unit were monitored daily. The pH of the nutrient solution was maintained within the range of 5.8-6.2 and the EC was kept within the range of 1.4-1.6 $dS \cdot m^{-1}$, using a portable pH/EC meter (HI98131, HANNA Instruments, Smithfield, RI). To adjust the pH, phosphoric and citric acid (reduce pH, General Hydroponics, Sebastopol, CA) and potassium hydroxide and potassium carbonate (raise pH, General Hydroponics, Sebastopol, CA) were used. EC was adjusted using deionized water and 2-1-6 and 5-0-1 liquid fertilizers. The greenhouse parameters, including average daylight hours, daily light integral (DLI), maximum and minimum greenhouse temperature, and humidity are shown in Supplemental Table 4-1.

4.2.2 LED treatment

Supplemental light is provided by red LED lighting strips (HighLight Series, Super Bright LEDs Inc., MI) from 0600 to 2000 HR (14 hrs./day), controlled by an outlet timer. The peak wavelength of red LED light produced by these strips was 631 nm. The NFT unit was placed under the red LED lighting system such that plants received an average PPFD of 100 $\mu mol \cdot m^{-2} \cdot s^{-1}$. The PPFD measurement across the growth area was performed by recording the light intensity of the LEDs without sunlight using a spectrometer (MK350S, UPRTek, Taiwan). The desired PPFD was achieved by adjusting the distance between LED and the plant canopy. As the plants grew taller, LEDs light sources were elevated to maintain a constant distance between LEDs and the plant canopy. Sunlight was measured with a quantum PAR light sensor (3668I, Spectrum Technologies, Aurora, IL) in a radiation shield (3663A, Spectrum Technologies, Aurora, IL) at 5 min intervals. The average daylight hours were between 12.12 to 13.59 hrs. (Supplemental Table 4-1). The average, maximum, and minimum mid-day PAR light value (from 11:00 a.m. to 1:00 p.m.) over the course of the experiment were 720.4, 1286.4, and 260.3 $\mu mol \cdot m^{-2} \cdot s^{-1}$, respectively.

4.2.3 Chemicals and standards

The chemicals and authentic standards for aroma compounds were purchased from the following vendors: n-alkane (C7-C30), *(E)*-anethole (≥99%), *p*-anisaldehyde (≥97.5%), carvacrol (≥99%), *p*-cymenene (≥98%), decane (≥99.8%), estragole (≥96%), fenchone (98%), linalool (≥97%), methyl eugenol (≥98%), 2-octanol (≥97%), 1-octen-3-ol (≥98%), α-phellandrene (≥75%), 1-phenylethanol (98%), phenyl acetaldehyde (≥95%), α-pinene (98%), and γ-terpinene (≥95%) were purchased from Sigma-Aldrich (St. Louis, MO). *(Z)*-Anethole was purchased from Toronto Research Chemicals (Toronto, Canada). *(Z)*-3-

hexenal (50% in triacetin) and *(E)*-2-hexenal (98%) were kindly provided by Bedoukian Research Inc. (Danbury, CT). Tridecane (>99%) was purchased from Tokyo Chemical Industry Co., Ltd. America (Portland, OR). (-)-bornyl acetate (95%) was purchased from Alfa Aesar (Haverhill, MA). Methanol (HPLC grade) was obtained from Fisher Scientific (Fair Lawn, NJ).

4.2.4 Extraction of aroma compounds with solid phase microextraction (SPME)

The extraction of fennel aroma compounds was conducted using the methodology described in our previous study (Liu et al., 2024). Briefly, frozen fennel tissue was ground to a fine powder using liquid nitrogen, and then 50 ± 0.5 mg of fennel powder was weighed into a 20 mL clear vial (Supelco, Bellefonte, PA). The vial was spiked with 36.4 ng decane, 4.8 ng 2-octanol, and 99.0 ng 1-phenylethanol as internal standards (IS) for quantitation. The headspace of the SPME vial was equilibrated for 10 min at 50 °C. Following equilibration, a preconditioned 1 cm 50/30 divinylbenzene/carboxen/polydimethylsiloxane (DVB/CAR/PDMS) fiber (Supelco, Bellefonte, PA) was exposed to the headspace for 30 min at 50 °C for the extraction of volatile compounds.

4.2.5 Aroma characterization by gas chromatography-mass spectrometry-olfactometry (GC-MS-O)

Aroma characterization was conducted with an Agilent 6890N GC (Santa Clara, CA), a 5975B mass selective detector (MSD) (Agilent Technologies Inc., Santa Clara, CA), and a PHASER sniff port (GL Sciences, Eindhoven, the Netherlands). The separation of volatile compounds was performed using a DB-WAX capillary column (30 m × 0.25 mm i.d., film thickness = 0.25 μm) (Supelco, Bellefonte, PA) with helium as the carrier gas at

a flow rate of 2 mL/min (67.9 cm/s). The injection port temperature was maintained at 230 °C in splitless mode. The column temperature program was as follows: hold for 5 min at 40 °C, 40-80 °C (8 °C/min), 80-152 °C (5 °C/min), 152-225 °C (8 °C/min), and hold for 15 min at 225 °C. Other parameters of MSD were as follows: interface temperature was 230 °C; ionization energy was 70 eV; mass range was 33-500 amu; EM voltage was Atune + 200V; scan rate was 5.15 scans/s. The effluent from the column was divided equally between the sniff port and the MSD. The eluting volatile compounds were combined with humidified air with a flow rate of 5 mL/min.

Three trained panelists (two females and one male) aged between 20 and 27 years old were selected to perform GC-O. All panelists participated in three training sessions using 27 aroma standards found in fennel so that they were able to recognize and describe common fennel aroma compounds. The sniffing of each fennel sample was 30 min, and panelists were asked to record retention time, aroma description, and intensity of the odorants perceived during the sniffing. Odor intensity was estimated based on a five-point scale.

4.2.6 Aroma identification and quantitation

Aroma compounds were screened based on GC-O results. These compounds were then identified by comparing mass spectra (NIST 17 library), retention indices, and odor characteristics with reference aroma standards. Retention indices of aroma compounds were calculated based on the equation described by van Den Dool & Kratz (1963) using the retention time of a C_7-C_{30} alkane solution.

Quantitation of aroma compounds was performed according to the methodology developed in a previous study (Liu et al., 2024). Briefly, a “blank” odorless fennel powder

was used as the sample matrix, which was spiked with a fixed concentration of IS and a series of aroma standards at different concentrations, then analyzed by GC-MS to construct linear regression equations. The "blank" fennel powder was achieved by incubating the sample under 50 °C with regular nitrogen purge of the headspace. Prior to the construction of linear regression equations, the "blank" fennel powder was analyzed by GC-MS to ensure the absence of or only negligible peaks in the resulting chromatogram. The linear regression equations were constructed using peak area ratio and mass ratio of aroma standards to their responding IS. The mass of each analyte in all fennel samples then can be determined using the corresponding regression equation, the known mass of IS, and the peak area ratio of target analyte to IS. The concentration of each analyte was calculated by dividing the mass of analyte by the mass of fennel powder in a vial. The odor activity value (OAV) was calculated by dividing the concentration of each analyte (fresh weight basis) by their previously published odor detection threshold in water (Erten & Cadwallader, 2017).

4.2.7 RNA extraction and sequencing

Total RNA was extracted from approximately 50 mg of fennel leaf tissue using the Qiagen RNeasy Plant Mini Kit (Hilden, Germany) and treated with the Qiagen RNase-free DNase Set (Hilden, Germany) according to manufacturer's instructions. There were three biological replicates for both control and red LED light treatments, each replicate contained leaf tissue from three different plants. After extraction, the sample quantity and quality were evaluated by the Thermo Scientific NanoDrop spectrophotometer (Waltham, MA) ($A260/A280 \geq 2.0$, $A260/A230 \geq 2.0$). In addition, the RNA integrity was analyzed using the Agilent RNA 6000 Pico Kit (Santa Clara, CA) and Agilent 2100 bioanalyzer (Santa

Clara, CA). Samples with an RNA Integrity Number (RIN) greater than 7 were considered suitable for sequencing. Library preparation and RNA-seq were conducted by Novogene (Sacramento, CA) using the Illumina NovaSeq platform (HWI-ST1276) with paired-end, 150 bp read sequencing strategy.

4.2.8 RNA sequencing based transcriptome analysis

RNA-seq reads from the three biological replicates were merged and assembled into a *de novo* transcriptome from all available reads using Trinity (v2.15.1), with the resulting assembly containing 211,514 contigs (Grabherr et al., 2011). Functional annotation of the assembly was performed using Trinotate (Bryant et al., 2017) for Gene Ontology (GO) and Kyoto Encyclopedia of Genes and Genomes (KEGG) pathway enrichment analysis. Differential gene expression data was obtained using the Bioconductor package DESeq2, version 1.42.1 (Love et al., 2014). Assembled transcripts with |log2Fold Change| > 1.5 (adjusted P-value < 0.05 using the Benjamini-Hochberg adjustment) were considered differentially expressed genes (DEG) and used in the analysis.

4.2.9 Statistical analysis

Growth parameters and aroma compounds concentrations between control and red LED light treated fennel plants were compared by t-test. The significance cutoff was set to $p<0.05$. Principal component analysis (PCA), hierarchical heatmap clustering, and graph construction were performed using R (version 4.3.1). R packages used for data analysis and graph construction were provided in Appendix D.

4.3 Results and discussion

4.3.1 Fennel growth affected by red LED light

As shown in Table 4-1, supplemental red LED light significantly affected several growth parameters of hydroponic fennel. Compared to the control group, fennel plants exposed to red LED light exhibited significant increases in fresh biomass, plant height, number of branches, and apparent moisture content, which indicates that red LED light has a positive impact on fennel growth and biomass production. The average dry biomass was also higher for plants exposed to supplemental red LED light, suggesting enhanced biomass accumulation despite increased apparent moisture content. Additionally, these plants appeared greener, as indicated by a significantly lower negative *a* value. Though not statistically significant, they also showed a lower positive *L* value (indicating a darker color) and a higher positive *b* value (indicating more yellowness) (Table 4-1). This is likely caused by the changes in chlorophyll content, which will be investigated in follow-up studies.

Remarkably, supplemental red LED light resulted in a 57% increase in fresh biomass and a 64% increase in dry biomass. Beyond natural sunlight, the supplemental red LED light provided an additional 5.04 $mol \cdot m^{-2} \cdot d^{-1}$ daily light integral (DLI) to the fennel plants, which was a major factor contributing to these increases. Previous research has extensively documented the critical role of photosynthetic DLI in plant biomass accumulation (Faust, Holcombe, Rajapakse, & Layne, 2005; Faust & Logan, 2018; Hammock, Kopsell, & Sams, 2023). Our findings are consistent with a recent study on dill and parsley, which demonstrated that increased DLI promoted dry mass accumulation, particularly when environmental temperatures range between 18.4 to 27.2 °C (Walters &

Lopez, 2021). Another contributing factor is the prolonged photoperiod of red LED light group. Since the growth experiment was performed from March to May, the average daylight hours ranged between 12.12 to 13.59 hrs. (Supplemental Table 4-1), shorter than the photoperiod provided by red LED light (14 hrs.). In terms of spectral quality, the addition of supplemental red LED light increased the R/FR ratio compared to the control group, which also affect photosynthesis and regulates plant development and morphology (Demotes-Mainard et al., 2016; Tan et al., 2022).

Table 4-1. Influences of supplemental red LED light on fennel morphology and growth

Growth parameters	Control fennel	Red LED light fennel	p value
Apparent moisture content (%)	85.64 ± 1.59	89.30 ± 1.08	0.030
Fresh biomass (g)	55.78 ± 22.33	87.56 ± 39.65	0.016
Dry biomass (g)	47.77 ± 19.13	78.19 ± 35.41	0.010
Number of branches	16.13 ± 5.17	21.00 ± 5.14	0.017
Height (cm)	33.87 ± 6.82	41.13 ± 10.41	0.033
Width (cm)	39.42 ± 6.16	41.02 ± 6.56	0.496
L	26.23 ± 2.93	22.76 ± 2.13	0.174
a	-12.63 ± 0.76	-14.17 ± 0.55	0.047
b	18.75 ± 1.58	20.25 ± 1.64	0.317

The width is calculated by taking the average of two perpendicular widths of plant canopy. The results are expressed as mean ± standard deviation, and p value is calculated with two-sample t-test assuming equal variances.

4.3.2 Fennel aroma compounds affected by red LED light

A total of 23 aroma compounds in fennel were identified by SPME-GC-MS-O, and their quantitation results by standard addition method (SAM) are shown in Table 4-2. Calibration curves for SAM quantitation are shown in Supplemental Table 4-2. Odor activity values (OAVs) were calculated for 16 compounds based on the quantitation results and published odor detection thresholds in water. Overall, *(Z)*-3-hexenal ("leafy, grassy") had the highest OAV. Other potent aroma compounds with relatively high OAVs (>50) in fennel were *(E)*-anethole ("sweet, anise"), estragole ("anise, herbal"), *α*-pinene ("pine, woody"), *(E)*-2-hexenal ("leafy, green"), *p*-anisaldehyde ("floral, sweet"), *α*-phellandrene ("herbal, woody"), phenyl acetaldehyde ("floral, sweet"), fenchone ("herbal") and linalool ("floral"). The identified aroma compounds include six phenylpropanoids, four monoterpenes, four aldehydes, three monoterpenoids, three sesquiterpenes, two alcohols, and one alkane. Among these compounds, phenylpropanoids were the most abundant group (Figure 4-1), accounting for approximately 65% ~ 83% of the total volatile compounds, followed by monoterpenes (6% ~ 17%), monoterpenoids (5% ~ 11%), and aldehydes (4% ~ 11%). Our fennel aroma characterization results align with previous studies (Afifi et al., 2021; Díaz-Maroto et al., 2005; Zeller et al., 2006), with some variations in aroma compounds and concentrations due to different cultivars and production location. Many of these volatile compounds also contribute to the "leafy", "woody", and "sweet" notes of other culinary herbs such as dill (Pino, Rosado, Goire, & Roncal, 1995), basil (Lee, Umano, Shibamoto, & Lee, 2005), and mint (Nguyen & Saleh, 2019), representing an essential aspect of herb flavor and quality.

Table 4-2. Concentration of aroma-active compounds in fennel grown under supplemental red LED light

No.	Compound	RI	RI Ref. [a]	Identification method [b]	Odor Description	Odor Intensity [c]		Odor threshold in water (μg/g)	Concentration (μg/g fennel, dry weight)		OAV	
						Control	Red LED		Control	Red LED	Control	Red LED
	Monoterpenes											
1	*α*-pinene	1011	1011	MS, RI, OD, AS	Pine, woody	W	W	0.006[1]	1078.91 ± 216.42^{A}	1556.28 ± 505.60^{A}	25813	27744
2	*α*-phellandrene	1153	1157	MS, RI, OD, AS	Herbal, woody	M	W	0.2[2]	1061.18 ± 125.49^{A}	1179.55 ± 364.40^{A}	762	631
3	*γ*-terpinene	1239	1233	MS, RI, OD, AS	Oily, herbal	M	M	1[3]	12.13 ± 4.78^{A}	18.67 ± 11.25^{A}	2	2
4	allo-ocimene	1371	1366	MS, RI, OD	Herbal, terpenic	M	M	0.727[4]	1.77 ± 0.07^{B}	2.47 ± 0.14 ^{A}	0.3	0.4
	Sesquiterpenes											
5	*γ*-muurolene	1697	1690	MS, RI, OD	Spice, woody	M	ND	ND	3.40 ± 0.36^{A}	3.93 ± 0.69^{A}	ND	ND
6	germacrene D	1719	1717	MS, RI, OD	Spice, clove	M	W	ND	11.17 ± 3.44^{A}	14.31 ± 2.81^{A}	ND	ND
7	*α*-cadinene	1816	1815	MS, RI, OD	Woody, fresh	W	W	ND	1.96 ± 0.32^{A}	2.47 ± 0.07^{A}	ND	ND
	Alkane											
8	tridecane	1303	1300	MS, RI, OD, AS	Mushroom, oily	M	W	ND	0.94 ± 0.01^{B}	1.26 ± 0.01^{A}	ND	ND
	Alcohols											
9	1-octen-3-ol	1451	1451	MS, RI, OD, AS	Earthy, mushroom	M	S	0.001[1]	ND	ND	ND	ND
10	linalool	1552	1552	MS, RI, OD, AS	Floral	W	M	0.006[1]	2.78 ± 0.74^{A}	5.35 ± 2.02^{A}	66	95
	Aldehydes											
11	*(Z)*-3-hexenal	1130	1134	MS, RI, OD, AS	Leafy, grassy	W	M	0.00025[1]	91.75 ± 51.20^{A}	155.09 ± 59.99^{A}	52681	66355
12	*(E)*-2-hexenal	1218	1218	MS, RI, OD, AS	Leafy, green	W	W	0.017[1]	638.62 ± 102.06^{A}	983.06 ± 452.49^{A}	5393	6185
13	phenyl acetaldehyde	1634	1632	MS, RI, OD, AS	Floral, sweet	W	M	0.004[1]	6.71 ± 7.37	ND	241	ND

14	*p*-anisaldehyde	2019	2016	MS, RI, OD, AS	Floral, sweet	M	M	0.047[5]	342.70 ± 82.18[B]	1179.15 ± 381.80[A]	1047	2684
	Monoterpenoids											
15	fenchone	1398	1392	MS, RI, OD, AS	Herbal	M	W	0.44[5]	1025.81 ± 339.24[A]	1888.42 ± 468.81[A]	340	459
16	bornyl acetate	1583	1580	MS, RI, OD, AS	Woody, pine	M	M	0.075[1]	3.67 ± 3.48[A]	5.78 ± 4.54[A]	7	8
17	carvacrol	2231	2233	MS, RI, OD	Herbal, oregano	M	S	1.7[4]	2.91 ± 0.34[B]	4.87 ± 0.30[A]	0.2	0.3
	Phenylpropanoids											
18	estragole	1669	1661	MS, RI, OD, AS	Anise, herbal	M	S	0.0075[2]	344.22 ± 23.08[B]	902.19 ± 107.08[A]	6588	12867
19	*(Z)*-anethole	1754	1732	MS, RI, OD	Sweet, anise	M	M	ND	84.42 ± 4.50[B]	116.38 ± 4.31[A]	ND	ND
20	*(E)*-anethole	1846	1838	MS, RI, OD, AS	Sweet, anise	S	S	0.073[5]	9040.43 ± 606.24[B]	23961.19 ± 1782.47[A]	17778	35110
21	methyl eugenol	2000	2003	MS, RI, OD, AS	Clove, sweet	W	W	0.82[1]	10.16 ± 1.39[B]	13.47 ± 0.23[A]	2	2
22	methyl isoeugenol	2174	2176	MS, RI, OD	Clove, woody	M	VW	1.6[5]	20.92 ± 4.88[A]	38.32 ± 10.06[A]	2	3
23	apiol	2361	2431	MS, RI, OD	Parsley, green	W	M	ND	106.62 ± 151.82[A]	21.45 ± 5.36[A]	ND	ND

[a] Reference retention indices are from NIST publication (Babushok, Linstrom, & Zenkevich, 2011).

[b] Identification method: mass spectra (MS), retention index (RI), odor descriptors (OD) against authentic aroma standards (AS).

[c] Odor intensity: very weak (VW), weak (W), medium (M), strong (S), and very strong (VS). Not determined (ND).

Two out of three panelists smelled the compound.

One out of three panelists smelled the compound.

[1] Odor threshold obtained from Leffingwell & Associates (http://www.leffingwell.com/odorthre.htm).

[2] Odor threshold obtained from literature (Rychlik, Schieberle, & Grosch, 1998).

[3] Odor threshold obtained from literature (van Gemert, 2003).

[4] Odor threshold obtained from literature (Zhang, Guan, Liang, Wang, Wu, & Liu, 2023).

[5] Odor threshold obtained from literature (Zeller et al., 2006).

[AB] represent the mean comparasion of compounds between control and red LED light samples by t-test at $p < 0.05$. The results are expressed as mean ± standard deviation.

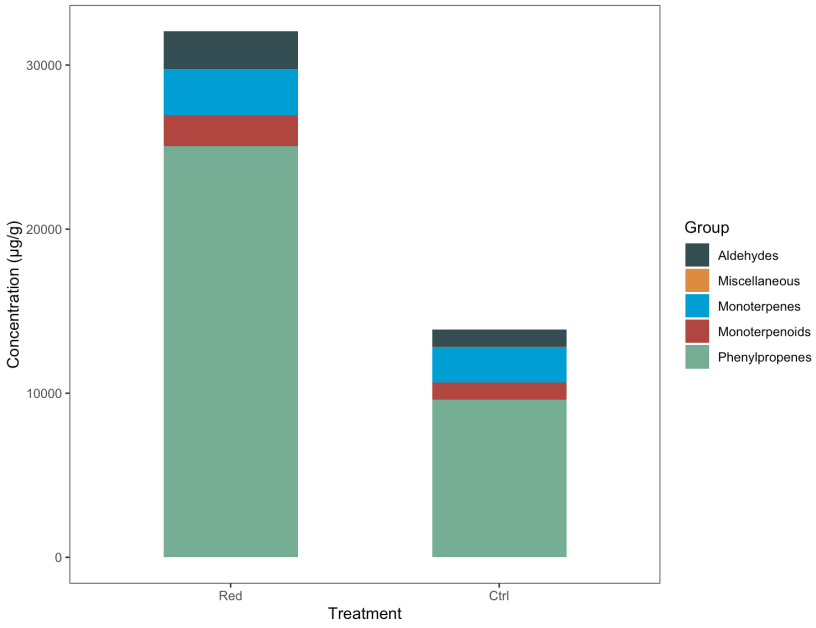

Figure 4-1. Bar graph of concentration of aroma compounds in different volatile groups affected by red LED light.

Supplemental red LED light significantly changed the volatile profile and aroma concentration of hydroponic fennel. The total aroma level (on a dry weight basis) increased by 130% under supplemental red LED, from 13.89 to 32.05 mg/g. The concentration of phenylpropanoids, the most important and character-impact aroma group, increased 2.6 times, from 9.61 to 25.05 mg/g. The increase primarily resulted from four aroma compounds: *(E)*-anethole, estragole, *(Z)*-anethole, and methyl eugenol, were all significantly elevated compared to the control group. Methyl eugenol also increased under red LED light but was not statistically different. Apiol was the only phenylpropene that decreased in concentration under red LED light, likely caused by an unusually high concentration in one outlier from the control group (Figure 4-2). Other chemical groups also showed varying degrees of increase under supplemental red LED light. Specifically, four other compounds increased significantly, including 1 monoterpene, allo-ocimene, 1

monoterpenoid, carvacrol, 1 aldehyde, *p*-anisaldehyde, and 1 alkane, tridecane. The increase in the rest of the aroma compounds was not significantly different. However, one aldehyde, phenyl acetaldehyde, was only detected and quantified by GC-MS in control fennel. These changes are crucial for elucidating the mechanisms of red light-induced changes in aroma accumulation and secondary metabolism.

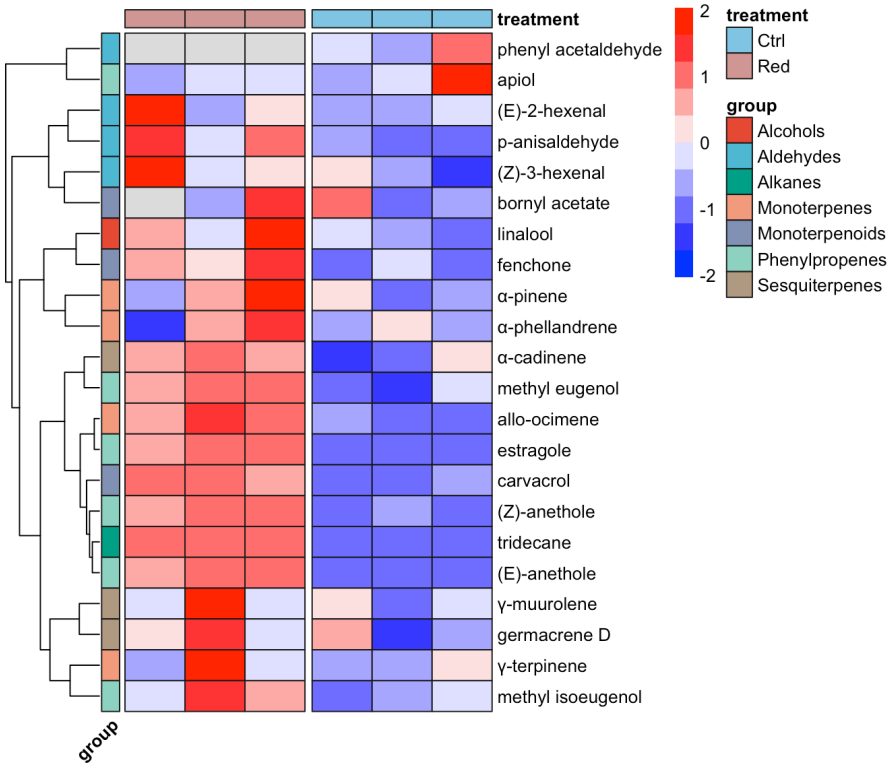

Figure 4-2. Hierarchical clustering heatmap showing the levels of aroma compounds in control and red LED light treated fennel.

The aroma compound concentrations of each sample are centered and scaled in the row direction, as indicated by the color scale between -2 to 2.

Principal component analysis (PCA) is a technique for examining the overall difference between groups and the variances within groups (Li et al., 2021). PCA was used to distinguish the aroma profiles between red LED light and control fennel, as shown in

the biplot in Figure 4-3. The PCA results indicated that the first principal component (PC1) accounted for 59.3% of the total variance and effectively separated the red LED light and control groups, while the second principal component (PC2) explained 17.9% of the total variance. The compounds with the most differentiation power on PC1 were *(E)*-anethole, *(Z)*-anethole, estragole, methyl eugenol, and carvacrol, consistent with quantitation results, as these compounds were significantly increased under red LED light. On the other hand, samples from control and red LED light groups did not distinctly separate on PC2, suggesting some variability in aroma composition within each treatment group. The loading plot further explained the variances in aroma compounds caused by supplemental red LED light. A positive correlation was observed between red LED light samples and most aroma compounds on the negative side of PC1, while a correlation between control samples and apiol was found on the positive side of PC1. These results suggest that the volatile profile and aroma accumulation in fennel dynamically changed under supplemental red LED light, with individual differences within plants of the same treatment.

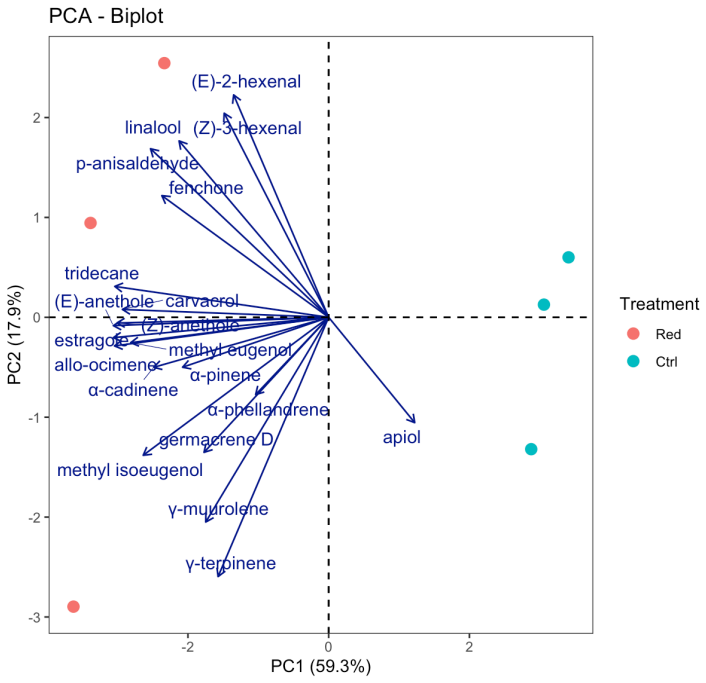

Figure 4-3. Principal component analysis based on aroma compound concentrations in control and red LED light treated fennel.

To further demonstrate the accumulation pattern of aroma compounds under the influence of red LED light, a hierarchical cluster heatmap was generated using normalized aroma concentrations from two treatment groups, with Euclidean distance as the clustering distance measure (Figure 4-2). There were two main clusters, showing that most aroma compounds had higher content in red LED light samples, except for phenyl acetaldehyde and apiol. The results suggest that supplemental red LED light is a promising tool for increasing aroma accumulation in hydroponic fennel.

4.3.3 Transcriptome analysis and differentially expressed genes (DEGs) in fennel leaf tissue

To further investigate the molecular mechanism underlying the positive effects of red light on fennel aroma and to identify potential genes involved in light-induced changes

in aroma composition, transcriptome analysis was performed using RNA-seq. Libraries from fennel leaf tissue generated an average of 58.4 million reads with 45.4% GC content (Supplemental Table 4-3).

Compared to the control samples, the number of upregulated DEGs was much higher than the number of downregulated DEGs in fennel treated with red LED light. Using the selection criteria of |log2Fold Change| >1.5 and adjusted p value <0.05, a total of 2236 DEGs were identified, with 1958 upregulated and 278 downregulated by red LED light treatment (Figure 4-4). Functional annotation of these DEGs with gene ontology and KEGG terms was performed using Trinotate. Among the upregulated DEGs, 829 GO terms were identified, while 343 GO terms were associated with the downregulated DEGs. In terms of biological process, the upregulated DEGs were primarily involved in the regulation of DNA-templated transcription, protein phosphorylation, response to light stimulus, light harvesting photosynthesis, circadian regulation of gene expression, and circadian rhythm (Figure 4-5). Conversely, the downregulated DEGs were mainly enriched in response to abiotic stress (such as salt stress, cold, and water deprivation), flavonoid biosynthetic process, and response to auxin (such as indole butyric acid) (Supplemental Figure 4-1). The enrichment analysis showed that genes associated with photosynthesis light harvesting, especially the light harvesting in photosystem I (PSI), circadian rhythm, and rhythmic processes were significantly activated in red LED light treated fennel samples (Figure 4-6). Additional top-enriched GO terms for both upregulated and downregulated DEGs are shown in Supplemental Figure 4-1.

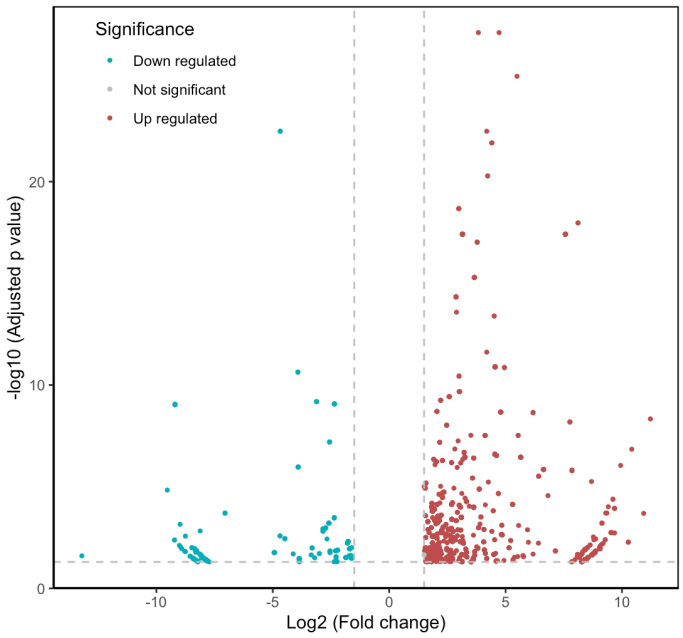

Figure 4-4. Volcano plot of up and down regulated DEGs affected by supplemental red LED light.

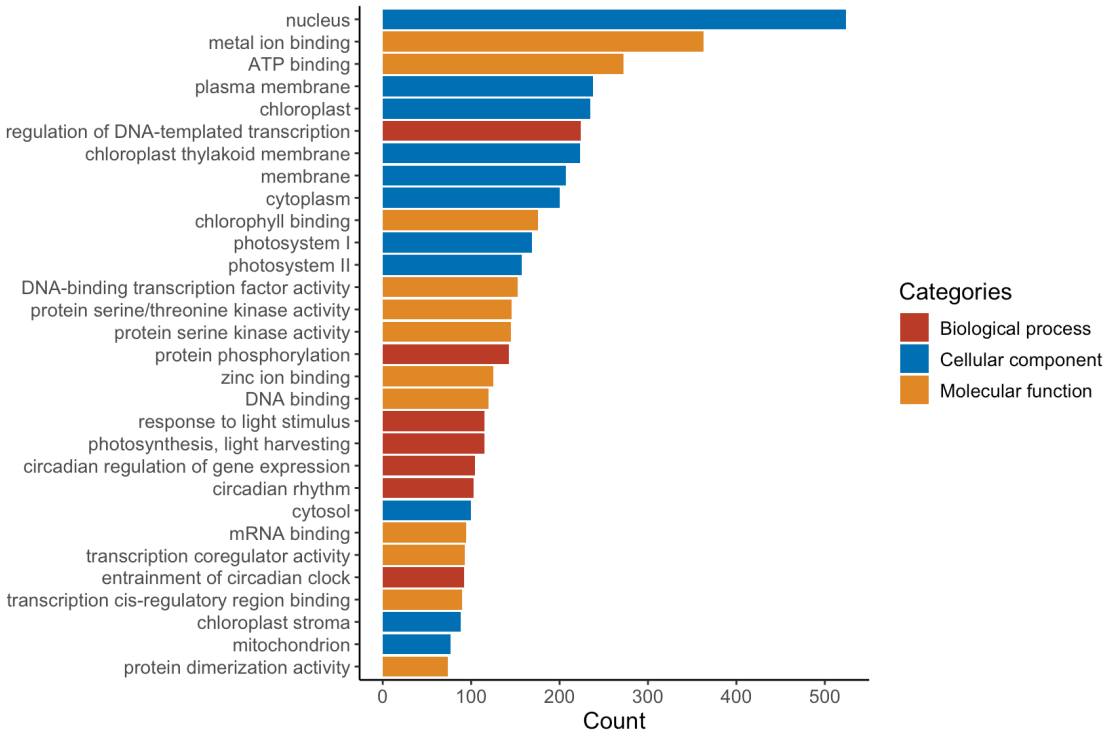

Figure 4-5. Enriched GO terms of genes upregulated by supplemental red LED light.

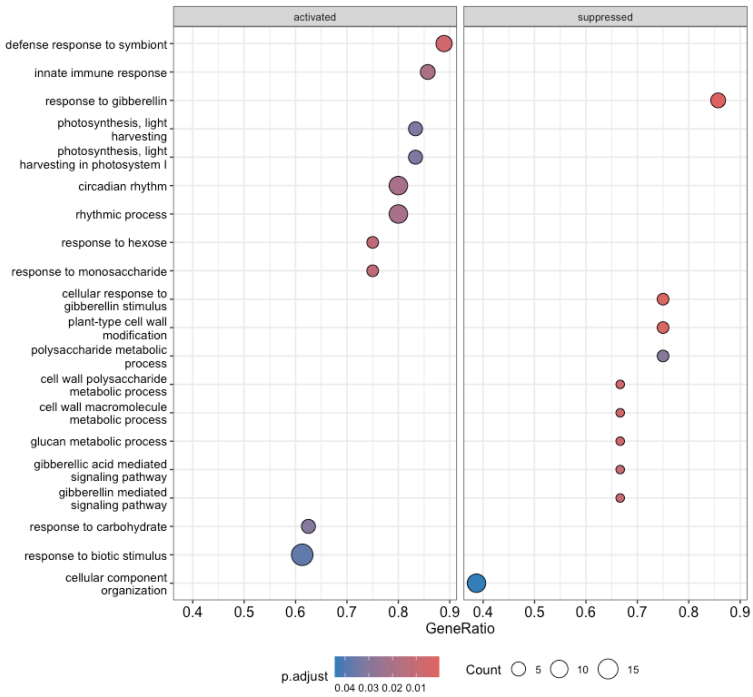

Figure 4-6. Gene set enrichment analysis on biological process GO terms affected by supplemental red LED light.

KEGG pathway enrichment analysis was performed with R package clusterProfiler using *Arabidopsis thaliana* as a model organism (Yu, Wang, Han, & He, 2012). Since a complete fennel genome was not available in KEGG at the time of this study, Trinotate was used to add KEGG annotations to transcripts based on homology. As shown in Figure 4-7, the only significantly enriched pathway identified is glutathione metabolism. Interestingly, the pathway "biosynthesis of secondary metabolites" was also enriched in upregulated DEGs, though it did not reach statistical significance (adjusted p value >0.05). As shown in Supplemental Figure 4-2, nine genes were putatively identified as being closely related to both "metabolic pathways" and "biosynthesis of secondary metabolites", including *CH1* (NCBI Gene ID 841029), *MS2* (NCBI Gene ID 821147), *ATTPS6* (NCBI Gene ID 843130), *TPPJ* (NCBI Gene ID 836638), *VTC2* (NCBI Gene ID 828792), *NRS/ER*

(NCBI Gene ID 842603), *AKR4C10* (NCBI Gene ID 818356), *SPDS3* (NCBI Gene ID 835392), and *PGK1* (NCBI Gene ID 820461). Additionally, *cPT4* (NCBI Gene ID 835991) was found to be closely related to "biosynthesis of secondary metabolites" but not to "metabolic pathways". A detailed description of these genes is provided in Supplemental Table 4-4. These identified genes may encode enzymes involved in red light-induced metabolic processes and changes in aroma composition. For example, the *PGK* (phosphoglycerate kinase) family of genes has been shown to play diverse roles in photosynthesis and glycolysis in maize (Massange-Sánchez, Casados-Vázquez, Juarez-Colunga, Sawers, & Tiessen, 2020).

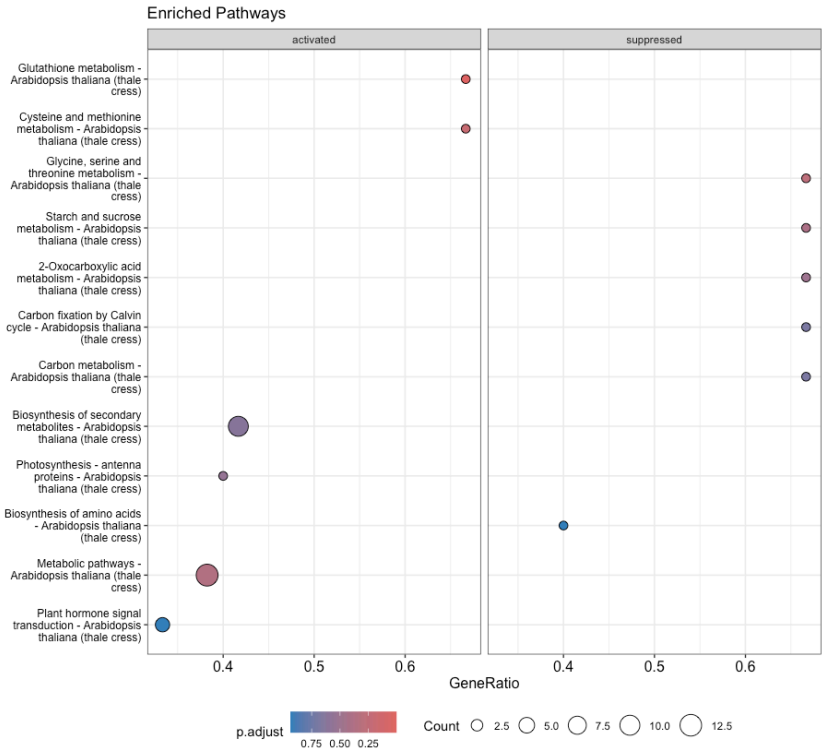

Figure 4-7. KEGG pathway enrichment analysis of DEGs affected by supplemental red LED light.

4.3.4 DEGs involved in secondary metabolite biosynthesis pathways

Phenylpropanoids are an important class of plant secondary metabolites and are the most abundant aroma compounds in hydroponic fennel. Analysis of aroma compounds revealed a significant increase in phenylpropanoids content in response to supplemental red LED light. We further investigated DEGs in the phenylpropanoid biosynthetic pathway (Figure 4-8). Phenylpropanoids are primarily derived from the aromatic acids L-phenylalanine (Phe) and L-tyrosine (Tyr) (Vogt, 2010), which are subsequently catalyzed by phenylalanine ammonia lyase (PAL) or tyrosine ammonia lyase (TAL) to cinnamic acid or *p*-coumaric acid. The phenylpropanoid biosynthetic pathway in plants involves many enzymes, including but not limited to, *trans*-cinnamate 4-monooxygenase (CYP73A), 4-coumarate CoA-ligase (4CL), cinnamoyl CoA reductase (CCR), cinnamyl alcohol dehydrogenase (CAD), and coniferyl alcohol acyltransferase (CFAT).

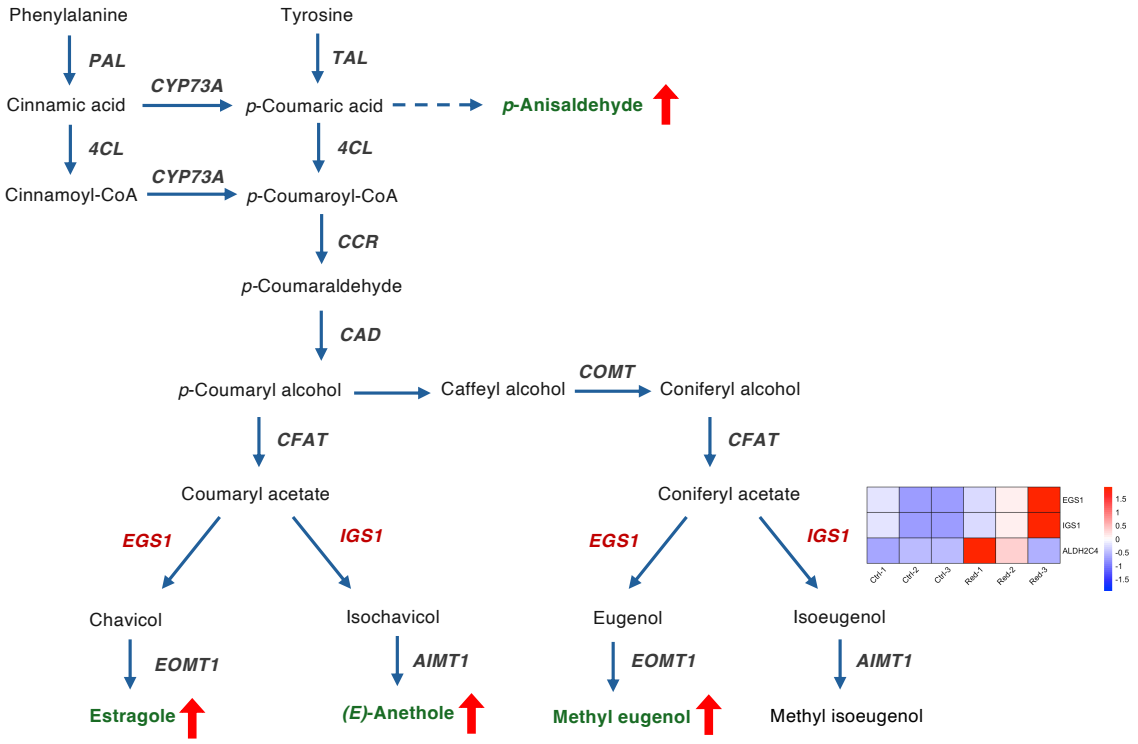

Figure 4-8. Biosynthesis pathway of phenylpropanoids in fennel affected by red LED light.

PAL: phenylalanine ammonia lyase, TAL: tyrosine ammonia lyase, CYP73A: trans-cinnamate 4-monooxygenase, 4CL: 4-coumarate CoA ligase, CCR: cinnamoyl CoA reductase, CAD: cinnamyl alcohol dehydrogenase, CFAT: coniferyl alcohol acyltransferase, EGS1: eugenol synthase, IGS1: isoeugenol synthase, AIMT1: trans-anol O-methyltransferase, EOMT1: eugenol O-methyltransferase, COMT: caffeic acid 3-O-methyltransferase, ALDH2C4: aldehyde dehydrogenase family 2 member C4. Volatile compounds that showed a significant increase under red LED treatment are highlighted in dark green. Solid arrows depict established enzymatic reactions, and dashed arrows depict unidentified enzymatic reactions. The gene expression levels of each sample are centered and scaled in the row direction, as indicated by the color scale.

Notably, three genes putatively encoding key enzymes involved in phenylpropanoid biosynthetic pathway were identified and exhibited higher expression levels in fennel samples exposed to red LED light. These includes eugenol synthase (EGS1), which catalyzes coumaryl acetate to chavicol and coniferyl acetate to eugenol; isoeugenol synthase (IGS1), which catalyzes coumaryl acetate to isochavicol, and coniferyl acetate to isoeugenol; and aldehyde dehydrogenase family 2 member C4 (ALDH2C4), which, while not directly involved in the phenylpropanoid biosynthetic pathway in fennel but is part of the broader family of enzymes contributing to diverse phenylpropanoid metabolism. The higher expression levels of these genes were consistent with the results of richer phenylpropanoids in red LED light treated fennel samples.

Fennel aroma compounds from other chemical groups, such as terpenoids and aldehydes, also showed increased concentrations in response to red LED light. Genes encoding key enzymes involved in terpenoid-related biosynthetic process (including monoterpenoid biosynthetic process, sesquiterpene biosynthetic process, isoprenoid metabolic process, terpene biosynthetic process, and terpenoid biosynthetic process), aromatic amino acid biosynthetic process, green leaf volatile biosynthetic process, aromatic compound biosynthetic, and secondary metabolic process were also identified, with higher expression levels observed in fennel samples exposed to red LED light (Figure 4-9). These findings suggest that the increased expression levels of many genes may be directly linked to the increased levels of various aroma compounds in fennel in response to supplemental red LED light.

Terpenoid biosynthetic process

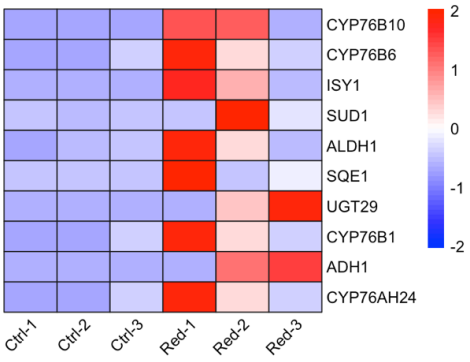

Gene name	Function
CYP76B10	Geraniol 8-hydroxylase
CYP76B6	Geraniol 8-hydroxylase
ISY1	(S)-8-oxocitronellyl enol synthase ISY1
SUD1	Probable E3 ubiquitin ligase SUD1
ALDH1	Aldehyde dehydrogenase 1
SQE1	Squalene monooxygenase SE1
UGT29	UDP-glucosyltransferase 29
CYP76B1	7-ethoxycoumarin O-deethylase
ADH1	Short chain aldehyde dehydrogenase 1
CYP76AH24	Ferruginol synthase

Aromatic amino acid biosynthetic process

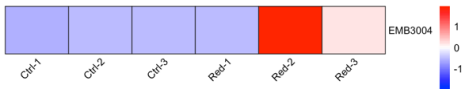

Gene name	Function
EMB3004	Bifunctional 3-dehydroquinate dehydratase/shikimate dehydrogenase, chloroplastic

Green leaf volatile biosynthetic process

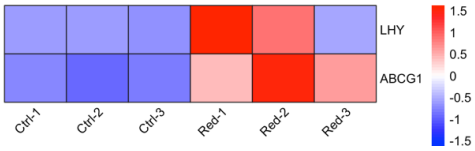

Gene name	Function
LHY	Protein late elongated hypocotyl
ABCG1	ABC transporter G family member 1

Aromatic compound biosynthetic and secondary metabolic process

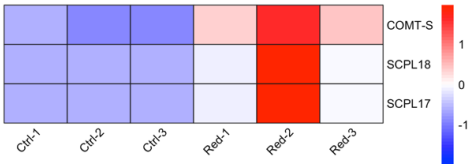

Gene name	Function
COMT-S	Esculetin O-methyltransferase
SCPL18	Serine carboxypeptidase-like 18
SCPL17	Serine carboxypeptidase-like 17

Figure 4-9. DEGs involved in biosynthesis of terpenoids, aromatic amino acids, green leaf volatiles, and aromatic compounds and their expression level.

For heatmap, blue represents low expression level and red represents high expression level. The gene expression levels of each sample are centered and scaled in the row direction, as indicated by the color scale.

4.3.5 Transcription factors involved in secondary metabolism

A search for transcription factors (TFs) among the DEGs identified 17 TFs, belonging to the bHLH, MYB, ERF, G2-like, MYC/bHLH, GATA, NFYA, and trihelix families. Their expression levels in control and red LED light treated fennel samples are shown in Figure 4-10. A hierarchical cluster heatmap was generated using normalized gene counts from the two treatment groups, revealing two main clusters: one consisting of TFs highly expressed in control samples, and another with higher expression in red LED light treated samples.

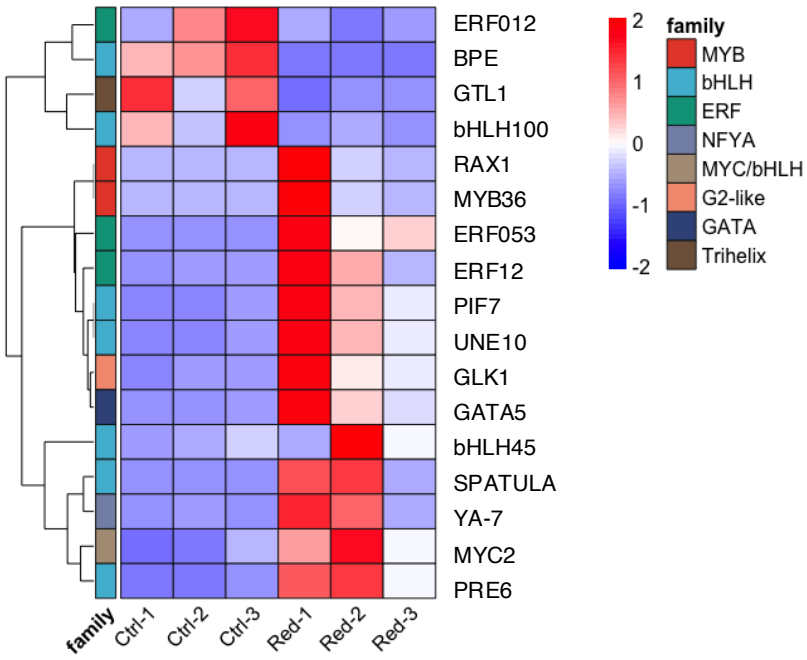

Figure 4-10. Transcription factors in fennel affected by red LED light.

The gene expression levels of each sample are centered and scaled in the row direction, as indicated by the color scale.

TFs that exhibited higher expression levels in control samples include ERF012, BPE, trihelix GTL1, and bHLH100. In contrast, TFs with higher expression levels in red

LED light samples include RAX1, MYB36, ERF053, ERF12, PIF7, UNE10, GLK1, GATA5, bHLH35, MYC2, PRE6, and nuclear transcription factor Y subunit A-7. MYB TFs, which are a family of proteins with the conserved MYB DNA binding domain (Stracke, Werber, & Weisshaar, 2001), have been shown to regulate biosynthetic genes in the phenylpropanoid pathway (Pratyusha & Sarada, 2022). The terpenoid biosynthesis pathway is reported to be regulated by AP2/ERF families (Patra, Schluttenhofer, Wu, Pattanaik, & Yuan, 2013), as well as the MYB and MYC/bHLH TF families (Wasternack & Strnad, 2019). Our findings suggest that these TFs are also involved in light-induced changes in secondary metabolism in fennel, highlighting the complex regulatory mechanisms of aroma formation influenced by narrow-wavelength red light.

4.4 Conclusion

In conclusion, this study comprehensively investigated the impact of supplemental red LED light on the growth, aroma profile, and gene expression of hydroponically cultivated fennel. *De novo* transcriptome assembly also contributes to further understanding of fennel genome. The results demonstrated that red LED light supplementation significantly enhanced fennel yield and aroma accumulation, making it an effective strategy for fennel cultivation in CEA, saving operational costs compared to traditional lighting, and adding profit for growers. Regarding aroma composition, red LED light increased the key aroma compounds in fennel, including *(E)*-anethole, estragole, *(Z)*-anethole, methyl eugenol, allo-ocimene, carvacrol, *p*-anisaldehyde, and tridecane. Transcriptome analysis revealed the upregulation of numerous genes under supplemental red LED light treatment, particularly those involved in primary and secondary metabolism, such as photosynthesis, phenylpropanoids biosynthesis, terpenoids biosynthesis, and green

leaf volatile biosynthesis. These gene expression changes help explain the observed enhancement in plant growth and aroma development. Additionally, this study identified various TFs that potentially regulate gene expression related to secondary metabolism under narrow-wavelength red light. Further research could explore the specific roles of these TFs in regulating the biosynthesis of volatile aroma compounds in fennel. Overall, these findings offer valuable insights into the optimization of aroma in culinary herbs under controlled environmental conditions and contribute to a deeper understanding of the molecular and genetic mechanisms governing plant development under supplemental red light. Future research can focus on charactering the key genes involved in phenylpropanoids biosynthesis, especially eugenol synthase and isoeugenol synthase, and investigating how their regulation is influenced by red light.

References

Afifi, S. M., El-Mahis, A., Heiss, A. G., & Farag, M. A. (2021). Gas chromatography–mass spectrometry-based classification of 12 fennel (*Foeniculum vulgare* Miller) varieties based on their aroma profiles and estragole levels as analyzed using chemometric tools. *ACS Omega*, *6*(8), 5775-5785. https://doi.org/10.1021/acsomega.0c06188.

Alrifai, O., Hao, X., Marcone, M. F., & Tsao, R. (2019). Current review of the modulatory effects of LED lights on photosynthesis of secondary metabolites and future perspectives of microgreen vegetables. *Journal of Agriculture and Food Chemistry, 67*(22), 6075-6090. https://doi.org/10.1021/acs.jafc.9b00819.

Amoozgar, A., Mohammadi, A., & Sabzalian, M. (2017). Impact of light-emitting diode irradiation on photosynthesis, phytochemical composition and mineral element content of lettuce cv. Grizzly. *Photosynthetica, 55*, 85-95. https://doi.org/10.1007/s11099-016-0216-8.

Appolloni, E., Pennisi, G., Zauli, I., Carotti, L., Paucek, I., Quaini, S., Orsini, F. & Gianquinto, G. (2022). Beyond vegetables: Effects of indoor LED light on specialized metabolite biosynthesis in medicinal and aromatic plants, edible flowers, and microgreens. *Journal of the Science of Food and Agriculture, 102*(2), 472-487. https://doi.org/10.1002/jsfa.11513.

Babushok, V. I., Linstrom, P. J., & Zenkevich, I. G. (2011). Retention indices for frequently reported compounds of plant essential oils. *Journal of Physical and Chemical Reference Data, 40*(4), 043101. https://doi.org/10.1063/1.3653552.

Badgujar, S. B., Patel, V. V., & Bandivdekar, A. H. (2014). *Foeniculum vulgare* Mill: A review of its botany, phytochemistry, pharmacology, contemporary application, and toxicology. *BioMed Research International,* 1, 842674. https://doi.org/10.1155/2014/842674.

Bantis, F., Smirnakou, S., Ouzounis, T., Koukounaras, A., Ntagkas, N., & Radoglou, K. (2018). Current status and recent achievements in the field of horticulture with the use of light-emitting diodes (LEDs). *Scientia Horticulturae, 235*, 437-451. https://doi.org/10.1016/j.scienta.2018.02.058.

Benke, K., & Tomkins, B. (2017). Future food-production systems: vertical farming and controlled-environment agriculture. *Sustainability: Science, Practice and Policy, 13*(1), 13-26. https://doi.org/10.1080/15487733.2017.1394054.

Brazaityte, A., Virsile, A., Samuoliene, G., Vastakaite-Kairiene, V., Jankauskiene, J., Miliauskiene, J., Novičkovas, A., Duchovskis, P. (2019). Response of mustard microgreens to different wavelengths and durations of UV-A LEDs. *Frontiers in Plant Science, 10*. https://doi.org/10.3389/fpls.2019.01153.

Bryant, D. M., Johnson, K., DiTommaso, T., Tickle, T., Couger, M. B., Payzin-Dogru, D., Lee, T. J., Leigh, N. D., Kuo, T.-H., Davis, F. G., Bateman, J., Bryant, S., Guzikowski, A. R., Tsai, S. L., Coyne, S., Ye, W. W., Freeman, R. M., Jr., Peshkin, L., Tabin, C. J., Regev, A., Haas, B. J., & Whited, J. L. (2017). A tissue-mapped axolotl *de novo* transcriptome enables identification of limb regeneration factors. *Cell Reports, 18*(3), 762-776. https://doi.org/10.1016/j.celrep.2016.12.063.

Chen, X.-l., Xue, X.-z., Guo, W.-z., Wang, L.-c., & Qiao, X.-j. (2016). Growth and nutritional properties of lettuce affected by mixed irradiation of white and supplemental light provided by light-emitting diode. *Scientia Horticulturae, 200*, 111-118. https://doi.org/10.1016/j.scienta.2016.01.007.

Contreras-Avilés, W., Heuvelink, E., Marcelis, L. F. M., & Kappers, I. F. (2024). Ménage à trois: light, terpenoids, and quality of plants. *Trends in Plant Science, 29*(5), 572-588. https://doi.org/10.1016/j.tplants.2024.02.007.

Demotes-Mainard, S., Péron, T., Corot, A., Bertheloot, J., Le Gourrierec, J., Pelleschi-Travier, S., Crespel, L., Morel, P., Huché-Thélier, L., Boumaza, R., Vian, A., Guérin, V., Leduc, N., & Sakr, S. (2016). Plant responses to red and far-red lights, applications in horticulture. *Environmental and Experimental Botany, 121*, 4-21. https://doi.org/10.1016/j.envexpbot.2015.05.010.

Díaz-Maroto, M. C., Díaz-Maroto Hidalgo, I. J., Sánchez-Palomo, E., & Pérez-Coello, M. S. (2005). Volatile components and key odorants of fennel (*Foeniculum vulgare* Mill.) and thyme (*Thymus vulgaris* L.) oil extracts obtained by simultaneous distillation−extraction and supercritical fluid extraction. *Journal of Agricultural and Food Chemistry, 53*(13), 5385-5389. https://doi.org/10.1021/jf050340.

El Haddaji, H., Akodad, M., Skalli, A., Moumen, A., Bellahcen, S., Elhani, S., Urrestarazu, M., Kolar, M., Imperl, J., Petrova, P., & Baghour, M. (2023). Effects of light-emitting diodes (LEDs) on growth, nitrates and osmoprotectant content in

microgreens of aromatic and medicinal plants. *Horticulturae*, 9(4). 494. https://doi.org/10.3390/horticulturae9040494.

Erten, E. S., & Cadwallader, K. R. (2017). Identification of predominant aroma components of raw, dry roasted and oil roasted almonds. *Food Chemistry, 217*, 244-253. https://doi.org/10.1016/j.foodchem.2016.08.091.

FAO (2022). Food and Agriculture Organization of the United Nations: Value of Agricultural Production. Retrived July 17, 2024, from https://www.fao.org/faostat/en/#data/QCL.

Faust, J. E., Holcombe, V., Rajapakse, N. C., & Layne, D. R. (2005). The effect of daily light integral on bedding plant growth and flowering. *HortScience, 40*(3), 645-649. https://doi.org/10.21273/HORTSCI.40.3.645.

Faust, J. E., & Logan, J. (2018). Daily light integral: A research review and high-resolution maps of the United States. *HortScience, 53*(9), 1250-1257. https://doi.org/10.21273/HORTSCI13144-18.

Grabherr, M. G., Haas, B. J., Yassour, M., Levin, J. Z., Thompson, D. A., Amit, I., Adiconis, X., Fan, L., Raychowdhury, R., Zeng, Q., Chen, Z., Mauceli, E., Hacohen, N., Gnirke, A., Rhind, N., di Palma, F., Birren, B. W., Nusbaum, C., Lindblad-Toh, K., Friedman, N., & Regev, A. (2011). Full-length transcriptome assembly from RNA-Seq data without a reference genome. *Nature Biotechnology*, *29*(7), 644-652. https://doi.org/10.1038/nbt.1883.

Hammock, H. A., Kopsell, D. A., & Sams, C. E. (2023). Application timing and duration of LED and HPS supplements differentially influence yield, nutrient

bioaccumulation, and light use efficiency of greenhouse basil across seasons. *Frontiers in Plant Science, 14*. https://doi.org/10.3389/fpls.2023.1174823.

Ibaraki, Y. (2017). LED Supplementary Lighting. In S. Dutta Gupta (Ed.), *Light Emitting Diodes for Agriculture: Smart Lighting* (pp. 27-36).Springer Singapore.

Lee, S. J., Umano, K., Shibamoto, T., & Lee, K. G. (2005). Identification of volatile components in basil (*Ocimum basilicum* L.) and thyme leaves (*Thymus vulgaris* L.) and their antioxidant properties. *Food Chemistry, 91*(1), 131-137. https://doi.org/10.1016/j.foodchem.2004.05.056.

Leffingwell & Associates. (1999). Odor & Flavor Detection Thresholds in Water (In Parts per Billion). Retrieved April 9, 2024, from http://www.leffingwell.com/odorthre.htm.

Li, C., Xin, M., Li, L., He, X., Yi, P., Tang, Y., Li, J., Zheng, F., Liu, G., Sheng, J., Li, Z., & Sun, J. (2021). Characterization of the aromatic profile of purple passion fruit (*Passiflora edulis* Sims) during ripening by HS-SPME-GC/MS and RNA sequencing. *Food Chemistry, 355*, 129685. https://doi.org/10.1016/j.foodchem.2021.129685.

Litvin, A. G., Currey, C. J., & Wilson, L. A. (2020). Effects of supplemental light source on basil, dill, and parsley growth, morphology, aroma, and flavor. *Journal of the American Society for Horticultural Science*,*145*(1), 18-29. https://doi.org/10.21273/JASHS04746-19.

Liu, J., Li, S., O'Keefe, S., Hurley, K., Rutto, L., Eriksen, R., & Yin, Y. (2024). Characterization of key aroma compounds in microgreens and mature plants of

hydroponic fennel (*Foeniculum vulgare* Mill.). *Food Research International*, 115229. https://doi.org/10.1016/j.foodres.2024.115229.

Livadariu, O., Maximilian, C., Rahmanifar, B., & Cornea, C. P. (2023). LED technology applied to plant development for promoting the accumulation of bioactive compounds: A review. *Plants, 12*(5). https://doi.org/10.3390/plants12051075.

Massange-Sánchez, J. A., Casados-Vázquez, L. E., Juarez-Colunga, S., Sawers, R. J. H., & Tiessen, A. (2020). The Phosphoglycerate Kinase (PGK) gene family of maize (*Zea mays* var. B73). *Plants, 9*(12), 1639. https://doi.org/10.3390/plants9121639

Meng, Q., & Runkle, E. S. (2018). *Using radiation to enhance quality attributes of leafy vegetables: a mini-review.* International Society for Horticultural Science (ISHS). https://doi.org/10.17660/ActaHortic.2018.1227.72.

Merico, D., Isserlin, R., Stueker, O., Emili, A., & Bader, G. D. (2010). Enrichment map: A network-based method for gene-set enrichment visualization and interpretation. *PLoS ONE, 5*(11), e13984. https://doi.org/10.1371/journal.pone.0013984.

Nguyen, T. L., & Saleh, M. A. (2019). Effect of exposure to light emitted diode (LED) lights on essential oil composition of sweet mint plants. *Journal of Environmental Science and Health Part a-Toxic/Hazardous Substances & Environmental Engineering, 54*(5), 435-440. https://doi.org/10.1080/10934529.2018.1562810.

Paik, I., & Huq, E. (2019). Plant photoreceptors: Multi-functional sensory proteins and their signaling networks. *Seminars in Cell & Developmental Biology, 92*, 114-121. https://doi.org/10.1016/j.semcdb.2019.03.007.

Palumbo, F., Vannozzi, A., Vitulo, N., Lucchin, M., & Barcaccia, G. (2018). The leaf transcriptome of fennel (*Foeniculum vulgare* Mill.) enables characterization of the *t*-anethole pathway and the discovery of microsatellites and single-nucleotide variants. *Scientific Reports, 8*(1), 10459. https://doi.org/10.1038/s41598-018-28775-2.

Patra, B., Schluttenhofer, C., Wu, Y., Pattanaik, S., & Yuan, L. (2013). Transcriptional regulation of secondary metabolite biosynthesis in plants. *Biochimica et Biophysica Acta (BBA) - Gene Regulatory Mechanisms, 1829*(11), 1236-1247. https://doi.org/10.1016/j.bbagrm.2013.09.006.

Pino, J. A., Rosado, A., Goire, I., & Roncal, E. (1995). Evaluation of flavor characteristic compounds in dill herb essential oil by sensory analysis and gas chromatography. *Journal of Agricultural and Food Chemistry, 43*(5), 1307-1309. https://doi.org/10.1021/jf00053a034.

Pratyusha, D. S., & Sarada, D. V. L. (2022). MYB transcription factors—master regulators of phenylpropanoid biosynthesis and diverse developmental and stress responses. *Plant Cell Reports, 41*(12), 2245-2260. https://doi.org/10.1007/s00299-022-02927-1.

Quail, P. H., Boylan, M. T., Parks, B. M., Short, T. W., Xu, Y., & Wagner, D. (1995). Phytochromes: photosensory perception and signal transduction. *Science*, *268*(5211), 675-680. https://doi.org/10.1126/science.7732376.

Rouphael, Y., Kyriacou, M. C., Petropoulos, S. A., De Pascale, S., & Colla, G. (2018). Improving vegetable quality in controlled environments. *Scientia Horticulturae, 234*, 275-289. https://doi.org/10.1016/j.scienta.2018.02.033.

Rychlik, M., Schieberle, P., & Grosch, W. (1998). *Compilation of odor thresholds, odor qualities and retention indices of key food odorants*. Garching: Deutsche Forschungsanstat für Lebensmittelchemie and Instit für Lebensmittelchemie der Technischen Universität München Garching.

Stracke, R., Werber, M., & Weisshaar, B. (2001). The R2R3-MYB gene family in Arabidopsis thaliana. *Current Opinion in Plant Biology, 4*(5), 447-456. https://doi.org/10.1016/S1369-5266(00)00199-0.

Tan, T., Li, S., Fan, Y., Wang, Z., Ali Raza, M., Shafiq, I., Wang, B., Wu, X., Yong, T., Wang, X., Wu, Y., Yang, F., & Yang, W. (2022). Far-red light: A regulator of plant morphology and photosynthetic capacity. *The Crop Journal, 10*(2), 300-309. https://doi.org/10.1016/j.cj.2021.06.007.

van Den Dool, H., & Dec. Kratz, P. (1963). A generalization of the retention index system including linear temperature programmed gas—liquid partition chromatography. *Journal of Chromatography A, 11*, 463-471. https://doi.org/10.1016/S0021-9673(01)80947-X.

van Gemert, A. F. (2003). *Compilations of Odour Threshold Values in Air, Water and Other Media*. Boelens Aroma Chemical Information Service.

Vogt, T. (2010). Phenylpropanoid Biosynthesis. *Molecular Plant, 3*(1), 2-20. https://doi.org/10.1093/mp/ssp106.

Walters, K. J., & Lopez, R. G. (2021). Modeling growth and development of hydroponically grown dill, parsley, and watercress in response to photosynthetic daily light integral and mean daily temperature. *PLoS ONE, 16*(3), e0248662. https://doi.org/10.1371/journal.pone.0248662.

Wasternack, C., & Strnad, M. (2019). Jasmonates are signals in the biosynthesis of secondary metabolites — Pathways, transcription factors and applied aspects — A brief review. *New Biotechnology, 48*, 1-11. https://doi.org/10.1016/j.nbt.2017.09.007.

Xiao, Z., Chen, J., Niu, Y., & Chen, F. (2017). Characterization of the key odorants of fennel essential oils of different regions using GC–MS and GC–O combined with partial least squares regression. *Journal of Chromatography B, 1063*, 226-234. https://doi.org/10.1016/j.jchromb.2017.07.053.

Yu, G., Wang, L.-G., Han, Y., & He, Q.-Y. (2012). clusterProfiler: an R package for comparing biological themes among gene clusters. *Omics: a journal of integrative biology, 16*(5), 284-287. https://doi.org/10.1089/omi.2011.0118.

Zeller, A., & Rychlik, M. (2006). Character impact odorants of fennel fruits and fennel tea. *Journal of Agricultural and Food Chemistry, 54*(10), 3686-3692. https://doi.org/10.1021/jf052944j.

Zhang, L., Huang, T., Zhang, Q., Wei, S., Escalona Contreras, V. H., Peng, J., Song, B., Li, Y., Yang, Q., & Yang, X. (2024). Plant factory technology as a powerful tool for improving vegetable quality: Lettuce as an application example. *Vegetable Research, 4*(1). https://doi.org/10.48130/vegres-0024-0015.

Zhang, S. C., Zhang, L., Zou, H. Y., Qiu, L., Zheng, Y. W., Yang, D. F., & Wang, Y. P. (2021). Effects of light on secondary metabolite biosynthesis in medicinal plants. *Frontiers in Plant Science, 12*. https://doi.org/10.3389/fpls.2021.781236.

Zhang, Z., Guan, W., Liang, M., Wang, R., Wu, Y., & Liu, Y. (2023). Characterization of the key odorants in fresh Amomum *tsao-ko* Crevost et Lemaire fruit by gas chromatography-olfactometry, quantitative analysis and aroma reconstitution. *LWT, 185*, 115154. https://doi.org/10.1016/j.lwt.2023.115154.

Chapter 5 Impact of Salinity Stress on Growth, Aroma, and Gene Expression of Hydroponic Fennel (*Foeniculum vulgare* Mill.)

This chapter is in preparation for submission to *Food Chemistry.*

Author Details: Jingsi Liu[1], Adam Sumner[2], Alex Harris[2], Wangyi Wei[1], Bastiaan Bargmann[2], David Haak[2], Yun Yin[1]

[1] Department of Food Science and Technology, Virginia Tech, Blacksburg, VA

[2] School of Plant and Environmental Sciences, Virginia Tech, Blacksburg, VA

Abstract

Water salinization poses a major threat to the agricultural and food systems. Previous research has shown that fennel can be utilized as a salt-tolerant plant to grow in arid regions. However, the impact of salinity stress on fennel aroma and the underlying molecular mechanisms are still unknown. The objective of this study was to investigate the impact of salinity on growth, aroma, and gene expression of fennel (*Foeniculum vulgare* Mill.) cultivated with nutrient film technique (NFT) hydroponic systems. Fennel was grown under varying salinity levels (0, 20, 40, and 60 mM additional NaCl) and growth parameters were measured upon harvest. Aroma characterization of fennel leaves was performed using headspace solid phase microextraction – gas chromatography – mass spectrometry – olfactometry (SPME-GC-MS-O). Quantitation of aroma compounds was performed using standard addition methods. RNA sequencing (RNA-seq) was performed to study the changes in gene expression levels. The results showed that the salinity stress caused a significant decrease in plant growth and yield in both week 3 and week 6 samples. However, the overall content of aroma-active compounds was not significantly discriminated by either salinity level or harvest time. RNA-seq results showed that salinity triggered defense mechanisms in fennel, particularly through the activation of plant hormone signal transduction and mitogen-activated protein kinase (MAPK) signaling pathways. The present study demonstrates the utilization of CEA and chemistry tools to evaluate the influence of abiotic factors on crop flavor quality.

Keywords

Fennel, salinity, aroma compounds, GC-MS-O, gene expression

5.1 Introduction

Soil and water salinization present a major thread to global agriculture and food production. The ongoing salinization of freshwater is driven by many anthropogenic activities, and it is estimated that over 50% of arable land could be affected by 2050 (Colin, Ruhnow, Zhu, Zhao, Zhao, & Persson, 2023; Jamil, Riaz, Ashraf, & Foolad, 2011; Shrivastava & Kumar, 2015). Salt stress is caused by high concentration of ions such as sodium (Na^+) and chloride (Cl^-), leading to inhibited plant growth and reduced yield (Machado & Serralheiro, 2017; Adhikari, Simko, & Mou, 2019; Mukhopadhyay, Sarkar, Jat, Sharma, & Bolan, 2021). Understanding the complex molecular mechanisms underlying salt stress in plants is critical for maintaining global food security. So far, three salt-induced stress pathways have been identified: osmotic stress, ionic stress, and secondary stress (Yang & Guo, 2018). Osmotic stress is caused by excessive soluble salts in the soil or water, and it limits water availability to plants (Hasegawa, Bressan, Zhu, & Bohnert, 2000). Ionic stress results from the cytotoxic ion levels in plant, which negatively affects various metabolic processes (Isayenkov & Maathuis, 2019; Yang et al., 2018). These primary stresses can trigger secondary stress, characterized by the buildup of harmful compounds and nutrient imbalances (Isayenkov et al., 2019). Furthermore, salt stress often leads to the accumulation of reactive oxygen species (ROS), which can cause severe damage to DNA, RNA, and proteins, ultimately resulting in cell death (Golldack, Li, Mohan, & Probst, 2014).

Given the increasing prevalence of salinization in agricultural areas, enhancing salt tolerance has become one of the key focuses of in breeding programs (An, Wang, Liu, Cao, & Chen, 2023). Advances in next-generation sequencing, such as RNA sequencing (RNA-

seq), now allow for the identification of salt-responsive genes and the regulatory networks governing these responses, which may serve as potential markers for breeding salt-tolerant plants (van Zelm, Zhang, & Testerink, 2020; Zhu, 2002). For example, genes involved in carbohydrate and amino acid metabolism are upregulated in rice (*Oryza sativa*) root systems under salt stress, potentially mitigating ROS damage (Chandran et al., 2019). Similarly, in wheat (*Triticum aestivum*), salinity adaptation is influenced by the expression of salt-induced proteins (Dell'Aquila & Spada, 1992). In Brazilian *Jatropha curcas* L. (physic nut), cultivar-dependent differences in gene expression have been observed, particularly in pathways related to phytohormones and secondary metabolites (de Souza et al., 2020).

Cultivating salt-tolerant plants in arid and semi-arid regions is another strategy to address challenge of salinization (Petropoulos, Karkanis, Martins, & Ferreira, 2018). Salt-tolerant plants can survive and reproduce in high salinity environment and maintain viable yield under stress conditions (Flowers & Colmer, 2008). Many previous studies have investigated the effects of salinity on plant biomass, growth, and secondary metabolite production (Acosta-Motos, Ortuño, Bernal-Vicente, Diaz-Vivancos, Sanchez-Blanco, & Hernandez, 2017; Adhikari, Olorunwa, Wilson, & Barickman, 2021; Hao, Wang, Yan, Liu, Wang, & Chen, 2021; Julkowska & Testerink, 2015; Karray-Bouraoui et al., 2009). Notably, many secondary metabolites, including terpenes and phenolic compounds, are antioxidants that help mitigate ROS damage under salt stress (Yang et al., 2018). These compounds also contribute to the essential oils and volatile aroma profiles of plants. Differences in volatile composition under salinity stress have been observed in many aromatic plants, such as coriander (Neffati, Sriti, Hamdaoui, Kchouk, & Marzouk, 2011),

mint (Karray-Bouraoui et al., 2009), and cumin (Bourgou, Bettaieb, Saidani, & Marzouk, 2010).

Fennel (*Foeniculum vulgare* Mill.), a valuable culinary and medicinal herb from the Apiaceae family, is now cultivated worldwide. The essential oils and fennel products are widely used in the food, pharmaceutical, and cosmetic industries. Native to the Mediterranean, fennel is suitable for cultivation in the arid and semi-arid environments (Ashraf & Akhtar, 2004). Previous research has shown that fennel has partial tolerance to salinity (30 – 60 mM NaCl) (Shafeiee & Ehsanzadeh, 2019). However, high salinity typically reduces fennel biomass and seed yield (Ashraf et al., 2004), with cultivar-dependent variations in salt tolerance (Zaki, Abou-Hussein, Abou El-Magd, & El-Abagy, 2009). In addition, salt stress reduced the germination percentage and germination rate of fennel seeds (Mohammadi, Pouryousef, & Farhang, 2023). Salinity has also been shown to affect the essential oil content of fennel. For example, *(E)*-anethole, the primary volatile compound of fennel, decreased significantly under salt stress, while the levels of estragole, limonene, and fenchone increased (Rebey, Rahali, Tounsi, Marzouk, & Ksouri, 2016). Despite these findings, the molecular mechanisms associated with salinity-induced changes in volatile aroma compounds and gene expression in fennel remain unknown. Since salt-induced signaling in plants is dynamic, it is also crucial to understand how these mechanisms function at different development and growth stages.

The objective of this study was to examine the effects of different levels of salinity stress on the growth, aroma composition, and gene expression of hydroponically grown fennel over time. Volatile aroma compounds were analyzed by gas chromatography-mass spectrophotometry-olfactometry (GC-MS-O) and quantified by standard addition method

with multiple internal standards. Gene expression levels in fennel leaf tissues were assessed through RNA-seq analysis. Additionally, we investigated key metabolic pathways responsive to salt stress and identified candidate genes that may serve as potential markers for breeding salt-tolerant crops. The metabolic and transcriptome data generated in this study offered valuable insights for crop improvement strategies, particularly under abiotic stress conditions such as salinity.

5.2 Materials and methods

5.2.1 Plant materials and growth conditions

The growth experiment was conducted at Virginia Tech greenhouses in Blacksburg, VA (lat. 37.2°N) from September to November 2023. The greenhouse is glass-glazed and equipped with environmental control systems. Fennel (*Foeniculum vulgare* Mill., cv. Grosfruchtiger) plants were grown in rockwool propagation cubes saturated with water and placed in germination trays. The seedlings were irrigated daily, allowed to grow for 3 weeks, and then transplanted into one of four nutrient film technology (NFT) hydroponic systems (NFT0406, CropKing, Lodi, OH). Each NFT unit accommodates 36 seedlings with an individual reservoir containing nutrient solution. Seedlings were randomly inserted into 2.54 × 2.54 cm square holes, spaced 20 cm apart, on the PVC channels of the NFT systems. The nutrient solution consisted of water supplemented with 2-1-6 and 5-0-1 (nitrogen-phosphate potash) liquid fertilizers (FloralGro and FloraMicro, General Hydroponics, Sebastopol, CA, US). A 400 GHP 24-W water pump (Active Aqua, Petaluma, CA, US) circulated the nutrient solution through the PVC channels, while the NFT units were adjusted to a 2-3° slope to ensure the nutrient solution return to the reservoir. To investigate the changes in growth and aroma of fennel plants affected by

salinity, 18 mature fennel plants were destructively harvested after three weeks under salinity stress, and another 18 mature fennel plants after six weeks. During the collection, data on plant height, fresh biomass, number of branches, apparent moisture content, and CIE *L a b* color parameters were also collected. The color of fennel leaves was measured using a Minolta CR-300 Chroma Meter (Minolta Co., Osaka, Japan).

The pH and EC of each NFT system were monitored daily. For the control group, the pH of the nutrient solution was maintained at the range of 5.8-6.2 while EC is maintained at the range of 1.2-1.6 $dS \cdot m^{-1}$ with a portable pH/EC meter (HI98131, HANNA Instruments, Smithfield, RI, US). The pH was adjusted with phosphoric and citric acid (pH Down, General Hydroponics, Sebastopol, CA, US) or potassium hydroxide and potassium carbonate (pH Up, General Hydroponics, Sebastopol, CA, US). EC was adjusted using deionized water and 2-1-6 and 5-0-1 liquid fertilizers.

The greenhouse temperature was set to 24°C during the day and 21°C during night, maintained by an environmental controller (Step Control, Wadsworth Control Systems, Arvada, CO, US). The average daylight hours are recorded by a Watchdog datalogger (1650 Micro Station, Spectrum Technologies, Aurora, IL). The environmental parameters, such as average daily light integral (DLI) per month, average daylight hours, greenhouse temperature, and average humidity are reported in Supplementary Table 5-1.

5.2.2 Salinity treatments

After transplantation, 4 different salinity levels were applied to fennel plants with a split block design. Each NFT hydroponic system's reservoir was adjusted individually, by adding NaCl until the desired salinity level. The nutrient composition for the salinity treatment groups was identical to the control group, which is water supplemented with 2-

1-6 and 5-0-1 fertilizers. The four treatment groups were as follows: control (0 mM additional NaCl, EC 1.2-1.6 $dS \cdot m^{-1}$), 20 mM NaCl (EC 3.2-3.6 $dS \cdot m^{-1}$), 40 mM NaCl (EC 5.2-5.6 $dS \cdot m^{-1}$), and 60 mM NaCl (EC 7.2-7.6 $dS \cdot m^{-1}$). These salinity levels were based on previous research, which suggested that fennel has partial tolerance to moderate salinity (30-60 mM NaCl) (Shafeiee et al., 2019). The pH of all groups was maintained between 5.8 to 6.2, as described in session 5.2.1.

5.2.3 Chemicals and standards

The chemicals and aroma compounds standards were sourced from the following suppliers: n-alkane (C7-C30), decane (≥99.8%), 2-octanol (≥97%), 1-phenylethanol (98%), *(E)*-anethole (≥99%), *α*-pinene (98%), *p*-cymenene (≥98%), methyl eugenol (≥98%), 1-octen-3-ol (≥98%), fenchone (98%), *p*-anisaldehyde (≥97.5%), linalool (≥97%), estragole (≥96%), phenyl acetaldehyde (≥95%), *α*-phellandrene (≥75%), and *γ*-terpinene (≥95%), all purchased from Sigma-Aldrich (St. Louis, MO). Methanol (HPLC grade) was obtained from Fisher Scientific (Fair Lawn, NJ). (-)-bornyl acetate (95%) was purchased from Alfa Aesar (Haverhill, MA). *(Z)*-Anethole was purchased from Toronto Research Chemicals (Toronto, Canada). *(Z)*-3-hexenal (50% in triacetin) and *(E)*-2-hexenal (98%) were generously supplied by Bedoukian Research Inc. (Danbury, CT). Tridecane (>99%) was purchased from Tokyo Chemical Industry Co., Ltd. America (Portland, OR).

5.2.4 Extraction of aroma compounds with solid phase microextraction (SPME)

Fennel aroma compounds was extracted using the method described in our previous work (chapter 3). Briefly, frozen fennel leaves were ground using a pestle and mortar with liquid nitrogen until a fine powder was achieved. Approximately 50 ± 0.5 mg of this

powder was weighed into a clear SPME vial (Supelco, Bellefonte, PA). 36.4 ng decane, 4.8 ng 2-octanol, and 99.0 ng 1-phenylethanol were added to the vial as quantitation internal standards (IS). The vial's headspace was kept at 50°C for 10 min to achieve equilibrium. Afterward, a 1 cm preconditioned 50/30 DVB/CAR/PDMS fiber (Supelco, Bellefonte, PA) was exposed to the headspace, and extracted the volatile compounds in the headspace for 30 min under 50°C.

5.2.5 Aroma characterization with gas chromatography-mass spectrometry-olfactometry (GC-MS-O)

Aroma characterization was performed using an Agilent 6890N GC (Santa Clara, CA) coupled with a 5975B mass selective detector (MSD) (Agilent Technologies Inc., Santa Clara, CA). GCO was performed with a PHASER sniff port (GL Sciences, Eindhoven, the Netherlands). Volatile compounds were separated using a DB-WAX capillary column (30 m × 0.25 mm i.d., film thickness = 0.25 μm) (Supelco, Bellefonte, PA) and helium was used as the carrier gas. The flow rate of helium was set to 2 mL/min (67.9 cm/s). The column temperature was programed as follows: hold at 40°C for 5 min, 40-80°C with an 8°C/min increase, 80-152°C with a 5°C/min increase, 152-225°C with an 8°C/min increase, and hold at 225°C for 15 min. The injection port temperature was 230°C and the fiber was injected in splitless mode. The interface temperature of MSD was set to 230°C, the ionization energy was set to 70 eV, the mass range was 33-500 amu, the EM voltage was Atune + 200V, and scan rate was 5.15 scans/s. The column effluent was divided equally between the sniff port and the MSD.

For GC-O, the eluting volatile compounds from GC were mixed with humidified air and detected with a flow rate of 5 mL/min. GC-O was performed by trained panelists

(aged between 20 and 28). All panelists participated in three training sessions using authentic standards of common aroma compounds in fennel, so that they were able to recognize and describe their odor. The sniffing session for one sample was 30 min. During the sniffing process, panelists were asked to record retention time, odor description, and intensity of the odorants perceived. Odor intensity was assessed using a five-point scale.

5.2.6 Aroma identification and quantitation

Aroma compounds were first tentatively screened based on GC-O results. Then, these compounds were identified by comparing mass spectra with library (NIST 17), retention indices, and aroma characteristics with authentic standards. The retention indices were calculated using the equation reported by van Den Dool & Kratz (1963) and the retention time of a C_7-C_{30} alkane solution.

Aroma compounds were quantified using the method developed in our previous study. Briefly, a "blank" fennel powder was created to mimic the sample matrix. The "blank" fennel powder was achieved by incubating the sample under 50°C with regular nitrogen purge of the headspace. The powder was then analyzed by GC-MS to ensure the absence of or only negligible peaks in the resulting chromatogram. After that, the power can be used as the sample matrix for constructing liner regression equations. The "blank" fennel powder was then spiked with fixed concentrations of IS and a series of aroma standards at different concentrations. The series of standard samples were analyzed by GC-MS to construct linear regression equations or calibration curves of each aroma standard, using peak area ratio and mass ratio of aroma standards to their corresponding IS. The mass of each analyte was determined using its regression equation, the known mass of IS, and the peak area ratio of the analyte to IS. The analyte concentration was calculated by

dividing its mass by the mass of fennel powder in the vial. The odor activity value (OAV) was calculated by dividing the concentration of each analyte (on a fresh weight basis) by its published odor detection threshold in water (Erten & Cadwallader, 2017).

5.2.7 RNA extraction and sequencing

Fennel RNA was extracted from approximately 50 mg of leaf tissue with Qiagen RNeasy Plant Mini Kit (Hilden, Germany) and treated with the Qiagen RNase-free DNase Set (Hilden, Germany) according to manufacturer's recommendations. Three replicates were performed for each treatment, and each replicate contained tissue from three different plants. Same plants were also used for aroma characterization. RNA quality was assessed using Thermo Scientific NanoDrop spectrophotometer (Waltham, MA) to confirm there was no degradation or contamination ($A260/A280 \geq 2.0$, $A260/A230 \geq 2.0$). RNA integrity was further analyzed using the Agilent RNA 6000 Pico Kit (Santa Clara, CA) and Agilent 2100 bioanalyzer (Santa Clara, CA). Samples with an RNA Integrity Number (RIN) above 7 were deemed suitable for sequencing. Library preparation and RNA-seq were performed by Novogene (Sacramento, CA) on the Illumina NovaSeq platform (HWI-ST1276) using a paired-end, 150 bp read sequencing strategy.

5.2.8 RNA sequencing based transcriptome analysis

RNA-seq reads were merged and assembled into a *de novo* transcriptome using Trinity software (v2.15.1) (Grabherr et al., 2011). Functional annotation of the assembly was performed using Trinotate (Bryant et al., 2017) for Gene Ontology (GO) and Kyoto Encyclopedia of Genes and Genomes (KEGG) pathway enrichment analysis. Differential gene expression data was obtained using the Bioconductor package DESeq2, version

1.42.1 (Love et al., 2014). Assembled transcripts with |log2Fold Change| > 1.5 and adjusted P-value < 0.05 were considered differentially expressed genes (DEG) and used in the analysis.

5.2.9 Statistical analysis

Growth parameters and aroma compounds concentrations between different salinity levels and two harvest times were compared by two-way analysis of variance (ANOVA) based on Tukey's honest significant difference (HSD) test for *post hoc* comparisons using R (version 4.3.1). The significance level was $p < 0.05$. R packages used for data analysis and graph construction were provided in Appendix D.

5.3 Results and discussion

5.3.1 Fennel growth affected by salinity

The impact of salinity stress on fennel growth parameters is presented in Figure 5-1. The addition of NaCl led to reductions in plant height, width, fresh weight, and the number of branches per plant, with more pronounced impact as the treatment duration increased. The results of two-way ANOVA revealed significant effects of harvest time, salinity level, and their interactions (harvest × salinity) (Supplemental Table 5-2). The control group showed the highest value for plant height and width (Figure 5-1A and 5-1B), followed by plants treated with 20 mM, 40 mM, and 60 mM additional NaCl. The differences in plant height and width were not significantly different after three weeks of salinity stress (first harvest). However, after six weeks (second harvest), plants exposed to 40 mM and 60 mM additional NaCl showed significantly reduced height and width. Additionally, at the second harvest, the fresh biomass and branches number per plant

decreased progressively with increased salinity (Figure 5-1C and 5-1D). These results demonstrated that salinity led to severe reduction in plant growth and limited the biomass production of fennel, especially with prolonged exposure.

Table 5-1 summarized the apparent moisture content and color parameters (measured on a CIE Lab scale) of fennel under salinity stress. Two-way ANOVA results (Supplemental Table 5-2) showed that apparent moisture content is significantly affected by harvest time, but not salinity level or the interaction between harvest and salinity. Apparent moisture content tended to be lower in fennel plants harvested later. Regarding color, *L*, or the brightness, was significantly influenced by both harvest time and salinity, though no interaction effects were found. Fennel leaves exhibited no significant difference in *L* across salinity levels, though plants exposed to 60 mM NaCl had a slightly less negative *a* value, indicating a shift towards a less green color. For *b*, the value indicating yellow-blue opponents, significant interactions between harvest and salinity were observed, although no clear trend in response to salinity stress was observed. Previous research showed that both long-term salinity and short-term drought could lead to clear changes in leaf pigment in Hybrid *Pennisetum* (Peidong Li, Zhu, Song, & Song, 2020). Similarly, in rice, chlorophyll content decreased under salt stress (Turan & Tripathy, 2015). This suggests that when plants are under salinity stress, chlorophyll content could decrease, leading to reduced photosynthesis efficiency and limited biomass production.

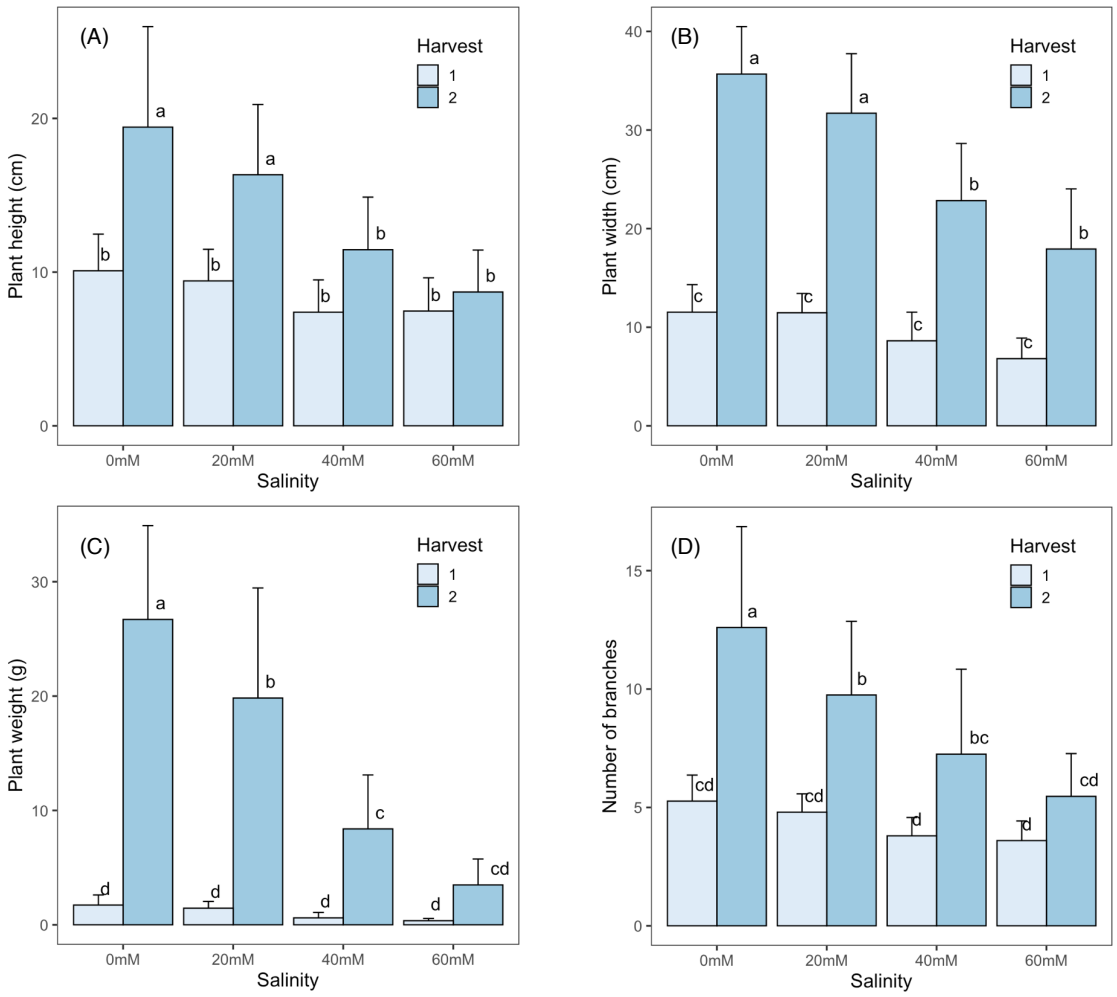

Figure 5-1. Influences of different salinity levels on fennel growth across two harvest times. (A). Plant height (B). Plant width. (C). Plant fresh weight. (D). Number of branches.

Analysis of variance and mean separation was performed using Tukey's HSD at $p < 0.05$.

Table 5-1. Apparent moisture content and color parameters of fennel affected by salinity stress

Parameters	Harvest 1				Harvest 2			
	Ctrl	20mM NaCl	40mM NaCl	60mM NaCl	Ctrl	20mM NaCl	40mM NaCl	60mM NaCl
Apparent moisture content (%)	89.50±0.56^{a}	89.59±1.43^{a}	87.88±1.49^{ab}	89.71±0.44^{a}	86.69±0.49^{b}	86.66±1.28^{b}	87.12±0.80^{ab}	88.47±0.50^{ab}
L	32.20±6.53^{a}	31.52±1.83^{a}	35.05±0.94^{a}	23.63±4.96^{a}	27.59±4.79^{a}	25.11±6.05^{a}	27.97±2.52^{a}	22.69±5.14^{a}
a	-16.38±2.99^{ab}	-15.52±1.23^{ab}	-18.42±0.30^{b}	-12.77±1.13^{a}	-15.62±1.56^{ab}	-14.80±1.89^{ab}	-14.47±0.96^{ab}	-13.24±1.97^{a}
b	26.48±5.90^{ab}	26.08±2.07^{ab}	30.32±1.66^{a}	21.21±1.09^{b}	24.24±2.23^{ab}	23.17±3.59^{ab}	22.38±1.94^{ab}	25.09±1.20^{ab}

The results are expressed as mean ± standard deviation. Mean separation is performed using analysis of variance (ANOVA) followed by Tukey's HSD.

Salinity stress is well-documented to inhibit plant growth and reduce crop yields (Machado et al., 2017; Mukhopadhyay et al., 2021). In our experiment, all NaCl treatments significantly reduced fennel growth parameters. This aligns with the findings of Semiz et al. (2012), that salinity levels ranging from 0.25 to 12 dS/m decreased plant height, fresh biomass, and seed yield of *F. vulgare*. Similarly, reductions in shoot and dry weight in fennel under salt stress were observed, likely linked to decreases in stomatal conductance, carbon dioxide assimilation and transpiration rate (Wasli et al., 2024). The negative impact of salinity on fennel growth is typically attributed to a combination of osmotic stress, ionic stress, and secondary stress, which can induce cytotoxicity, limit water uptake, disrupt plant cell structure, and inhibit metabolic processes (Yang et al., 2018).

5.3.2 Fennel aroma compounds affected by salinity

A total of 27 aroma-active compounds were identified by GC-MS-O, including 6 phenylpropanoids, 5 aldehydes, 4 monoterpenes, 3 sesquiterpenes, 3 alcohols, 2 monoterpenoids, 2 ketones, 1 alkane, and 1 unidentified compound. The unidentified compound was detected by GC-O panelists, however showed no peaks in chromatograms. The GC-O panelists' evaluation of these aroma-active compounds are shown in Table 5-2. These compounds were also quantified using standard addition methods, with results summarized in Table 5-3. Their odor activity values (OAVs), calculated based on their concentrations and published odor threshold in water, are shown in Table 5-4. Calibration curves for SAM quantitation are provided in Supplemental Table 5-2.

Table 5-2. Aroma-active compounds in fennel grown under different salinity levels identified by GC-MS-O

No.	Compound	RI	RI Ref. [a]	Identification method [b]	Odor Description	Odor Intensity [c]							
						H1-Ctrl	H1-20 mM	H1-40 mM	H1-60 mM	H2-Ctrl	H2-20mM	H2-40mM	H2-40mM
	Monoterpenes												
1	*α*-pinene	1011	1011	MS, RI, OD, AS	Pine, woody	W	W	M	M	W	W	M	M
2	*α*-phellandrene	1153	1157	MS, RI, OD, AS	Herbal, woody	W	M	S	S	M	M	S	W
3	*γ*-terpinene	1239	1233	MS, RI, OD, AS	Oily, herbal	W	S	W	M	M	S	S	S
4	allo-ocimene	1371	1366	MS, RI, OD	Herbal, terpenic	S	S	VS	VS	VS	S	VS	S
	Sesquiterpenes												
5	*γ*-muurolene	1697	1690	MS, RI, OD	Spice, woody	M	M	S	S	S	S	S	M
6	germacrene D	1719	1717	MS, RI, OD	Spice, clove	/	S	/	/	M	/	S	S
7	*α*-cadinene	1816	1815	MS, RI, OD	Woody, fresh	W	M	/	M	/	/	M	M
	Alkane												
8	tridecane	1303	1300	MS, RI, OD, AS	Mushroom, gasoline-like	M	/	S	M	S	M	S	S
	Alcohols												
9	*(Z)*-3-hexen-1-ol	1384	1377	MS, RI, OD, AS	Leafy, green	/	/	/	/	M	M	W	M
10	1-octen-3-ol	1451	1451	MS, RI, OD, AS	Earthy, mushroom	S	VS	VS	VS	VS	S	S	S
11	linalool	1552	1552	MS, RI, OD, AS	Floral	W	/	/	/	/	/	/	/
	Aldehydes												
12	hexenal	1076	1078	MS, RI, OD	Green, grassy	W	/	/	W	VW	M	W	W

13	*(Z)*-3-hexenal	1130	1134	MS, RI, OD, AS	Leafy, grassy	M	M	M	M	M	M	M	S
14	*(E)*-2-hexenal	1218	1218	MS, RI, OD, AS	Leafy, green	W	M	M	S	W	M	M	M
15	phenyl acetaldehyde	1634	1632	MS, RI, OD, AS	Floral, sweet	/	S	S	S	M	/	S	M
16	*p*-anisaldehyde	2019	2016	MS, RI, OD, AS	Floral, sweet	S	S	S	S	S	S	S	S
	Monoterpenoids												
17	fenchone	1398	1392	MS, RI, OD, AS	Herbal	/	W	S	W	/	VW	W	W
18	bornyl acetate	1583	1580	MS, RI, OD, AS	Woody, pine	M	S	VS	S	VS	S	M	S
	Ketones												
19	*β*-ionone	1940	1940	MS, RI, OD, AS	Floral, sweet	/	M	VS	VS	VS	VS	VS	VS
20	anisketone	2150	2170	MS, RI, OD, AS	Licorice, sweet	/	/	M	/	/	M	M	/
	Phenylpropanoids												
21	estragole	1669	1661	MS, RI, OD, AS	Anise, herbal	M	S	VS	S	S	S	VS	VS
22	*(Z)*-anethole	1754	1732	MS, RI, OD	Sweet, anise	M	M	S	S	S	M	S	S
23	*(E)*-anethole	1846	1838	MS, RI, OD, AS	Sweet, anise	VS	VS	VS	VS	VS	VS	VS	VS
24	methyl eugenol	2000	2003	MS, RI, OD, AS	Clove, sweet	S	S	S	S	S	S	S	S
25	methyl isoeugenol	2174	2176	MS, RI, OD	Clove, woody	M	M	S	W	S	/	/	/
26	apiol	2361	2431	MS, RI, OD	Parsley, green	W	W	W	VW	M	/	/	/
	Unknown												
27	Unknown 1	2057	NA	OD	Fruity, green	S	W	W	S	S	S	S	S

[a] Reference retention indices are from NIST publication (Babushok, Linstrom, & Zenkevich, 2011).

[b] Identification method: mass spectra (MS), retention index (RI), odor descriptors (OD) against authentic aroma standards (AS).

[c] Odor intensity: very weak (VW), weak (W), medium (M), strong (S), and very strong (VS). Not determined (ND).

One of the panelists smelled the compound.

Table 5-3. Concentrations of aroma-active compounds in fennel under different salinity stress

No.	Compound	Concentration (μg/g fennel, fresh weight)							
		Harvest 1				*Harvest 2*			
		Ctrl	20mM NaCl	40mM NaCl	60mM NaCl	Ctrl	20mM NaCl	40mM NaCl	60mM NaCl
1	*α*-pinene	25.39±14.51^{c}	27.84±11.09^{bc}	26.00±15.57^{c}	50.94±8.87^{abc}	36.56±11.76^{abc}	67.42±10.40^{ab}	66.89±22.38^{ab}	68.09±13.83^{a}
2	*α*-phellandrene	61.84±18.11^{a}	81.93±13.89^{a}	85.53±30.83^{a}	96.99±6.17^{a}	80.90±10.80^{a}	88.43±7.35^{a}	100.81±32.89^{a}	119.01±32.37^{a}
3	*γ*-terpinene	3.91±2.01^{ab}	4.24±1.19^{ab}	6.15±3.47^{ab}	6.58±1.04^{a}	2.93±1.01^{ab}	1.29±0.09^{b}	2.96±1.73^{ab}	3.46±1.96^{ab}
4	allo-ocimene	0.24±0.01^{a}	0.25±0.01^{a}	0.25±0.00^{a}	0.25±0.00^{a}	0.24±0.00^{a}	0.24±0.01^{a}	0.25±0.00^{a}	0.24±0.00^{a}
5	*γ*-muurolene	0.25±0.01^{a}	0.26±0.01^{a}	0.25±0.00^{a}	0.26±0.01^{a}	0.25±0.00^{a}	0.25±0.00^{a}	0.26±0.00^{a}	0.26±0.01^{a}
6	germacrene D	0.26±0.00^{b}	0.25±0.01^{b}	0.25±0.01^{b}	0.27±0.01^{b}	0.57±0.29^{a}	0.26±0.00^{b}	0.28±0.00^{ab}	0.27±0.01^{b}
7	*α*-cadinene	ND	ND	ND	ND	ND	ND	ND	ND
8	tridecane	ND	ND	0.15	0.15±0.01	ND	ND	ND	ND
9	*(Z)*-3-hexen-1-ol	0.54±0.36^{a}	1.09±0.71^{a}	0.65±0.51^{a}	0.49^{a}	1.10±0.43^{a}	0.72±0.38^{a}	1.68±0.91^{a}	1.45±0.13^{a}
10	1-octen-3-ol	ND	ND	ND	ND	ND	ND	ND	ND
11	linalool	0.06±0.03^{a}	0.06±0.03^{a}	0.09±0.10^{a}	0.05±0.03^{a}	0.03±0.01^{a}	0.03±0.00^{a}	0.03±0.00^{a}	0.04±0.01^{a}
12	hexenal	12.29±6.94^{c}	16.66±2.33^{bc}	21.93±6.20^{bc}	29.24±19.46^{bc}	52.13±13.36^{ab}	40.81±16.92^{abc}	48.75±18.30^{abc}	71.58±8.47^{a}
13	*(Z)*-3-hexenal	7.38±3.78^{ab}	4.39±2.58^{b}	5.58±3.66^{b}	3.94±2.71^{b}	15.47±2.00^{a}	7.54±3.00^{ab}	7.33±2.03^{ab}	7.04±3.71^{ab}
14	*(E)*-2-hexenal	19.54±7.83^{b}	13.61±3.37^{b}	10.08±5.93^{b}	14.81±11.52^{b}	46.11±14.95^{a}	25.24±7.46^{ab}	28.52±6.79^{ab}	31.27±7.19^{ab}
15	phenyl acetaldehyde	ND	ND	ND	ND	ND	ND	ND	ND
16	*p*-anisaldehyde	9.32±2.72^{a}	9.97±1.50^{a}	9.99±1.70^{a}	10.48±3.93^{a}	13.80±8.59^{a}	11.15±3.75^{a}	9.48±0.59^{a}	13.10±4.24^{a}
17	fenchone	36.77±17.24^{a}	5.12^{a}	98.82±3.25^{a}	3.92^{a}	ND	ND	ND	21.32^{a}
18	bornyl acetate	ND	0.22	0.28	0.47	ND	ND	ND	ND
19	*β*-ionone	0.34±0.05^{a}	0.69±0.54^{a}	0.39^{a}	0.36±0.33^{a}	0.97±0.83^{a}	0.55±0.07^{a}	0.14±0.07^{a}	0.58±0.14^{a}
20	anisketone	1.47±0.63^{a}	1.53±0.56^{a}	1.50±0.14^{a}	1.44±0.41^{a}	1.67±0.79^{a}	1.87±0.32^{a}	1.65±0.21^{a}	1.81±0.31^{a}
21	estragole	15.99±5.91^{a}	17.33±5.15^{a}	32.08±24.97^{a}	14.09±3.23^{a}	16.45±6.59^{a}	19.47±2.45^{a}	18.32±3.16^{a}	18.96±5.71^{a}
22	*(Z)*-anethole	9.59±0.38^{a}	9.77±0.36^{a}	10.13±0.37^{a}	9.63±0.26^{a}	10.02±0.62^{a}	10.81±0.74^{a}	10.09±0.38^{a}	9.80±0.51^{a}
23	*(E)*-anethole	379.57±202.22^{a}	409.77±115.38^{a}	473.32±55.49^{a}	315.33±112.34^{a}	314.53±175.75^{a}	373.69±61.28^{a}	360.41±68.73^{a}	362.67±135.53^{a}
24	methyl eugenol	1.50±0.04^{a}	1.59±0.11^{a}	1.45±0.08^{a}	1.53±0.03^{a}	1.41±0.05^{a}	1.41±0.06^{a}	1.42±0.05^{a}	1.46±0.15^{a}
25	methyl isoeugenol	2.03±0.47^{a}	2.13±0.54^{a}	2.90±1.36^{a}	2.14±0.10^{a}	1.63±0.23^{a}	1.51±0.09^{a}	1.64±0.33^{a}	1.99±0.51^{a}
26	apiol	4.56±1.63^{b}	7.76±0.91^{b}	5.76±3.68^{b}	53.85±36.75^{a}	2.78±2.02^{b}	1.78±0.32^{b}	1.72±0.03^{b}	7.23±4.16^{b}

Results are expressed as mean ± SD (unless the compound is detected in only one of the replicates). ND = not determined. Mean separation is performed using analysis of variance (ANOVA) followed by Tukey's HSD.

Table 5-4. Odor activity values (OAV) of aroma-active compounds in fennel under different salinity stress

No.	Compound	Odor threshold in water (μg/g)	OAV							
			Harvest 1				*Harvest 2*			
			Ctrl	20mM NaCl	40mM NaCl	60mM NaCl	Ctrl	20mM NaCl	40mM NaCl	60mM NaCl
1	*α*-pinene	0.006[1]	4231	4640	4334	8490	6093	11236	11148	11349
2	*α*-phellandrene	0.2[2]	309	410	428	485	405	442	504	595
3	*γ*-terpinene	1[3]	4	4	6	7	3	1	3	3
4	allo-ocimene	0.727[4]	0.3	0.3	0.3	0.3	0.3	0.3	0.3	0.3
5	*γ*-muurolene	ND	ND	ND	ND	ND	ND	ND	ND	ND
6	germacrene D	ND	ND	ND	ND	ND	ND	ND	ND	ND
7	*α*-cadinene	ND	ND	ND	ND	ND	ND	ND	ND	ND
8	tridecane	ND	ND	ND	ND	ND	ND	ND	ND	ND
9	*(Z)*-3-hexen-1-ol	0.007[1]	8	16	9	7	16	10	24	21
10	1-octen-3-ol	0.001[1]	ND	ND	ND	ND	ND	ND	ND	ND
11	linalool	0.006[1]	10	9	16	9	5	5	5	6
12	hexenal	0.0045[2]	2732	3703	4873	6499	11583	9068	10834	15906
13	*(Z)*-3-hexenal	0.00025[1]	29518	17549	22319	15766	61866	30142	29305	28153
14	*(E)*-2-hexenal	0.017[1]	1150	800	593	871	2713	1485	1678	1839
15	phenyl acetaldehyde	0.004[1]	ND	ND	ND	ND	ND	ND	ND	ND
16	*p*-anisaldehyde	0.047[5]	198	212	213	223	294	237	202	279
17	fenchone	0.44[5]	84	12	225	9	ND	ND	ND	48
18	bornyl acetate	0.075[1]	ND	3	4	6	ND	ND	ND	ND
19	*β*-ionone	0.0005[2]	684	1386	774	714	1931	1101	286	1155
20	anisketone	1.8[5]	1	1	1	1	1	1	1	1
21	estragole	0.0075[2]	2132	2311	4278	1878	2194	2596	2442	2529
22	*(Z)*-anethole	ND	ND	ND	ND	ND	ND	ND	ND	ND
23	*(E)*-anethole	0.073[5]	5200	5613	6484	4320	4309	5119	4937	4968
24	methyl eugenol	0.82[1]	2	2	2	2	2	2	2	2
25	methyl isoeugenol	1.6[5]	1	1	2	1	1	1	1	1
26	apiol	ND	ND	ND	ND	ND	ND	ND	ND	ND

[1] Odor threshold obtained from Leffingwell & Associates (http://www.leffingwell.com/odorthre.htm).

[2] Odor threshold obtained from literature (Rychlik, Schieberle, & Grosch, 1998).

[3] Odor threshold obtained from literature (van Gemert, 2003).

[4] Odor threshold obtained from literature (Zhang, Guan, Liang, Wang, Wu, & Liu, 2023).

[5] Odor threshold obtained from literature (Zeller et al., 2006).

ND = Not determined.

Among the identified compounds, those with relatively high OAVs (>50) in fennel included *α*-pinene (pine, woody), *α*-phellandrene (herbal, woody), hexenal (green, grassy), (*Z)*-3-hexenal (leafy, grassy), *(E)*-2-hexenal (leafy, green), *p*-anisaldehyde (floral, sweet), fenchone (herbal), *β*-ionone (floral, sweet), estragole (anise, herbal), and *(E)*-anethole (sweet, anise). These compounds contribute significantly to the overall aroma profiles of fennel, with *(E)*-anethole being the most characteristic aroma compound. It has been characterized in many previous studies as one of the main aroma compounds in fennel (Afifi, El-Mahis, Heiss, & Farag, 2021; Bilia, Flamini, Taglioli, Morelli, & Vincieri, 2002; Zeller & Rychlik, 2006). In addition to *(E)*-anethole, many of these aroma compounds are key components of fennel-based products, such as fennel essential oils and fennel tea (Bilia et al., 2002; Xiao, Chen, Niu, & Chen, 2017). However, variations in the composition of fennel aroma compounds can occur due to differences in cultivar and geological locations (Afifi et al., 2021).

The composition of aroma compounds in fennel under different salinity levels is shown in Figure 5-2. A two-way ANOVA indicated no significant effects of harvest time, salinity, or their interactions on the total aroma concentration. Phenylpropanoids were the most abundant group in fennel aroma, accounting for 54.2% ~ 72.7% of the total volatile aroma compounds across all treatments. Other chemical groups include terpenoids (19.5% ~ 28.7%), aldehydes (6.0% ~ 21.3%), and minor compounds, including ketones, alcohols, and alkane, which accounted for less than 0.6% of the total volatile profile. According to 2-way ANOVA, terpenoids concentration was significantly affected by salinity, while the concentrations of aldehydes and miscellaneous groups were significantly affected by

harvest time. In general, the concentration of terpenoids showed an increasing trend with increased salinity level.

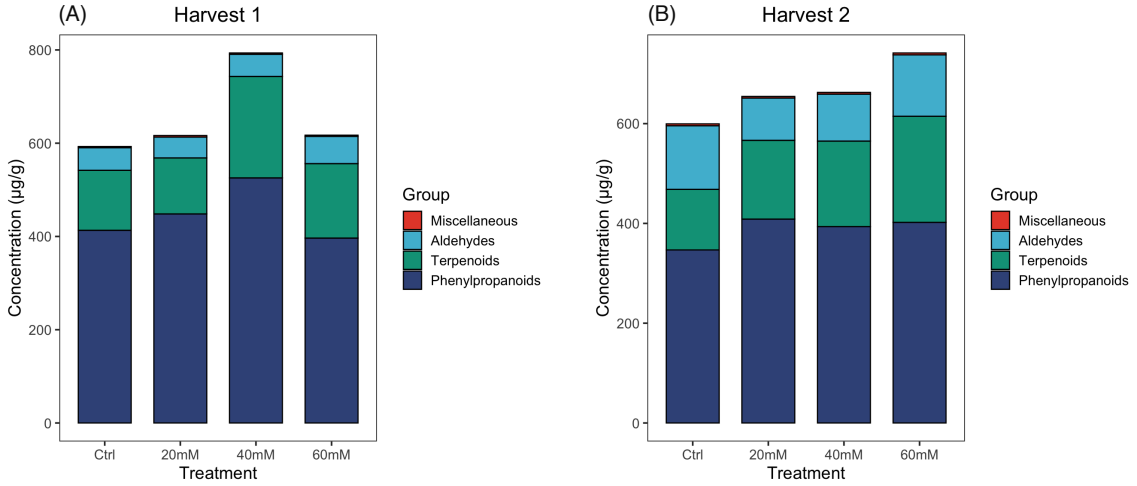

Figure 5-2. Aroma composition of fennel under different salinity stress at (A) the first harvest, (B) the second harvest.

This trend in terpenoid accumulation under salinity stress has also been observed in other species. For example, a threefold increase in limonene (monoterpene) was reported in Tunisian fennel under 75 mM NaCl (Rebey et al., 2016). Similarly, increased levels of terpenoids have been observed in *Salvia mirzayanii* (Valifard, Mohsenzadeh, Kholdebarin, Rowshan, Niazi, & Moghadam, 2019), *Citrus aurantium* (Eirini, Paschalina, Ioannis, & Kortessa, 2017), and *Camellia sinensis* (Zhou, Shamala, Yi, Yan, & Wei, 2020) under salinity stress. The rise in terpenoids level is likely linked to their role in plants' antioxidant defense mechanisms. Under normal conditions, there is an equilibrium between the production and scavenging of ROS; however, under stress, ROS levels can rise, causing oxidative damages (Miller, Shulaev, & Mittler, 2008). Terpenoids, as plant secondary metabolites, can mitigate ROS overgeneration and help reduce oxidative stress.

To further examine how salinity stress affects aroma compounds over two harvest times, a hierarchical cluster heatmap was graphed using normalized aroma concentrations, with Euclidean distance as the clustering metric (Figure 5-3). Each row represents an individual compound, and each column corresponds to a sample. Darker shades of red indicate higher compound concentrations, while darker blue represents lower concentrations. The heatmap showed distinct differences in aroma concentrations between the two harvests. Compounds such as *γ*-terpinene, allo-ocimene, and methyl isoeugenol, showed higher concentration in the earlier harvest, while others, including *α*-phellandrene, *α*-pinene, and hexenal, were more abundant in the second harvest.

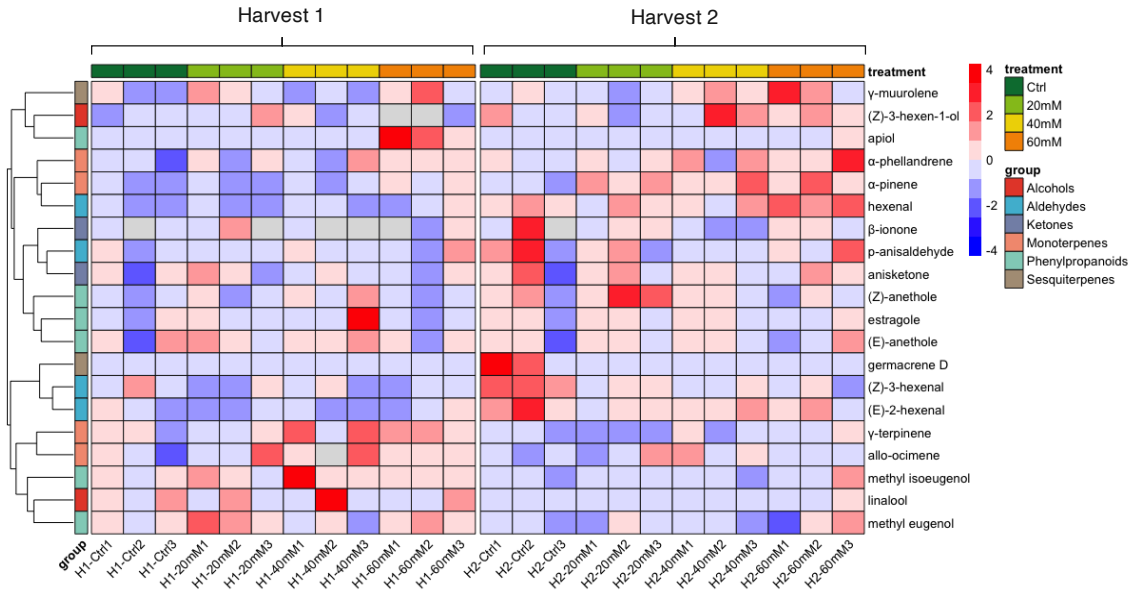

Figure 5-3. Hierarchical cluster heatmap of fennel aroma compounds under different salinity levels.

Four aroma compounds, including *α*-pinene, (*Z)*-3-hexenal, hexenal, and apiol, were significantly influenced by salinity. Figure 5-4 is the bar graph showing their concentrations across different treatments, and the p values of two-way ANOVA are

provided in Table 5-5. The concentrations of *α*-pinene, hexenal, and *(Z)*-3-hexenal were significantly affected by both harvest time and salinity levels, though no significant interactions between these factors was observed. In contrast, apiol showed significant effects not only from harvest time and salinity but also from their interaction, indicating a more complex response. Apiol showed higher concentrations in the earlier harvest, consistent with the findings in Chapter 3, while *α*-pinene, hexenal, and *(Z)*-3-hexenal showed higher concentrations in the second harvest. Under 60 mM NaCl, fennel accumulated the highest levels of *α*-pinene, hexenal, and apiol. However, except for apiol, the differences in concentrations were not statistically significant. The highest concentration of *(Z)*-3-hexenal was observed in the control group at the second harvest, though this difference was also not statistically significant when compared to other salinity treatments within the same harvest. Changes in volatile composition due to salinity stress have been previously reported in various plant species, such as C*oriandrum sativum* (Neffati et al., 2011), *Mentha piperita* L. (Khorasaninejad, Mousavi, Soltanloo, Hemmati, & Khalighi, 2010), and *Rosmarinus officinalis* L. (Sarmoum, Haid, Biche, Djazouli, Zebib, & Merah, 2019). The impact of salinity on a plant's volatile profile largely depends on the salt concentration and the species' salinity tolerance, which may be linked to specific enzymes involved in the biosynthesis pathways of volatile compounds under salinity stress (Sarmoum et al., 2019).

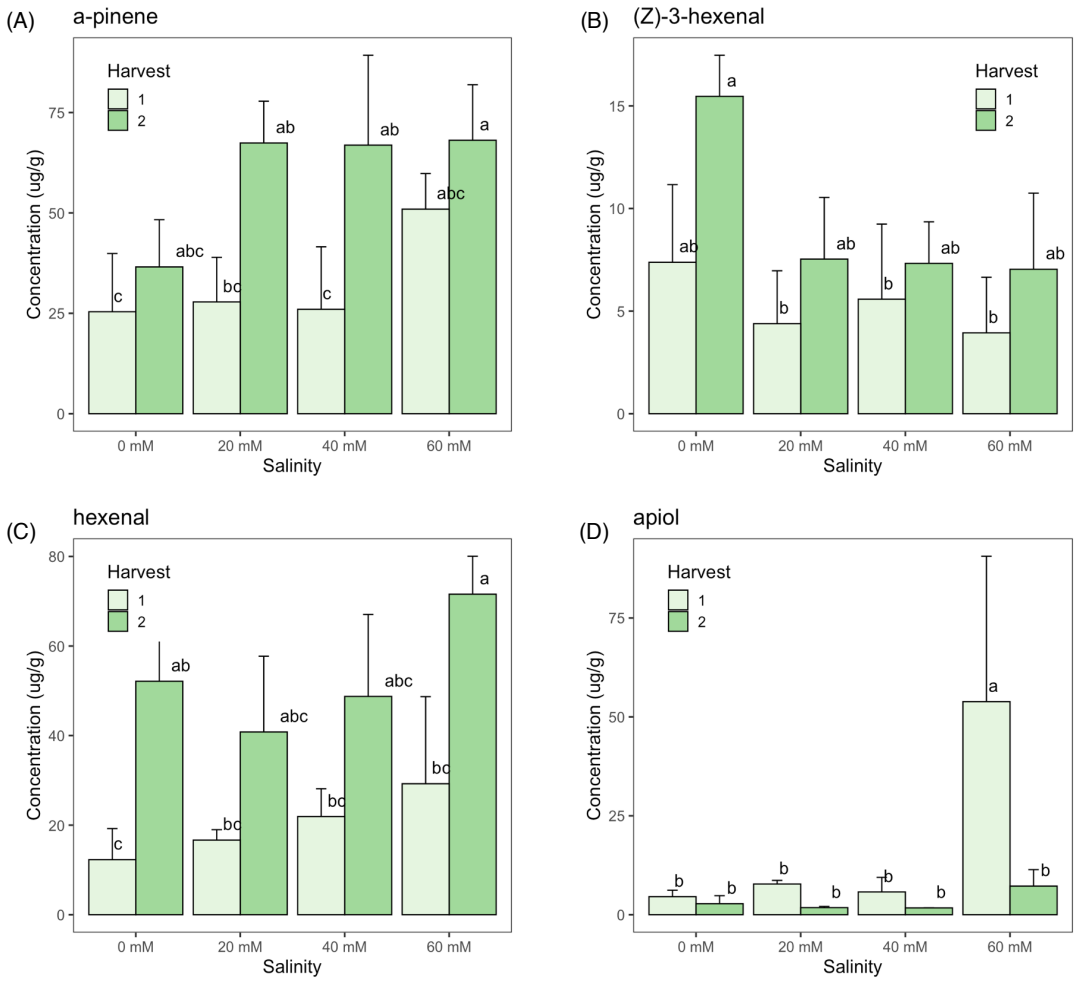

Figure 5-4. Aroma compounds significantly affected by salinity treatment. (A) α-pinene. (B) (Z)-3-hexenal. (C) hexenal. (D) apiol.

Analysis of variance and mean separation was performed using Tukey's HSD at $p < 0.05$.

Table 5-5. p values of two-way ANOVA for selected aroma compounds.

Source of variance	p value			
	α-pinene	hexenal	*(Z)*-3-hexenal	apiol
Harvest	0.0002	<0.0001	0.0048	0.0153
Salinity	0.0240	0.0491	0.0122	0.0059
Harvest × Salinity	0.1965	0.5407	0.3135	0.0274

5.3.3 Transcriptome analysis and differentially expressed genes (DEGs) in fennel leaf tissue under salinity stress

To investigate the genetic basis underlying fennel's response to salinity stress across two harvest times, RNA-seq analysis was performed on fennel leaf tissues under different treatments to generate their transcriptome profiles. The number of reads, raw data size, and other quality parameters of samples were provided in Supplemental Table 5-4. The expression levels of *de novo* transcripts were quantified using Trinity software and differential expression analysis was performed using Bioconductor package DESeq2 (Love, Anders, Kim, & Huber, 2016). A principal component analysis (PCA) was performed using the expression levels of transcripts from all 24 samples. As shown in Figure 5-5, the first two principal components (PC) accounted for 33% of the total variance. Overall, samples from different harvest times distinguished well on PC1.

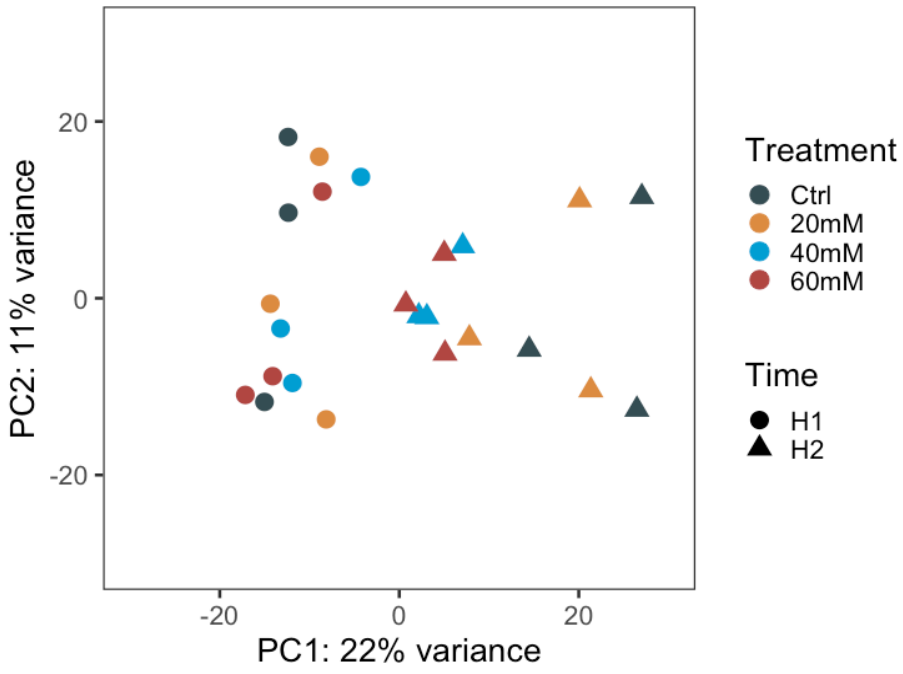

Figure 5-5. Principal component analysis with gene expression levels of fennel samples.

Figure 5-6 is a hierarchical clustering heatmap showing sample correlations. It can be observed that the correlation coefficient was close to 1 for replicates. The heatmap of the sample-to-sample distances is shown in Supplemental Figure 5-1, which shows an overview on similarities and dissimilarities between samples. The results suggested that two samples from the control and 20 mM NaCl treatment at the second harvest clustered together, while the remaining samples formed another cluster. Overall, these findings suggest some variation within replicates of the same treatment, likely due to the relatively small replicate size (n=3) in this study.

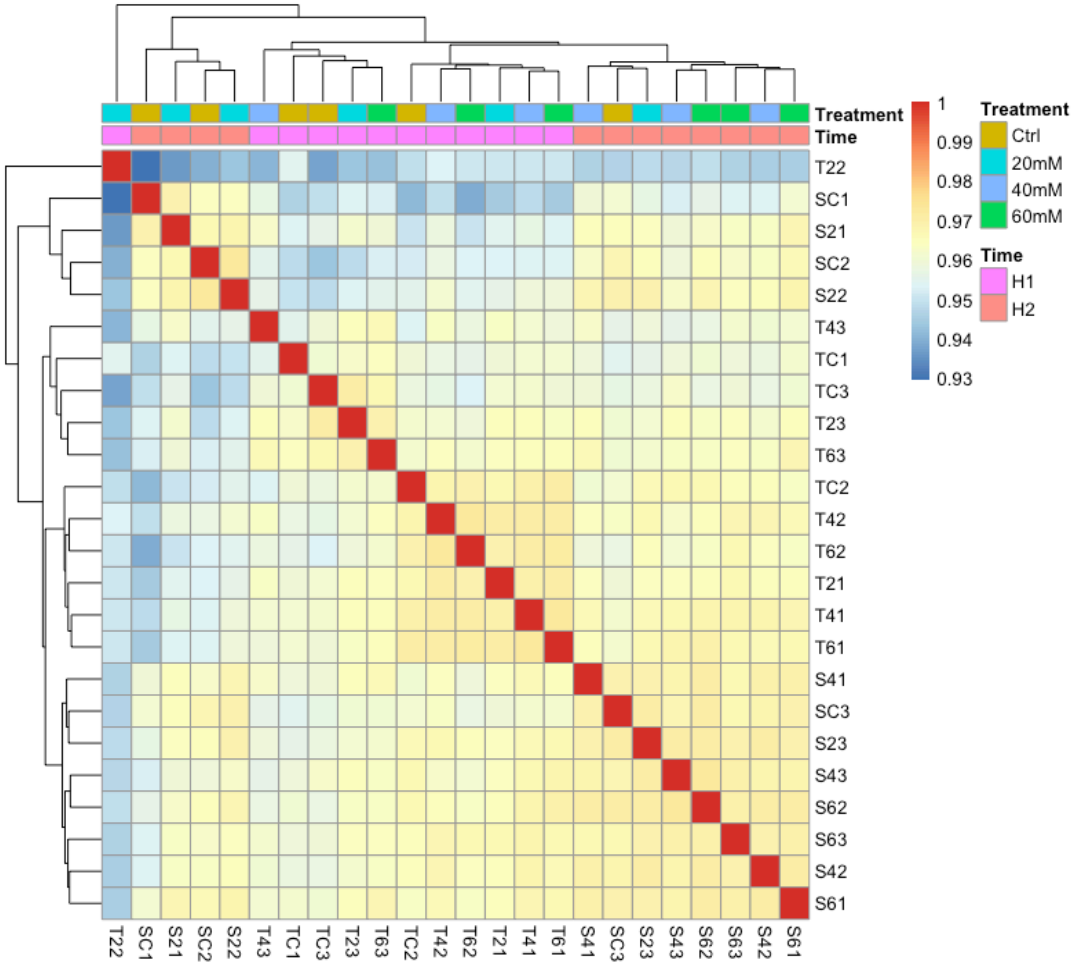

Figure 5-6. Hierarchical clustering heatmap showing sample correlation based on gene expression data.

To determine whether any salinity level induced changes in gene expression at any time point, a design with a time factor, a salinity factor, and the interaction between these two was employed in DESeq2. Using the criteria of |log2Fold Change| >1.5 and adjusted p value < 0.05, a total of 388 DEGs were identified, including 337 upregulated and 51 downregulated transcripts (Figure 5-7). Among the DEGs, 6 transcription factors (TFs) were identified, including transcription factor MYB102, WRKY42, WRKY6, heat stress transcription factor B-3, JUNGBRUNNEN 1, and bHLH041. All TFs were upregulated in response to salinity. TFs play a key role in regulating molecular response at transcription level (Stevens, Mariconti, Rossignol, Perennes, Cella, & Bergounioux, 2002). The results are similar with previous research in *Aeluropus littoralis*, where TFs from WRKY family were up-regulated in 200 mM and 400 mM NaCl treatments (Younesi-Melerdi, Nematzadeh, Pakdin-Parizi, Bakhtiarizadeh, & Motahari, 2020). Additionally, genes from MYB family are known to play key roles in stress adaptive pathways (Golldack, Lüking, & Yang, 2011). Previous studies have also suggested TFs from ERF family also contribute to salinity response (Licausi, Ohme‐Takagi, & Perata, 2013), but no ERF TFs were identified in this study.

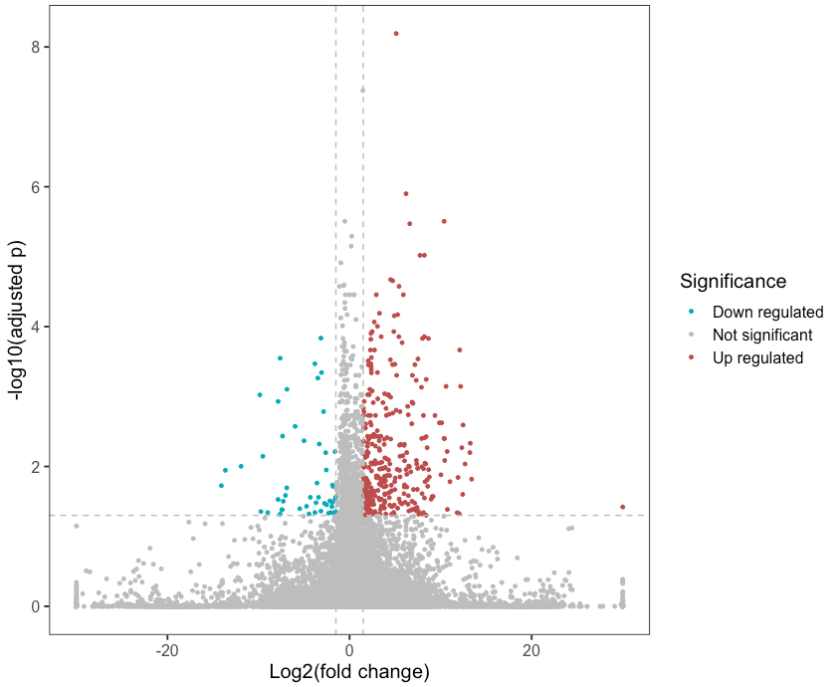

Figure 5-7. Volcano plot of differentially expressed genes.

5.3.4 Functional enrichment of DEGs

Gene ontology (GO) enrichment analysis was performed to investigate the functions of the identified DEGs. The most enriched biological process (BP) GO terms, and the numbers of their occurrence were shown in Figure 5-8. Notably, more GO terms were associated with upregulated DEGs than with downregulated ones. Among the upregulated transcripts, the most enriched BP terms were “phosphorylation”, “defense response”, “response to salt stress”, and “response to water deprivation”. Phosphorylation, the process in which a phosphate group is added to a molecule, plays a crucial role in the mitogen-activated protein kinase cascade (MAPK or MPK) pathway, which is involved in salinity stress signal transduction (Ichimura et al., 2002). For the downregulated transcripts, “double-strand break repair via homologous recombination” was the most enriched BP term. Homologous recombination plays a vital role in both the repair of DNA damage

during mitosis and in the pairing and exchange of chromosomes during meiosis (Krejci, Altmannova, Spirek, & Zhao, 2012). This suggest that salinity may impair fennel's DNA repair capacity, leading to inhibited growth and reduced crop productivity (Balestrazzi, Confalonieri, Macovei, Donà, & Carbonera, 2011).

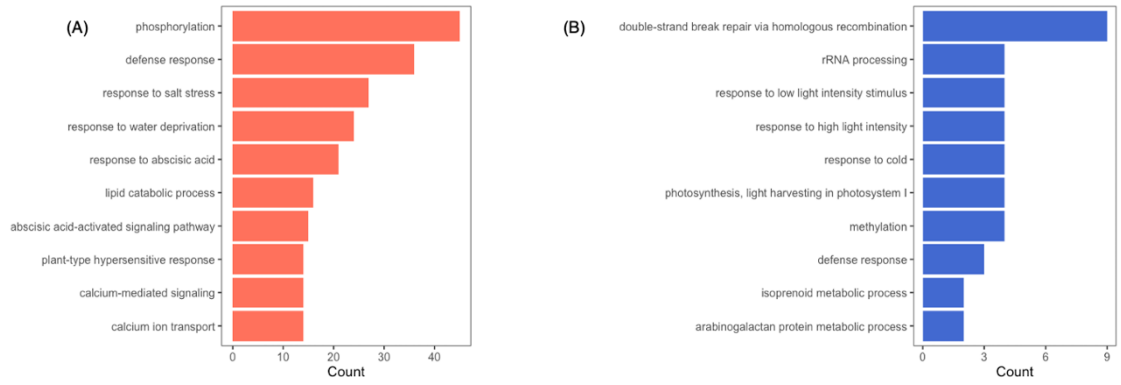

Figure 5-8. Most enriched biological process GO terms in (A) upregulated DEGs and (B) downregulated DEGs.

As shown in Figure 5-9A, the most enriched GO terms among the upregulated transcripts included "oxidoreductase activity", "nucleotide binding", "nucleoside phosphate binding", "catalytic activity", and "heterocyclic compound binding". Most of them belong to the molecular function and cellular component categories of GC terms. The role of oxidoreductase in enhancing salinity resistance has been reported in *Chrysanthemum morifolium* (Li, Fang, Chong, Chen, Yue, & Wang, 2024). The significantly downregulated GO terms are "outer membrane", "organelle outer membrane", "binding membrane of organelle", "negative regulation of biological process", and "cell wall macromolecule metabolic process". This suggested that salinity significantly affected the structural integrity of the cell membrane in fennel. These results align with previous research findings in *Sorghum bicolor*, where salinity altered the organization of

cellulose microfibril in cell walls (Koyro, 1997). For BP terms, as shown in Figure 5-9B, "phosphorus metabolic process", "phosphate-containing compound metabolic process", and "response to stimulus" were significantly activated, while "negative regulation of biological process" and "cell wall macromolecule metabolic process" were suppressed. Phosphorus is an essential plant macronutrient for energy metabolism and macromolecules formation (Stigter & Plaxton, 2015). Previous studies have shown that increasing phosphorus levels in nutrient solutions enhances salt tolerance by reducing sodium and increasing potassium in barley shoots (Chen, Zhou, Newman, Mendham, Zhang, & Shabala, 2007). Similarly, the increased phosphorus metabolism observed may contribute to the defense mechanism of fennel in response to salinity.

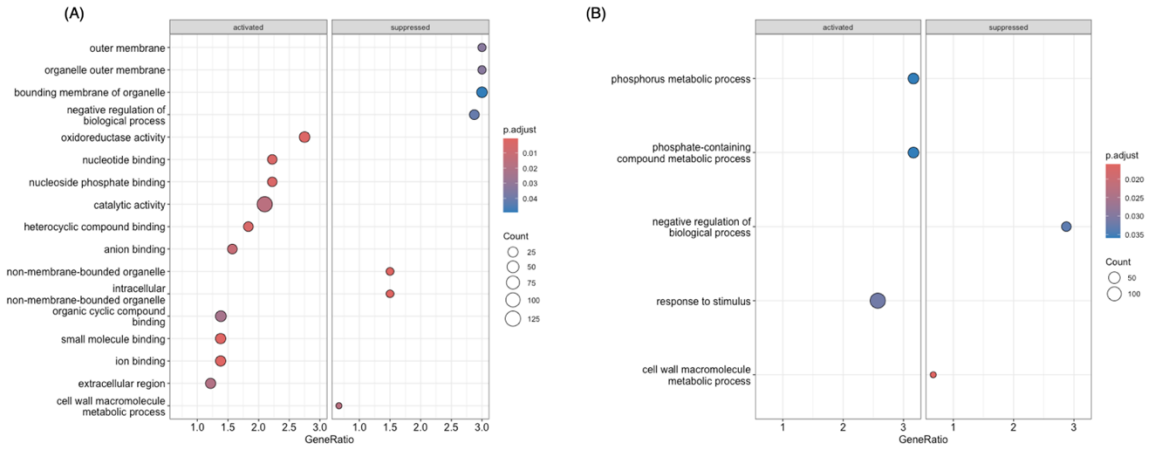

Figure 5-9. Enrichment map of (A) all GO terms and (B) biological process GO terms.

KEGG enrichment analysis was conducted using *Arabidopsis thaliana* as the reference organism. As shown in Supplemental Figure 5-2, the "plant hormone signal transduction" pathway was significantly activated by salinity. Other pathways, such as "biosynthesis of secondary metabolites", "metabolic pathways", and "α-linolenic acid metabolism" were also enriched but did not show statistical significance. This suggested

that salinity affected secondary metabolism, which may potentially alter the aroma and fatty acid composition of fennel. Supplemental Figure 5-3 further illustrate the influences of salinity on plant hormone signal transduction pathway. Several key genes and enzymes, including auxin response factors (ARF), auxin responsive GH3 gene family (GH3), protein phosphatases 2C (PP2C and ABI1/2), and calcium-dependent protein kinase (CPK28), were significantly activated by salinity. These genes regulate important biological processes, such as plant growth, cell enlargement, and abscisic acid response. Interestingly, PP2C and ABI1/2 are also involved in the MAPK signaling pathway, which is known to play a pivotal role in abiotic stress responses (Younesi-Melerdi et al., 2020). In previous studies, up-regulation of genes involved in plant hormone signal transduction pathway under salinity stress was also reported in other plant species, such as sorghum (Wang et al., 2010), legumes (Singh, Jain, & Garg, 2015), and rice (Kong et al., 2019).

5.4 Conclusion

In this study, the response of fennel to salinity stress over a six-week period was investigated. Salinity caused significant reductions in fennel growth, especially in plant height, width, and yield, with more pronounced impacts as the duration of exposure increased. While no significant effect of salinity, harvest time, or the interactions between these two on total aroma concentration was observed, salinity significantly affected terpenoids concentration, and several aroma compounds, including α-pinene, (*Z)*-3-hexenal, hexenal, and apiol. These changes are likely linked to specific genes and enzymes involved in the biosynthesis pathways of volatile compounds under salinity stress. The results from *de novo* RNA-seq highlighted the detrimental effects of salinity on cellular structures and metabolic processes, as well as the activation of salt tolerance and defense

mechanisms in fennel. Plant hormone signal transduction and MAPK signaling pathways were upregulated, and several TFs from MYB, bHLH, and WRKY families were identified in our study, which may involve in stress adaption. To summarize, this study provides new insights into the growth, aroma formation, and adaptive responses of fennel in response to salinity stress. Future research could focus on the influences of salinity stress on fennel fatty acids composition, as well as the identification of genes responsible for salinity tolerance and their regulatory mechanisms.

References

Acosta-Motos, J. R., Ortuño, M. F., Bernal-Vicente, A., Diaz-Vivancos, P., Sanchez-Blanco, M. J., & Hernandez, J. A. (2017). Plant responses to salt stress: Adaptive mechanisms. *Agronomy, 7*(1), 18. https://doi.org/10.3390/agronomy7010018.

Adhikari, B., Olorunwa, O. J., Wilson, J. C., & Barickman, T. C. (2021). Morphological and physiological response of different lettuce genotypes to salt stress. *Stresses, 1*(4), 285–304. https://doi.org/10.3390/stresses1040021.

Adhikari, N. D., Simko, I., & Mou, B. (2019). Phenomic and physiological analysis of salinity effects on lettuce. *Sensors, 19*(21), 4814. https://doi.org/10.3390/s19214814.

Afifi, S. M., El-Mahis, A., Heiss, A. G., & Farag, M. A. (2021). Gas chromatography–mass spectrometry-based classification of 12 fennel (*Foeniculum vulgare* Miller) varieties based on their aroma profiles and estragole levels as analyzed using chemometric tools. *ACS Omega*, *6*(8), 5775-5785. https://doi.org/10.1021/acsomega.0c06188.

An, Y., Wang, Z., Liu, B., Cao, Y., & Chen, L. (2023). Translational landscape of medicago truncatula seedlings under salt stress. *Journal of Agricultural and Food Chemistry*, *71*(44), 16657-16668. https://doi.org/10.1021/acs.jafc.3c03922.

Ashraf, M., & Akhtar, N. (2004). Influence of salt stress on growth, ion accumulation and seed oil content in sweet fennel. *Biologia Plantarum, 48*(3), 461-464. https://doi.org/10.1023/B:BIOP.0000041105.89674.d1.

Babushok, V. I., Linstrom, P. J., & Zenkevich, I. G. (2011). Retention indices for frequently reported compounds of plant essential oils. *Journal of Physical and Chemical Reference Data*, *40*(4), 043101. https://doi.org/10.1063/1.3653552.

Balestrazzi, A., Confalonieri, M., Macovei, A., Donà, M., & Carbonera, D. (2011). Genotoxic stress and DNA repair in plants: Emerging functions and tools for improving crop productivity. *Plant Cell Reports, 30*(2), 287–295. https://doi.org/10.1007/s00299-010-0975-9.

Bilia, A. R., Flamini, G., Taglioli, V., Morelli, I., & Vincieri, F. F. (2002). GC-MS analysis of essential oil of some commercial Fennel teas. *Food Chemistry, 76*(3), 307-310. https://doi.org/10.1016/S0308-8146(01)00277-1.

Bourgou, S., Bettaieb, I., Saidani, M., & Marzouk, B. (2010). Fatty acids, essential oil, and phenolics modifications of black cumin fruit under nacl stress conditions. *Journal of Agricultural and Food Chemistry, 58*(23), 12399-12406. https://doi.org/10.1021/jf103415q.

Bryant, D. M., Johnson, K., DiTommaso, T., Tickle, T., Couger, M. B., Payzin-Dogru, D., Lee, T. J., Leigh, N. D., Kuo, T.-H., Davis, F. G., Bateman, J., Bryant, S., Guzikowski, A. R., Tsai, S. L., Coyne, S., Ye, W. W., Freeman, R. M., Jr., Peshkin, L., Tabin, C. J., Regev, A., Haas, B. J., & Whited, J. L. (2017). A tissue-mapped axolotl *de novo* transcriptome enables identification of limb regeneration factors. *Cell Reports, 18*(3), 762-776. https://doi.org/10.1016/j.celrep.2016.12.063.

Chandran, A. K. N., Kim, J.-W., Yoo, Y.-H., Park, H. L., Kim, Y.-J., Cho, M.-H., & Jung, K.-H. (2019). Transcriptome analysis of rice-seedling roots under soil–salt stress

using RNA-Seq method. *Plant Biotechnology Reports, 13*(6), 567-578. https://doi.org/10.1007/s11816-019-00550-3.

Chen, Z., Zhou, M., Newman, I. A., Mendham, N. J., Zhang, G., & Shabala, S. (2007). Potassium and sodium relations in salinised barley tissues as a basis of differential salt tolerance. *Functional Plant Biology, 34*(2), 150-162. https://doi.org/10.1071/fp06237.

Colin, L., Ruhnow, F., Zhu, J.-K., Zhao, C., Zhao, Y., & Persson, S. (2023). The cell biology of primary cell walls during salt stress. *The Plant Cell, 35*(1), 201-217. https://doi.org/10.1093/plcell/koac292.

de Souza, M. C. P., da Silva, M. D., Binneck, E., de Lima Cabral, G. A., Benko Iseppon, A. M., Pompelli, M. F., Endres, L., & Kido, É. A. (2020). RNA-Seq transcriptome analysis of *Jatropha curcas* L. accessions after salt stimulus and unigene-derived microsatellite mining. *Industrial Crops and Products, 147*, 112168. https://doi.org/10.1016/j.indcrop.2020.112168.

Dell'Aquila, A., & Spada, P. (1992). Regulation of protein synthesis in germinating wheat embryos under polyethylene glycol and salt stress. *Seed Science Research, 2*(2), 75-80. https://doi.org/10.1017/S0960258500001161.

Eirini, S., Paschalina, C., Ioannis, T., & Kortessa, D.-T. (2017). Effect of drought and salinity on volatile organic compounds and other secondary metabolites of *Citrus aurantium* leaves. *Natural Product Communications, 12*(2), 193-196.

Erten, E. S., & Cadwallader, K. R. (2017). Identification of predominant aroma components of raw, dry roasted and oil roasted almonds. *Food Chemistry, 217,* 244-253. https://doi.org/10.1016/j.foodchem.2016.08.091.

Flowers, T. J., & Colmer, T. D. (2008). Salinity tolerance in halophytes. *The New Phytologist, 179*(4), 945-963. https://doi.org/10.1111/j.1469-8137.2008.02531.x.

Golldack, D., Li, C., Mohan, H., & Probst, N. (2014). Tolerance to drought and salt stress in plants: Unraveling the signaling networks. *Frontiers in Plant Science, 5.* https://doi.org/10.3389/fpls.2014.00151.

Golldack, D., Lüking, I., & Yang, O. (2011). Plant tolerance to drought and salinity: stress regulating transcription factors and their functional significance in the cellular transcriptional network. *Plant Cell Reports, 30*(8), 1383-1391. https://doi.org/10.1007/s00299-011-1068-0.

Grabherr, M. G., Haas, B. J., Yassour, M., Levin, J. Z., Thompson, D. A., Amit, I., Adiconis, X., Fan, L., Raychowdhury, R., Zeng, Q., Chen, Z., Mauceli, E., Hacohen, N., Gnirke, A., Rhind, N., di Palma, F., Birren, B. W., Nusbaum, C., Lindblad-Toh, K., Friedman, N., & Regev, A. (2011). Full-length transcriptome assembly from RNA-Seq data without a reference genome. *Nature Biotechnology*, *29*(7), 644-652. https://doi.org/10.1038/nbt.1883.

Hao, S., Wang, Y., Yan, Y., Liu, Y., Wang, J., & Chen, S. (2021). A review on plant responses to salt stress and their mechanisms of salt resistance. *Horticulturae, 7*(6), 132. https://doi.org/10.3390/horticulturae7060132.

Hasegawa, P. M., Bressan, R. A., Zhu, J.-K., & Bohnert, H. J. (2000). Plant cellular and molecular responses. *Annual Review of Plant Biology, 51,* 463-499. https://doi.org/10.1146/annurev.arplant.51.1.463.

Ichimura, K., Shinozaki, K., Tena, G., Sheen, J., Henry, Y., Champion, A., Kreis, M., Zhang, S., Hirt, H., Wilson, C., Heberle-Bors, E., Ellis, B. E., Morris, P. C., Innes, R. W., Ecker, J. R., Scheel, D., Klessig, D. F., Machida, Y., Mundy, J., & Walker, J. C. (2002). Mitogen-activated protein kinase cascades in plants: a new nomenclature. *Trends in Plant Science, 7*(7), 301-308. https://doi.org/10.1016/S1360-1385(02)02302-6.

Isayenkov, S. V., & Maathuis, F. J. M. (2019). Plant salinity stress: Many unanswered questions remain. *Frontiers in Plant Science*, *10*. https://doi.org/10.3389/fpls.2019.00080.

Jamil, A., Riaz, S., Ashraf, M., & Foolad, M. R. (2011). Gene expression profiling of plants under salt stress. *Critical Reviews in Plant Sciences, 30*(5), 435-458. https://doi.org/10.1080/07352689.2011.605739.

Julkowska, M. M., & Testerink, C. (2015). Tuning plant signaling and growth to survive salt. *Trends in Plant Science, 20*(9), 586-594. https://doi.org/10.1016/j.tplants.2015.06.008.

Karray-Bouraoui, N., Rabhi, M., Neffati, M., Baldan, B., Ranieri, A., Marzouk, B., Lachaâl, M., & Smaoui, A. (2009). Salt effect on yield and composition of shoot essential oil and trichome morphology and density on leaves of *Mentha pulegium*.

Industrial Crops and Products, 30(3), 338-343. https://doi.org/10.1016/j.indcrop.2009.06.003.

Khorasaninejad, S., Mousavi, A., Soltanloo, H., Hemmati, K., & Khalighi, A. (2010). The effect of salinity stress on growth parameters, essential oil yield and constituent of peppermint (*Mentha piperita* L.). *World Applied Sciences Journal, 11*(11), 1403-1407.

Kong, W., Zhong, H., Deng, X., Gautam, M., Gong, Z., Zhang, Y., Zhao, G., Liu, C., & Li, Y. (2019). Evolutionary analysis of *GH3* genes in six *Oryza* species/subspecies and their expression under salinity stress in *Oryza sativa* ssp. *japonica*. *Plants, 8*(2), 30. https://doi.org/10.3390/plants8020030.

Koyro, H.-W. (1997). Ultrastructural and physiological changes in root cells of Sorghum plants (*Sorghum bicolor*× S. *sudanensis* cv. Sweet Sioux) induced by NaCl. *Journal of Experimental Botany, 48*(3), 693-706. https://doi.org/10.1093/jxb/48.3.693.

Krejci, L., Altmannova, V., Spirek, M., & Zhao, X. (2012). Homologous recombination and its regulation. *Nucleic Acids Research, 40*(13), 5795-5818. https://doi.org/10.1093/nar/gks270.

Li, P., Fang, T., Chong, X., Chen, J., Yue, J., & Wang, Z. (2024). CmDOF18 positively regulates salinity tolerance in *Chrysanthemum morifolium* by activating the oxidoreductase system. *BMC Plant Biology, 24*(1), 232. https://doi.org/10.1186/s12870-024-04914-y.

Li, P., Zhu, Y., Song, X., & Song, F. (2020). Negative effects of long-term moderate salinity and short-term drought stress on the photosynthetic performance of Hybrid *Pennisetum*. *Plant Physiology and Biochemistry, 155*, 93-104. https://doi.org/10.1016/j.plaphy.2020.06.033.

Licausi, F., Ohme-Takagi, M., & Perata, P. (2013). APETALA 2/Ethylene Responsive Factor (AP 2/ERF) transcription factors: Mediators of stress responses and developmental programs. *New Phytologist, 199*(3), 639-649. https://doi.org/10.1111/nph.12291.

Machado, R. M., & Serralheiro, R. P. (2017). Soil salinity: Effect on vegetable crop growth. Management practices to prevent and mitigate soil salinization. *Horticulturae, 3*(2), 30. https://doi.org/10.3390/horticulturae3020030.

Miller, G., Shulaev, V., & Mittler, R. (2008). Reactive oxygen signaling and abiotic stress. *Physiologia plantarum, 133*(3), 481-489. https://doi.org/10.1111/j.1399-3054.2008.01090.x.

Mohammadi, M., Pouryousef, M., & Farhang, N. (2023). Study on germination and seedling growth of various ecotypes of fennel (*Foeniculum vulgare* Mill.) under salinity stress. *Journal of Applied Research on Medicinal and Aromatic Plants*, 34, 100481. https://doi.org/10.1016/j.jarmap.2023.100481.

Mukhopadhyay, R., Sarkar, B., Jat, H. S., Sharma, P. C., & Bolan, N. S. (2021). Soil salinity under climate change: Challenges for sustainable agriculture and food security. *Journal of Environmental Management, 280*, 111736. https://doi.org/10.1016/j.jenvman.2020.111736.

Neffati, M., Sriti, J., Hamdaoui, G., Kchouk, M. E., & Marzouk, B. (2011). Salinity impact on fruit yield, essential oil composition and antioxidant activities of *Coriandrum sativum* fruit extracts. *Food Chemistry, 124*(1), 221-225. https://doi.org/10.1016/j.foodchem.2010.06.022.

Petropoulos, S. A., Karkanis, A., Martins, N., & Ferreira, I. C. F. R. (2018). Halophytic herbs of the Mediterranean basin: An alternative approach to health. *Food and Chemical Toxicology, 114*, 155-169. https://doi.org/10.1016/j.fct.2018.02.031.

Rebey, I. B., Rahali, F. Z., Tounsi, M. S., Marzouk, B., & Ksouri, R. (2016). Variation in fatty acid and essential oil composition of sweet fennel (*Foeniculum vulgare* Mill) seeds as affected by salinity. *Journal of New Sciences, 15*.

Rychlik, M., Schieberle, P., & Grosch, W. (1998). *Compilation of odor thresholds, odor qualities and retention indices of key food odorants*. Garching: Deutsche Forschungsanstat für Lebensmittelchemie and Instit für Lebensmittelchemie der Technischen Universität München Garching.

Sarmoum, R., Haid, S., Biche, M., Djazouli, Z., Zebib, B., & Merah, O. (2019). Effect of salinity and water stress on the essential oil components of rosemary (*Rosmarinus officinalis* L.). *Agronomy, 9*(5), 214. https://doi.org/10.3390/agronomy9050214.

Semiz, G., Ünlükara, A., Yurtseven, E., Suarez, D., & Telci, I. (2012). Salinity impact on yield, water use, mineral and essential oil content of fennel (*Foeniculum vulgare* Mill.). *Journal of Agricultural Sciences, 18*(3), 177-186.

Shafeiee, M., & Ehsanzadeh, P. (2019). Physiological and biochemical mechanisms of salinity tolerance in several fennel genotypes: Existence of clearly-expressed

genotypic variations. *Industrial Crops and Products, 132*, 311-318. https://doi.org/10.1016/j.indcrop.2019.02.042.

Shrivastava, P., & Kumar, R. (2015). Soil salinity: A serious environmental issue and plant growth promoting bacteria as one of the tools for its alleviation. *Saudi Journal of Biological Sciences, 22*(2), 123-131. https://doi.org/10.1016/j.sjbs.2014.12.001.

Singh, V. K., Jain, M., & Garg, R. (2015). Genome-wide analysis and expression profiling suggest diverse roles of *GH3* genes during development and abiotic stress responses in legumes. *Frontiers in Plant Science, 5.* https://doi.org/10.3389/fpls.2014.00789.

Stevens, R., Mariconti, L., Rossignol, P., Perennes, C., Cella, R., & Bergounioux, C. (2002). Two E2F sites in the Arabidopsis MCM3 promoter have different roles in cell cycle activation and meristematic expression. *Journal of Biological Chemistry*, 277(36), 32978-32984. https://doi.org/10.1074/jbc.m205125200.

Stigter, K. A., & Plaxton, W. C. (2015). Molecular mechanisms of phosphorus metabolism and transport during leaf senescence. *Plants, 4*(4), 773-798. https://doi.org/10.3390/plants4040773.

Turan, S., & Tripathy, B. C. (2015). Salt‐stress induced modulation of chlorophyll biosynthesis during de‐etiolation of rice seedlings. *Physiologia plantarum, 153*(3), 477-491. https://doi.org/10.1111/ppl.12250.

Valifard, M., Mohsenzadeh, S., Kholdebarin, B., Rowshan, V., Niazi, A., & Moghadam, A. (2019). Effect of salt stress on terpenoid biosynthesis in Salvia mirzayanii: from gene to metabolite. *The Journal of Horticultural Science and Biotechnology, 94*(3), 389-399. https://doi.org/10.1080/14620316.2018.1505443.

van Den Dool, H., & Dec. Kratz, P. (1963). A generalization of the retention index system including linear temperature programmed gas—liquid partition chromatography. *Journal of Chromatography A, 11*, 463-471. https://doi.org/10.1016/S0021-9673(01)80947-X.

van Gemert, A. F. (2003). *Compilations of Odour Threshold Values in Air, Water and Other Media*. Boelens Aroma Chemical Information Service.

van Zelm, E., Zhang, Y., & Testerink, C. (2020). Salt tolerance mechanisms of plants. *Annual Review of Plant Biology, 71*, 403-433. https://doi.org/10.1146/annurev-arplant-050718-100005.

Wang, S., Bai, Y., Shen, C., Wu, Y., Zhang, S., Jiang, D., Guilfoyle, T. J., Chen, M., & Qi, Y. (2010). Auxin-related gene families in abiotic stress response in *Sorghum bicolor*. *Functional & Integrative Genomics, 10*, 533-546. https://doi.org/10.1007/s10142-010-0174-3.

Wasli, H., Ben Mansour, R., Hessini, K., Abid, C., Herchi, W., Cardoso, S. M., & Jelali, N. (2024). Combined effects of salinity and iron availability on growth, gas exchange, and antioxidant status of *Foeniculum vulgare*. *Russian Journal of Plant Physiology, 71*(1), 15. https://doi.org/10.1134/S1021443723602392.

Xiao, Z., Chen, J., Niu, Y., & Chen, F. (2017). Characterization of the key odorants of fennel essential oils of different regions using GC–MS and GC–O combined with partial least squares regression. *Journal of Chromatography B, 1063,* 226-234. https://doi.org/10.1016/j.jchromb.2017.07.053.

Yang, Y., & Guo, Y. (2018). Elucidating the molecular mechanisms mediating plant salt-stress responses. *New Phytologist, 217*(2), 523-539. https://doi.org/10.1111/nph.14920.

Younesi-Melerdi, E., Nematzadeh, G.-A., Pakdin-Parizi, A., Bakhtiarizadeh, M. R., & Motahari, S. A. (2020). *De novo* RNA sequencing analysis of *Aeluropus littoralis* halophyte plant under salinity stress. *Scientific Reports, 10*(1), 9148. https://doi.org/10.1038/s41598-020-65947-5.

Zaki, M. F., Abou-Hussein, S. D., Abou El-Magd, M. M., & El-Abagy, H. M. H. (2009). Evaluation of some sweet fennel cultivars under saline irrigation water. *European Journal of Scientific Research, 30*(1), 67-78.

Zeller, A., & Rychlik, M. (2006). Character impact odorants of fennel fruits and fennel tea. *Journal of Agricultural and Food Chemistry, 54*(10), 3686-3692. https://doi.org/10.1021/jf052944j.

Zhang, Z., Guan, W., Liang, M., Wang, R., Wu, Y., & Liu, Y. (2023). Characterization of the key odorants in fresh Amomum *tsao-ko* Crevost et Lemaire fruit by gas chromatography-olfactometry, quantitative analysis and aroma reconstitution. *LWT, 185,* 115154. https://doi.org/10.1016/j.lwt.2023.115154.

Zhou, H.-C., Shamala, L. F., Yi, X.-K., Yan, Z., & Wei, S. (2020). Analysis of terpene synthase family genes *in Camellia sinensis* with an emphasis on abiotic stress conditions. *Scientific Reports, 10*(1), 933. https://doi.org/10.1038/s41598-020-57805-1.

Zhu, J.-K. (2002). Salt and drought stress signal transduction in plants. *Annual Review of Plant Biology, 53*, 247-273. https://doi.org/10.1146/annurev.arplant.53.091401.143329.

Chapter 6 Conclusions and Future Works

6.1 Conclusions

The primary aim of this study is to understand how key aroma compounds in fennel are influenced by growth stage, supplemental red LED light, and varying levels of salinity. Leafy fennel was cultivated using nutrient film technique (NFT) hydroponic systems in Virginia Tech greenhouse, under relatively stable environmental conditions. Aroma characterization was performed using gas chromatography – mass spectrometry – olfactometry (GC-MS-O), and the concentrations of aroma compounds were quantified using standard addition method with multiple internal standards. RNA sequencing and transcriptome analysis were conducted to investigate the molecular mechanisms underlying changes in fennel growth and aroma formation in response to environmental variables, particularly supplemental red LED and salinity. To summarize, notably differences were observed between fennel microgreens and mature plants. Supplemental red LED significantly enhanced fennel aroma concentration, likely by inducing changes in the expression of genes involved in the secondary metabolism pathways. While salinity stress significantly reduced fennel growth and yield, its influences on aroma concentration and composition were less pronounced.

Chapter 3 investigated the aroma profile and volatile constitutes of hydroponically grown fennel at different growth stages. The aroma profiles of fennel microgreens and mature fennel at the vegetative stages were thoroughly characterized. GC-MS of these samples identified 35 aroma-active compounds, including 8 phenylpropenes, 5 aldehydes, 5 monoterpenes, 4 monoterpenoids, 3 sesquiterpenes, 3 alcohols, 2 ketones, 1 ester, 1 alkane, and 3 unknown compounds. Of these, 32 were detected in microgreens, while 28

were found in mature fennel. In addition, the total concentration of aroma compounds was higher in microgreens. Microgreens also contained a higher proportion of monoterpenes. In contrast, early harvested mature fennel exhibited a higher level of aldehydes. Despite differences in individual compound concentrations, phenylpropenes (or phenylpropanoids) represented the most abundant chemical group across all growth stages. Collectively, these compounds contributed to the anise-like, sweet, herbal, and woody notes of fennel. This chapter established baseline information for understanding aroma development of fennel and lays the foundation for future studies aimed at optimizing cultivation practices to enhance fennel flavor.

Chapter 4 comprehensively explored the influences of supplemental red LED on the growth, aroma profile, and gene expression of hydroponic fennel. The application of supplemental red LED significantly promoted biomass accumulation and improved fennel growth. GC-MS analysis identified 23 aroma compounds, with red LED light notably enhancing the overall volatile profile and aroma concentration. This included a 130% increase in the dominant fennel aroma compound, *(E)*-anethole, from 13.89 mg/g to 32.05 mg/g under red LED treatment. Transcriptome analysis showed upregulation of key genes and transcription factors by supplemental red LED, particularly those involved in plant primary and secondary metabolism, including photosynthesis, phenylpropanoids biosynthesis, terpenoids biosynthesis, and green leaf volatile biosynthesis. Overall, these findings offer valuable insights into optimizing aroma biosynthesis in culinary herbs through controlled lighting in CEA, while also deepening the understanding of the molecular and genetic mechanisms governing plant development under supplemental red light.

Chapter 5 focused on the response of fennel to varying levels of salinity stress. Significant reductions in fennel growth parameters were observed, with more severe effects corresponding to longer exposure. However, salinity did not significantly affect the total aroma concentration in fennel. A two-way ANOVA showed that while terpenoid concentrations were influenced by salinity levels, these differences were not statistically significant and were not separated by Tukey's HSD. Four aroma compounds, including *α*-pinene, (*Z)*-3-hexenal, hexenal, and apiol, were significantly affected by salinity but exhibited different trends across various salinity levels. RNA-seq results highlighted negative impact of salinity on cell structure and metabolic processes, alongside the activation of salt tolerance and defense mechanisms in fennel, particularly plant hormone signal transduction and mitogen-activated protein kinase cascade (MAPK) signaling pathways. This chapter adds to fundamental knowledge on growth, aroma formation, and adaptive strategies of fennel under salinity stress.

Overall, this project provides comprehensive information regarding the aroma chemistry of hydroponic fennel, particular the biological, molecular, and transcriptomic aspects of aroma biosynthesis affected by various environmental stimuli. These findings offer guidance for industry seeking to enhance herb flavor through precise environmental control in CEA.

6.2 Future works

The primary focus of this project is to evaluate fennel aroma in response to various environmental factors. However, from a consumer perspective, taste-active compounds may be equally important. Future research could focus on the instrumental analysis of fennel taste compounds in response to environmental stimuli, as well as the interaction or

synergy between aroma compounds and taste compounds to gain a holistic view. Additionally, while distinct differences in aroma profiles were identified in this study (e.g., microgreens vs. mature fennel, control vs. red LED), it remains unclear whether these differences are perceivable to consumers. A future sensory study would be valuable to explore whether consumer can detect and/or prefer these flavor variations.

Regarding aroma characterization techniques, this study utilized solid phase microextraction (SPME), gas chromatography-mass spectrometry-olfactometry, and standard addition method for detailed quantification. The contribution of individual volatile compounds to the overall aroma profile was assessed using odor activity values (OAV). Future research could incorporate recombination and omission studies to further validate the sensory relevance of fennel aroma compounds.

Aroma biosynthesis in fennel, as well as in other culinary herbs, is a complex and dynamic process affected by factors beyond growth stage, light, and salinity. Future work could investigate other key variables, such as temperature, nutrients, endophyte, and the interaction of different environmental stimuli on fennel aroma chemistry. CEA remains an ideal platform for such research, offering precise control over cultivation conditions to optimize herb flavor.

This study focused on the effects of supplemental red LED light due to its established role in enhancing secondary metabolite production. However, the impact of other visible spectrum and ultraviolet radiation, is also worth investigating. Further research could explore the influence of other visible spectrum, ultraviolet radiation, and combinations of spectra on fennel growth and aroma formation, so that the optimal light regime for fennel cultivation could be obtained.

Contrary to initial expectations based on literature, moderate salinity in this study did not enhance fennel aroma but significantly reduced growth. This may be due to the use of higher-than-optimal salinity levels or that the treatment time was too long. Future research could evaluate lower salinity levels and short-term salinity treatments, such as mild stress applied shortly before harvest, to potentially enhance aroma accumulation while minimizing growth reduction.

De novo RNA seq showed significant transcriptomic changes in fennel under different environmental conditions, providing insights into stress-induced regulation of aroma compounds. Further investigation could focus on the role of transcription factors in the biosynthesis of key secondary metabolites and their regulatory mechanisms, advancing the understanding of genes governing fennel aroma formation.

Appendix A. Supplemental Materials for Chapter 3.

Supplemental Table 3-1. Average daylight hours, daily light integral (DLI), maximum greenhouse temperature, minimum greenhouse temperature, and relative humidity in Blacksburg, VA during the growth experiment

Month	Daylight Hours (h)	DLI ($mol \cdot m^{-2} \cdot d^{-1}$)	Max temp (°C)	Min temp (°C)	Relative humidity (%)
October 2022	10.81	10.37	25.26	21.78	43.80
November 2022	10.14	7.63	24.99	20.69	46.95
December 2022	9.48	5.77	24.12	20.50	40.64

Data were collected by the Watchdog data logger and were expressed as mean values of each month.

Since fennel seeds were germinated on 10/23/2022, the data for October 2022 were collected from 10/23/2022 to 10/31/2022.

Supplemental Table 3-2. Concentration of aroma-active compounds in Week 3 microgreens (individual replicates)

No.	Compound	Concentration (μg/g fennel, fresh weight)					
		Replicate 1	*Replicate 2*	*Replicate 3*	*Replicate 4*	*Replicate 5*	*Replicate 6*
1	*α*-pinene	22.86 ± 1.65	24.52 ± 5.43	46.52 ± 0.04	11.35 ± 2.00	18.71 ± 2.45	21.59 ± 2.95
2	*α*-phellandrene	161.28 ± 29.64	188.93 ± 32.42	303.90 ± 25.80	143.04 ± 17.38	180.61 ± 27.50	203.76 ± 25.49
3	*γ*-terpinene	23.24 ± 4.22	27.84 ± 4.77	38.15 ± 4.04	22.13 ± 2.78	28.23 ± 2.23	31.36 ± 3.38
4	allo-ocimene	0.29 ± 0.02	0.26 ± 0.01	0.26 ± 0.01	0.26 ± 0.01	0.26 ± 0.00	0.27 ± 0.00
5	*p*-cymenene	0.27 ± 0.01	0.35 ± 0.01	0.28 ± 0.04	0.28 ± 0.01	0.28 ± 0.00	0.32 ± 0.00
6	*γ*-muurolene	0.43 ± 0.05	0.54 ± 0.09	0.53 ± 0.01	0.46 ± 0.03	0.57 ± 0.02	0.65 ± 0.02
7	germacrene D	0.95 ± 0.06	0.76 ± 0.11	1.12 ± 0.07	0.79 ± 0.01	0.65 ± 0.02	0.81 ± 0.09
8	*α*-cadinene	0.26 ± 0.00	0.26 ± 0.01	0.25 ± 0.01	0.26 ± 0.00	0.25 ± 0.00	0.24 ± 0.09
9	tridecane	0.45 ± 0.08	0.50 ± 0.10	0.85 ± 0.05	0.40 ± 0.11	0.49 ± 0.08	0.36 ± 0.20
10	*(Z)*-3-hexen-1-ol	0.08 ± 0.00	0.02 ± 0.00	0.16 ± 0.02	0.17 ± 0.03	0.11 ± 0.04	0.20 ± 0.00
11	1-octen-3-ol	ND	ND	ND	ND	ND	ND
12	linalool	0.12 ± 0.01	0.10 ± 0.01	0.17 ± 0.02	0.07 ± 0.00	0.05 ± 0.00	0.04 ± 0.00
13	*(Z)*-3-hexenal	10.26 ± 0.06	5.08 ± 1.20	2.16 ± 0.37	3.85 ± 0.94	3.25 ± 0.66	2.76 ± 0.06
14	*(E)*-2-hexenal	29.28 ± 1.30	28.63 ± 1.24	26.51 ± 1.16	14.87 ± 0.06	21.38 ± 0.88	16.85 ± 0.48
15	phenyl acetaldehyde	ND	ND	ND	ND	ND	ND
16	*p*-anisaldehyde	9.17 ± 1.50	12.34 ± 0.99	12.21 ± 0.51	8.07 ± 0.86	7.88 ± 0.17	5.25 ± 0.79
17	4-methoxycinnamaldehyde	1.90 ± 0.21	1.54 ± 0.00	2.54 ± 0.56	1.79 ± 0.09	1.59 ± 0.14	0.83 ± 0.00
18	fenchyl acetate	ND	ND	0.14	6.21	ND	ND
19	camphor	ND	ND	0.77 ± 0.04	ND	ND	ND
20	bornyl acetate	0.46 ± 0.03	0.56 ± 0.13	1.06 ± 0.17	1.22 ± 0.13	0.82 ± 0.13	0.36 ± 0.10
21	carvacrol	0.26 ± 0.02	0.28 ± 0.01	0.31 ± 0.05	0.16 ± 0.01	0.17 ± 0.00	0.14 ± 0.00
22	3-octanol acetate	ND	ND	ND	ND	ND	ND
23	*β*-ionone	0.92 ± 0.17	1.17 ± 0.07	1.24 ± 0.20	0.77 ± 0.14	1.79 ± 0.19	0.75 ± 0.21
24	anisketone	2.36 ± 0.18	2.85 ± 0.05	2.61 ± 0.10	2.19 ± 0.15	2.39 ± 0.04	1.41 ± 0.10
25	*p*-propyl-anisole	0.08 ± 0.01	0.09 ± 0.01	0.09 ± 0.00	0.08 ± 0.00	0.08 ± 0.00	0.08 ± 0.01
26	estragole	22.68 ± 1.05	25.01 ± 1.32	28.66 ± 0.67	23.05 ± 0.07	22.06 ± 0.87	14.74 ± 2.59
27	*(Z)*-anethole	9.50 ± 0.14	9.49 ± 0.04	9.64 ± 0.07	9.76 ± 0.18	9.66 ± 0.26	9.21 ± 0.32
28	*(E)*-anethole	524.68 ± 29.87	622.51 ± 66.03	718.77 ± 2.91	561.44 ± 7.54	536.12 ± 20.22	295.17 ± 66.52
29	methyl eugenol	1.58 ± 0.20	1.43 ± 0.12	1.72 ± 0.09	1.56 ± 0.00	1.48 ± 0.09	1.37 ± 0.05
30	methyl isoeugenol	2.61 ± 0.07	2.63 ± 0.07	3.10 ± 0.07	2.91 ± 0.16	2.78 ± 0.01	2.02 ± 0.10
31	myristicin	0.75 ± 0.03	2.92 ± 0.19	5.26 ± 1.24	2.74 ± 1.40	2.77 ± 0.71	8.66 ± 4.58
32	apiol	129.91 ± 10.06	173.70 ± 7.27	164.31 ± 1.33	130.77 ± 18.94	199.22 ± 16.07	111.68 ± 10.54

Each replicate was measured twice by GC-MS and the results are expressed as mean ± SD. ND = not determined.

Supplemental Table 3-3. Concentration of aroma-active compounds in Week 8 mature fennel (individual replicates)

No.	Compound	Concentration (µg/g fennel, fresh weight)					
		Replicate 1	*Replicate 2*	*Replicate 3*	*Replicate 4*	*Replicate 5*	*Replicate 6*
1	*α*-pinene	36.03 ± 8.40	27.17 ± 5.54	70.67 ± 6.81	33.10 ± 6.61	45.45 ± 2.30	44.39 ± 10.14
2	*α*-phellandrene	64.24 ± 6.18	98.32 ± 3.06	82.87 ± 7.50	74.92 ± 12.30	138.87 ± 7.79	85.07 ± 7.20
3	*γ*-terpinene	1.80 ± 0.18	1.49 ± 0.03	4.98 ± 0.49	2.03 ± 0.41	6.67 ± 0.26	6.43 ± 0.33
4	allo-ocimene	0.24 ± 0.00	0.24 ± 0.00	0.25 ± 0.01	0.24 ± 0.00	0.24 ± 0.00	0.26 ± 0.00
5	*p*-cymenene	0.26 ± 0.01	0.25 ± 0.00	0.27 ± 0.00	0.26 ± 0.01	0.27 ± 0.01	0.26 ± 0.01
6	*γ*-muurolene	0.65 ± 0.01	0.83 ± 0.04	0.59 ± 0.05	0.39 ± 0.00	0.32 ± 0.01	0.44 ± 0.09
7	germacrene D	0.37 ± 0.02	0.36 ± 0.01	0.35 ± 0.05	0.34 ± 0.02	0.42 ± 0.01	0.33 ± 0.01
8	*α*-cadinene	0.30 ± 0.03	0.28 ± 0.01	0.30 ± 0.01	0.30 ± 0.01	0.25 ± 0.02	0.26 ± 0.03
9	tridecane	0.16 ± 0.01	0.15 ± 0.01	0.14 ± 0.00	0.14 ± 0.00	0.14 ± 0.00	0.14 ± 0.00
10	*(Z)*-3-hexen-1-ol	0.62 ± 0.04	2.61 ± 0.14	1.33 ± 0.24	0.93 ± 0.13	1.22 ± 0.09	1.07 ± 0.13
11	1-octen-3-ol	ND	ND	ND	ND	ND	ND
12	linalool	0.02 ± 0.00	0.03 ± 0.00	0.03 ± 0.00	0.03 ± 0.00	0.05 ± 0.01	0.03 ± 0.00
13	*(Z)*-3-hexenal	7.65 ± 0.56	4.90 ± 0.84	5.27 ± 1.18	8.26 ± 0.28	7.86 ± 1.46	6.57 ± 0.40
14	*(E)*-2-hexenal	39.26 ± 2.66	22.24 ± 2.67	17.93 ± 1.14	38.56 ± 2.95	25.58 ± 1.29	20.04 ± 3.52
15	phenyl acetaldehyde	ND	ND	ND	ND	ND	ND
16	*p*-anisaldehyde	6.58 ± 0.39	9.16 ± 0.61	7.36 ± 1.25	6.87 ± 1.76	30.19 ± 4.58	9.79 ± 0.60
17	4-methoxycinnamaldehyde	0.86 ± 0.03	1.55 ± 0.26	1.39 ± 0.01	0.98 ± 0.13	3.07 ± 0.62	1.69 ± 0.16
18	fenchyl acetate	ND	ND	ND	ND	ND	ND
19	camphor	ND	ND	ND	ND	0.78 ± 0.23	ND
20	bornyl acetate	ND	ND	ND	ND	ND	0.04
21	carvacrol	0.14 ± 0.01	0.16 ± 0.04	0.18 ± 0.01	0.19 ± 0.01	0.29 ± 0.01	0.23 ± 0.03
22	3-octanol acetate	ND	ND	ND	ND	ND	ND
23	*β*-ionone	0.64 ± 0.14	1.54 ± 0.09	1.62 ± 0.07	1.71 ± 0.20	3.35 ± 0.10	1.39 ± 0.12
24	anisketone	1.75 ± 0.05	2.27 ± 0.06	2.45 ± 0.10	2.12 ± 0.24	6.35 ± 0.06	2.56 ± 0.01
25	*p*-propyl-anisole	0.08 ± 0.01	0.09 ± 0.00	0.09 ± 0.01	0.08 ± 0.01	0.28 ± 0.04	0.08 ± 0.01
26	estragole	20.70 ± 1.54	26.75 ± 3.08	23.74 ± 1.05	24.29 ± 2.08	66.07 ± 8.29	26.99 ± 0.64
27	*(Z)*-anethole	10.13 ± 0.05	11.46 ± 0.49	11.87 ± 0.19	12.38 ± 0.07	15.38 ± 1.27	12.84 ± 0.22
28	*(E)*-anethole	438.91 ± 44.23	586.52 ± 84.40	528.86 ± 66.51	574.44 ± 8.27	1786.97 ± 152.66	678.27 ± 32.39
29	methyl eugenol	1.38 ± 0.02	1.54 ± 0.03	1.51 ± 0.02	1.42 ± 0.06	1.48 ± 0.00	1.48 ± 0.03
30	methyl isoeugenol	1.69 ± 0.04	2.44 ± 0.16	2.79 ± 0.18	2.59 ± 0.29	5.16 ± 0.07	3.32 ± 0.04
31	myristicin	ND	ND	ND	0.08 ± 0.01	0.15 ± 0.03	0.01
32	apiol	1.86 ± 0.15	1.31 ± 0.01	3.56 ± 0.55	12.23 ± 3.97	5.77 ± 0.57	2.82 ± 0.10

Each replicate was measured twice by GC-MS and the results are expressed as mean ± SD. ND = not determined.

Supplemental Table 3-4. Concentration of aroma-active compounds in Week 9 mature fennel (individual replicates)

No.	Compound	Concentration (µg/g fennel, fresh weight)					
		Replicate 1	*Replicate 2*	*Replicate 3*	*Replicate 4*	*Replicate 5*	*Replicate 6*
1	*α*-pinene	27.70 ± 6.72	58.39 ± 8.84	27.06 ± 3.30	39.26 ± 4.91	20.09 ± 1.78	1.75 ± 0.07
2	*α*-phellandrene	53.73 ± 8.55	138.56 ± 5.76	114.09 ± 13.91	83.18 ± 3.34	71.53 ± 2.00	135.76 ± 9.59
3	*γ*-terpinene	1.04 ± 0.22	13.49 ± 0.87	6.25 ± 0.68	6.23 ± 0.18	4.14 ± 0.00	4.98 ± 0.55
4	allo-ocimene	0.25 ± 0.01	0.24 ± 0.01	0.36 ± 0.01	0.25 ± 0.00	0.24 ± 0.00	0.24 ± 0.00
5	*p*-cymenene	0.24 ± 0.01	0.26 ± 0.01	0.27 ± 0.01	0.26 ± 0.01	0.25 ± 0.00	0.26 ± 0.01
6	*γ*-muurolene	0.42 ± 0.01	0.31 ± 0.01	0.42 ± 0.04	0.46 ± 0.01	0.30 ± 0.00	0.38 ± 0.02
7	germacrene D	0.38 ± 0.03	0.48 ± 0.02	0.39 ± 0.05	0.29 ± 0.02	0.28 ± 0.00	0.31 ± 0.00
8	*α*-cadinene	0.25 ± 0.01	0.29 ± 0.00	0.29 ± 0.02	0.24 ± 0.00	0.24 ± 0.00	0.24 ± 0.00
9	tridecane	0.14 ± 0.00	0.14 ± 0.00	0.14 ± 0.00	0.14 ± 0.00	0.14 ± 0.00	0.14 ± 0.00
10	*(Z)*-3-hexen-1-ol	1.73 ± 0.06	1.86 ± 0.08	4.65 ± 0.43	2.69 ± 0.04	1.17 ± 0.09	2.30 ± 0.14
11	1-octen-3-ol	ND	ND	ND	ND	ND	ND
12	linalool	0.02 ± 0.00	0.05 ± 0.01	0.02 ± 0.00	0.02 ± 0.00	0.02 ± 0.00	0.02 ± 0.00
13	*(Z)*-3-hexenal	7.01 ± 0.10	6.38 ± 1.40	3.91 ± 0.67	3.74 ± 0.92	2.40 ± 0.62	1.28 ± 0.30
14	*(E)*-2-hexenal	14.30 ± 2.37	24.44 ± 4.59	14.49 ± 0.03	16.15 ± 2.88	11.00 ± 0.00	9.44 ± 1.00
15	phenyl acetaldehyde	ND	ND	ND	ND	ND	ND
16	*p*-anisaldehyde	4.16 ± 0.40	15.01 ± 0.17	7.26 ± 0.70	4.72 ± 0.85	3.86 ± 0.33	4.20 ± 1.13
17	4-methoxycinnamaldehyde	1.46 ± 0.10	3.16 ± 0.44	1.24 ± 0.08	0.79 ± 0.15	0.45 ± 0.11	0.47 ± 0.07
18	fenchyl acetate	ND	ND	ND	ND	ND	ND
19	camphor	ND	ND	ND	ND	ND	ND
20	bornyl acetate	ND	ND	ND	ND	ND	ND
21	carvacrol	0.14 ± 0.00	0.22 ± 0.03	0.19 ± 0.01	0.13 ± 0.01	0.15 ± 0.01	0.15 ± 0.02
22	3-octanol acetate	ND	ND	ND	ND	ND	ND
23	*β*-ionone	0.02	1.16 ± 0.16	2.42 ± 0.48	0.65 ± 0.06	1.01 ± 0.19	1.06 ± 0.21
24	anisketone	1.02 ± 0.15	4.12 ± 0.10	2.10 ± 0.23	1.10 ± 0.17	1.00 ± 0.08	0.94 ± 0.18
25	*p*-propyl-anisole	0.08 ± 0.00	0.10 ± 0.02	0.08 ± 0.01	0.08 ± 0.00	0.07 ± 0.00	0.07 ± 0.00
26	estragole	13.67 ± 2.43	62.70 ± 1.60	23.25 ± 1.99	15.90 ± 0.28	11.17 ± 0.14	10.16 ± 1.07
27	*(Z)*-anethole	9.48 ± 0.14	15.47 ± 0.04	10.43 ± 0.39	9.67 ± 0.04	9.10 ± 0.06	9.72 ± 0.35
28	*(E)*-anethole	255.52 ± 59.52	1583.58 ± 9.40	496.72 ± 56.01	293.36 ± 3.62	176.93 ± 19.49	146.38 ± 31.15
29	methyl eugenol	1.49 ± 0.01	1.47 ± 0.01	1.33 ± 0.01	1.31 ± 0.02	1.35 ± 0.01	1.45 ± 0.03
30	methyl isoeugenol	1.63 ± 0.07	3.46 ± 0.04	1.65 ± 0.12	1.97 ± 0.12	1.37 ± 0.03	1.51 ± 0.10
31	myristicin	ND	0.21	ND	ND	ND	ND
32	apiol	2.13 ± 0.20	3.28 ± 0.38	2.01 ± 0.23	2.02 ± 0.04	2.22 ± 0.09	2.20 ± 0.26

Each replicate was measured twice by GC-MS and the results are expressed as mean ± SD. ND = not determined.

Supplemental Table 3-5. Concentration of aroma-active compounds in Week 10 mature fennel (individual replicates)

No.	Compound	Concentration (μg/g fennel, fresh weight)					
		Replicate 1	*Replicate 2*	*Replicate 3*	*Replicate 4*	*Replicate 5*	*Replicate 6*
1	*α*-pinene	27.70 ± 6.72	58.39 ± 8.84	27.06 ± 3.30	39.26 ± 4.91	20.09 ± 1.78	1.75 ± 0.07
2	*α*-phellandrene	53.73 ± 8.55	138.56 ± 5.76	114.09 ± 13.91	83.18 ± 3.34	71.53 ± 2.00	135.76 ± 9.59
3	*γ*-terpinene	1.04 ± 0.22	13.49 ± 0.87	6.25 ± 0.68	6.23 ± 0.18	4.14 ± 0.00	4.98 ± 0.55
4	allo-ocimene	0.25 ± 0.01	0.24 ± 0.01	0.36 ± 0.01	0.25 ± 0.00	0.24 ± 0.00	0.24 ± 0.00
5	*p*-cymenene	0.24 ± 0.01	0.26 ± 0.01	0.27 ± 0.01	0.26 ± 0.01	0.25 ± 0.00	0.26 ± 0.01
6	*γ*-muurolene	0.42 ± 0.01	0.31 ± 0.01	0.42 ± 0.04	0.46 ± 0.01	0.30 ± 0.00	0.38 ± 0.02
7	germacrene D	0.38 ± 0.03	0.48 ± 0.02	0.39 ± 0.05	0.29 ± 0.02	0.28 ± 0.00	0.31 ± 0.00
8	*α*-cadinene	0.25 ± 0.01	0.29 ± 0.00	0.29 ± 0.02	0.24 ± 0.00	0.24 ± 0.00	0.24 ± 0.00
9	tridecane	0.14 ± 0.00	0.14 ± 0.00	0.14 ± 0.00	0.14 ± 0.00	0.14 ± 0.00	0.14 ± 0.00
10	*(Z)*-3-hexen-1-ol	1.73 ± 0.06	1.86 ± 0.08	4.65 ± 0.43	2.69 ± 0.04	1.17 ± 0.09	2.30 ± 0.14
11	1-octen-3-ol	ND	ND	ND	ND	ND	ND
12	linalool	0.02 ± 0.00	0.05 ± 0.01	0.02 ± 0.00	0.02 ± 0.00	0.02 ± 0.00	0.02 ± 0.00
13	*(Z)*-3-hexenal	7.01 ± 0.10	6.38 ± 1.40	3.91 ± 0.67	3.74 ± 0.92	2.40 ± 0.62	1.28 ± 0.30
14	*(E)*-2-hexenal	14.30 ± 2.37	24.44 ± 4.59	14.49 ± 0.03	16.15 ± 2.88	11.00 ± 0.00	9.44 ± 1.00
15	phenyl acetaldehyde	ND	ND	ND	ND	ND	ND
16	*p*-anisaldehyde	4.16 ± 0.40	15.01 ± 0.17	7.26 ± 0.70	4.72 ± 0.85	3.86 ± 0.33	4.20 ± 1.13
17	4-methoxycinnamaldehyde	1.46 ± 0.10	3.16 ± 0.44	1.24 ± 0.08	0.79 ± 0.15	0.45 ± 0.11	0.47 ± 0.07
18	fenchyl acetate	ND	ND	ND	ND	ND	ND
19	camphor	ND	ND	ND	ND	ND	ND
20	bornyl acetate	ND	ND	ND	ND	ND	ND
21	carvacrol	0.14 ± 0.00	0.22 ± 0.03	0.19 ± 0.01	0.13 ± 0.01	0.15 ± 0.01	0.15 ± 0.02
22	3-octanol acetate	ND	ND	ND	ND	ND	ND
23	*β*-ionone	0.02	1.16 ± 0.16	2.42 ± 0.48	0.65 ± 0.06	1.01 ± 0.19	1.06 ± 0.21
24	anisketone	1.02 ± 0.15	4.12 ± 0.10	2.10 ± 0.23	1.10 ± 0.17	1.00 ± 0.08	0.94 ± 0.18
25	*p*-propyl-anisole	0.08 ± 0.00	0.10 ± 0.02	0.08 ± 0.01	0.08 ± 0.00	0.07 ± 0.00	0.07 ± 0.00
26	estragole	13.67 ± 2.43	62.70 ± 1.60	23.25 ± 1.99	15.90 ± 0.28	11.17 ± 0.14	10.16 ± 1.07
27	*(Z)*-anethole	9.48 ± 0.14	15.47 ± 0.04	10.43 ± 0.39	9.67 ± 0.04	9.10 ± 0.06	9.72 ± 0.35
28	*(E)*-anethole	255.52 ± 59.52	1583.58 ± 9.40	496.72 ± 56.01	293.36 ± 3.62	176.93 ± 19.49	146.38 ± 31.15
29	methyl eugenol	1.49 ± 0.01	1.47 ± 0.01	1.33 ± 0.01	1.31 ± 0.02	1.35 ± 0.01	1.45 ± 0.03
30	methyl isoeugenol	1.63 ± 0.07	3.46 ± 0.04	1.65 ± 0.12	1.97 ± 0.12	1.37 ± 0.03	1.51 ± 0.10
31	myristicin	ND	0.21	ND	ND	ND	ND
32	apiol	2.13 ± 0.20	3.28 ± 0.38	2.01 ± 0.23	2.02 ± 0.04	2.22 ± 0.09	2.20 ± 0.26

Each replicate was measured twice by GC-MS and the results are expressed as mean ± SD. ND = not determined.

Supplemental Figure 3-1. Representative SPME-GC-MS total ion chromatograms of volatile compounds from microgreen (week 3, red line) and mature herbs (week 10, blue line). The quantified aroma-active compounds are labeled with numbers representing different compounds, see Table 3-1

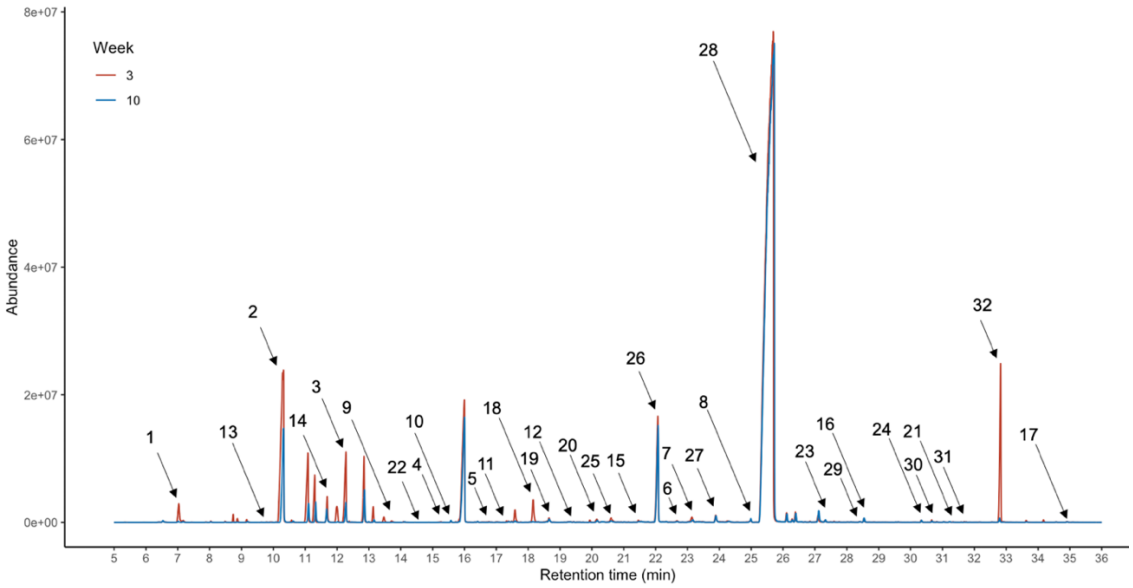

Supplemental Figure 3-2. Percentage of variances in fennel aroma compounds explained by different principal components

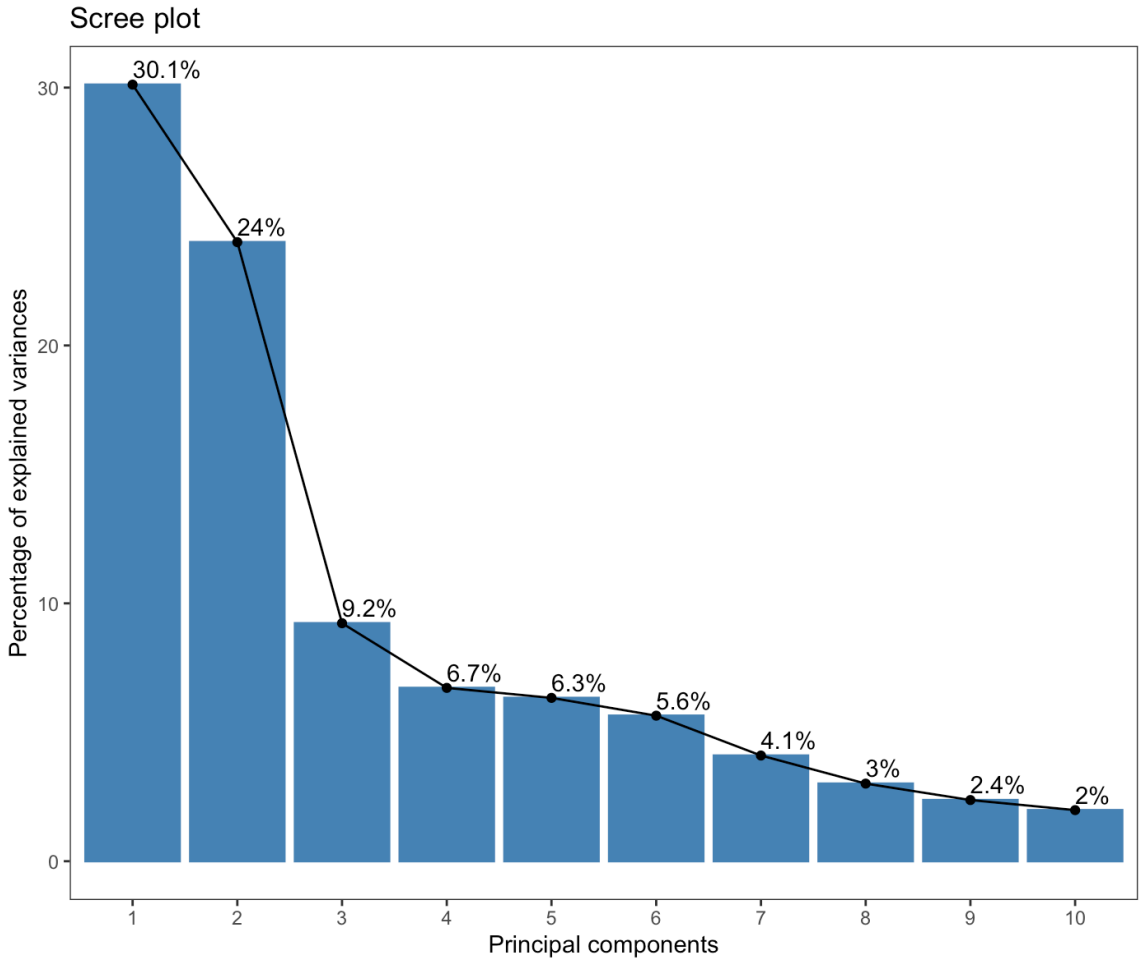

Supplemental Figure 3-3. PCA of fennel aroma-active compounds and the corresponding loading plot. (A) PCA of the 1st and 3rd principal components. (B) Loading plot of the 1st and 3rd principal components. (C) PCA of the 2nd and 3rd principal components. (D) Loading plot of the 2nd and 3rd principal components.

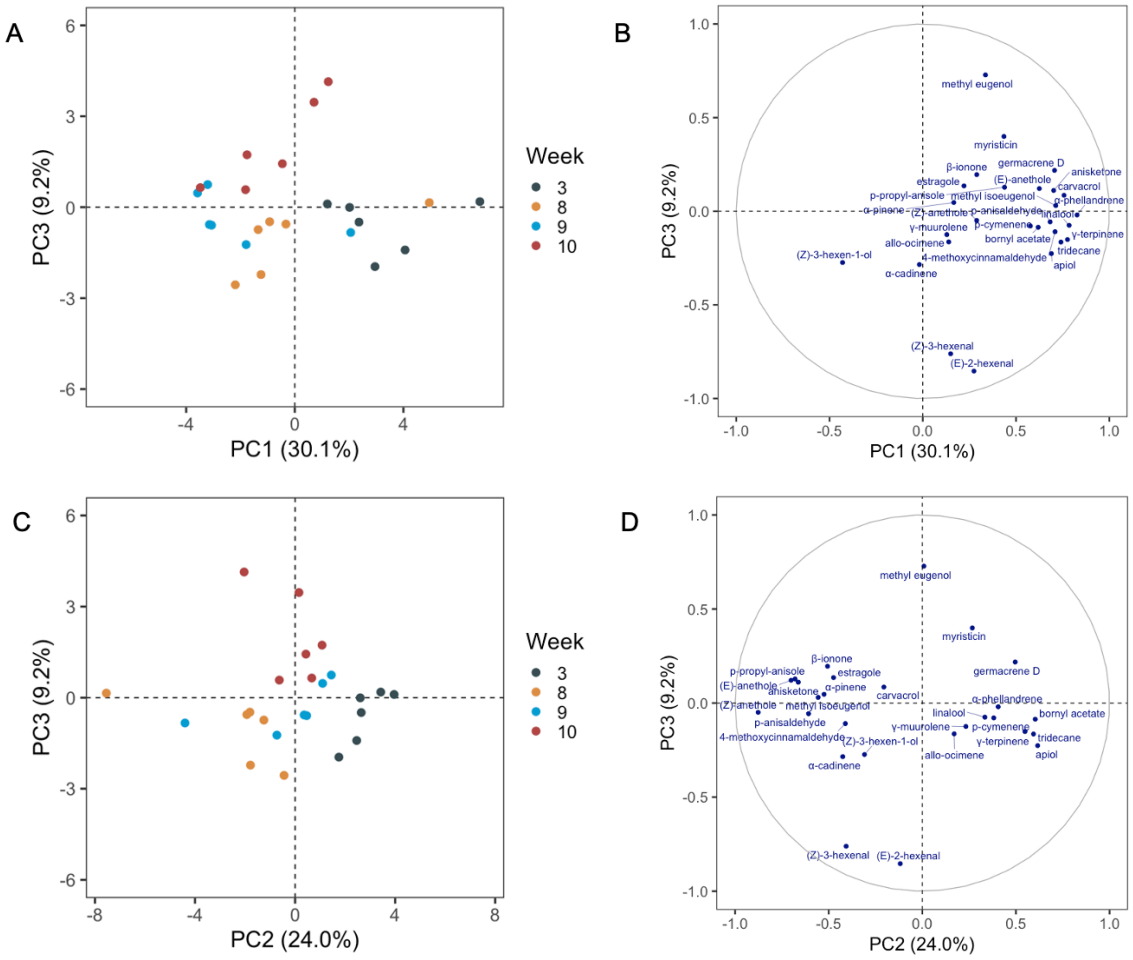

Appendix B. Supplemental Materials for Chapter 4.

Supplemental Table 4-1. Average daylight hours, daily light integral, maximum and minimum temperature, and relative humidity in the greenhouse

Date	Average daylight Hours (h)	DLI (mol·m^{-2}·d^{-1})	Max temp (°C)	Min temp (°C)	Relative humidity (%)
3/16/2023-3/31/2023	12.12	17.24	26.69	21.07	41.88
4/1/2023-4/30/2023	12.81	18.28	25.61	21.31	48.60
5/1/2023-5/19/2023	13.59	22.05	26.78	21.99	40.65

Data collected by Watchdog data logger. Seeds were germinated on 3/16/2023. Data from 3/17/2023, 4/11/2023-4/14/2023 were excluded because of data loss.

Supplemental Table 4-2. Regression equations of standard addition method for aroma-active compounds in fennel

No.	Compound	IS	Regression Equation [a]	R^2	Linear range	LOD	LOQ
1	*α*-pinene	decane	y = 0.3418x + 0.0527	0.9975	0.36~143.28	0.39	1.29
2	*α*-phellandrene	decane	y = 0.7269x + 3.6977	0.9947	1.21~484.50	0.11	0.38
3	*γ*-terpinene	decane	y = 1.1434x + 1.8957	0.9948	0.49~197.60	0.33	1.10
4	allo-ocimene	decane	y = 3.3571x - 1.0863	0.9941	0.08~33.32	0.01	0.04
5	*γ*-muurolene	decane	y = 3.3571x - 1.0863	0.9941	0.08~33.32	0.01	0.04
6	germacrene D	decane	y = 3.3571x - 1.0863	0.9941	0.08~33.32	0.01	0.04
7	*α*-cadinene	decane	y = 3.3571x - 1.0863	0.9941	0.08~33.32	0.01	0.04
8	tridecane	decane	y = 2.3394x - 0.4302	0.9941	0.02~7.52	0.00	0.01
9	1-octen-3-ol	2-octanol	y = 0.4363x + 1.3773	0.9955	0.01~1.65	0.16	0.54
10	linalool	2-octanol	y = 0.5871x - 0.1086	0.9965	0.01~3.34	0.01	0.05
11	*(Z)*-3-hexenal	2-octanol	y = 0.0035x + 0.0266	0.9942	0.01~16.00	0.07	0.25
12	*(E)*-2-hexenal	2-octanol	y = 0.1129x + 3.1690	0.9886	0.17~66.64	1.17	3.90
13	phenyl acetaldehyde	2-octanol	y = 0.0836x + 1.4775	0.9957	0.01~3.91	0.20	0.67
14	*p*-anisaldehyde	2-octanol	y = 0.0581x - 0.7592	0.9822	0.11~43.68	0.65	2.15
15	fenchone	1-phenylethanol	y = 0.6193x + 39.8030	0.9823	5.81~2322.60	1.37	4.57
16	bornyl acetate	1-phenylethanol	y = 2.0570x + 0.8921	0.9966	0.19~75.24	0.07	0.22
17	carvacrol	1-phenylethanol	y = 0.8875x - 0.0478	0.9989	0.07~29.11	0.02	0.05
18	estragole	1-phenylethanol	y = 3.7210x - 3.4301	0.9999	3.80~1520.96	0.38	1.01
19	*(Z)*-anethole	1-phenylethanol	y = 3.4311x - 14.1430	0.9799	0.53~213.41	0.04	0.11
20	*(E)*-anethole	1-phenylethanol	y = 2.9579x + 62.2620	0.9935	14.70~5880.60	1.96	6.52
21	methyl eugenol	1-phenylethanol	y = 0.7534x - 0.4722	0.9996	0.07~285.38	0.18	0.61
22	methyl isoeugenol	1-phenylethanol	y = 0.7534x - 0.4722	0.9996	0.07~285.38	0.18	0.61
23	apiol	1-phenylethanol	y = 0.7534x - 0.4722	0.9996	0.07~285.38	0.18	0.61

[a] Regression equation: $y = \frac{Peak\ area\ of\ analyte}{Peak\ area\ of\ IS}$, $x = \frac{Mass\ of\ analyte}{Mass\ of\ IS}$

Pure standards not available, calibration curve was built based against compounds with similar chemical structure. Specifically, allo-ocimine, *γ*-muurolene, germacrene D, and *α*-cadinene were quantified against *p*-cymenene; methyl isoeugenol and apiol were quantified against methyl eugenol.

Supplemental Table 4-3. Summary of RNA-seq data quality

Sample	Raw reads	Raw data (G)	Effective (%)	Error (%)	Q20 (%)	Q30 (%)	GC (%)
CTRL1	51184196	7.7	98.91	0.02	98.29	94.49	45.2
CTRL2	51997162	7.8	98.62	0.02	98.26	94.35	45.28
CTRL3	65048582	9.8	98.62	0.02	98.36	94.62	44.62
RED1	67491354	10.1	98.81	0.02	98.27	94.41	45.65
RED2	58809584	8.8	98.86	0.02	98.33	94.59	45.95
RED3	56056864	8.4	96.6	0.02	98.26	94.4	45.87

Supplemental Table 4-4. Genes (*Arabidopsis thaliana*) involved in KEGG biosynthesis of secondary metabolites pathway

Gene symbol	NCBI Gene ID	Description
AKR4C10	818356	NAD(P)-linked oxidoreductase superfamily protein
ATTPS6	843130	UDP-Glycosyltransferase / trehalose-phosphatase family protein
cPT4	835991	Undecaprenyl pyrophosphate synthetase family protein
CH1	841029	Pheophorbide a oxygenase family protein with Rieske 2Fe-2S domain-containing protein
MS2	821147	Methionine synthase 2
NRS/ER	842603	Nucleotide-rhamnose synthase/epimerase-reductase
PGK1	820461	Phosphoglycerate kinase 1
SPDS3	835392	Spermidine synthase 3
TPPJ	836638	Haloacid dehalogenase-like hydrolase (HAD) superfamily protein
VTC2	828792	GDP-L-galactose phosphorylase 1

Supplemental Figure 4-1. GO-term enrichment for DEGs of fennel affected by supplemental red LED light. (A) Top upregulated and downregulated biological process terms. (B) Top upregulated and downregulated cellular component terms. (C) Top upregulated and downregulated molecular function terms

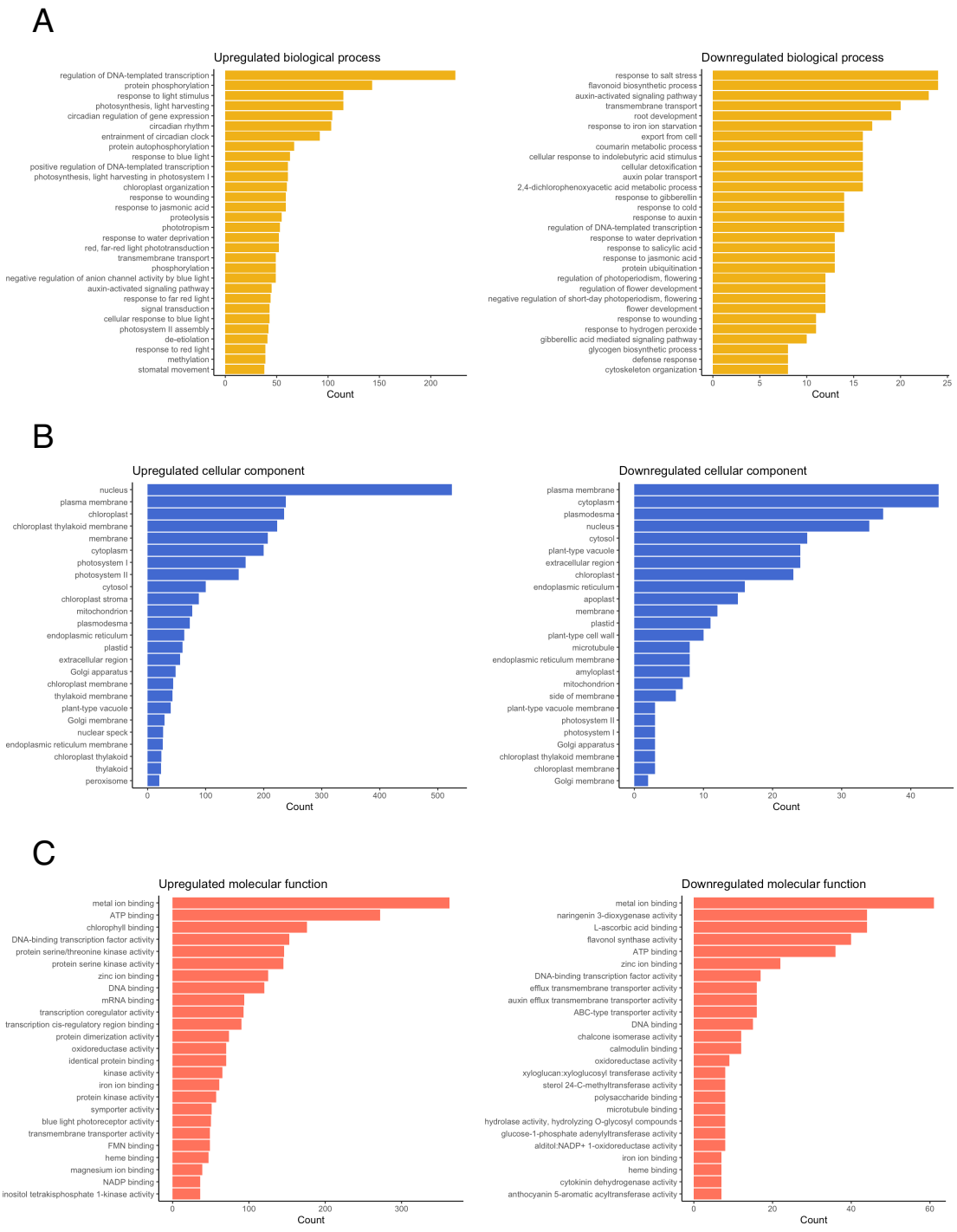

Supplemental Figure 4-2. Category net plot of KEGG pathway enrichment analysis. Yellow dots represent different biological pathways, with the size of each dot reflecting adjusted p value, larger dots indicate more significant pathways. Blue and red dots represent genes labeled with their NCBI Gene ID

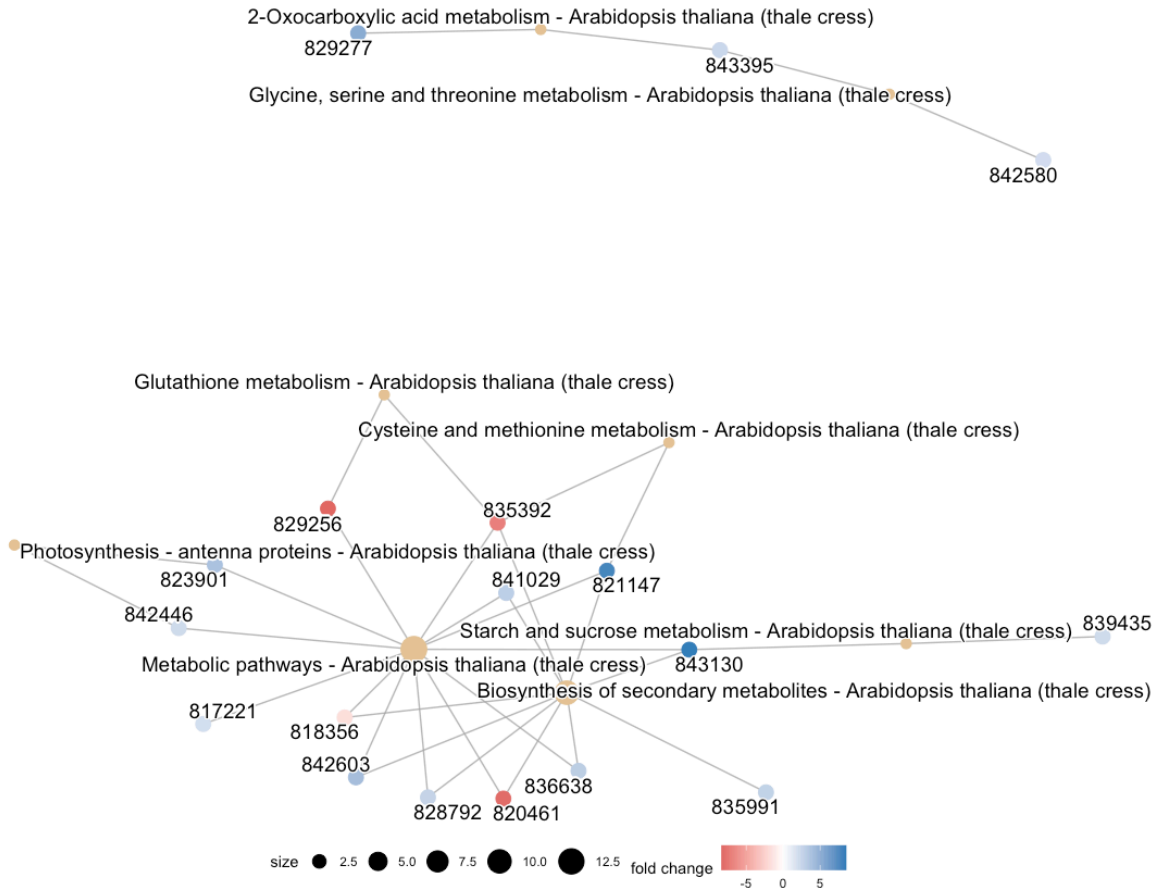

Appendix C. Supplemental Materials for Chapter 5.

Supplemental Table 5-1. Average daylight hours and daily light integral (DLI) at Blacksburg, VA during fennel growth period

Date	Average daylight Hours (h)	DLI ($mol \cdot m^{-2} \cdot d^{-1}$)	Max temperature (°C)	Min temperature (°C)	Relative humidity (%)
9/19/2023-9/30/2023	11.57	12.47	26.57	22.26	65.71
10/1/2023-10/31/2023	10.96	14.24	28.31	21.37	54.36
11/1/2023-11/23/2023	9.98	9.09	24.98	19.27	45.54

Average daylight hours and DLI were calculated based on data collected by Watchdog data logger. Seeds were germinated on 9/19/2023.

Supplemental Table 5-2. p values of two-way ANOVA for growth parameters.

Source of variance	p value							
	Height (cm)	Width (cm)	Fresh weight (g)	Number of branches	Moisture	*L*	*a*	*b*
Harvest	<0.0001	<0.0001	<0.0001	<0.0001	0.0002	0.0202	0.0896	0.0677
Salinity	<0.0001	<0.0001	<0.0001	<0.0001	0.0789	0.0304	0.0128	0.3047
Harvest × Salinity	0.0002	<0.0001	<0.0001	0.0003	0.1671	0.6532	0.1678	0.0218

Supplemental Table 5-3. Regression equations of standard addition method for aroma-active compounds in fennel

No.	Compound	IS	Regression Equation [a]	R^2	Linear range	LOD	LOQ
1	*α*-pinene	decane	y = 0.3418x + 0.0527	0.9975	0.36~143.28	0.39	1.29
2	*α*-phellandrene	decane	y = 0.7269x + 3.6977	0.9947	1.21~484.50	0.11	0.38
3	*γ*-terpinene	decane	y = 1.1434x + 1.8957	0.9948	0.49~197.60	0.33	1.10
4	allo-ocimene	decane	y = 3.3571x - 1.0863	0.9941	0.08~33.32	0.01	0.04
5	*γ*-muurolene	decane	y = 3.3571x - 1.0863	0.9941	0.08~33.32	0.01	0.04
6	germacrene D	decane	y = 3.3571x - 1.0863	0.9941	0.08~33.32	0.01	0.04
7	*α*-cadinene	decane	y = 3.3571x - 1.0863	0.9941	0.08~33.32	0.01	0.04
8	tridecane	decane	y = 2.3394x - 0.4302	0.9941	0.02~7.52	0.00	0.01
9	*(Z)*-3-hexen-1-ol	2-octanol	y = 0.2213x + 0.6373	0.9970	0.02~8.33	0.04	0.14
10	1-octen-3-ol	2-octanol	y = 0.4363x + 1.3773	0.9955	0.01~1.65	0.16	0.54
11	linalool	2-octanol	y = 0.5871x - 0.1086	0.9965	0.01~3.34	0.01	0.05
12	hexenal	2-octanol	y = 0.0035x + 0.0266	0.9942	0.01~16.00	0.07	0.25
13	*(Z)*-3-hexenal	2-octanol	y = 0.0035x + 0.0266	0.9942	0.01~16.00	0.07	0.25
14	*(E)*-2-hexenal	2-octanol	y = 0.1129x + 3.1690	0.9886	0.17~66.64	1.17	3.90
15	phenyl acetaldehyde	2-octanol	y = 0.0836x + 1.4775	0.9957	0.01~3.91	0.20	0.67
16	*p*-anisaldehyde	2-octanol	y = 0.0581x - 0.7592	0.9822	0.11~43.68	0.65	2.15
17	fenchone	1-phenylethanol	y = 0.6193x + 39.8030	0.9823	5.81~2322.60	1.37	4.57
18	bornyl acetate	1-phenylethanol	y = 2.0570x + 0.8921	0.9966	0.19~75.24	0.07	0.22
19	*β*-ionone	1-phenylethanol	y = 0.5634x + 0.3565	0.9971	0.16~63.84	0.02	0.07
20	anisketone	1-phenylethanol	y = 0.4849x - 0.0254	0.9973	0.08~31.14	0.03	0.11
21	estragole	1-phenylethanol	y = 3.7210x - 3.4301	0.9999	3.80~1520.96	0.38	1.01
22	*(Z)*-anethole	1-phenylethanol	y = 3.4311x - 14.1430	0.9799	0.53~213.41	0.04	0.11
23	*(E)*-anethole	1-phenylethanol	y = 2.9579x + 62.2620	0.9935	14.70~5880.60	1.96	6.52
24	methyl eugenol	1-phenylethanol	y = 0.7534x - 0.4722	0.9996	0.07~285.38	0.18	0.61
25	methyl isoeugenol	1-phenylethanol	y = 0.7534x - 0.4722	0.9996	0.07~285.38	0.18	0.61
26	apiol	1-phenylethanol	y = 0.7534x - 0.4722	0.9996	0.07~285.38	0.18	0.61

Pure standards not available, calibration curve was built based against compounds with similar chemical structure. Specifically, allo-ocimine, γ-muurolene, germacrene D, and α-cadinene were quantified against p-cymenene; hexenal was quantified against (Z)-3-hexenal; methyl isoeugenol and apiol were quantified against methyl eugenol.

Supplemental Table 5-4. Summary of RNA Seq data quality

Sample	Raw reads	Raw data (G)	Effective (%)	Error (%)	Q20 (%)	Q30 (%)	GC (%)
TC1	63113046	9.5	98.51	0.03	97.79	93.91	43.51
TC2	56240808	8.4	97.94	0.03	97.85	93.90	43.66
TC3	61181340	9.2	98.66	0.03	97.82	93.91	43.52
T21	52318694	7.8	98.72	0.03	97.83	93.88	43.46
T22	41283310	6.2	98.75	0.03	97.79	93.79	43.38
T23	96877550	14.5	98.35	0.03	97.73	93.73	43.67
T41	57306570	8.6	98.63	0.03	97.83	93.86	43.65
T42	57632164	8.6	98.25	0.03	97.78	93.78	43.25
T43	69718982	10.5	98.61	0.03	97.36	93.08	42.54
T61	62505046	9.4	97.98	0.03	97.72	93.66	43.56
T62	67542192	10.1	98.02	0.03	97.74	93.66	43.40
T63	42663814	6.4	98.66	0.03	97.77	93.75	43.65
SC1	49428944	7.4	98.71	0.03	97.57	93.51	42.83
SC2	46801636	7.0	97.84	0.03	97.76	93.73	42.89
SC3	46194432	6.9	98.16	0.03	97.74	93.61	43.37
S21	43574512	6.5	98.66	0.03	97.84	93.88	43.65
S22	47031270	7.1	98.16	0.03	97.83	93.92	43.21
S23	41777694	6.3	97.77	0.03	97.76	93.65	43.64
S41	53534056	8.0	98.81	0.03	97.72	93.73	43.22
S42	45641236	6.8	98.32	0.03	97.91	94.10	43.28
S43	41161484	6.2	98.14	0.03	97.65	93.46	43.66
S61	55120480	8.3	98.24	0.03	97.85	93.99	43.60
S62	58706020	8.8	98.46	0.03	97.68	93.63	43.47
S63	44122136	6.6	98.42	0.03	97.49	93.01	43.82

Supplemental Figure 5-1. Heatmap of sample-to-sample distances

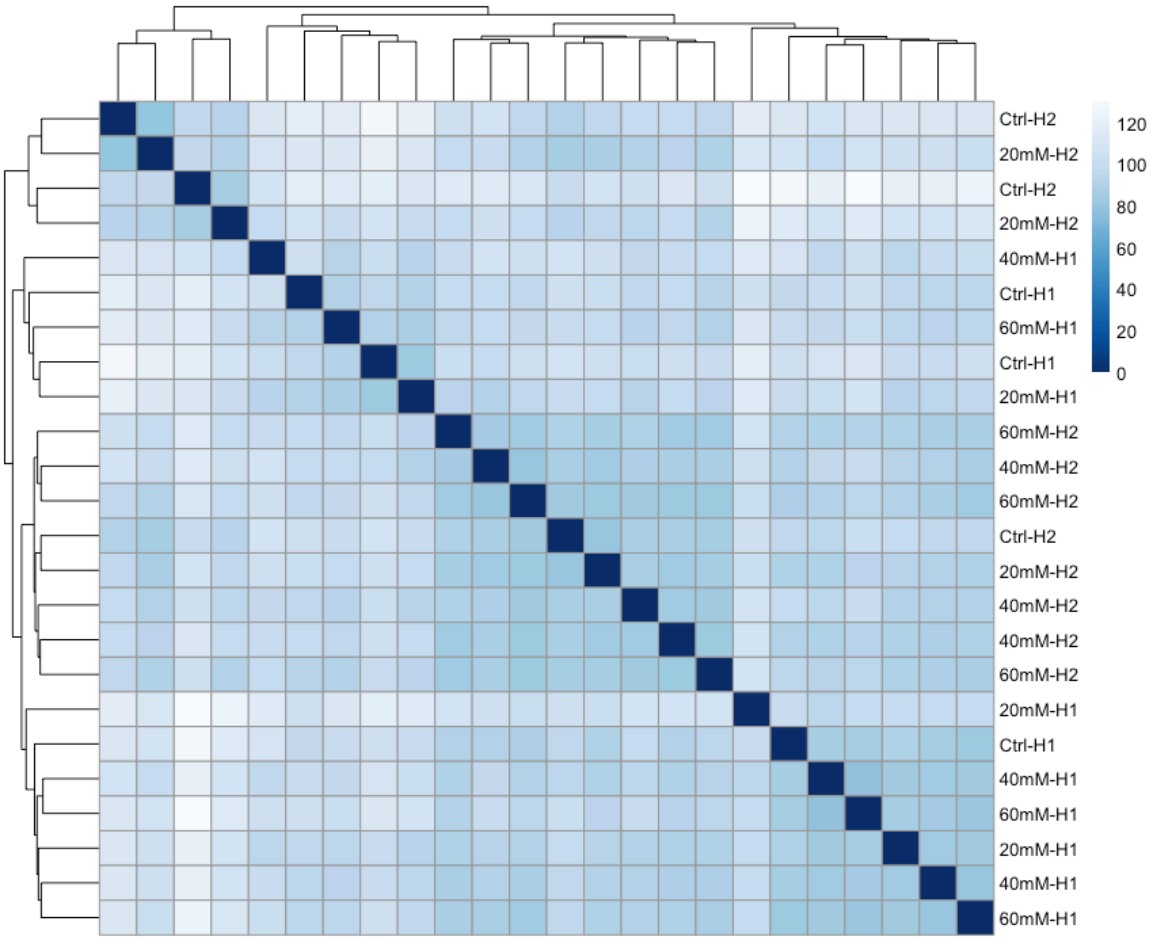

Supplemental Figure 5-2. KEGG pathway enrichment analysis of DEGs

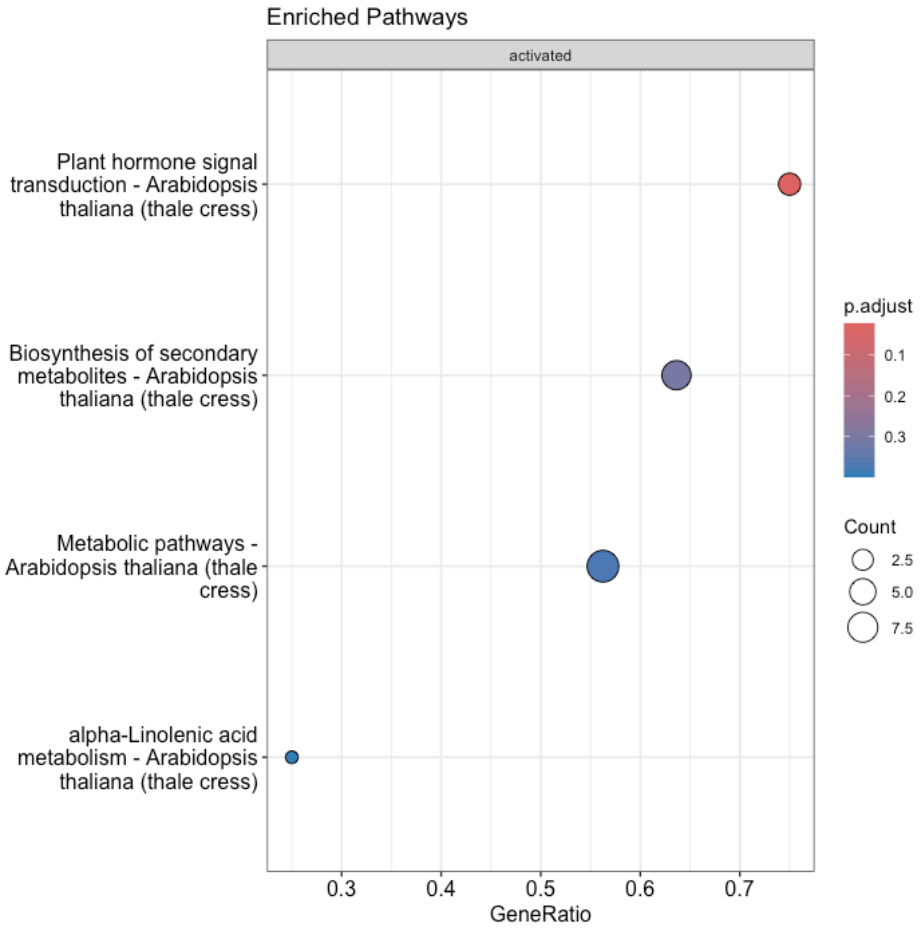

Supplemental Figure 5-3. DEGs involved in KEGG plant hormone signal transduction pathway (ath04075)

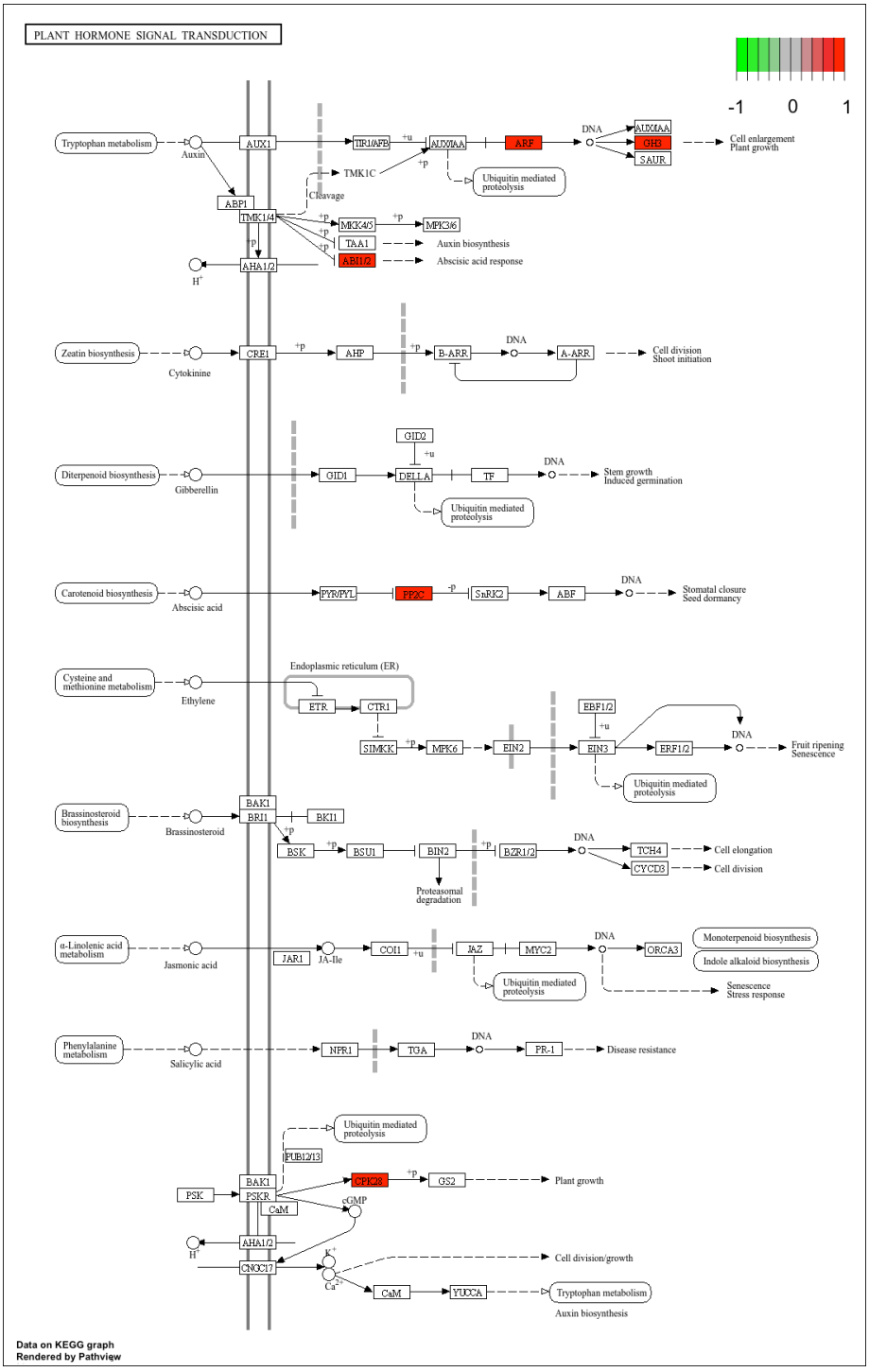

Appendix D. R Packages Used for Data Analysis and Graph Construction.

Ahlmann-Eltze, C., & Hickey, P. (2024). MatrixGenerics: S4 Generic Summary Statistic Functions that Operate on Matrix-Like Objects (Version 1.16.0) [R package]. Bioconductor. https://doi.org/10.18129/B9.bioc.MatrixGenerics.

Arora, S., Morgan, M., Carlson, M., & Pagès, H. (2024). GenomeInfoDb: Utilities for manipulating chromosome names, including modifying them to follow a particular naming style (Version 1.40.1) [R package]. Bioconductor. https://doi.org/10.18129/B9.bioc.GenomeInfoDb.

Bache, S., & Wickham, H. (2022). magrittr: A Forward-Pipe Operator for R (Version 2.0.3) [R package]. CRAN. https://CRAN.R-project.org/package=magrittr.

Bengtsson, H. (2024). matrixStats: Functions that Apply to Rows and Columns of Matrices (and to Vectors) (Version 1.4.1) [R package]. CRAN. https://CRAN.R-project.org/package=matrixStats.

Carlson, M. (2024). org.At.tair.db: Genome wide annotation for Arabidopsis (Version 3.19.1) [R package]. Bioconductor.

Huber, W., Carey, V. J., Gentleman, R., Anders, S., Carlson, M., Carvalho, B. S., Bravo, H. C., Davis, S., Gatto, L., Girke, T., Gottardo, R., Hahne, F., Hansen, K. D., Irizarry, R. A., Lawrence, M., Love, M. I., MacDonald, J., Obenchain, V., Ole's, A. K., Pagès, H., Reyes, A., Shannon, P., Smyth, G. K., Tenenbaum, D., Waldron, L., & Morgan, M. (2015). Orchestrating high-throughput genomic analysis with Bioconductor. *Nature Methods, 12*(2), 115–121. https://doi.org/10.1038/nmeth.3252.

Kolde, R. (2019). pheatmap: Pretty Heatmaps (Version 1.0.12) [R package]. CRAN. https://CRAN.R-project.org/package=pheatmap.

Lawrence, M., Huber, W., Pagès, H., Aboyoun, P., Carlson, M., Gentleman, R., Morgan, M., & Carey, V. (2013). Software for computing and annotating genomic ranges. *PLoS Computational Biology, 9.* https://doi.org/10.1371/journal.pcbi.1003118.

Love, M. I., Huber, W., & Anders, S. (2014). Moderated estimation of fold change and dispersion for RNA-seq data with DESeq2. *Genome Biology, 15*, 550. https://doi.org/10.1186/s13059-014-0550-8.

Luo, W., & Brouwer, C. (2013). Pathview: an R/Bioconductor package for pathway-based data integration and visualization. *Bioinformatics, 29*(14), 1830–1831. https://doi.org/10.1093/bioinformatics/btt285.

Makowski, D., Lüdecke, D., Patil, I., Thériault, R., Ben-Shachar, M., & Wiernik, B. (2023). Automated results reporting as a practical tool to improve reproducibility and methodological best practices adoption. CRAN. https://easystats.github.io/report/.

Morgan, M., Obenchain, V., Hester, J., & Pagès, H. (2024). SummarizedExperiment: SummarizedExperiment container (Version 1.34.0) [R package]. Bioconductor. https://doi.org/10.18129/B9.bioc.SummarizedExperiment.

Neuwirth, E. (2022). RColorBrewer: ColorBrewer Palettes (Version 1.1-3) [R package]. CRAN. https://CRAN.R-project.org/package=RColorBrewer.

Pagès, H., Carlson, M., Falcon, S., & Li, N. (2024). AnnotationDbi: Manipulation of SQLite-based annotations in Bioconductor (Version 1.66.0) [R package]. Bioconductor. https://doi.org/10.18129/B9.bioc.AnnotationDbi.

Pagès, H., Lawrence, M., & Aboyoun, P. (2024). S4Vectors: Foundation of vector-like and list-like containers in Bioconductor (Version 0.42.1) [R package]. Bioconductor. https://doi.org/10.18129/B9.bioc.S4Vectors.

R Core Team. (2024). R: A language and environment for statistical computing [Software]. R Foundation for Statistical Computing. https://www.R-project.org/.

Wickham, H. (2016). ggplot2: Elegant graphics for data analysis. Springer-Verlag. https://ggplot2.tidyverse.org.

Wickham, H. (2023). stringr: Simple, Consistent Wrappers for Common String Operations (Version 1.5.1) [R package]. CRAN. https://CRAN.R-project.org/package=stringr.

Wickham, H., François, R., Henry, L., Müller, K., & Vaughan, D. (2023). dplyr: A grammar of data manipulation (Version 1.1.4) [R package]. CRAN. https://CRAN.R-project.org/package=dplyr.

Wickham, H., Hester, J., & Bryan, J. (2024). readr: Read rectangular text data (Version 2.1.5) [R package]. CRAN. https://CRAN.R-project.org/package=readr.

Xiao, N. (2024). ggsci: Scientific Journal and Sci-Fi Themed Color Palettes for 'ggplot2' (Version 3.2.0) [R package]. CRAN. https://CRAN.R-project.org/package=ggsci

Xu, S., Hu, E., Cai, Y., Xie, Z., Luo, X., Zhan, L., Tang, W., Wang, Q., Liu, B., Wang, R., Xie, W., Wu, T., Xie, L., & Yu, G. (2024). Using clusterProfiler to characterize multiomics data. *Nature Protocols*. https://doi.org/10.1038/s41596-024-01020-z.

Wu, T., Hu, E., Xu, S., Chen, M., Guo, P., Dai, Z., Feng, T., Zhou, L., Tang, W., Zhan, L., Fu, X., Liu, S., Bo, X., & Yu, G. (2021). clusterProfiler 4.0: A universal enrichment tool for interpreting omics data. *The Innovation, 2*(3), 100141. https://doi.org/10.1016/j.xinn.2021.100141.

Yu, G., Wang, L., Han, Y., & He, Q. (2012). clusterProfiler: an R package for comparing biological themes among gene clusters. *OMICS: A Journal of Integrative Biology, 16*(5), 284–287. https://doi.org/10.1089/omi.2011.0118.

Yu, G. (2024). enrichplot: Visualization of Functional Enrichment Result (Version 1.24.4) [R package]. Bioconductor. https://doi.org/10.18129/B9.bioc.enrichplot.

Yu, G., Wang, L., & Yan, G. (2015). DOSE: an R/Bioconductor package for Disease Ontology Semantic and Enrichment analysis. *Bioinformatics, 31*(4), 608–609. https://doi.org/10.1093/bioinformatics/btu684.

Zhu, A., Ibrahim, J. G., & Love, M. I. (2018). Heavy-tailed prior distributions for sequence count data: Removing the noise and preserving large differences. *Bioinformatics*. https://doi.org/10.1093/bioinformatics/bty895.

Appendix E. IRB Approval Letter.

VIRGINIA TECH

Division of Scholarly Integrity and Research Compliance
Institutional Review Board
North End Center, Suite 4120 (MC 0497)
300 Turner Street NW
Blacksburg, Virginia 24061
540/231-3732
irb@vt.edu
http://www.research.vt.edu/sirc/hrpp

MEMORANDUM

DATE: May 27, 2022

TO: Yun Yin, Jingsi Liu

FROM: Virginia Tech Institutional Review Board (FWA00000572)

PROTOCOL TITLE: Aroma characterization of six culinary herbs: basil, dill, fennel, lemon balm, tarragon, and thyme

IRB NUMBER: **22-509**

Based on the submitted project description and items listed in the Special Instructions section found on Page 2, the Virginia Tech Human Research Protection Program (HRPP) has determined that the proposed activity is not research involving human subjects as defined by HHS and FDA regulations.

Further review and approval by the Virginia Tech Human Research Protection Program (HRPP) is not required because this is not human research. This determination applies only to the activities described in the submitted project description and does not apply should any changes be made. If changes are made you must immediately submit an Amendment to the HRPP for a new determination. Your amendment must include a description of the changes and you must upload all revised documents. At that time, the HRPP will review the submission activities to confirm the original "Not Human Subjects Research" decision or to advise if a new application must be made.

If there are additional undisclosed components that you feel merit a change in this initial determination, please contact our office for a consultation.

Please be aware that receiving a "Not Human Subjects Research" Determination is not the same as IRB review and approval of the activity. You are NOT to use IRB consent forms or templates for these activities. If you have any questions, please contact the Virginia Tech HRPP office at 540-231-3732 or irb@vt.edu.

PROTOCOL INFORMATION:

Determined As:	**Not Human Subjects Research**
Protocol Determination Date:	**May 27, 2022**

ASSOCIATED FUNDING:

The table on the following page indicates whether grant proposals are related to this protocol, and which of the listed proposals, if any, have been compared to this protocol, if required.